

AD-A070 233

MISSOURI UNIV-COLUMBIA DEPT OF CIVIL ENGINEERING

F/6 13/2

METAL HYDROXIDES FROM ELECTROPLATING: SLUDGE CHARACTERIZATION A--ETC(U)

MAY 79 J T NOVAK, M M GHOSH, W KNOCH

F08635-77-C-0281

UNCLASSIFIED

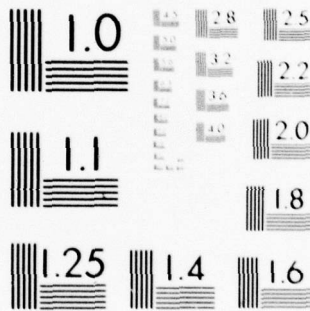
AFESC/ESL-TR-79-09

NL

1 OF 3

AD
A070233





MICROCOPY RESOLUTION TEST CHART
NATIONAL BUREAU OF STANDARDS-1963-A

AD A070233

DDC FILE COPY



LEVEL

ES-TR-79-09

②

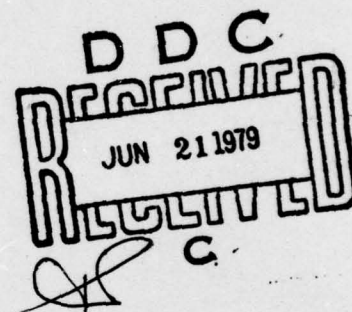
METAL HYDROXIDES FROM ELECTROPLATING: SLUDGE CHARACTERIZATION AND METAL RECOVERY

JOHN T. NOVAK THOMAS CLEVINGER MRIGANKA M. GHOSH
CHARLES YEH WILLIAM KNOCH
DEPARTMENT OF CIVIL ENGINEERING
UNIVERSITY OF MISSOURI-COLUMBIA
COLUMBIA, MO 65201

MAY 1979

FINAL REPORT

29 JULY 1977 - 18 FEBRUARY 1978



APPROVED FOR PUBLIC RELEASE;
DISTRIBUTION UNLIMITED

AFEGSC

ENGINEERING AND SERVICES LABORATORY
AIR FORCE ENGINEERING AND SERVICES CENTER
TYNDALL AIR FORCE BASE, FLORIDA 32403

79 06 18 023

UNCLASSIFIED

SECURITY CLASSIFICATION OF THIS PAGE (When Data Entered)

REPORT DOCUMENTATION PAGE		READ INSTRUCTIONS BEFORE COMPLETING FORM
1. REPORT NUMBER ESL-TR-79-09	2. GOVT ACCESSION NO.	3. RECIPIENT'S CATALOG NUMBER
4. TITLE (and Subtitle) METAL HYDROXIDES FROM ELECTROPLATING: SLUDGE CHARACTERIZATION AND METAL RECOVERY		5. TYPE OF REPORT & PERIOD COVERED Final Report 29 July 77 - 18 Feb 78
6. AUTHOR(s) John T. Novak, Thomas/Clevenger Mriganka M. Ghosh, Charles/Yeh William P. Knoche		7. CONTRACT OR GRANT NUMBER(s) F08635-77-C-0281
8. PERFORMING ORGANIZATION NAME AND ADDRESS Department of Civil Engineering University of Missouri - Columbia Columbia MO 65201		9. PROGRAM ELEMENT, PROJECT, TASK JON: 20543W24 Program Element 647008F
11. CONTROLLING OFFICE NAME AND ADDRESS HQ AFESC/RDVW Tyndall AFB FL 32403		10. REPORT DATE May 9979 12. NUMBER OF PAGES 260
14. MONITORING AGENCY NAME & ADDRESS (if different from Controlling Office) AFESC/ESL		15. SECURITY CLASS. (of this report) UNCLASSIFIED 15a. DECLASSIFICATION/DOWNGRADING SCHEDULE
16. DISTRIBUTION STATEMENT (of this Report) Approved for public release; distribution unlimited.		
17. DISTRIBUTION STATEMENT (of the abstract entered in Block 20, if different from Report)		
18. SUPPLEMENTARY NOTES Available in DDC		
19. KEY WORDS (Continue on reverse side if necessary and identify by block number) Electroplating Dewatering Sludge Filtration Heavy Metals Liquid Extraction Metal Hydroxides Precipitation		
20. ABSTRACT (Continue on reverse side if necessary and identify by block number) The purpose of this project was to investigate the precipitation of metals from plating facilities, to determine the dewatering characteristics of the resultant metal hydroxide slurries and to evaluate the solvent extraction process for metal recovery and reuse. Individual metals were found to precipitate according to the theoretical solubility calculations, however, mixed metals solutions containing Cr (III) often would form "co-precipitants." The co-precipitation would result in certain		

DD FORM 1 JAN 73 1473

410 687
SECURITY CLASSIFICATION OF THIS PAGE (When Data Entered)

UNCLASSIFIED

SECURITY CLASSIFICATION OF THIS PAGE(When Data Entered)

BLOCK 20 (continued)

metals precipitating at pH levels below the range of predicted insolubility.

Colloidal metal hydroxides remaining after settling could be removed by filtration using either a gravity filter or diatomaceous precoat pressure filter. Metal removal was effective (>95%) but the filtrate metal concentrations were not sufficiently low to meet effluent requirements.

Sludges produced by hydroxide precipitation varied depending upon the pH of precipitation and the specific metals in the sludge. Sludge dewatering characteristics were found to be determined by the mean particle size of the flocs. Polymers improved dewatering rates by increasing the mean floc size. Freshly precipitated chromium hydroxide sludges were found to pass through filtering media because of floc break-up. Polymer conditioning was necessary to prevent sludge penetration through the filter media.

Solvent extraction could be used to selectively extract individual metals from a mixed metal sludge but the process was not economical.

UNCLASSIFIED

SECURITY CLASSIFICATION OF THIS PAGE(When Data Entered)

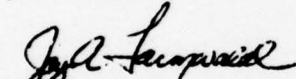
PREFACE

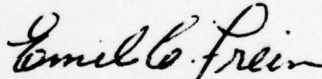
This report was prepared by the Department of Civil Engineering, University of Missouri-Columbia, under Contract No. FO8635-77-C-0281 with the Civil and Environmental Engineering Development Office, Detachment 1, Armament Development and Test Center (AFSC), Tyndall AFB FL. Effective 1 March 1979 CEEDO was inactivated and became the Engineering and Services Laboratory (ESL) a Directorate of the Air Force Engineering and Services Center located on Tyndall AFB Florida 32403.

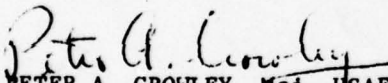
Captain Jay A. Farmwald was program manager for this work.

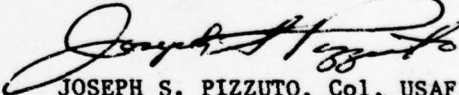
This report has been reviewed by the Information Office (OI) and is releasable to the National Technical Information Service (NTIS). At NTIS it will be available to the general public, including foreign nations.

This technical report has been reviewed and is approved for publication.


JAY A. FARMWALD, Capt, USAF, BSC
Project Officer


EMIL C. FREIN, Maj, USAF
Chief, Envmtl Engrg and Energy
Research Branch


PETER A. CROWLEY, Maj, USAF, BSC
Chief, Environics Division


JOSEPH S. PIZZUTO, Col, USAF, BSC
Director, Engineering and Services
Laboratory

(The reverse of this page is blank)

Accession For	
NTIS GRA&I	<input checked="checked" type="checkbox"/>
DDC TAB	<input type="checkbox"/>
Unannounced	<input type="checkbox"/>
Justification	
By _____	
Distribution/	
Availability Codes	
Dist	Avail and/or special
A	

TABLE OF CONTENTS

Section	Title	Page
I.	INTRODUCTION	1
	A. Nature of Problem	1
	B. Present Study	2
	C. Objectives	4
II.	METHODS AND MATERIALS	7
	A. Insolubilization/Precipitation Studies	7
	B. Sludge Characterization and Testing	9
	1. Filtration Parameters	9
	2. Particle Size Measurements	14
	3. Sludge Conditioning Studies	16
	4. Sedimentation/Thickening Studies	16
	C. Filtration Studies	17
	1. Samples	17
	2. Dual Media Filtration Studies	17
	3. Diatomaceous Earth Filtration	19
	D. Solvent Extraction	19
	1. Method Verification and Percent Extraction Curves	19
	2. Separation Scheme Determination	29
	3. Pilot Plant	29
III.	RESULTS AND DISCUSSION	32
	A. Metal Insolubilization Studies	32
	1. Individual Metal Systems	32

TABLE OF CONTENTS (Continued)

Section	Title	Page
	2. Effect of Sulfate Ions on Chromium Stability	47
	3. Chromium Mixed-Metal Systems	51
	4. Mixed-Metal Studies (Fe-Ni)	78
	5. Mixed-Metal Studies (Cu-Ni)	78
	6. Mixed-Metal Studies (Chromium-Cadmium-Copper-Nickel)	85
	7. OC-ALC Electroplating Waste Treatment Studies	90
B.	Sludge Characterization	94
	1. Introduction	94
	2. Individual Metal Hydroxide Sludges	95
	3. Mixed-Metal Sludges	105
	4. Effects of Particle Size on the Dewatering of Metal Hydroxide Sludges	109
	5. Statistical Modelling	115
	6. Solids Penetration During Dewatering	120
	7. Sludge Compressibility	131
	8. Polymer Treatment of Metal Hydroxide Sludges	135
	9. Thickening of Metal Hydroxide Suspensions	141
C.	Dual Media Filtration of Metal Oxide Suspensions	150
	1. Effect of Flow Rate	150
	2. Polymer Addition	150

TABLE OF CONTENTS (Concluded)

Section	Title	Page
	3. Precoat Filtration	157
	D. Precoat Filtration With Diatomaceous Earth	163
	1. Effect of Body Feed	170
	2. Effect of Precoat Variations	179
	E. Liquid-Liquid Extraction	179
IV	CONCLUSIONS	242
V	RECOMMENDATIONS	246
	REFERENCES	249
	APPENDIX	253
	A. Estimation of Current Bed Utilization	253
	B. Calculation of Simulated Sample Content for Cation Regenerant	258

LIST OF FIGURES

Figure	Title	Page
1.	Proposed metal recovery and treatment process for Air Force facilities.	5
2.	Schematic of the experimental apparatus utilized in metals insolubilization studies.	8
3.	Laboratory filtration apparatus.	11
4.	Results of studies examining the statistical error of "S", the coefficient of compressibility.	13
5.	Replicate sampling of a particle size distribution using the HIAC particle counter.	15
6.	Gravity filter apparatus.	21
7.	Clean bed head loss.	22
8.	Precoat filter cell assembly.	23
9.	Schematic diagram of the precoat filter apparatus.	24
10.	Percent extraction curve for 8HQ.	27
11.	Percent extraction curve for NaDDC.	28
12.	Pilot plant design.	32
13.	Concentration (theoretical and experimental) of supernatant nickel ion as a function of pH.	33
14.	Concentration (theoretical and experimental) of supernatant zinc as a function of pH.	34
15.	Concentration (theoretical and experimental) of supernatant cadmium as a function of pH.	35
16.	Concentration (theoretical and experimental) of supernatant copper as a function of pH.	36
17.	Concentration (theoretical and experimental) of supernatant chromium ion as a function of pH.	37
18.	Supernatant chrome concentration and supernatant turbidity as a function of pH for a settled sample containing 130 mg/l Cr(III) initially.	38

LIST OF FIGURES (continued)

Figure	Title	Page
19.	The characteristic size of chromium hydroxide flocs as a function of pH.	39
20.	The characteristic surface potential of chromium hydroxide flocs as a function of pH (no sulfates present in solution).	41
21.	Supernatant nickel concentration as a function of pH for a settled sample containing 50 mg/l Ni(II) initially.	42
22.	Supernatant copper concentration and supernatant turbidity as a function of pH for a settled sample containing 90 mg/l Cu(II) initially.	43
23.	Supernatant zinc concentration and supernatant turbidity as a function of pH for a settled sample containing 90 mg/l Zn(II) initially.	44
24.	Supernatant cadmium concentration and supernatant turbidity as a function of pH for a settled sample containing 90 mg/l Cd(II) initially.	45
25.	Representative results from Thomas and Theis (20).	48
26.	Supernatant chromium concentration and supernatant turbidity as a function of pH for a settled sample containing 130 mg/l Cr(III) initially. (Sulfates present in solution)	49
27.	The characteristic surface potential of chromium hydroxide flocs as a function of pH. (Sulfates present in solution)	50
28.	Supernatant chromium, zinc and sulfate concentrations as a function of pH for a settled sample containing 37 mg/l Cr(III), 40 mg/l Zn(II) and 52 mg/l SO ₄ initially.	52
29.	Supernatant chromium and nickel concentrations as a function of pH for a settled sample containing 40 mg/l Cr(II) and 30 mg/l Ni(II) initially.	53
30.	Supernatant chromium and cadmium concentrations and supernatant turbidity as a function of pH for a settled sample containing 147 mg/l Cr(III) and 180 mg/l Cd(II) initially.	54

LIST OF FIGURES (continued)

Figure	Title	Page
31.	Comparative data from this study and similar studies performed by Thomas and Theis (20).	55
32.	The effect of chromium content and pH on the concentration of nickel remaining in the supernatant liquor.	57
33.	The effect of chromium content and pH on the concentration of nickel remaining in the supernatant liquor.	58
34.	Alkimetric titration curves for several initial Cr(III) ion concentrations.	59
35.	Alkimetric titration curves for several initial Ni(II) ion concentrations.	60
36.	Alkimetric titration curve for zinc.	61
37.	Alkimetric titration curves for several initial Cd(II) ion concentrations.	62
38.	An alkimetric titration curve for a Cr(III) - Ni(II) metal mixture.	64
39.	An alkimetric titration curve for a Cr(III) - Ni(II) metal mixture.	65
40.	Alkimetric titration curves for two Cr(III) - Ni(II) mixtures.	66
41.	An alkimetric titration curve for a Cr(III) - Ni(II) metal mixture.	67
42.	Alkimetric titration curves (theoretical and experimental) for a Cr(III) - Ni(II) metal mixture.	68
43.	Distribution of Cr(III) species as a function of pH ($Cr_T = 10^{-2}M$).	72
44.	Distribution of Cr(III) species as a function of pH ($Cr_T = 10^{-3}M$).	73
45.	Alkimetric titration curves for a Cr(III) - Ni(II) metal mixture ($Cr(III) = 12.2 \text{ meq}$, $Ni(II) = 12.2 \text{ meq}$).	75

LIST OF FIGURES (continued)

Figure	Title	Page
46.	Alkimetric titration curves for Fe(III) - Ni(II) metal mixtures.	79
47.	Alkimetric titration curves for several Fe(III) - Ni(II) metal mixtures.	80
48.	Supernatant iron and nickel concentrations as a function of pH for a settled sample containing 200 mg/l Fe(III) and 900 mg/l Ni(II) initially.	81
49.	Alkimetric titration curves for several Cu(II) - Ni(II) metal mixtures.	82
50.	An alkimetric titration curve for a Cu(II) - Ni(II) metal mixture, showing the possibilities for the application of "selective precipitation".	83
51.	An alkimetric titration curve for a Cu(II) - Ni(II) metal mixture, showing the possibilities for the application of "selective precipitation".	84
52.	Supernatant copper and nickel concentrations as a function of pH for a settled sample containing 350 mg/l Cu(II) and 900 mg/l Ni(II) initially.	86
53.	Supernatant metals and sulfate concentrations and supernatant turbidity as a function of pH (mixed-metal system containing no Cr(III).)	88
54.	Supernatant metal and sulfate concentrations and supernatant turbidity as a function of pH (mixed-metal system containing Cr(III).)	89
55.	Representative data from Thomas and Theis (20). Note: All supernatant Cu(II), Cd(II) and Zn(II) concentrations were less than 1 to 2 mg/l.	91
56.	Supernatant metals concentration as a function of pH (insolubilization using NaOH) OC-ALC cation regenerant.	92
57.	Supernatant metals concentration as a function of pH (insolubilization using CaO). OC-ALC cation regenerant.	93

LIST OF FIGURES (continued)

Figure	Title	Page
58.	The characteristic sludge floc size and corresponding specific resistance of nickel hydroxide sludges as a function of pH.	96
59.	Filtrate quality obtained during vacuum filtration as a function of pH for several nickel hydroxide sludges.	97
60.	Effect of pH on the compressibility of nickel hydroxide sludges.	98
61.	Effect of pH on the cake solids concentration obtained following vacuum filtration (nickel hydroxide sludges).	99
62.	The specific resistance of cupric hydroxide sludges as a function of pH.	101
63.	Variations in the characteristic size of cupric hydroxide and cupric oxide flocs as a function of pH.	102
64.	Degree of solids penetration obtained during vacuum filtration as a function of pH for cupric hydroxide sludges.	103
65.	Variations in the specific resistance of metal hydroxide sludges as a function of the size of sludge flocs.	112
66.	Variations in the specific resistance of metal hydroxide sludges as a function of the size of sludge flocs.	113
67.	Effect of specific surface area (measured as $(1/u)^2$) on the specific resistance of metal hydroxide sludges.	114
68.	Variations in sludge specific resistance as a function of the stated sludge particle size range (5 - 10u).	116
69.	Variations in sludge specific resistance as a function of the stated sludge particle size range (10 - 20u).	117
70.	A comparison of the specific resistance values of two metal hydroxide sludges possessing similar particle size distributions.	118
71.	A comparison of the specific resistance values of two metal hydroxide sludges possessing similar particle size distributions.	119

LIST OF FIGURES (continued)

Figure	Title	Page
72.	Comparison between experimentally observed specific resistance values and values predicted through the use of statistical models.	123
73.	The effect of sludge "fines" on the filtrate turbidity obtained during vacuum filtration.	125
74.	Sludge specific resistance and filtrate quality as a function of time of "aging".	127
75.	Vacuum filtrate quality as a function of applied pressure differential.	129
76.	Filtrate quality as a function of applied pressure differential using a laboratory filter press.	130
77.	Effects of polymer conditioning on filtrate quality.	132
78.	Variations in sludge compressibility as a function of the sludge mean floc size (data for metal hydroxide sludges).	133
79.	The effect of pH on the polymer dose required for effective conditioning of metal hydroxide sludges (nickel dominant sludges).	138
80.	Effects of polymer conditioning dosage on the rate of thickening of metal hydroxide suspensions.	142
81.	Effects of polymer conditioning dosage on the size of flocs present in metal hydroxide suspensions.	143
82.	Particle size effects on the thickening rates of metal hydroxide suspensions.	144
83.	Comparative results from the use of several polymer types for the improvement of metal hydroxide suspension thickening rates.	148
84.	Sludge thickening rates and dewatering rates as a function of polymer conditioning dose.	149
85.	Filtration of mixed-metal hydroxide suspension without polymer addition - effluent profile.	151
86.	Filtration of mixed metal hydroxide suspension without polymer addition - headloss profile.	152

LIST OF FIGURES (continued)

Figure	Title	Page
87.	Filtration of mixed-metal hydroxide suspensions without polymer addition - effluent profile.	153
88.	Filtration of mixed-metal hydroxide suspension without polymer addition - headloss profile.	154
89.	Filtration of mixed-metal hydroxide suspensions with polymer addition - effluent profile.	155
90.	Filtration of mixed-metal hydroxide suspensions with polymer addition - headloss profile.	155
91.	Filtration of mixed-metal hydroxide suspensions with polymer addition - effluent profile.	158
92.	Filtration of mixed-metal hydroxide suspensions with polymer addition - effluent profile.	159
93.	Filtration of mixed-metal hydroxide suspensions with polymer addition - effluent profile.	160
94.	Filtration of mixed-metal hydroxide suspensions with polymer precoat - effluent profile.	161
95.	Filtration of mixed-metal hydroxide suspensions with polymer precoat - effluent profile.	162
96.	Filtration of mixed-metal hydroxide suspensions with anionic polymer addition - effluent profile.	164
97.	Filtration of mixed-metal hydroxide suspensions with anionic polymer addition - headloss profile.	165
98.	Filtration of mixed-metal hydroxide suspensions using larger graded media - effluent profile.	166
99.	Filtration of mixed-metal hydroxide suspensions using larger graded media - headloss profile.	167
100.	Effect of body feed variations on headloss in a diatomaceous earth filter.	172
101.	Effect of body feed on filtrate turbidity.	173
102.	Effect of body feed on the quantity of water produced.	174

LIST OF FIGURES (continued)

Figure	Title	Page
103.	Effect of body feed variations on headloss and water production.	175
104.	Effect of body feed variations on filtrate turbidity.	175
105.	Effect of body feed variations on headloss and water production.	177
106.	Effect of body feed variations on filtrate turbidity.	178
107.	Effect of precoat variations on headloss.	180
108.	Effect of precoat variations on filtrate turbidity.	181
109.	Effect of precoat variations on head loss.	182
110.	Effect of precoat variations on filtrate turbidity.	183
111.	Precision study using 8HQ.	189
112.	Percent extraction curve for AcA.	190
113.	Percent extraction curve for cupferron.	191
114.	Percent extraction curve for BZA.	192
115.	Percent extraction curve for dithizone.	193
116.	Percent extraction curve for TTA.	194
117.	Liquid-liquid extraction flow diagram.	195
118.	Sequential extraction scheme using A(8HQ, pH = 0.5), B(8HQ, pH = 4.0) and C(8HQ, pH = 5.5).	207
119.	Sequential extraction scheme using A(TTA, pH = 3), B(8HQ, pH = 5.3) and C(8HQ, pH = 7.2).	208
120.	Sequential extraction scheme using A(TTA, pH = 2.6), B(8HQ, pH = 4.0) and C(TTA, pH = 7.0).	210
121.	Sequential extraction scheme using A(8HQ, pH = 2.5), B(8HQ, pH = 4.0) and C(NaDDC, pH = 4.0).	211

LIST OF FIGURES (continued)

Figure	Title	Page
122.	Sequential extraction scheme using A(AcA, pH = 5.5), B(8HQ, pH = 2.5), C(8HQ, pH = 4.0) and D(NaDDC, pH = 4.0).	212
123.	Sequential extraction scheme using A(TTA, pH = 3.0), B(8HQ, pH = 2.5), C(8HQ, pH = 4.0), D(8HQ, pH = 5.3) and E(NaDDC, pH = 5.3).	213
124.	Sequential extraction scheme using A(TTA, pH = 4.0), B(TTA, pH = 4.0), C(8HQ, pH = 4.0), D(8HQ, pH = 5.5) and E(NaDDC, pH = 5.5)	214
125.	Sequential extraction scheme using A(TTA, pH = 4.0), B(TTA, pH = 4.0), C(8HQ, pH = 4.0), and D(NaDDC, pH = 4.0).	215
126.	Percent extraction for TTA for four consecutive extractions of a synthetic regenerate solution.	217
127.	Percent extraction for 8HQ for four consecutive extractions of a synthetic regenerate solution.	218
128.	Percent extraction for NaDDC for four consecutive extractions of a synthetic regenerate solution.	219
129.	Percent extraction for TTA for five independent runs containing the synthetic regenerate solution spiked with various metals.	220
130.	Percent extraction for 8HQ for five independent runs containing the synthetic regenerate solution spiked with various metals.	222
131.	Metal content in stripped TTA solution from high Cu run.	225
132.	Metal content in stripped 8HQ solution from high Cu run.	226
133.	Metal content in stripped 8HQ solution from high Ni run.	227
134.	Metal content in stripped 8HQ solution from high Zn run.	228
135.	Metal content in stripped 8HQ solution from high Cd run.	229
136.	Metal content in stripped NaDDC solution from high Cu run.	230

LIST OF FIGURES (concluded)

Figure	Title	Page
137.	Metal content in stripped NaDDC solution from high Ni run.	231
138.	Metal content in stripped NaDDC solution from high Zn run.	232
139.	Metal content in stripped NaDDC solution from high Cd run.	233
140.	Metal content in stripped NaDDC solution from high Cr run.	234
141.	Percent extraction in 8HQ extraction of a precipitated synthetic regenerate solution. Three consecutive extractions.	238
142.	Metal content in stripped 8HQ solution from precipitated synthetic regenerate run.	239

LIST OF TABLES

Table	Title	Page
1.	Effluent Limitations and Monitoring Requirements: Industrial Waste Treatment Plant Effluent, Tinker AFB OK (NPDES Permit No. OK0000809)	3
2.	Composition of Synthetic Waste	18
3.	Operational Parameters for the Dual Media Filter Studies	20
4.	List of the Seven Chelating Compounds Evaluated	25
5.	Literature Isoelectric Point Values for Certain Metal Hydroxides (20)	46
6.	Results of Chromium - Nickel "Coprecipitation" Studies	69
7.	Results of Cr - Ni "Coprecipitation" Studies	71
8.	Water Exchange Rates for Certain Metal Ions	77
9.	Results of Cu - Ni "Selective Precipitation" Studies	87
10.	Effect of pH and Sludge Age on the Filtrate Quality of $\text{Cu}(\text{OH})_2$ Sludges	104
11.	$\text{Cr}(\text{OH})_3$ Insolubilization Using Lime and NaOH	106
12.	Characteristics of Synthetic Mixed-Metal Sludges	107
13.	Characteristics of Sludges from Tinker Air Force Base	108
14.	Particle Size Ranges Utilized for HIAC Size Analysis	110
15.	Description of Independent Variables Utilized in Statistical Models	121
16.	Statistical Modelling - Sludge Specific Resistance	122
17.	Statistical Modelling - Filtrate Turbidity (NTU)	126
18.	Statistical Modelling - Coefficient of Compressibility (CC)	134
19.	Summary of Metal Hydroxide Sludge Conditioning Studies	136

LIST OF TABLES

Table	Title	Page
20.	Optimum Polymer Dose for Sludge Conditioning (OP)	140
21.	Statistical Modelling - Interfacial Settling Velocity (ISV)	141
22.	Effluent Metal Concentration for Dual Media Studies	163
23.	Different Grades of Diatomaceous Earth and the Filtrate Turbidity of Buchner Funnel Test	171
24.	Influent and Effluent Metal Concentration of Diatomaceous Earth Filtration	184
25.	Settling Effects on Extraction Efficiencies of Three Different Chelating Compounds	186
26.	Shaking Time Effects on Extraction Efficiencies 8HQ and NaDDC	188
27.	Percent Extraction and Stripping for NaDDC	197
28.	Percent Extraction and Stripping for BZA	198
29.	Percent Extraction and Stripping for Cupferron	199
30.	Percent Extraction and Stripping for Dithizone	200
31.	Percent Extraction and Stripping for AcA	201
32.	Re-extraction Capabilities of Various Chelating Compounds	202
33.	Re-extraction of Thenylotrifluoroacetone and Sodium Diethyldithiocarbamate Using Different Metal Concentrations	204

SECTION I

INTRODUCTION

A. Nature of Problem

In recent years there has been considerable interest in treating industrial wastewaters prior to their entry into the environment. Legislation has been enacted which mandates resource recovery, whenever economically feasible, Resource Conservation and Recovery Act-1976 (RCRA), and establishes guidelines for the control of toxic and hazardous material discharged into the environment, Toxic Substances Control Act-1976 (TSCA). Such legislation has prompted government and industry to develop/modify control technologies in an effort to meet these new challenges in an economic and timely manner.

The metal finishing industry, having been identified as a major industry of concern in the Federal Water Pollution Control Act (1972), faces major new challenges in wastewater treatment. Those pollutants of primary concern include the heavy metals and cyanides. Sufficient technology is not generally available for the economic removal or recovery of these materials from wastewaters discharged from such facilities. Of the 20,000 metal finishing operations within the United States only 5,000 can be classified as large independent plants or captive facilities where ample technology is available at reasonable costs (1).

Those methods most widely accepted by the metal finishing industry for the treatment of waste discharges include: oxidative destruction of cyanides, reduction of hexavalent chrome, precipitation of heavy metals, sludge dewatering and ultimate disposal. The slurries generated in this conventional scheme are often difficult to handle and resist most dewatering processes. Cherry (2) indicates that these sludges often yield less than 1% solids upon thickening and less than 20% solids by filter pressing. Dewatering rates are slow and therefore process yields are low resulting in high costs per volume of liquid handled. To date it is unclear to what extent disposal of these sludges will be regulated under RCRA and/or TSCA. However, EPA has, in their proposed Guidelines and Regulations on Hazardous Waste Management (Federal Register-18 Dec 78) specifically classified electroplating wastewater treatment sludge as a "hazardous waste". It has been shown that environmental problems are often encountered in the disposal of metal hydroxide sludges, slurries or dewatered residues, on land. The success of lagooning as a method of sludge disposal depend largely on the type of soil and also on climatological factors, such as rainfall and evaporation. Acidic groundwaters or soil may make metals mobile in a short period of time following disposal. Recent advances in disposal technologies involve the immobilization of metals with strong chelating compounds. Several fixative and encapsulating techniques are now available for fixing metals in a solidified matrix, which can ultimately be used as construction material. Cementation of heavy metals in ferrous sulfate matrix is the basis of the "ferrite process" recently marketed in Japan by Nippon Electric Company (3). (Patterson has provided an excellent summary of some

recent technological developments for the disposed of metal-finished waste sludges (4)).

Interest in developing possible methods for reclaiming metals from plating wastes is also on the rise. The value of nickel and chromium lost in plating wastes in the United States has been estimated at 25 to 30 million dollars. Some large electroplating facilities discard sludges containing metals values at \$150,000 to \$200,000 per year (5). Of those recovery schemes available all require point source segregation of individual metal streams. For the most part these processes involve either direct precipitation, adsorption followed by precipitation, evaporative/membrane processes, or ion exchange followed by precipitation of metals from the concentrated regeneration wastewaters.

B. Present Study

The United States Air Force (USAF) maintains five Air Logistics Centers (ALC's) that operate extensive aircraft related plating facilities. These centers, located in Oklahoma City, OK (OC-ALC), San Antonio, TX (SA-ALC), Ogden, UT (O,ALC), Sacramento, CA (S-ALC) and Macon, GA (M-ALC) employ ion exchange as a water reuse/metal concentration process discharging concentrated cyanide and metal solutions to their respective base industrial waste treatment plants (IWTP) in the form of slug regenerant waste streams. Those newer facilities (SA-ALC and S-ALC) segregate chrome and cyanide waste streams from the remaining mixed metal stream (Ni, Cu, Zn, Cd). Chrome is recovered in an evaporative process whereas cyanide is held for batch delivery to the IWTP. Present operations make it difficult for the IWTP's to efficiently reduce hexavalent chrome and precipitate metal hydroxides. A representative discharge permit for one such IWTP (OC-ALC) is shown in Table 1 and indicates the high level of treatment which has been imposed on such facilities by the regulatory agencies.

It is also noteworthy that the final pretreatment regulations for existing point sources within the electroplating industry as recently promulgated by EPA may be enforced at the actual plating facility as opposed to the IWTP. These considerations make it imperative that research and development continue with respect to the optimization of proven treatment technologies and potential recovery processes which might have application at the ALC plating facilities.

In 1977 the Department of Civil Engineering, University of Missouri-Columbia, completed a preliminary study entitled, "Optimum Dewatering and Metal Recovery from Metal Plating Waste Sludges" (6). The major recommendations from this study were to conduct an in-depth investigation into the effects of important physiochemical parameters on the precipitation of metals from mixed metal solutions, to determine the dewatering behavior of sludges that result, and to study the effectiveness of dual media gravity feed filters and pressure precoated diatomaceous earth filters in removing carryover metal hydroxide particulates from the settler effluent and from the vacuum

TABLE 1. EFFLUENT LIMITATIONS AND MONITORING REQUIREMENTS:
INDUSTRIAL WASTE TREATMENT PLANT EFFLUENT,
TINKER AFB OK (NPDES PERMIT NO. OK0000809)

<u>EFFLUENT CHARACTERISTIC</u>	<u>DISCHARGE LIMITATIONS (Lb/day)</u>	
	<u>Daily Avg</u>	<u>Daily Max</u>
Flow (MGD)	--	--
COD	312	938
Total Suspended Solids	125	280
Cadium	.12	.54
Chromium, Total	.62	270
Chromium, Hexavalent	.30	.90
Cyanide, A	.03	.14
Copper	.07	.32
Lead	.37	1.66
Nickel	1.25	5.62
Zinc	.62	2.70
phenols	.05	.22
Oil and grease	125	280
Cyanide, Total	.06	.27
pH	Not less than 6.0 standard units nor greater than 9.0 standard units	

There shall be no discharge of floating solids or visible foam in other than trace amounts.

Effective Dates: 7-01-77 through 12-15-79

Monitoring Requirements: Three 24 hour composites per week.

filtrate from dewatering operations. Further, it was recommended that liquid-liquid extraction process be explored in an attempt to develop a pilot unit for separating and recovering metals from the mixed metal sludges obtained from the precipitation of regeneration backwash wastes.

Many different methods are being tried for reclaiming metals from hydroxide sludges (5), but a common problem found in all is the inability to handle mixed sludges containing several metals with varying concentrations. Therefore, if the various waste streams in a plating plant can be kept separate, several processes for recovery of individual metals exist, with electrodeposition and membrane processes being widely used. However, for established facilities where many different metals are being plated, segregation of individual metal sludges is not practical. A process is needed which can separate several metals at one time. Furthermore, the process must lend itself to automation resulting in reduced labor load. These requirements eliminate multi-technique processes employing combinations of precipitation, distillation, electrodeposition and others. Solvent extraction methods using high molecular weight amines for the removal of toxic metal ions, such as cadmium, chromium, copper, nickel, and zinc, have been extensively investigated (7-10). It has, however, seen surprisingly limited application in the reclamation of plating wastes. The Bureau of Mines (11) used liquid-liquid exchange to remove Co in the reclaiming of superalloy scrap. This was, however, only one part of a multi-technique procedure. Liquid-liquid exchange also has been evaluated using naphthenic acid in kerosene as the extracting medium (5). The authors concluded unsatisfactory overall results from this approach. However, naphthenic acid is a non-chelating organic acid and should not be expected to possess sufficient selectivity for different metals in a multi-component matrix for the type encountered in this situation. Several industrial processes utilizing solvent extraction procedures have recently been employed in Europe (12). The Gullspang process uses high molecular-weight amine Alamine 336 to remove molybdenum, chromium, cobalt, and nickel from solid wastes such as scrap lathe turnings, and mill shavings. The Soderfors process is used to recover metals from stainless steel pickling both. The Valberg process is being used to recover zinc from effluent water from rayon manufacturing. All of these processes use solvent extraction on an industrial scale.

A scheme for the precipitation of metals from the regeneration backwashes from ion exchange units at OC-ALC, followed by dewatering of resultant sludges, and recovery of metals by solvent extraction was proposed (6), as shown in Figure 1.

C. Objectives

The intent of this study was to determine the operational characteristics that govern the vacuum and gravity dewatering of hydroxide sludges obtained from the insolubilization of mixed-metal electroplating wastes. Additionally, the feasibility of recovery of metals from dewatered sludges was to be investigated.

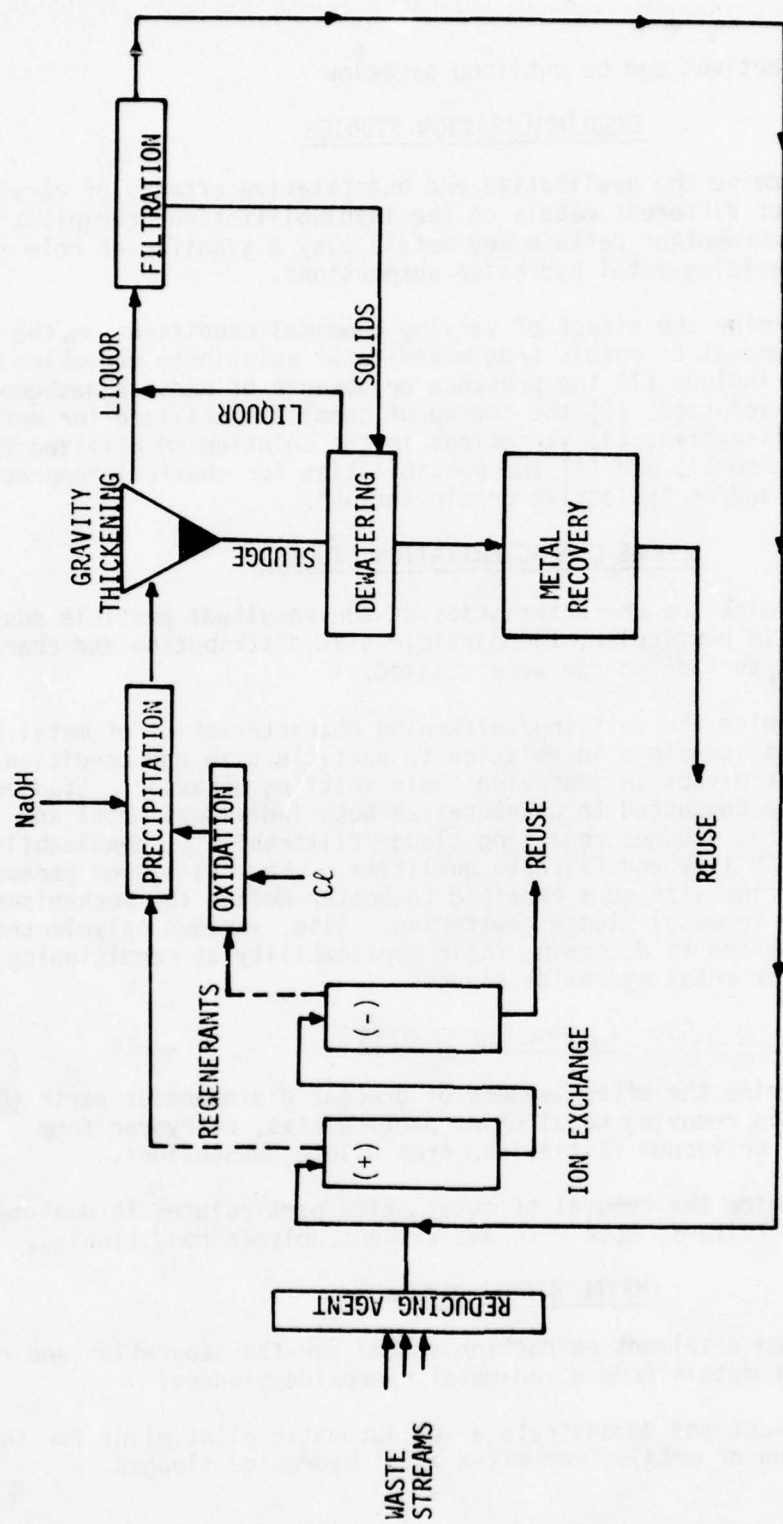


Figure (1). Proposed metal recovery and treatment process for Air Force facilities.

The specific objectives can be outlined as below

INSOLUBILIZATION STUDIES

1. To determine the qualitative and quantitative effects of varying ratios of different metals on the insolubilization/precipitation of metals and whether certain key metals play a significant role in characterizing metal hydroxide suspensions.
2. To determine the effect of varying chemical conditions on the efficient removal of metals from mixed-metal solutions; variables considered include (1) the presence or absence of certain background ions in solution, (2) the choice of chemicals utilized for metals insolubilization, (3) variations in the solution pH utilized for metals removal, and (4) the possibilities for chemical "coprecipitation" and/or "selective precipitation".

SLUDGE CHARACTERIZATION STUDIES

3. To determine the characteristics of the resultant particle suspensions. In particular, the particle size distribution and characteristic surface charge were studied.
4. To determine the settling/thickening characteristics of metal hydroxide suspensions in relation to particle size and conditioning polyelectrolytes in improving their settling behavior. Studies were also conducted to characterize both individual metal and mixed-metal sludges regarding sludge filterability, handleability, compressibility and filtrate qualities. Various sludge parameters such as floc size were examined to better define the mechanisms applicable to metal sludge dewatering. Also, various polyelectrolytes were examined to determine their applicability as conditioning agents for metal hydroxide sludges.

FILTRATION STUDIES

5. To determine the effectiveness of precoat diatomaceous earth (DE) filters in removing metal oxide particulates, carryover from settling or vacuum filtration, from dilute suspensions.
6. To determine the removal of metal oxide particulates in dual-media granular filters, both with and without polymer conditioning.

METAL RECOVERY STUDIES

7. To develop a solvent extraction scheme for the separation and recovery of metals from mixed-metal hydroxide sludges.
8. To construct and demonstrate a semiautomatic pilot plant for the separation of metals from mixed-metal hydroxide sludges.

SECTION II

METHODS AND MATERIALS

A. Insolubilization/Precipitation Studies

Metals examined during the insolubilization/precipitation studies included chromium copper, nickel and zinc. Insolubilization studies were performed using each metal individually and several metal combinations. Solutions were prepared by dissolving metal nitrate salts in distilled water. The solution pH was then lowered to pH 1.5 to 2.0, simulating the acidic regenerate of an ion exchange unit. In addition to those solutions prepared in the laboratory cation regenerate samples were obtained from the plating facility at OC-ALC. Tests were performed to determine if these actual wastewater samples behaved in a manner similar to the laboratory solutions with respect to metals insolubilization.

The general procedure of insolubilization studies began by placing a defined volume of waste solution into a beaker which contained a pH electrode for monitoring solution pH levels. Mixing was initiated through the use of a magnetic mixer and stirring bar. Base was added volumetrically to the solution, with the rate of base addition between 4 to 8 ml per minute. Base addition continued through the pH range of metal insolubilization until a predetermined level was reached. Mixing was continued at the pH level for approximately 20 minutes to provide flocculation time. Continual readjustment of the solution pH was practiced through the addition of HNO_3 or NaOH to maintain the proper pH level. Following flocculation, the beaker was removed from the mixer and a portion of the suspension placed into a 250 ml or 1 liter graduated cylinder. A one-hour sedimentation time was then provided, after which a supernatant liquor sample was collected and analyzed for residual turbidity and metals concentration, both soluble and insoluble. A schematic of the equipment utilized for insolubilization studies is shown in Figure 2.

Metal removal through hydroxide insolubilization was chosen as the method of treatment based upon the following reasons:

(1) All metals under consideration could be efficiently insolubilized from solution by hydroxide addition (13). In relation to the overall goals of the research project, the supernatant waters from the insolubilization/precipitation process will not be discharged to the environment; rather, they will be recycled within the rinse water system. Thus, it is only necessary to lower the concentration of metals to the 1 to 2 mg/l range which is characteristic of most rinse waters. Hydroxide insolubilization has been shown in the literature to be extremely efficient in this regard.

(2) Carbonate precipitation was not utilized based upon the findings of Patterson et al. (14). Their research indicated no significant benefits could be derived through the use of carbonate precipitation.

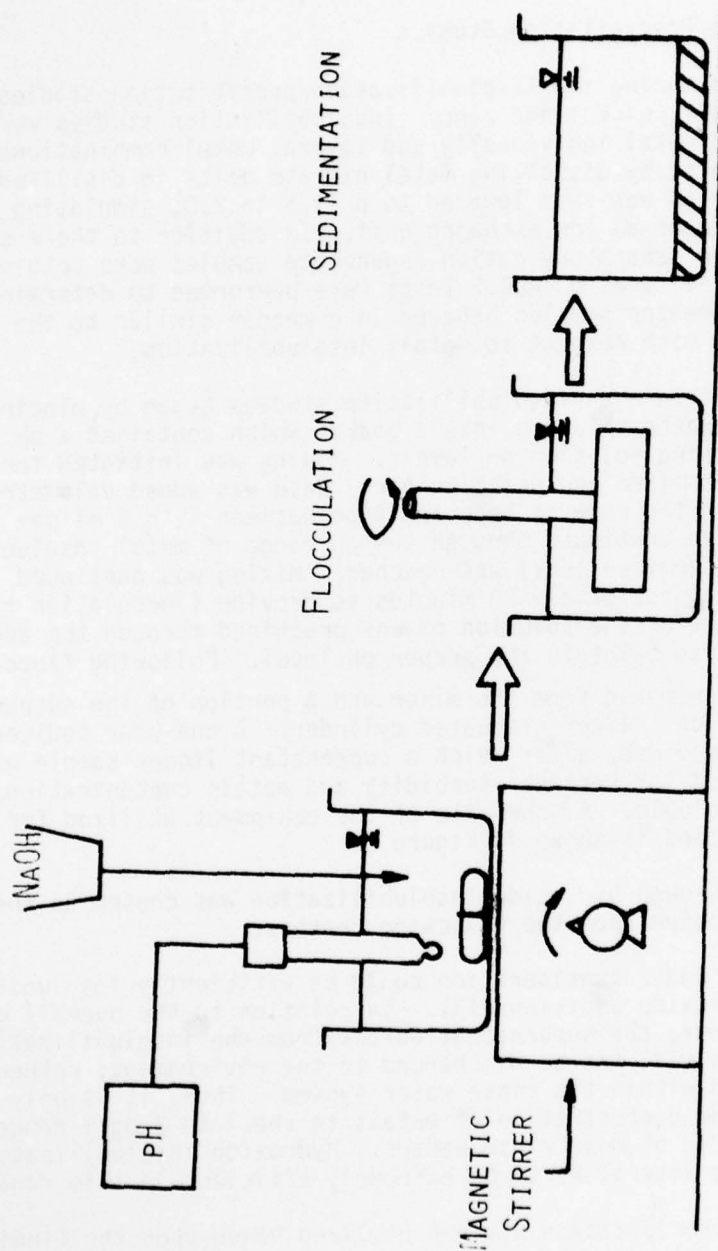


Figure (2). Schematic of the experimental apparatus utilized in metals insolubilization studies.

(3) A major requirement of the proposed metal recovery system is the eventual resolubilization of metal sludges prior to liquid-liquid extraction, the ultimate recovery process to be utilized. For this reason, sulfide precipitation (15) was not considered a viable treatment alternative because the extreme insolubility of metal sulfide species make recovery difficult.

Sodium hydroxide was used for a vast majority of the studies conducted; lime was used periodically in parallel studies. The choice of NaOH is related to the proposed waste treatment system at OC-ALC. Their present ion exchange system shows a high selectivity for calcium. Thus, it was felt that the use of lime would result in significantly high calcium concentrations in the rinse waters. This would produce a corresponding increase in the percentage of the ion exchange bed which would be utilized for water softening. Sodium hydroxide, although more expensive on a comparative chemical cost basis, will reduce the above mentioned problem because the exchange resin possesses a lower capacity for sodium exchange.

Samples of the initial synthetic solution and final supernatant liquor were collected for each study and stored in 50 ml Nalgene sample bottles. Each bottle contained approximately 1 ml of 1+1 HNO_3 to maintain a soluble metal environment. Samples were analyzed using a Perkin-Elmer 360 Atomic Absorption Spectrophotometer. Samples were diluted prior to analysis using 1% HNO_3 from an automatic diluter. Representative dilution ratios included: 1:2, 1:5, 1:10, 1:50, 1:100, 1:500 and 1:1,000. Analyses were run on several dilutions of each sample to ensure that at least 3 dilutions could be found within the linear range of the spectrophotometer. External standards for each metal under consideration were prepared through dilution of purchased metal standards in 1% HNO_3 . Standards were prepared periodically to ensure freshness and reliability.

Metal insolubilization studies were also conducted to examine the stoichiometric requirements necessary for complete metals removal. Methods similar to those presented by Stumm and Morgan (16) were utilized to obtain acidimetric titration curves for each metal and/or combination of metals. Synthetic solutions were prepared as described previously. Base was added to solution in known quantities, and the pH was monitored as a function of the amount of base added. Comparing the quantity of base required to reach the inflection point with the initial quantity of metals present allows for the calculation and comparison of stoichiometric requirements for complete insolubilization.

B. Sludge Characterization and Testing

1. Filtration Parameters

Sludge samples were obtained by (1) collecting the settled samples following insolubilization/precipitation studies, and (2) collection of OC-ALC wastewater samples. In general, sludge samples obtained from

insolubilization studies were not analyzed until one day following precipitation. This was done to minimize variations between sludge samples due to aging effects.

Sludge filtration rate studies were performed using a standard Buchner funnel apparatus as shown in Figure 3. Equipment utilized included a 9 cm Buchner funnel, No. 40 ashless filter paper, a 100 ml graduated cylinder and a vacuum pump. One hundred ml samples were used throughout all of the filtration studies. Specific directions regarding the procedure utilized are given by Eckenfelder and O'Connor (17). In general, once the vacuum was initiated, filtrate volumes were collected in the graduated cylinder and recorded as a function of time. Unless otherwise noted, the vacuum level was maintained at 15 inches Hg (approximately 7.5 psi).

Prior to each filtration test the initial solids concentration was measured; likewise, the cake solids concentration was determined following cake failure. Both a total solids and dissolved solids test were performed for the prefiltered sludges according to the procedures defined in Standard Methods (18). This was because certain metal plating waste solutions contain large dissolved solids levels such that over 60% of the total solids may be in a dissolved state. Thus, it was felt that dissolved solids must be corrected for in each sludge sample.

Following the completion of filtration rate studies, the data collected was used to determine the specific resistance for each sludge according to the following equation:

$$r = \frac{2bPA^2}{c}$$

where

r = specific resistance (m/Kg)

b = slope t/V versus V plot (sec/m⁶)

t = time (sec)

V = filtrate volume (m³)

P = vacuum pressure (N/m²)

A = filtration area (m²)

c = filtrate viscosity assumed to be identical to water at 20°C
(N-sec/m²)

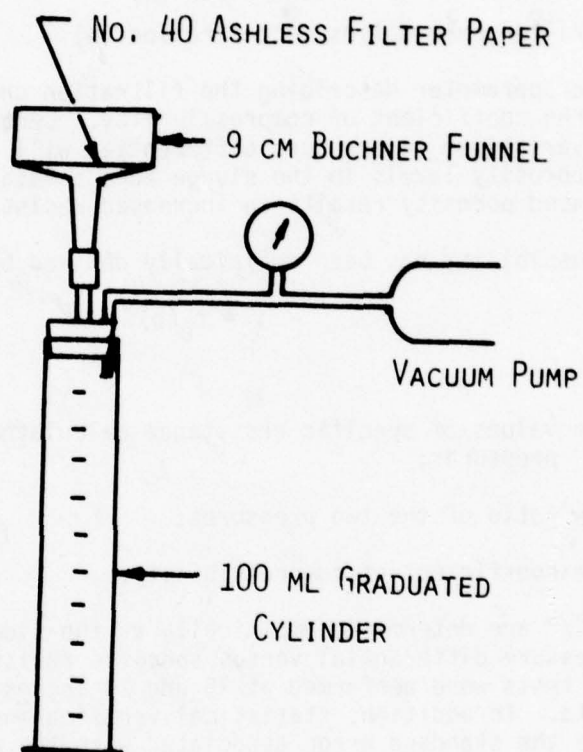


Figure (3). Laboratory filtration apparatus.

$$c = \frac{1}{\frac{100 - c_i}{c_i} - \frac{100 - c_f}{c_f}} \quad (\text{Kg/m}^3)$$

c_i = initial solids concentration (%)

c_f = filter cake solids concentration (%)

Another parameter describing the filtration characteristics of a sludge is the coefficient of compressibility. Certain sludges when subjected to variations in pressure differential will deform, resulting in decreased porosity levels in the sludge cake strata near the filter medium. This decreased porosity results in increased resistance to flow.

Compressibility has been empirically defined by the equation

$$r = r_0(p)^s$$

where

r, r_0 = values of specific resistance calculated at two different pressures;

p = ratio of the two pressures;

s = coefficient of compressibility.

Values of "s" are determined empirically as the slope of a logarithmic plot of pressure differential versus specific resistance. In this study, filtration tests were performed at 15 and 20 inches Hg to obtain compressibility data. In addition, statistical verification studies were performed to estimate the standard error associated with the empirical determination of "s". Each sludge was tested alternately at 15 and then 20 inches Hg and, from each data-pair, a coefficient of compressibility was calculated. The results from one such study is shown in Figure 4. It can be seen that considerable error is associated with the determination of "s".

Filtrate quality obtained during dewatering was also a parameter which was investigated. Samples of the vacuum filtrate were taken following cake failure; only the last 50 ml of filtrate were used for testing. Initial filtrate quantities were not considered truly reflective because the cake structure may not be fully developed during the initial stages of filtration. Each sample was analyzed for turbidity using a Hach 2100 Turbidimeter*. In cases of high filtrate turbidity, suspended solids tests were performed. Suspended solids testing was not done on all filtrate samples since most has residual turbidities less than 10 FTU. In this range, the suspended solids test was found to be inadequate.

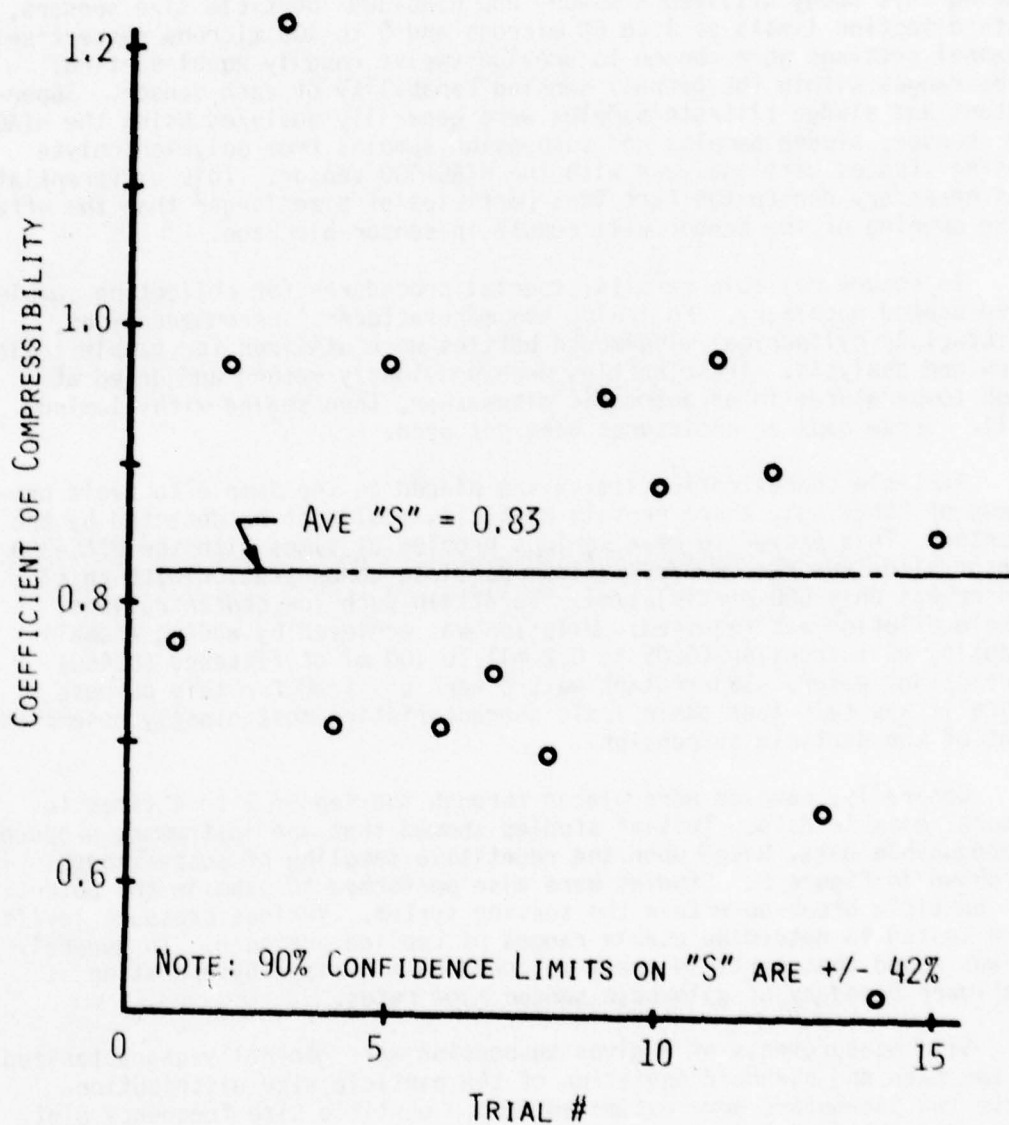


Figure (4). Results of studies examining the statistical error of "S", the coefficient of compressibility.

2. Particle Size Measurements

Through the course of this investigation, particles and their characteristic size distribution were an important consideration. For this study, a HIAC-320 • 12-channel particle size analyzer was utilized. Analysis during this study utilized HIAC-60 and HIAC-300 particle size sensors, with detection limits of 1 to 60 microns and 5 to 300 microns respectively. Channel settings were chosen to provide twelve roughly equal particle size ranges within the overall sensing capability of each sensor. Supernatant and sludge filtrate samples were generally analyzed using the HIAC-60 sensor; sludge samples and suspension samples from polyelectrolyte dosing studies were analyzed with the HIAC-300 sensor. This differentiation was necessary due to the fact that particles of size larger than the effective opening of the sensor will result in sensor blockage.

To ensure reliable results, special procedures for collecting samples were deemed necessary. Following the manufacturers' recommendations, flint-glass cylindrical wide-mouth bottles were utilized for sample collection and analysis. These bottles were previously washed and dried at high temperatures in an automatic dishwasher, then sealed with aluminum foil. Screw caps or enclosures were not used.

Particle concentration limits are placed on the sample to avoid problems of "shading", where certain particles would not be detected by the counter. This proved to be a serious problem at times with the HIAC-300 sensor since the recommended maximum particle concentration with this sensor was only 500 particles/ml. To attain such low concentrations, sample dilution was required. Dilution was achieved by adding a small quantity of suspension (0.05 to 0.2 ml) to 100 ml of filtered (0.45u) supernatant water. Supernatant waters were utilized for this purpose since it was felt that their ionic characteristics most closely resembled that of the particle suspension.

Generally, samples were placed through the sensor 2 to 4 times to ensure reliable data. Initial studies showed that the instrument produced reproducible data, based upon the repetitive sampling of suspensions, as shown in Figure 5. Studies were also performed to examine the potential for particle break-up within the sensing system. Various pressure levels were tested to determine usable ranges of applied pressure. In general, it was found that particle break-up could be minimized by operating at the lower boundary of allowable sensor flow rates.

Size measurements of a given suspension were generally characterized by the mean and standard deviation of the particle size distribution. These two parameters were estimated from a particle size frequency plot. Size distribution plots were also made showing the relative fractions of particles present in different size ranges.

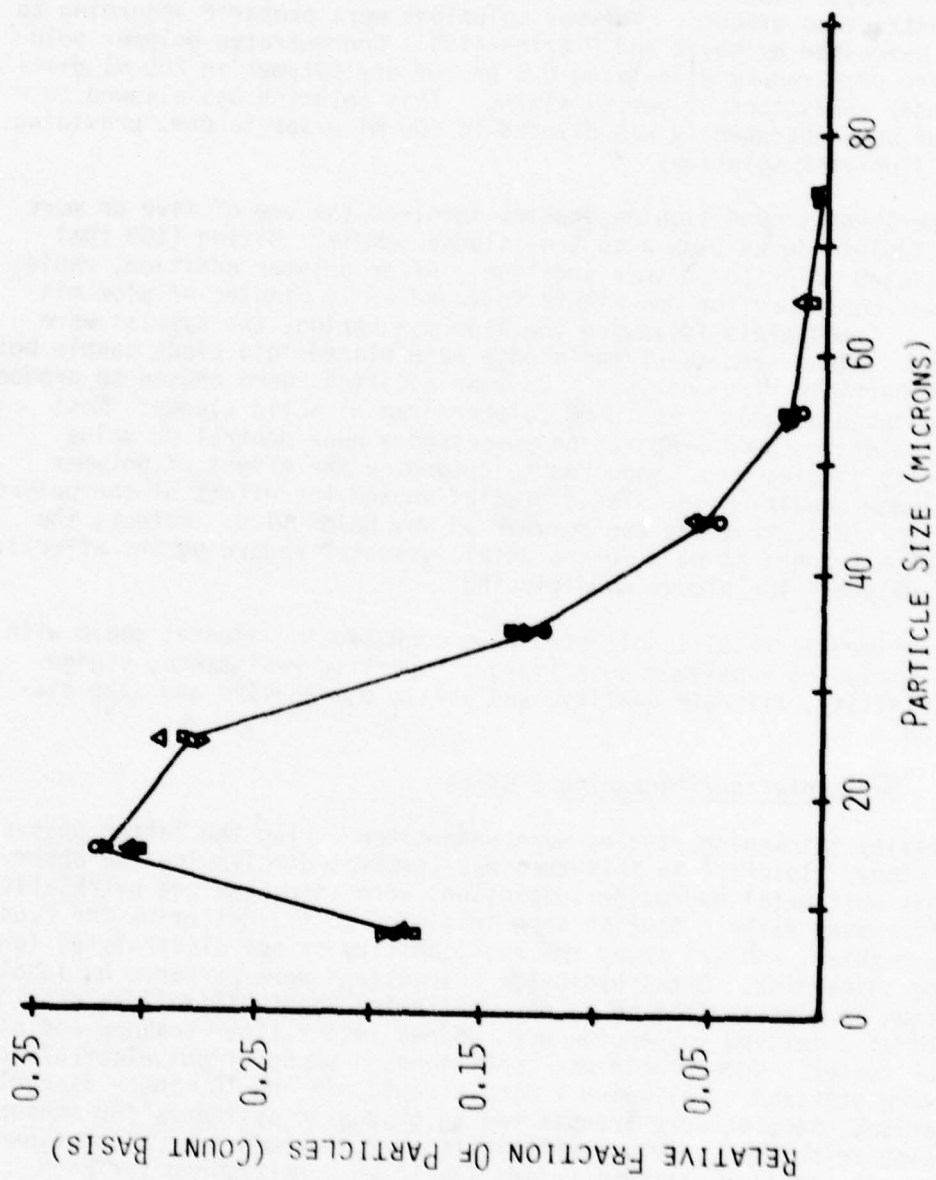


Figure (5). Replicate sampling of a particle size distribution using the HIAC particle counter.

3. Sludge Conditioning Studies

Only synthetic polyelectrolytes were examined for metal hydroxide sludge conditioning. Since a major goal was the ultimate resolubilization and extraction of metals, the incorporation of iron or aluminum through inorganic sludge conditioning may lead to unnecessary cation contamination of the extraction process. Polymer solutions were prepared according to methods described by Novak and O'Brien (19). Concentrated polymer solutions were prepared by dissolving 0.5 gr. of dry polymer in 200 ml distilled water under conditions of vortex mixing. This solution was allowed to mix overnight and subsequently was diluted to 500 ml prior to use, providing a 1 mg/ml polymer solution.

Experimental conditioning studies involved the use of five or more polyelectrolyte doses plus a control sludge sample. Mixing (150 rpm) was initiated prior to polymer addition. After polymer addition, rapid mixing was continued for one minute followed by 10 minutes of slow mix (30 rpm). Immediately following the slow-mix period, the samples were dewatered. Also, samples of the sludge were placed into clean sample bottles for particle size analysis. Polymer additions were chosen to produce a dosing range between 0 to 10 mg polymer/gram of solid sludge. Most polymer solutions upon preparation possessed a near neutral pH value. Preliminary studies were conducted to determine the effect of polymer pH on sludge conditioning. These studies showed the effect of the polymer pH to be minimal, provided the polymer pH was below 11.0. Rather, the sludge pH was found to be a more crucial parameter regarding the effectiveness of polymers for sludge conditioning.

Experimental results collected from conditioning studies dealt with several variables - polymer dose (mg/gr), specific resistance, sludge compressibility, filtrate quality, and particle mean size and size distribution.

4. Sedimentation/Thickening Studies

Gravity thickening studies were undertaken during the latter phases of the study. Interest in this area was stimulated following the observation that most metal hydroxide suspensions were characterized by relatively slow thickening rates. Studies were initiated to (1) determine the cause of this problem, and (2) study the applicability of polyelectrolytes for improved thickening. Metal hydroxide suspensions were prepared by insolubilization at a prescribed pH value. Following insolubilization, equal aliquots of a settled suspension were poured into 1 liter beakers and placed on a jar tester. Under rapid mix conditions, a range of polyelectrolyte doses were utilized. Following 1 minute rapid mix and 10 minute flocculation periods, samples were transferred to graduated cylinders for measuring thickening velocities. Interface heights were determined as a function of time. In addition, initial solids levels were determined for each suspension. Samples of each suspension were likewise stored for future particle size analysis. Thickening data was collected over a 90 minute

period, except in cases of dilute suspensions which settled much faster.

Data collected from these studies were analyzed by plotting interfacial settling velocity curves. The zone settling velocity was estimated from the straight-line portion of each settling curve. Comparison of settling velocities showed the effect of polyelectrolyte dosing.

C. Filtration Studies

1. Samples

Several samples of OC-ALC anion and cation regenerant wastes were evaluated at the University of Missouri. The results of analyses on these samples are summarized in Appendix A. It is clear from these data that the ion exchange operation at OC-ALC is inefficient with respect to column utilization and regeneration. The major problems seem to be associated with:

- (1) Using the columns for the treatment of both makeup and rinse water
- (2) Inefficient water/resin contact

These areas are more fully discussed in Appendix A. Based on these findings it was obvious that the bench scale filtration studies would have to be accomplished using a simulated sample if excessive delays in data collection were to be avoided. In this regard the University of Missouri investigating team and the Air Force program manager jointly agreed to generate the required data based on representative simulated samples. The derivation of the basic sample composition is summarized in Appendix B. Table 2 outlines the resultant composition which formed the basis for generating samples during the filtration and recovery studies.

It should be noted that only the cation exchange regeneration waste was simulated since from initial results it became apparent that comparative recovery of chromium directly from the anion exchange regenerant would be more economical than mixing the two wastes followed by recovery of all metals separately.

2. Dual Media Filtration Studies

Studies were conducted to determine if suspended metal hydroxides could be effectively removed by conventional filtration and to attempt to define the optimum operational conditions for filtration. It is expected that filtration will be necessary to "polish" the effluent from the metal precipitation process so that this water can be reused in the plating operation. A stock metal hydroxide suspension was prepared from a mixed metal solution containing 1200 mg/l nickel, 240 mg/l zinc and 60 mg/l copper by precipitating the metals by NaOH addition at pH 10.5. This mixed metal composition was believed to be representative of the "carry over" from a metal precipitation process and would represent the feed

TABLE 2. COMPOSITION OF SYNTHETIC WASTE

Element	meq/l	mg/l
Cd	0.3	18.5
Ni	59.9	1550.0
Cr	5.3	91.0
Cu	4.1	129.0
Fe	10.4	191.0
Zn	8.6	279.0
Ca	4.9	97.0
Mg	3.3	40.4
	95.8 meq/l	

solution which would require filtering. The stock suspension was then diluted by tap water addition to yield a turbidity of either 10 NTU or 25 NTU. The pH was approximately 8.6. A summary of standard operational parameters is included in Table 3.

The filter which was used in this study is shown in Figure 6. The filter media consisted on 18.5 inches of anthracite (effective size 0.7 mm, porosity 0.55) on top of 10 inches of sand (effective size 0.5 mm, porosity 0.42). The intermixing of media was minimal after several backwashes. The clean bed head loss at different flow rates is shown in Figure 7.

3. Diatomaceous Earth Filtration

Laboratory scale diatomaceous earth filters were designed and constructed for use in this study. The precoat filter cell as shown in Figure 8 uses a 2-inch septum. The flow scheme under the three modes of pumping, during each cycle, namely precoat, filtration, and backwashing, are shown in Figure 9. A representative mixed metal hydroxide suspension, identical to that used in dual-media filter studies was employed. Studies were conducted at three rates of filtration, namely 0.5, 0.75 and 1.0 gpm/ft². In order to determine the effect of precoat grain size, several different DE sizes were employed in the precoat.

D. Solvent Extraction

1. Method Verification and Percent Extraction Curves

In this study five metals were considered for recycling from electroplating waste streams. These were nickel, copper, chromium, cadmium, and zinc. The preliminary work included method verification and calculation of extraction curves for each of the seven chelates listed in Table 4. This preliminary work was conducted using solutions containing only the above five elements. These were made by taking the appropriate dilution of 1 mg/ml commercial Fisher standard solutions of each element. These standards were prepared by the Fisher Scientific Company with the following chemicals: (1) Cr - potassium dichromate in distilled water (2) Cd - cadmium metal in dilute nitric acid (3) Cu - copper oxide in dilute nitric acid, (4) Zn - zinc oxide in dilute nitric acid (5) Ni - nickel metal in dilute nitric acid. All dilutions were made with 1% nitric acid. All pH adjustments were made with sodium hydroxide or nitric acid. The organic solvent used for the extractions was chloroform. All chemicals used were ACS Reagent Grade.

The Extraction method used for most of the work consisted of shaking a solution of a particular chelate in chloroform (10 ml) with an equal volume of an aqueous phase containing the appropriate metals. This aqueous phase was adjusted, previous to the extraction, to the desired pH using either sodium hydroxide or nitric acid. This method, which used a new chloroform and aqueous phase at each desired pH, was termed "independent batch". The aqueous and organic

TABLE 3. OPERATIONAL PARAMETERS FOR
THE DUAL MEDIA FILTER STUDIES

SPECIFICATION OF FILTER MEDIA

	Depth	Effective Size	Uniformity Coefficient
Anthracite	20 in	0.7 mm	1.3
Sand	12 in	0.5 mm	1.2

METALS CONCENTRATION OF INFLUENT

	Stock Metal Hydroxide Suspensions	Dilute to 25 NTU	Dilute to 10 NTU
Nickel	1200 mg/l	120 mg/l	40 mg/l
Zinc	240 mg/l	24 mg/l	8 mg/l
Copper	60 mg/l	6 mg/l	2 mg/l

POLYMERS EVALUATED

Manufacturer Name	Type	Molecular Weight
Betz 1100	Anionic	5×10^6
Betz 1175	Cationic	1×10^4

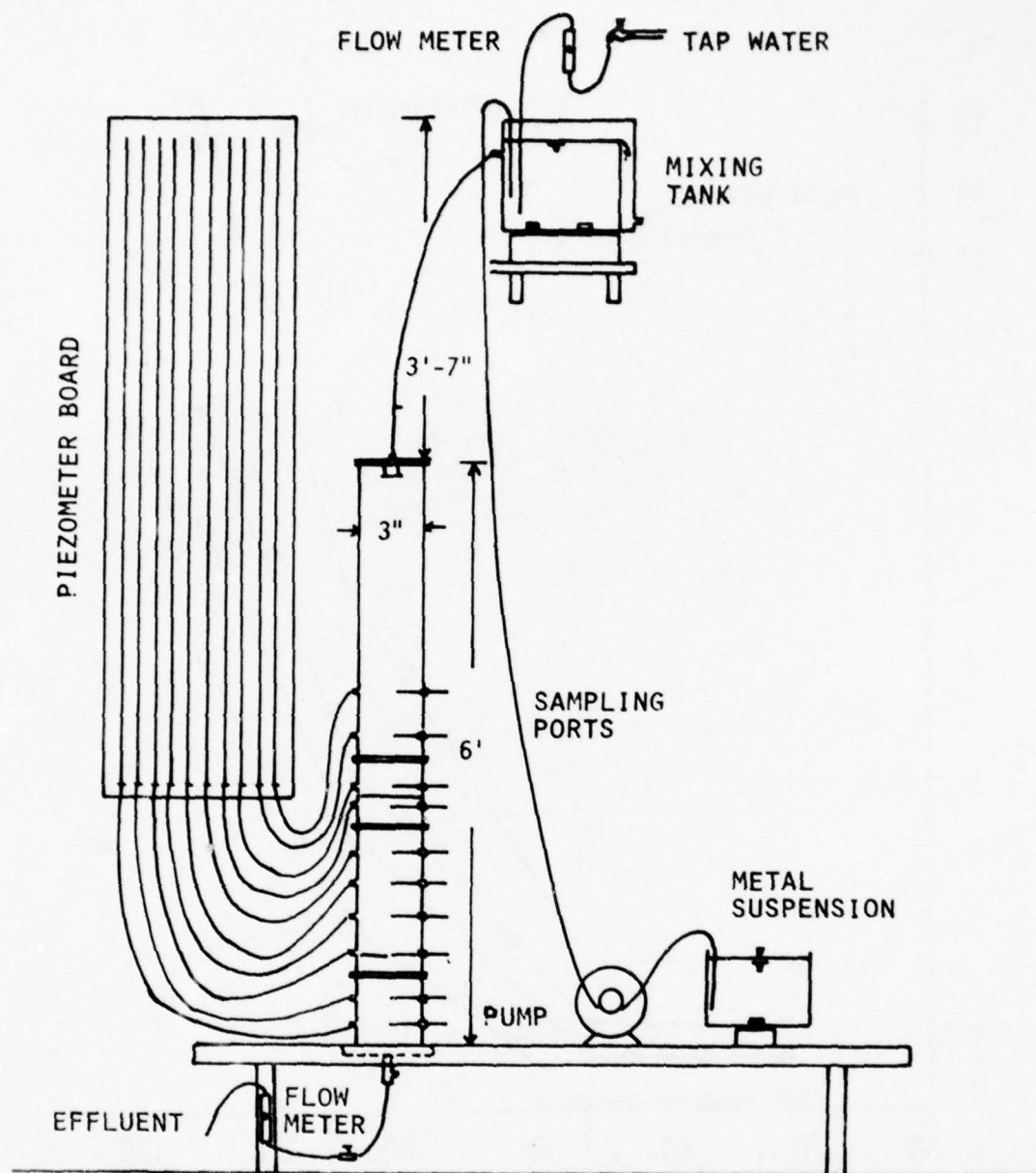


Figure (6). Gravity filter apparatus.

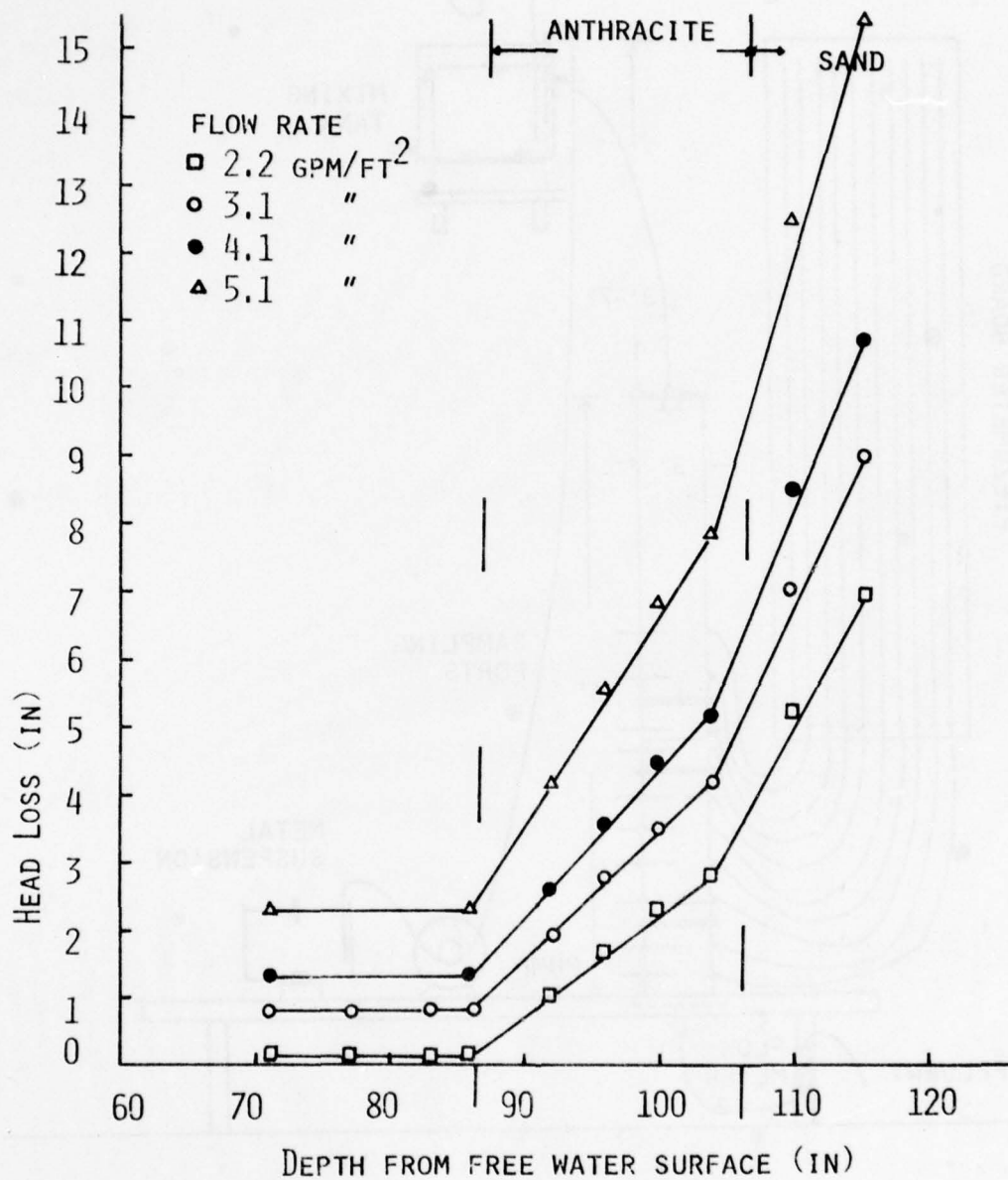
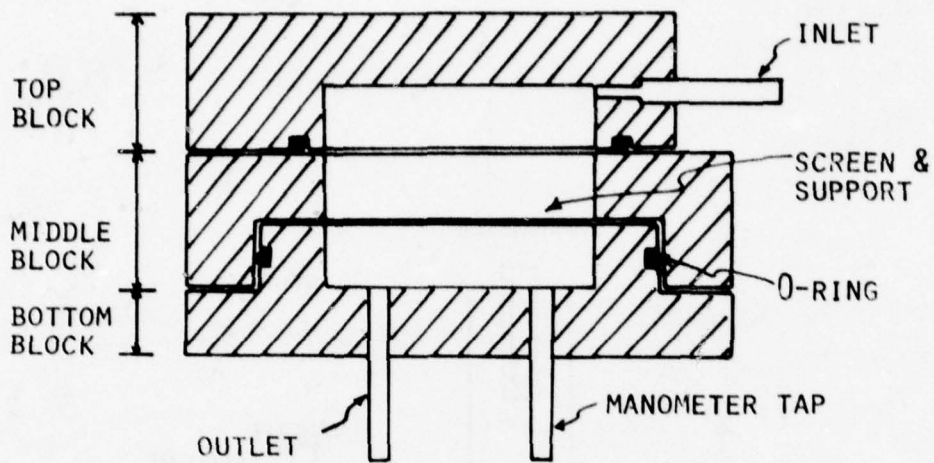
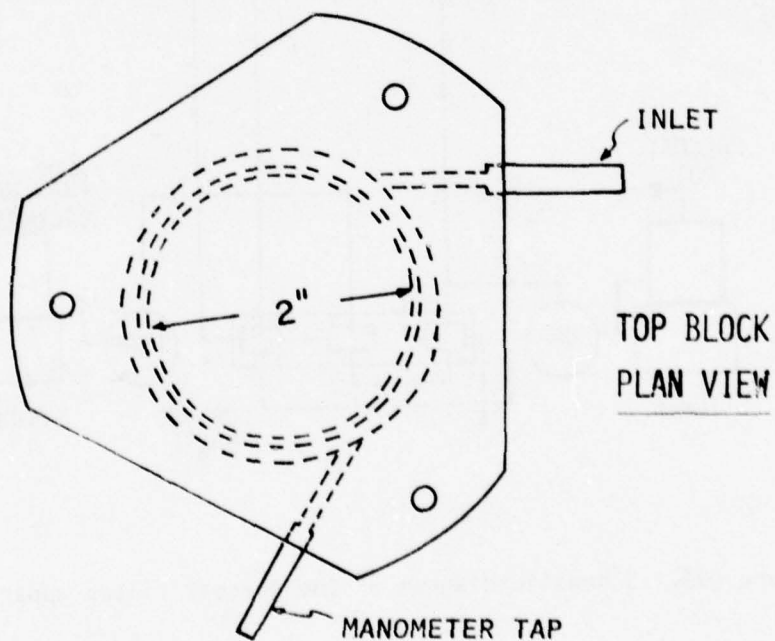


Figure (7). Clean bed head loss.



FILTRATION CELL SECTIONAL VIEW



TOP BLOCK
PLAN VIEW

Figure (8). Precoat filter cell assembly.

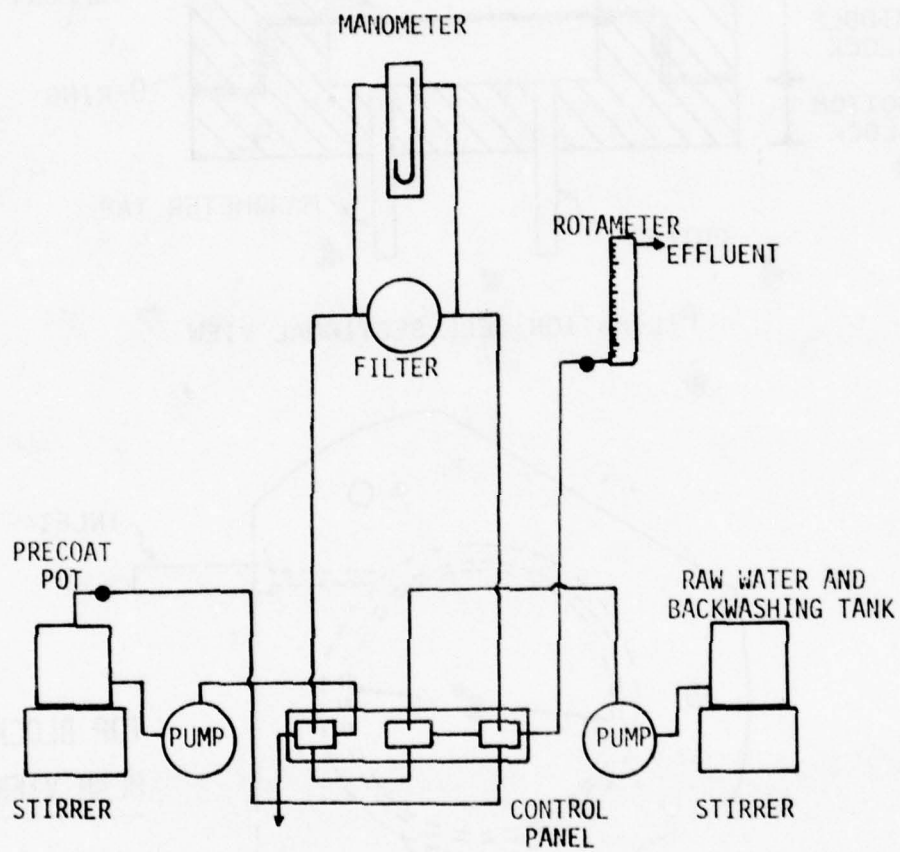


Figure (9). Schematic diagram of the precoat filter apparatus.

TABLE 4
LIST OF THE SEVEN CHELATING COMPOUNDS EVALUATED

<u>Chelating Agent</u>
Thenyltrifluoroacetone
Acetylacetone
Benzoylacetone
Dithizone
Cupferron
Diethyldithiocarbamate
8-Hydroxyquinoline

phases were not mutually presaturated before equilibration; however, volume changes were negligible and were ignored. After shaking two minutes, the two phases were separated and the concentration of the metal in the aqueous phase was determined by atomic absorption using an Instrumental Laboratories 453 atomic absorption spectrophotometer*.

The data from these experiments were plotted on graphs showing the percent of metal extracted versus pH. Two typical graphs are shown in Figures 10 and 11. Figure 10 shows a chelate that produces good separation while Figure 11 shows one that does not.

The following calculation was used to obtain %E.

$$\%E = \frac{100 D}{(D + \frac{V_w}{V_o})}$$

where

$$D = \frac{\text{Activity organic phase}}{\text{Activity water phase}}$$

V_w = volume of water

V_o = volume of organic

Since most of the experiments used equal volumes of organic and water, the equation simplifies to

$$\%E = \frac{100 (A)_o / (A)_w}{(A)_o / (A)_w + 1} = \frac{100 (A)_o}{(A)_o + (A)_w} = \frac{100 (A)_o}{(A)_t}$$

where

$(A)_o$ = concentration in organic phase

$(A)_w$ = concentration in water phase

$(A)_t$ = total concentration present in all phases

The concentration in the water phase was obtained by direct analysis by atomic absorption. The total concentration present in all phases was determined by direct analysis of the water phase before extraction. The difference between the total and that in the water phase after extraction is assumed to be that in the organic layer.

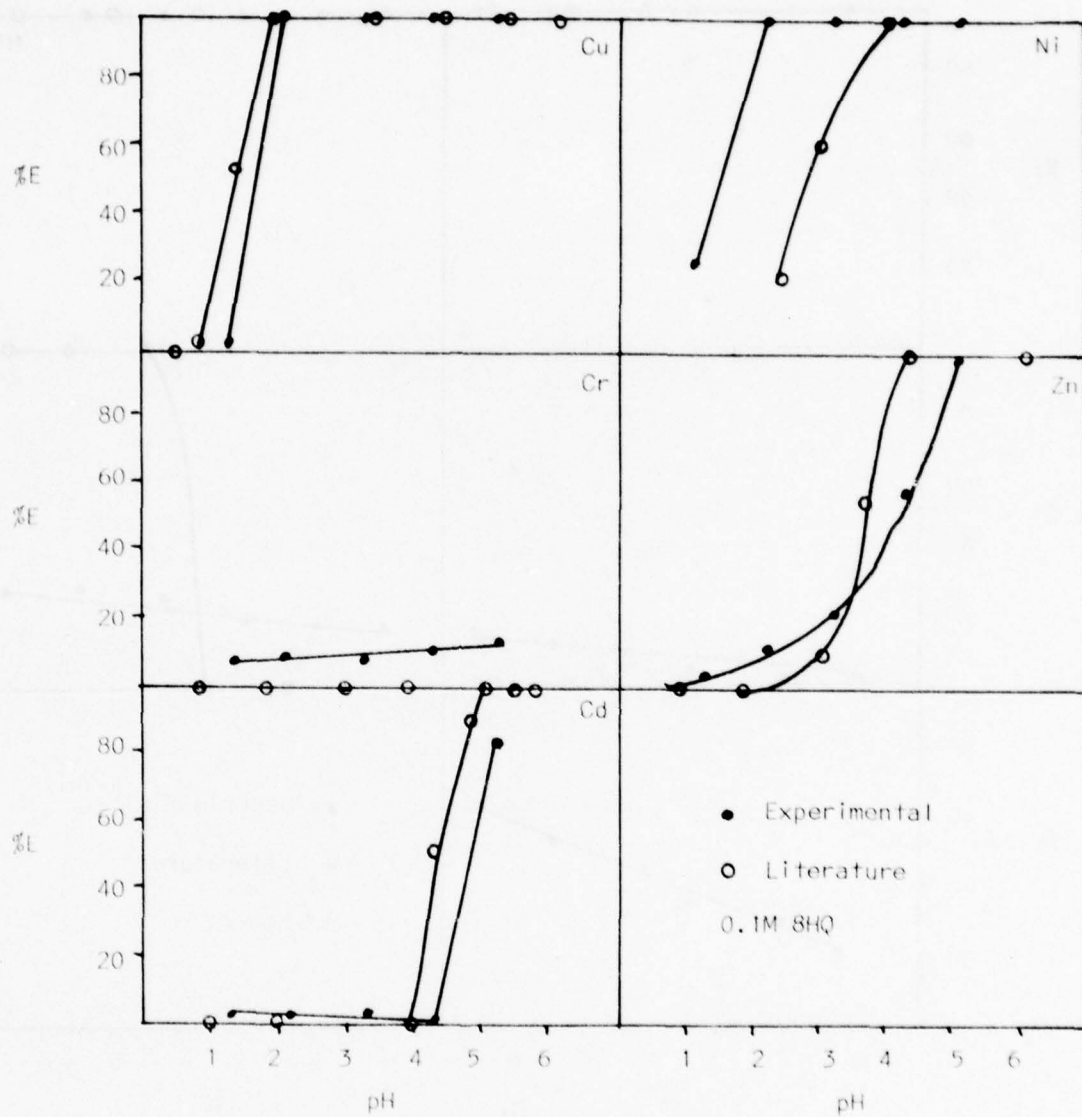


Figure (10). Percent extraction curve for 8HQ.

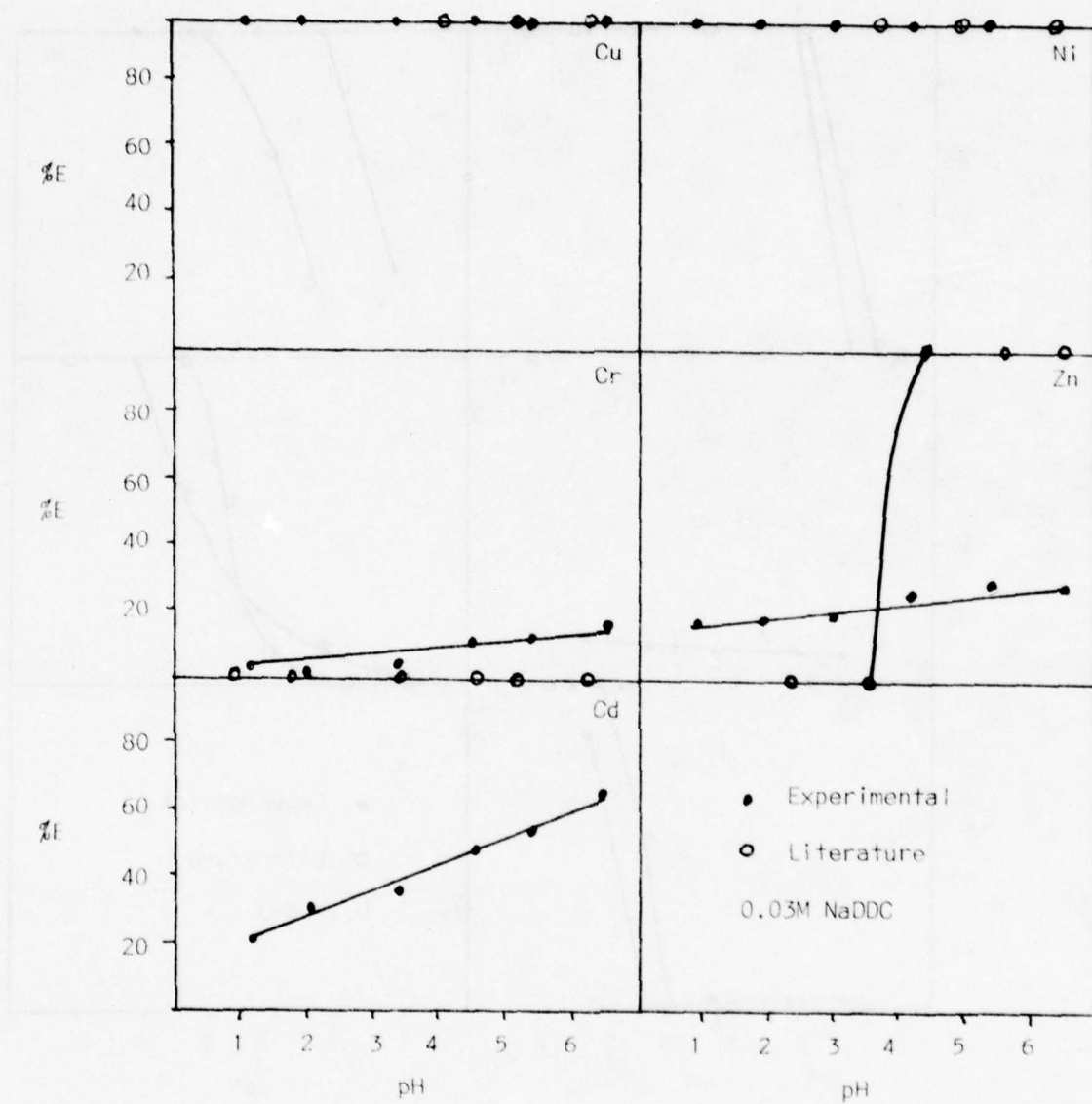


Figure (11). Percent extraction curve for NaDDC.

2. Separation Scheme Determination

During this part of the study various chelates were tested in a sequential extraction scheme in order to obtain a clean separation of each metal. For this study a synthetic regenerate sample was used. This was prepared by dissolving: (1) 0.05g cadmium nitrate, (2) 1.55g nickel metal, (3) 0.7g chromium nitrate, (4) 0.13g copper metal, (5) 0.92g iron (III) chloride, (6) 0.28g zinc metal, (7) 0.27g calcium chloride, and (8) 0.04g magnesium metal. After dissolving, the solution was diluted to one liter with 0.6M hydrochloric acid.

The extraction method consisted of shaking a solution of a particular chelate in chloroform (10 ml) with an equal volume of an aqueous phase containing the regenerate solution adjusted to the proper pH with sodium hydroxide or hydrochloric acid. After shaking two minutes, the two phases were separated and an aliquot was taken from the aqueous phase for analysis. The aqueous phase was then transferred to the next solution of a chelate in chloroform. This procedure was followed through the total number of chelates in the scheme. The data from these experiments were used to calculate the %E as described previously.

The analysis of the aqueous phase was done using a Jarrel-Ash Model 975 Plasma Atomcop®, an inductively coupled argon plasma spectrometer. This instrument could simultaneously analyze for all of the elements present in the synthetic regenerate.

In some cases the regenerate was spiked with cadmium, chromium, or copper.

3. Pilot Plant

For the experiments using the pilot plant, the synthetic regenerate described above was used. For one run, the nickel level was decreased while the other metal concentrations remained the same.

In the pilot plant, a series of 500 ml Kimax Conical Beakers®, with a side arm midway down the beaker, served as the extraction vessels. As can be seen in Figure 12, the synthetic regenerate solution is put in a large storage reservoir where the pH is then adjusted. The regenerate is then gravity feed to the first extraction vessel which contains 150 ml of chloroform and the desired chelate. The two phases are then mixed with a stirring bar and magnetic stirring unit. The initial mixing time was two minutes, but later it was found that this had to be increased to 20 minutes. The two phases were allowed to separate. The clamp on the side arm tubing was then opened and the water layer was transferred to the next extraction vessel, again by gravity feed. This process can

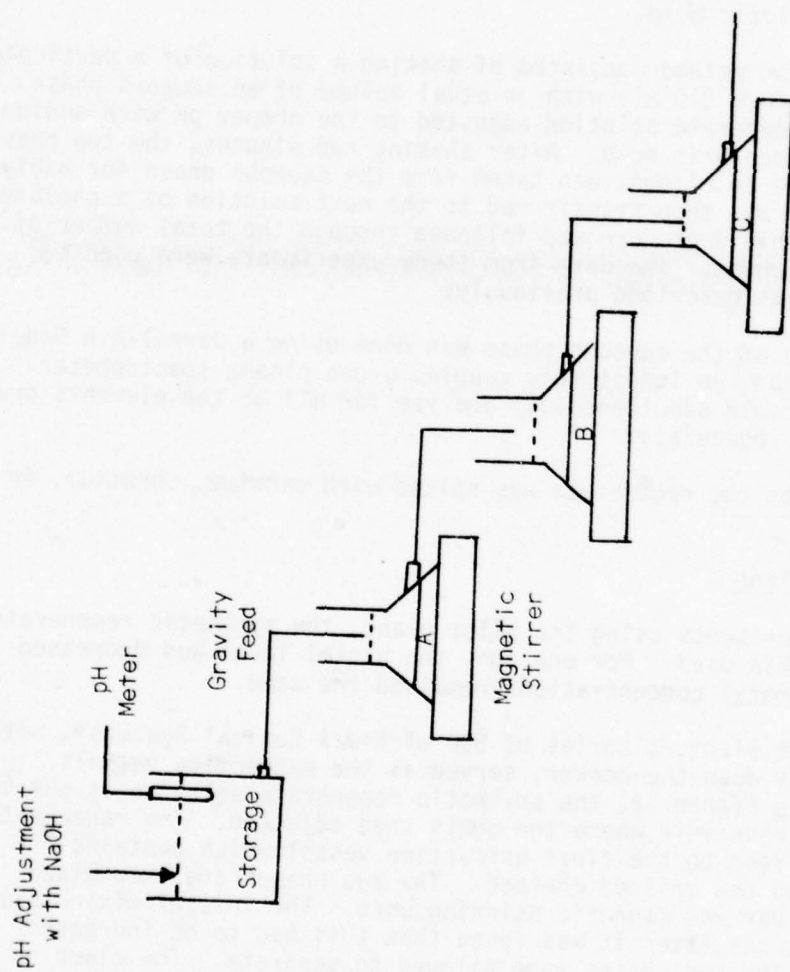


Figure (12). Pilot plant design.

be carried out for as many extraction steps as are in the separation scheme. After the extractions were completed the organic phases were shaken with 2.4M HCl and the metals stripped.

The analysis of the aqueous and stripping phases were done using the inductively coupled plasmas described previously. The data were again used to calculate the %E as previously described.

SECTION III

RESULTS AND DISCUSSION

A. Metal Insolubilization Studies

1. Individual Metal Systems

In Figures 13 through 17 the results of studies related to the insolubilization and precipitation of various plating metals from solution are presented. In general, the concentration of each metal remaining in the supernatant following a one-hour sedimentation period is in good agreement with that predicted by equilibrium chemistry. The discrepancy between measured copper concentrations and those predicted by equilibrium chemistry may be the result of experimental limitations. The minimum theoretical solubility for copper is approximately $10^{-8}M$; however, the atomic absorption spectrophotometer used for this study had a minimum detection limit of approximately $10^{-6}M$ for copper. Thus, the copper concentrations reported in the pH range 8.5 to 10.5 may in fact be much higher than the actual concentrations present in the supernatant liquor.

Chromium was the only metal investigated which showed a marked variation from equilibrium chemistry predictions. Figure 13 clearly shows that higher chromium concentrations remain after sedimentation than would be expected from equilibrium considerations. Chromium suspensions were often characterized by relatively high residual turbidity levels (8 to 25 FTU) following a one-hour sedimentation period. Other metal hydroxide suspensions were found to settle to supernatant turbidity levels of 1 to 5 FTU. Also, it should be noted that the level of soluble chromium in the supernatant was always found to be below 0.5 mg/l in the pH range 6.5 to 10. Thus, it appears that the residual chromium is present in an insoluble, colloidal form.

In Figure 18 data is presented relating to the effect of pH on the residual turbidity and chromium levels remaining in the supernatant liquor after sedimentation. The data shown was obtained using chromium solutions containing no sulfates. The role of sulfates in chromium removal will be discussed in a later section. In general, these figures show efficient removal of both turbidity and chromium between pH 7.5 to 10.0. This is in agreement with the results of Thomas and Theis (20). Outside this pH range, the suspension appeared to be colloidal, exhibiting little or no settling over extended periods of time.

The size distribution of particles present in each chromium suspension as a function of insolubilization pH were determined. Results of particle size analyses are presented in Figure 19 showing the mean particle size of the suspension and the size distribution. Suspensions outside the pH range 7.5 to 10.0 are characterized by extremely small particles with

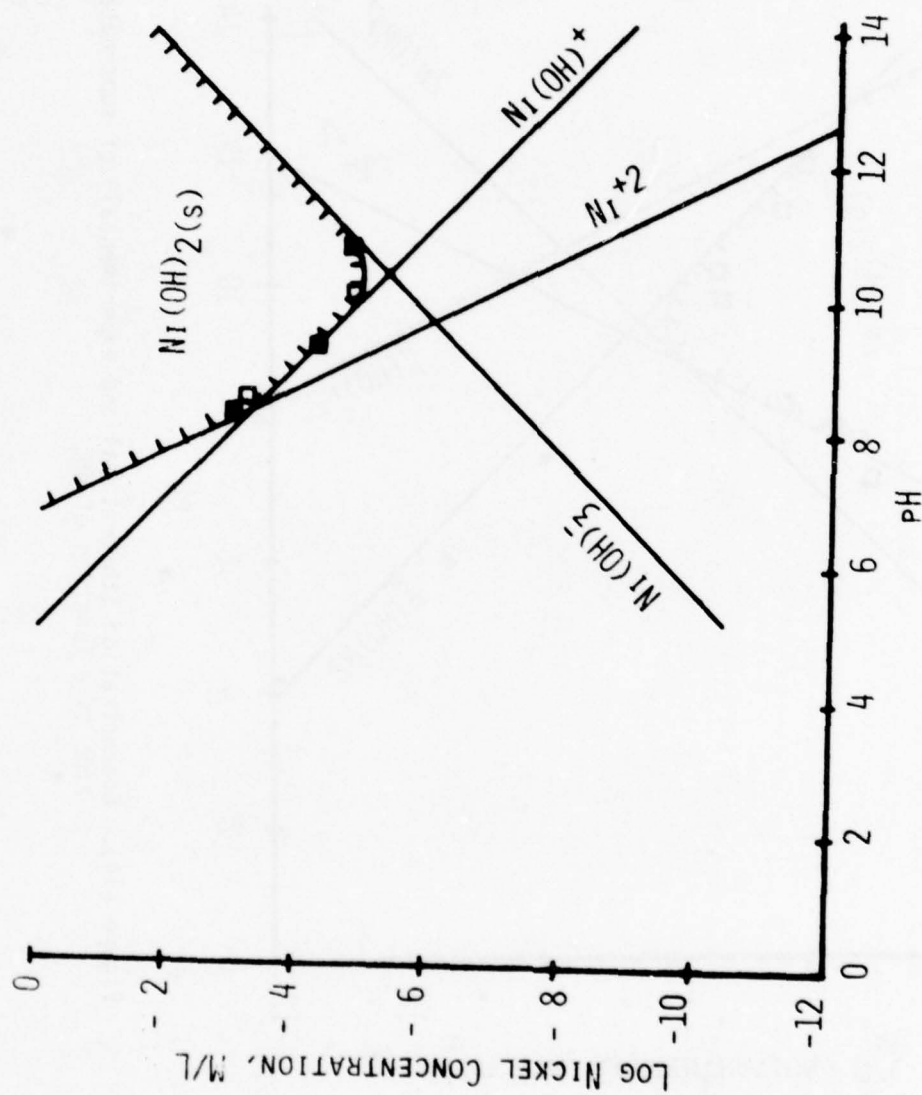


Figure (13). Concentration (theoretical and experimental) of supernatant nickel ion as a function of pH.

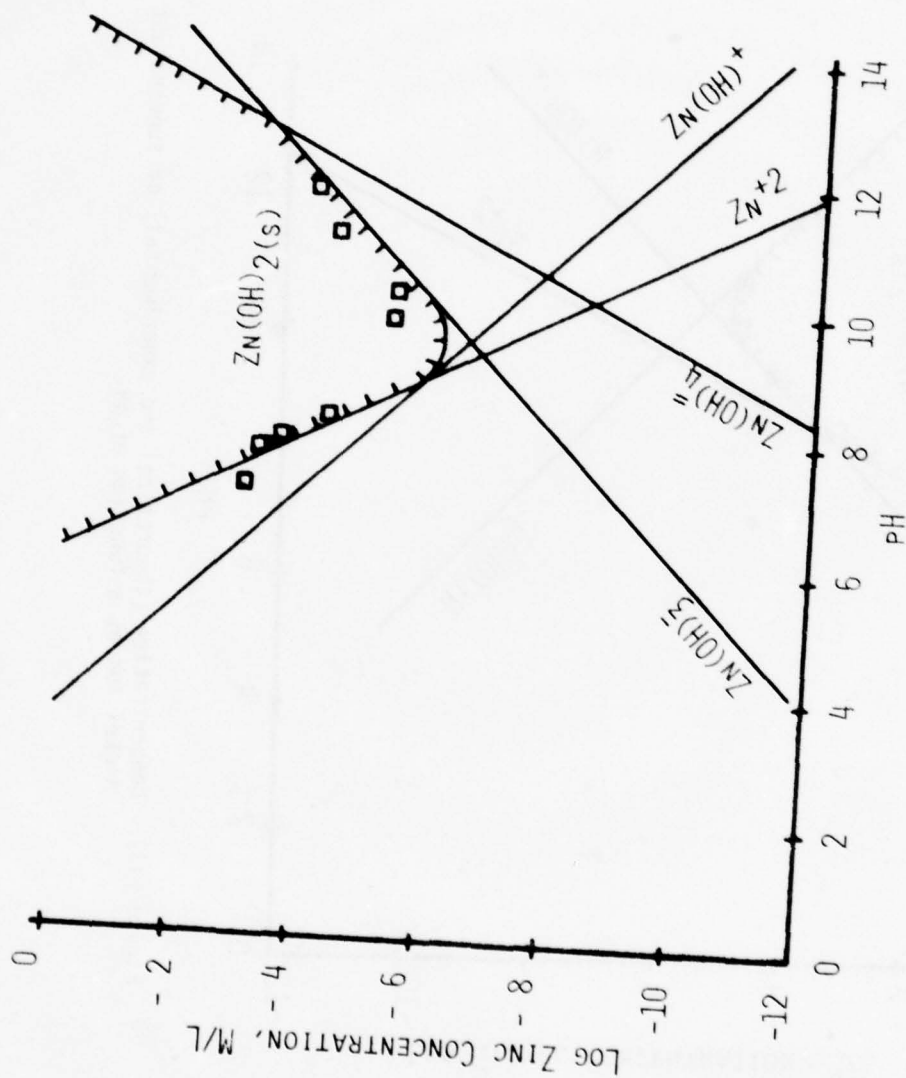


Figure (14). Concentration (theoretical and experimental) of supernatant zinc as a function of pH.

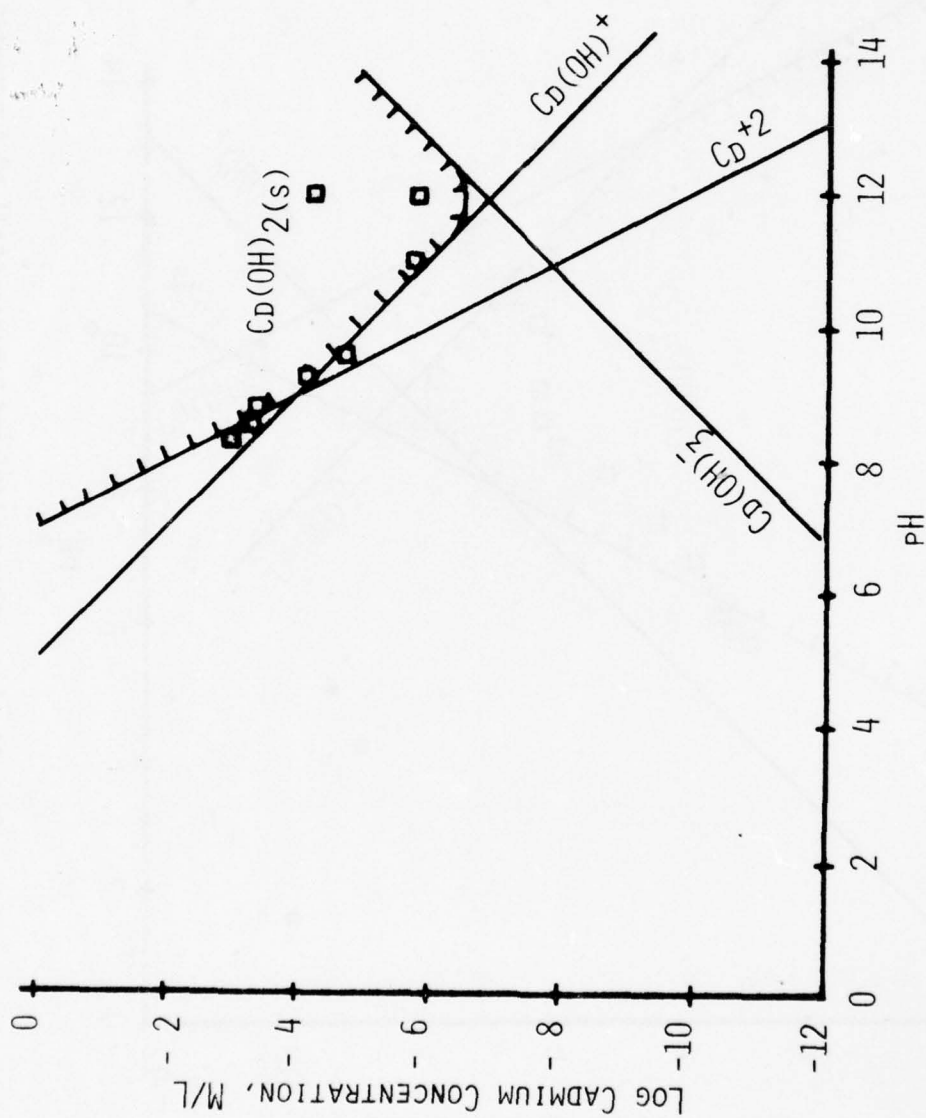


Figure (15). Concentration (theoretical and experimental) of supernatant cadmium as a function of pH.

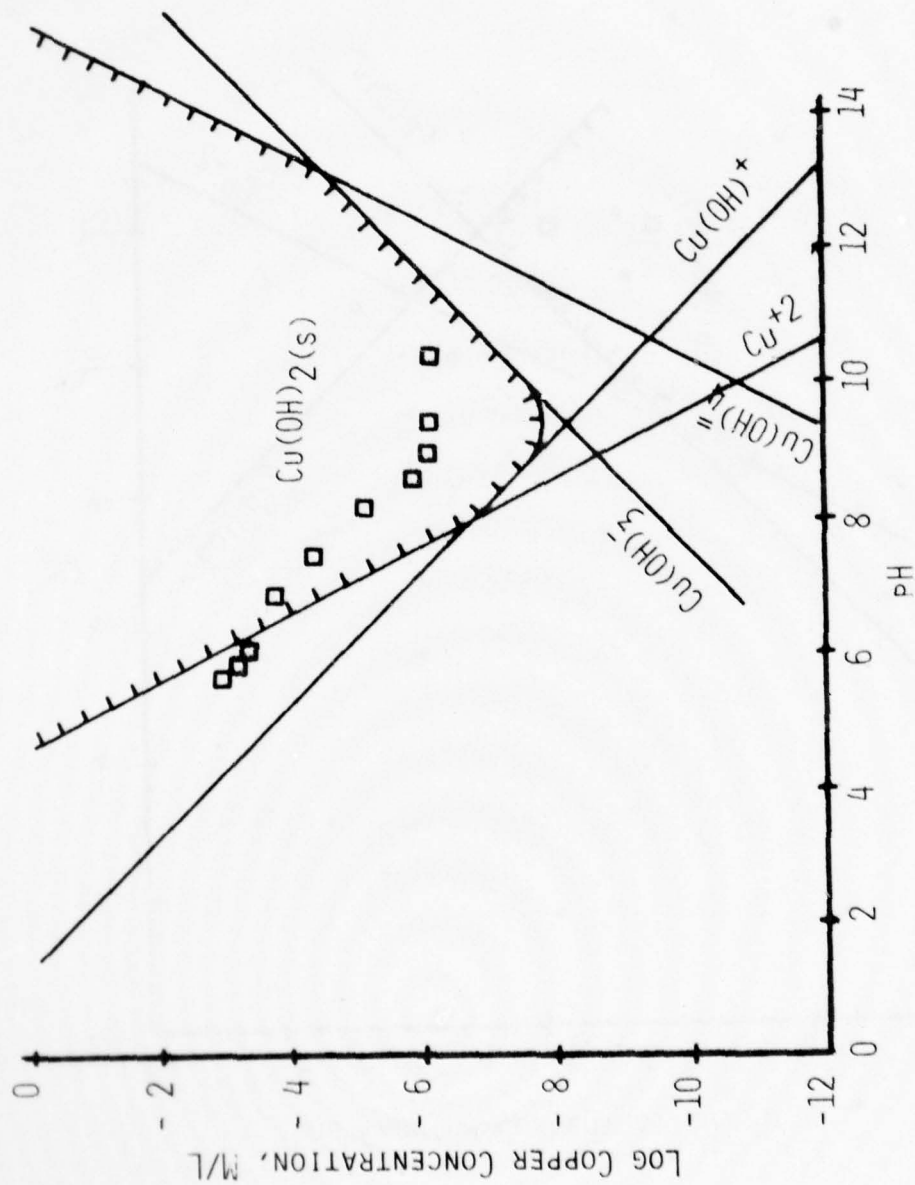


Figure (16). Concentration (theoretical and experimental) of supernatant copper as a function of pH.

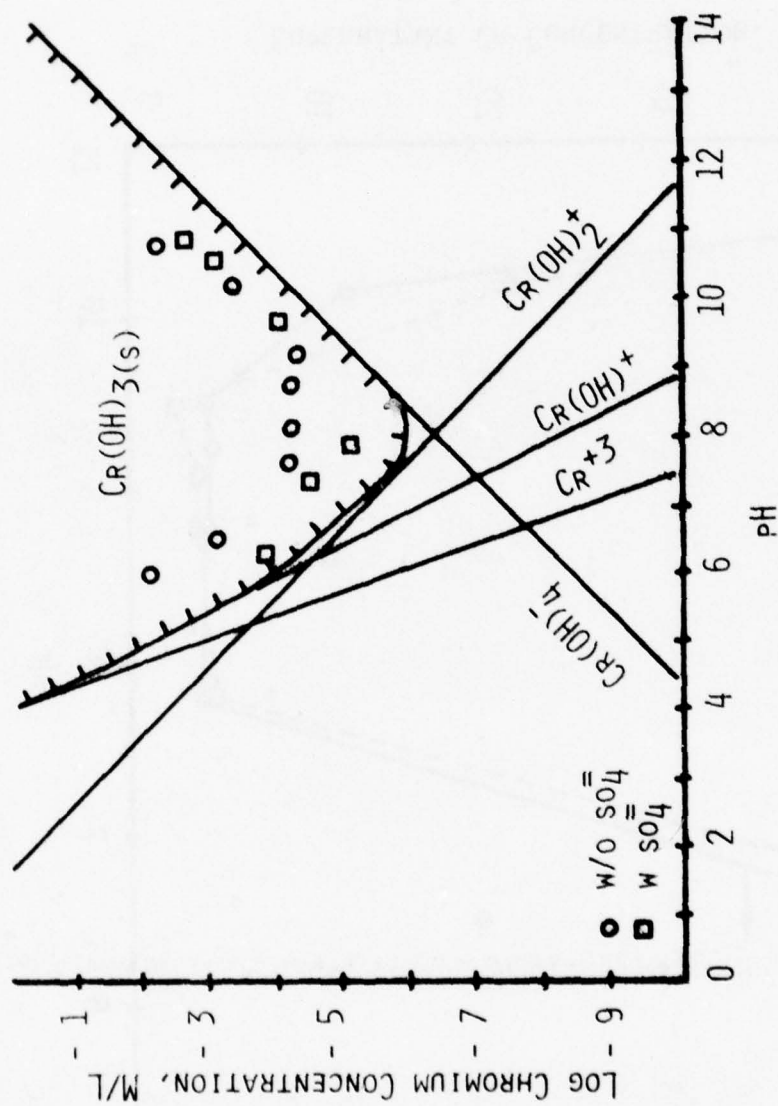


Figure (17). Concentration (theoretical and experimental) of supernatant chromium ion as a function of pH.

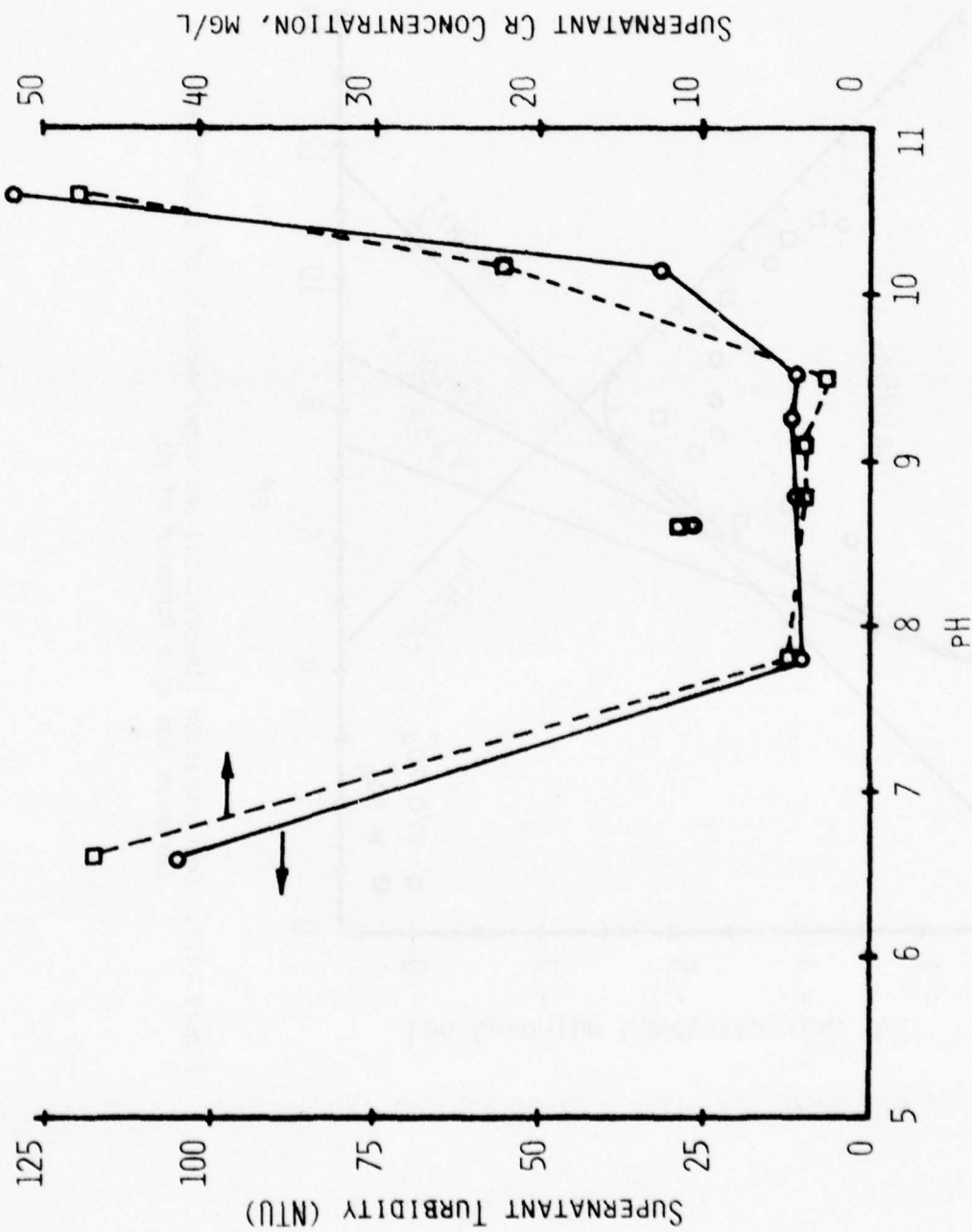


Figure (18). Supernatant chrome concentration and supernatant turbidity as a function of pH for a settled sample containing 130 mg/l Cr(III) initially.

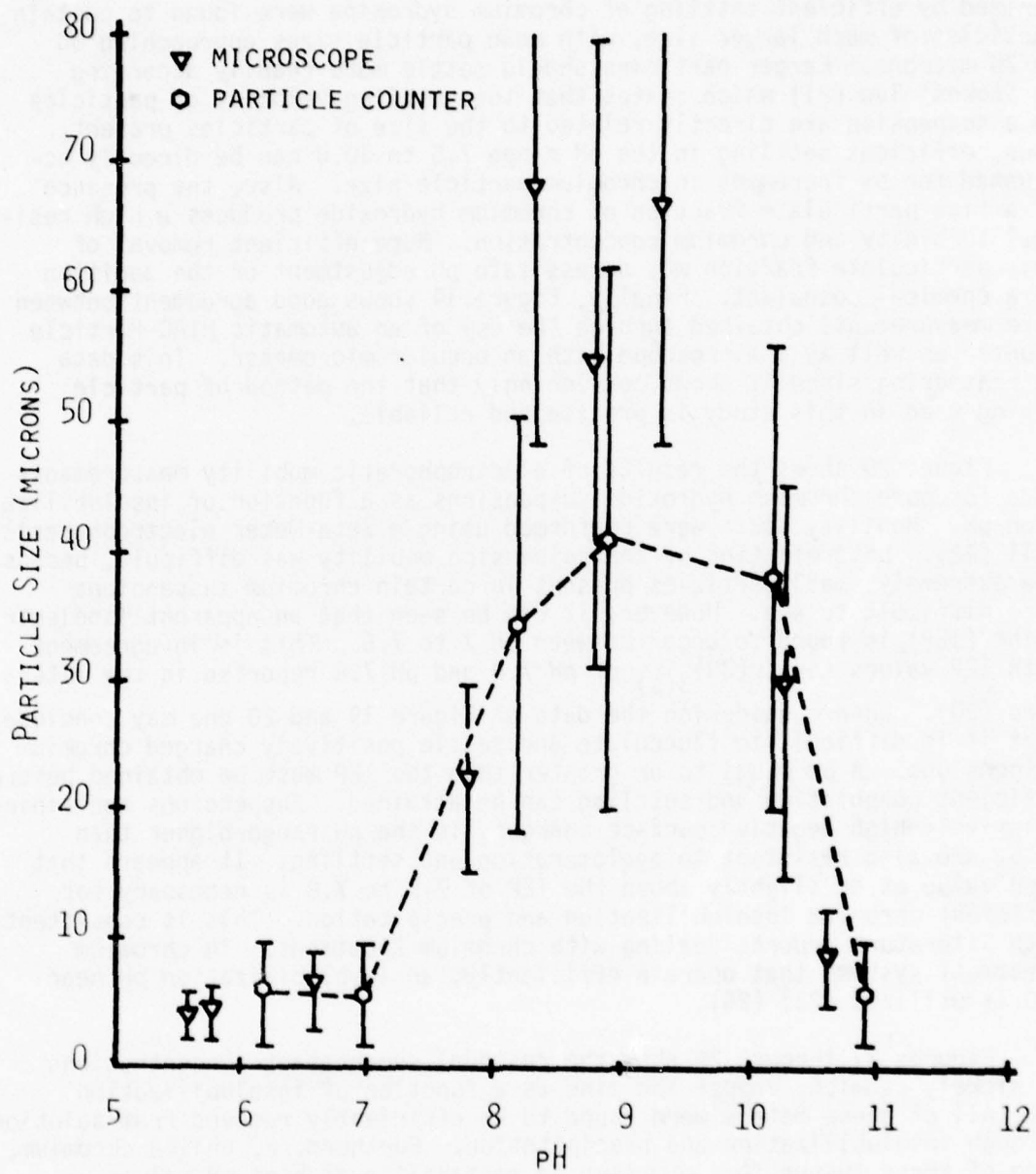


Figure (19). The characteristic size of chromium hydroxide flocs as a function of pH.

mean particles sizes between 3-8 microns. Suspensions which were characterized by efficient settling of chromium hydroxide were found to contain particles of much larger size, with mean particle sizes approaching 50 to 70 microns. Larger particles should settle more readily according to Stokes' law (21) which states that the settling velocity of particles in a suspension are directly related to the size of particles present. Thus, efficient settling in the pH range 7.5 to 10.0 can be directly accounted for by increases in chromium particle size. Also, the presence of a fine particulate fraction of chromium hydroxide produces a high residual turbidity and chromium concentration. More efficient removal of this particulate fraction may necessitate pH adjustment or the addition of a chemical coagulant. Finally, Figure 19 shows good agreement between size measurements obtained through the use of an automatic HIAC Particle Counter as well as a microscope with an ocular micrometer. This data is reassuring since it shows convincingly that the method of particle sizing used in this study is precise and reliable.

Figure 20 shows the results of electrophoretic mobility measurements made for pure chromium hydroxide suspensions as a function of insolubilization pH. Mobility tests were performed using a Zeta-Meter electrophoresis cell (22). Determination of the suspension mobility was difficult, because the extremely small particles present in certain chromium suspensions were difficult to see. However, it can be seen that an apparent isoelectric point (IEP) is found to occur between pH 7 to 7.5. This is in agreement with IEP values for $\text{Cr}(\text{OH})_3(\text{s})$ of pH 7.0 and pH 7.8 reported in the literature (20). When considering the data of Figure 19 and 20 one may conclude that it is difficult to flocculate and settle positively charged chromium suspensions. A pH equal to or greater than the IEP must be obtained before efficient coagulation and settling can be attained. Suspensions containing relatively high negative surface charges, in the pH range higher than 10.5, are also resistant to agglomeration and settling. It appears that a pH value at or slightly above the IEP of 7.5 to 7.8 is necessary for efficient chromium insolubilization and precipitation. This is consistent with literature reports dealing with chromium treatment. In chromium treatment systems that operate efficiently, an insolubilization pH near 8.0 is utilized (23) (24).

Figures 21 through 24 show the residual supernatant concentrations of nickel, cadmium, copper and zinc as a function of insolubilization pH. All of these metals were found to be efficiently removed from solution through insolubilization and precipitation. Furthermore, unlike chromium, none of these suspensions were seen to restabilize at high pH values. This may be because the IEP values for these metals occur at a higher pH than the IEP of chromium. Table 5 shows representative literature values for the IEP of each metal hydroxide under consideration; all fall within the pH range 9.5 to 11.0. Thus, the pH values used in this study may not have been sufficiently high to promote restabilization of these four metal hydroxide suspensions.

Changes were detected in the physical appearance of the copper

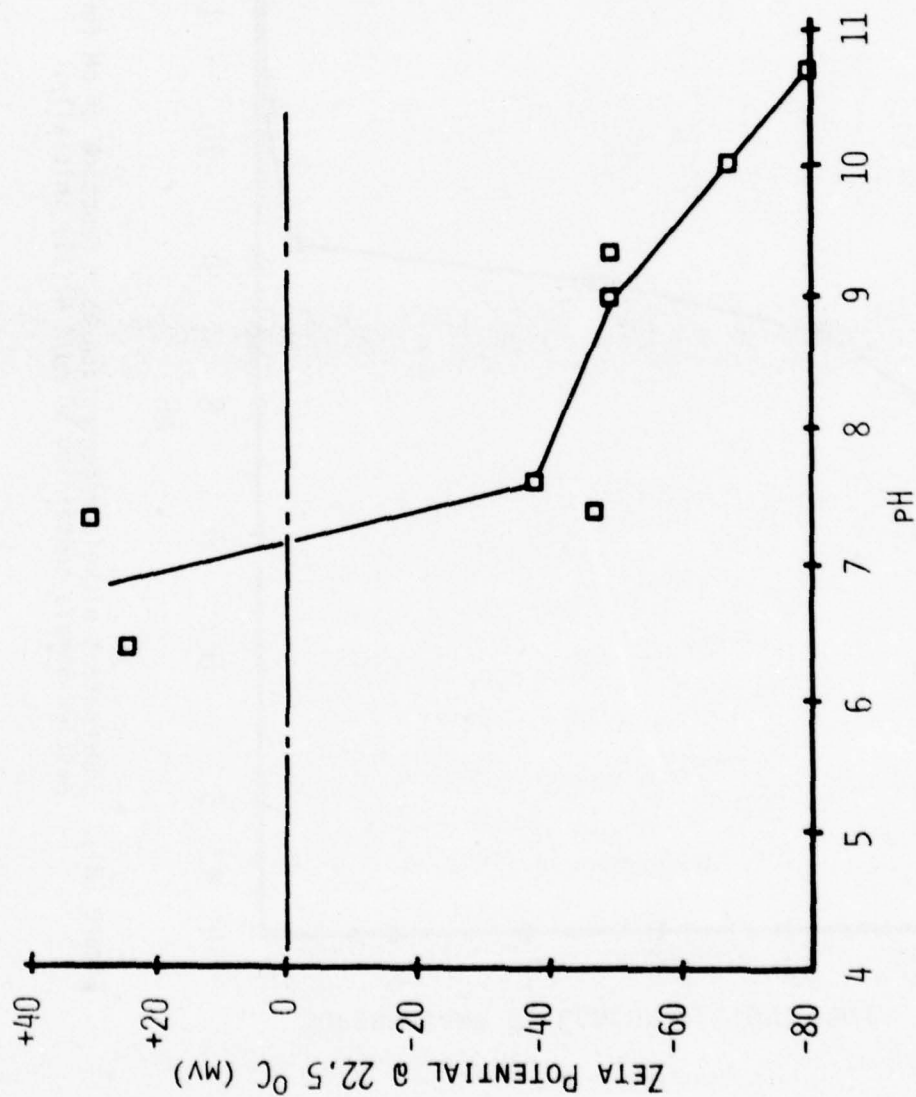


Figure (20). The characteristic surface potential of chromium hydroxide flocs as a function of pH (no sulfates present in solution).

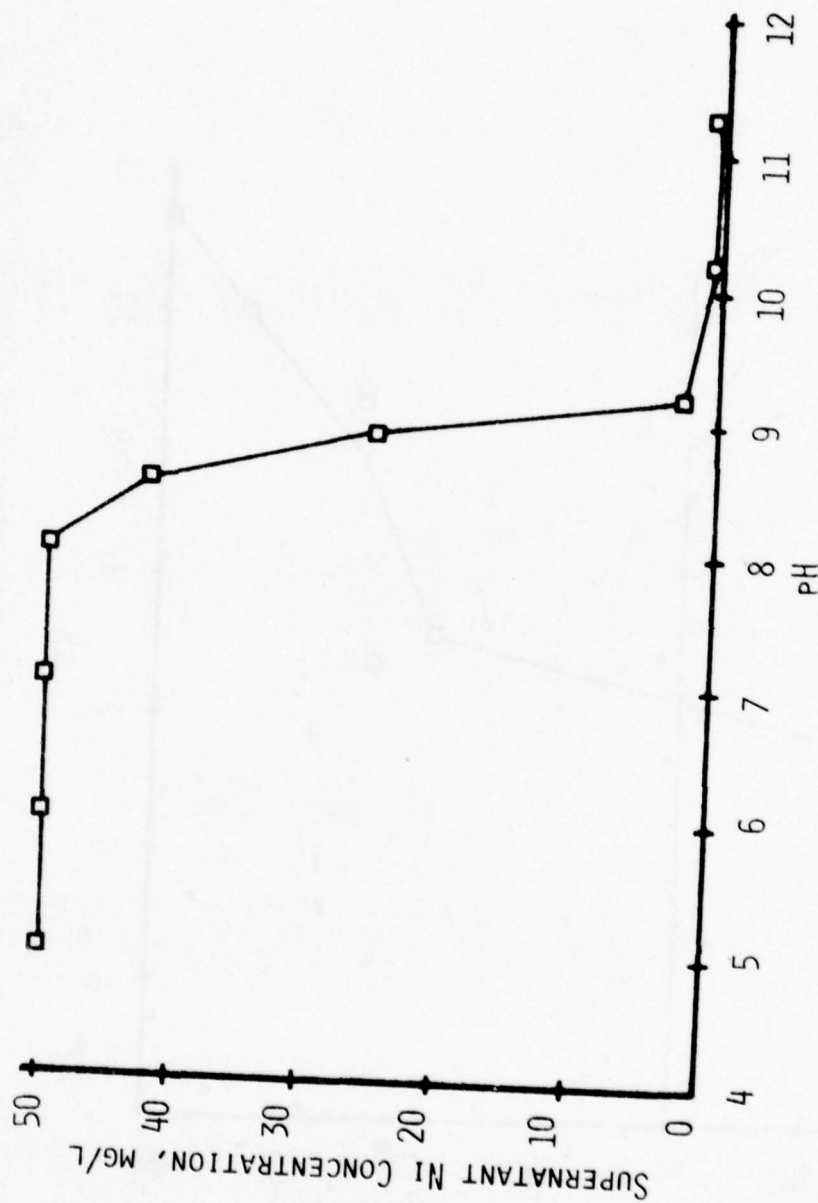


Figure (21). Supernatant nickel concentration as a function of pH for a settled sample containing 50 mg/l Ni(II) initially.

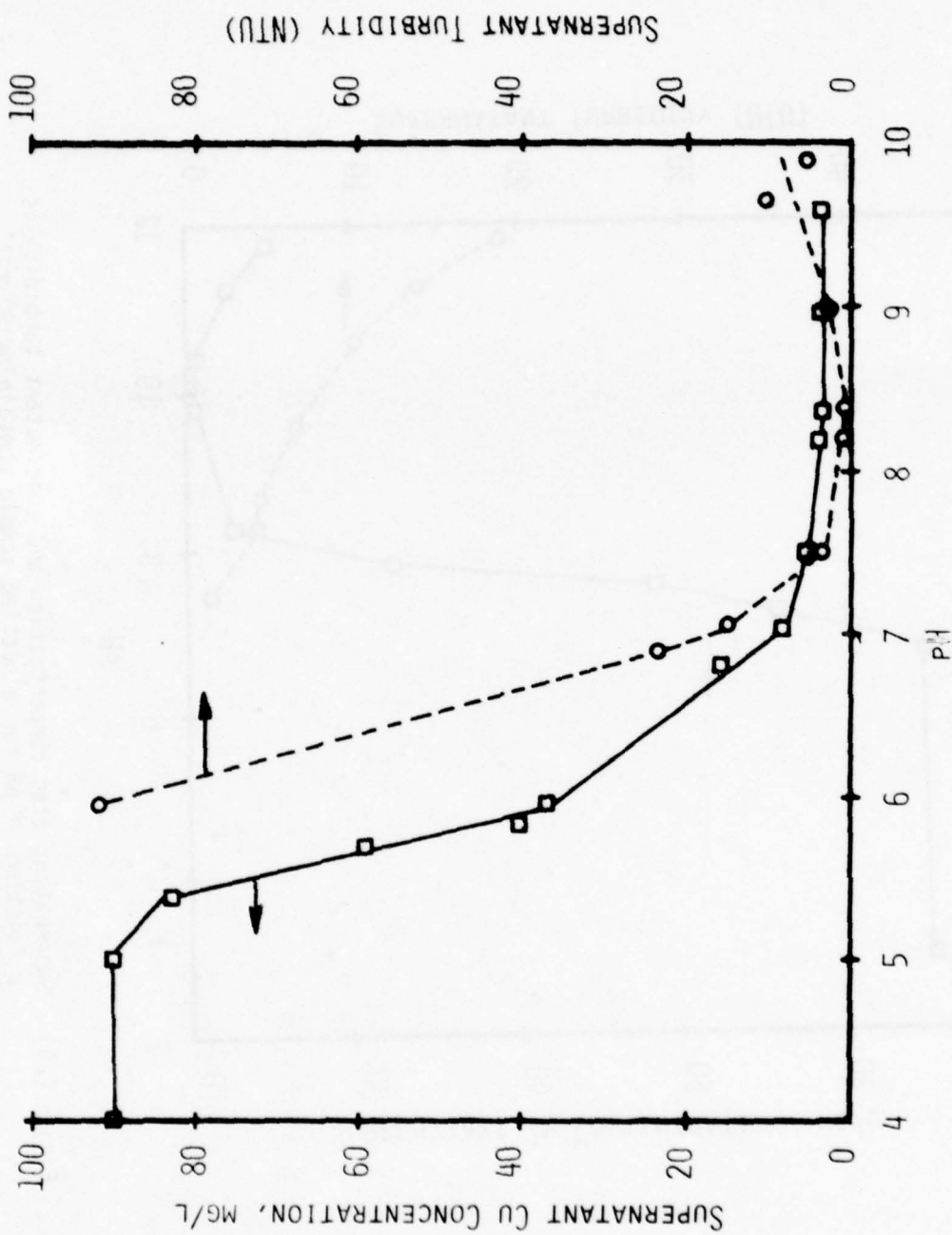


Figure (22). Supernatant copper concentration and supernatant turbidity as a function of pH for a settled sample containing 90 mg/l Cu(II) initially.

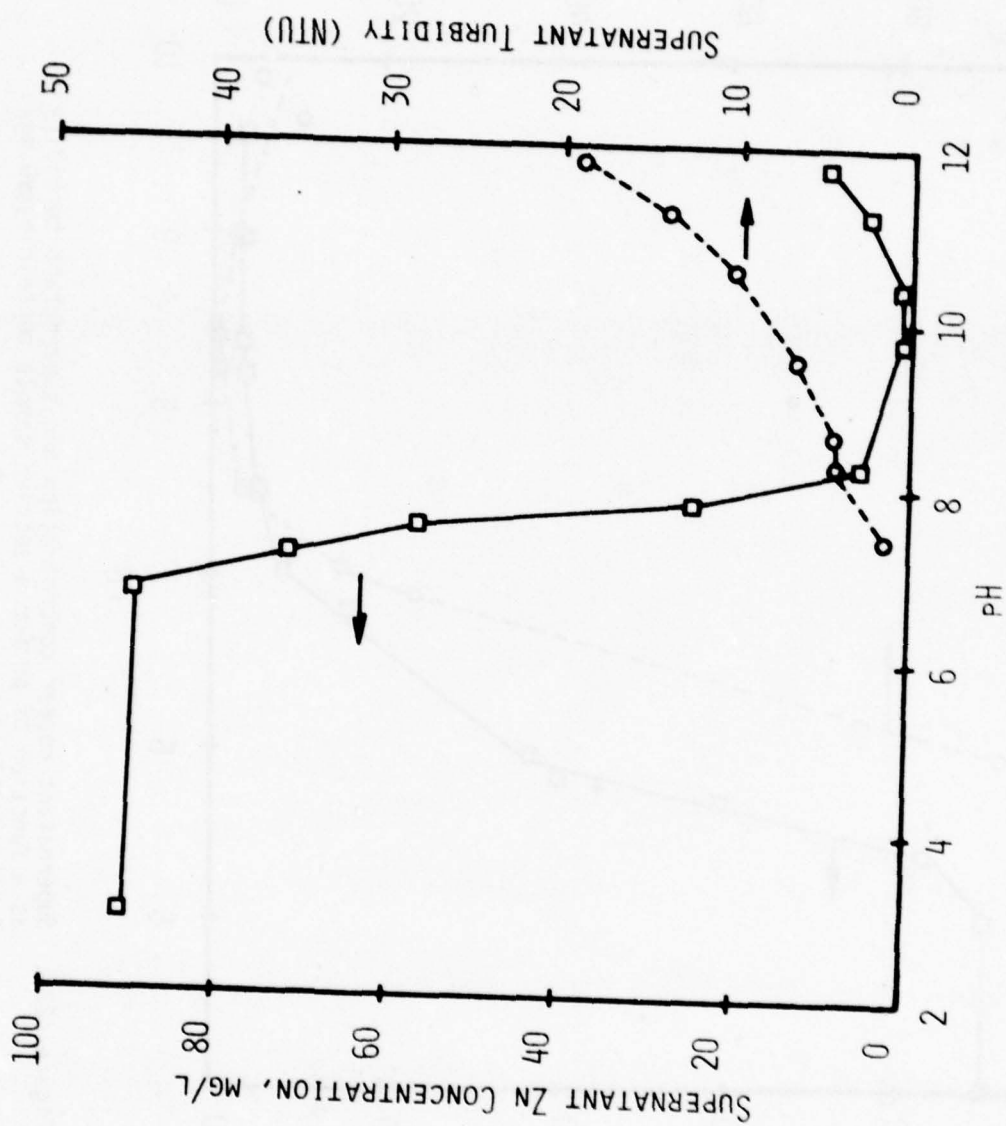


Figure (23). Supernatant zinc concentration and supernatant turbidity as a function of pH for a settled sample containing 90 mg/l Zn(II) initially.

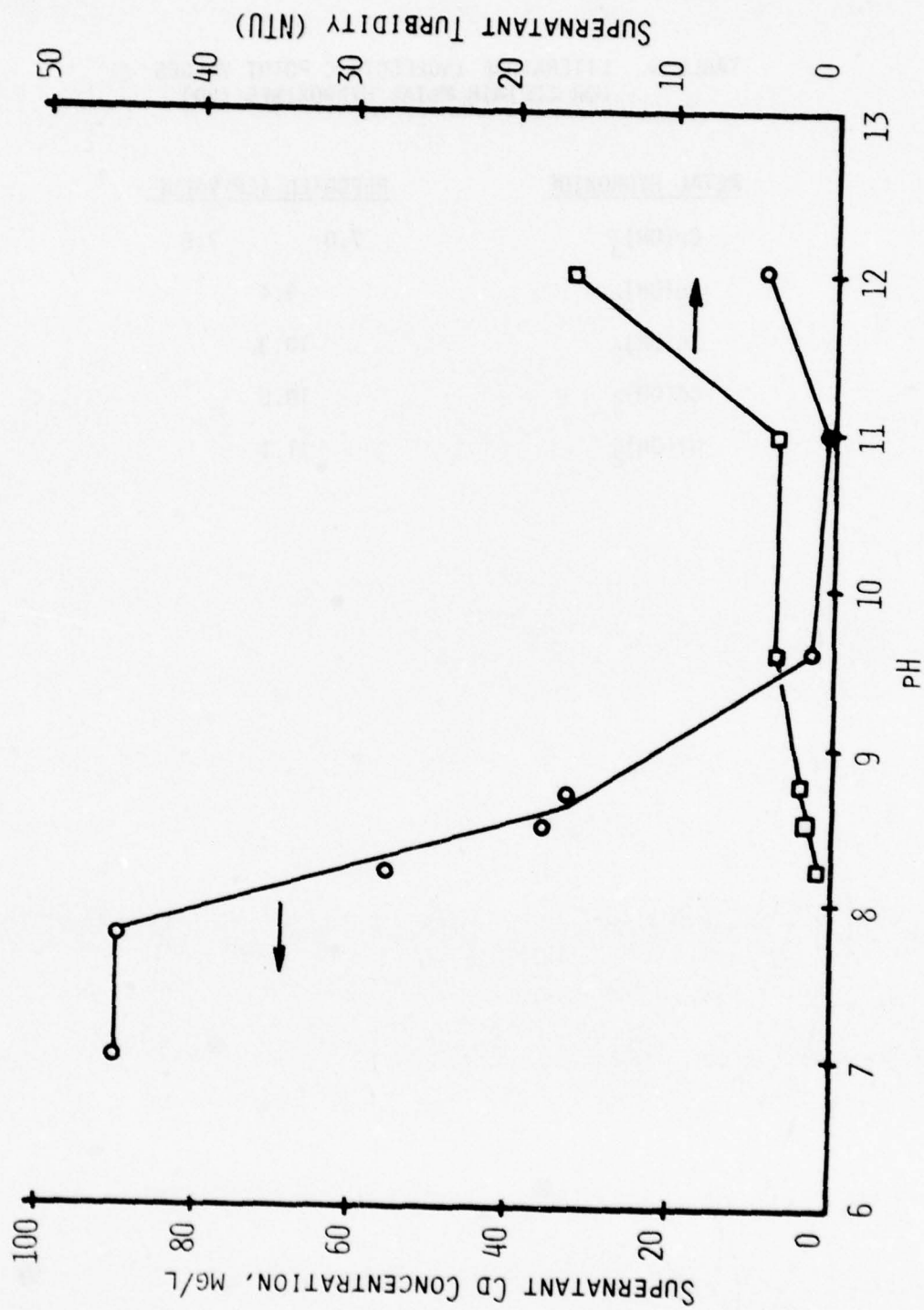


Figure (24). Supernatant cadmium concentration and supernatant turbidity as a function of pH for a settled sample containing 90 mg/l Cd(II) initially.

TABLE 5. LITERATURE ISOELECTRIC POINT VALUES
FOR CERTAIN METAL HYDROXIDES (20)

<u>METAL HYDROXIDE</u>	<u>REPORTED IEP VALUE</u>	
	7.0	7.8
Cr(OH)_3		
Cu(OH)_2		9.4
Zn(OH)_2		10.3
Cd(OH)_2		10.5
Ni(OH)_2		11.1

suspensions, especially at high pH values of insolubilization (pH 10.5 to 11.0). These suspensions were noted to change from a bluish color to a dark-brown color within relatively short periods of time. The time necessary to observe this change in appearance was found to decrease as the insolubilization pH increased, reaching a minimum of a few minutes at pH 11.0. Also, subsequent attempts to resolubilize these brown suspensions showed they were much more difficult to resolubilize than the freshly precipitated blue suspensions. This chemical phenomenon is apparently related to the "aging" of copper from a cupric hydroxide ($\text{Cu}(\text{OH})_2$) to cupric oxide (CuO). Tewari (25) has reported upon the increased difficulty in resolubilizing metal hydroxide suspensions following longer periods of "aging". In the case of copper, it can be seen that this "aging" phenomenon occurs rapidly while other metal hydroxides have been noted to "age" much more slowly, with aging periods up to and exceeding one year (26).

2. Effect of Sulfate Ions on Chromium Stability

Thomas and Theis (20) studied the effect of various anions on the precipitation of chromium hydroxide from solution. They concluded that some ions effect the stability of chromium suspensions by causing double-layer compression, while other ions appear to alter stability through specific ion adsorption to the hydroxide surface. Representative data from Thomas' study is shown in Figure 25. It is apparent that high concentrations of sulfate ions affected the stability of chromium hydroxide at pH 6.5 but not at pH 9.0. Unfortunately, in Thomas' study, the concentration of sulfate was not measured during the precipitation of chromium from solution. Data related to sulfate concentrations before and after chromium precipitation would be useful since it would help to explain the mechanism whereby sulfate ions affect the stability of chromium hydroxide suspensions.

It was the intent of this study to determine the fate of sulfate ions during the insolubilization and precipitation of chromium hydroxide. Sulfates were chosen for examination because they are found in a majority of chromium-bearing wastewaters, especially those which use $\text{SO}_2(\text{g})$ for the reduction of Cr(VI) to Cr(III). Also, sulfates have been shown to effect the stability of chromium hydroxide (20).

Figure 26 shows the effect of sulfate ions on the stability of a pure chromium hydroxide suspension. Sulfates were added to solution as H_2SO_4 prior to the insolubilization of chromium from solution. Comparing the results presented in Figures 18 and 26, it may be concluded that the presence of sulfate ions results in the precipitation of chromium hydroxide in the pH range 6 to 7. However, no effect is noted regarding the stability of the suspension at high pH. Furthermore, Figure 27 shows the effect of sulfate ions on the zeta potential of chromium hydroxide suspensions. Comparing these results to Figure 20, it can be seen that the point of zero charge has been shifted to a lower pH value, implying the adsorption

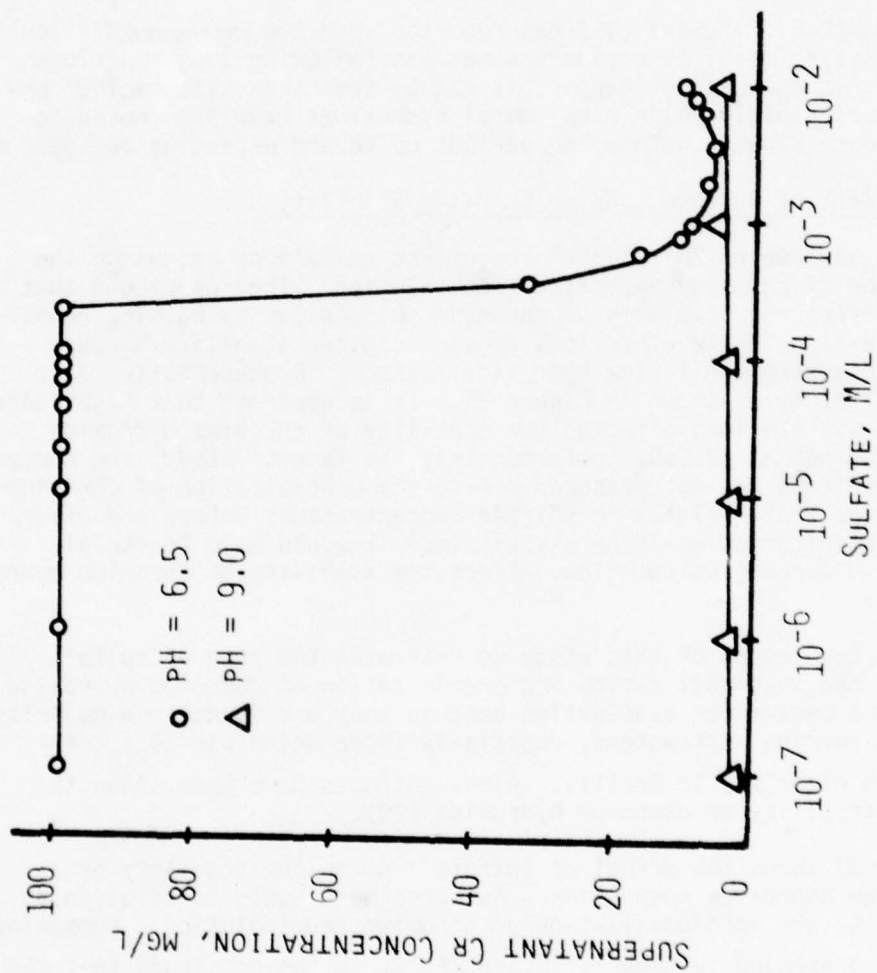


Figure (25). Representative results from Thomas and Theis (20).

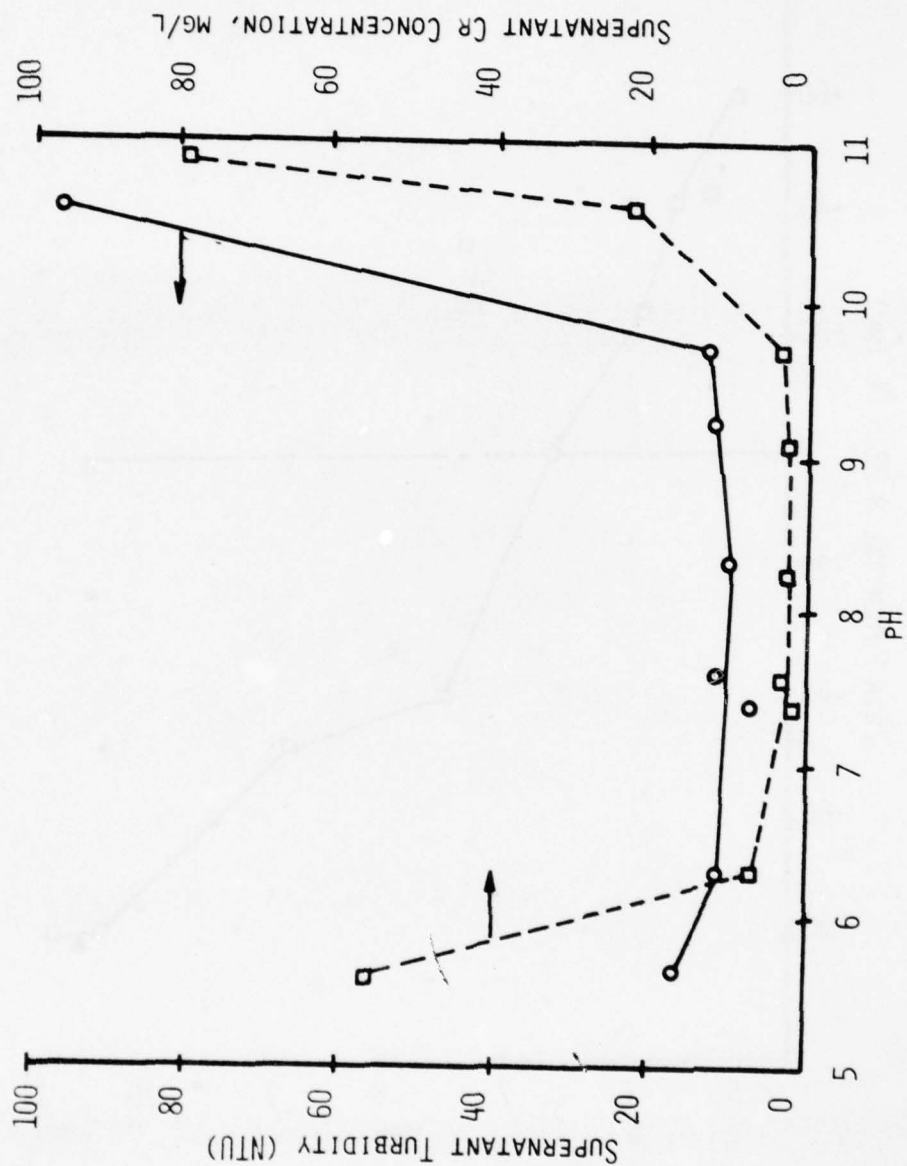


Figure (26). Supernatant chromium concentration and supernatant turbidity as a function of pH for a settled sample containing 130 mg/l Cr(III) initially. (Sulfates present in solution)

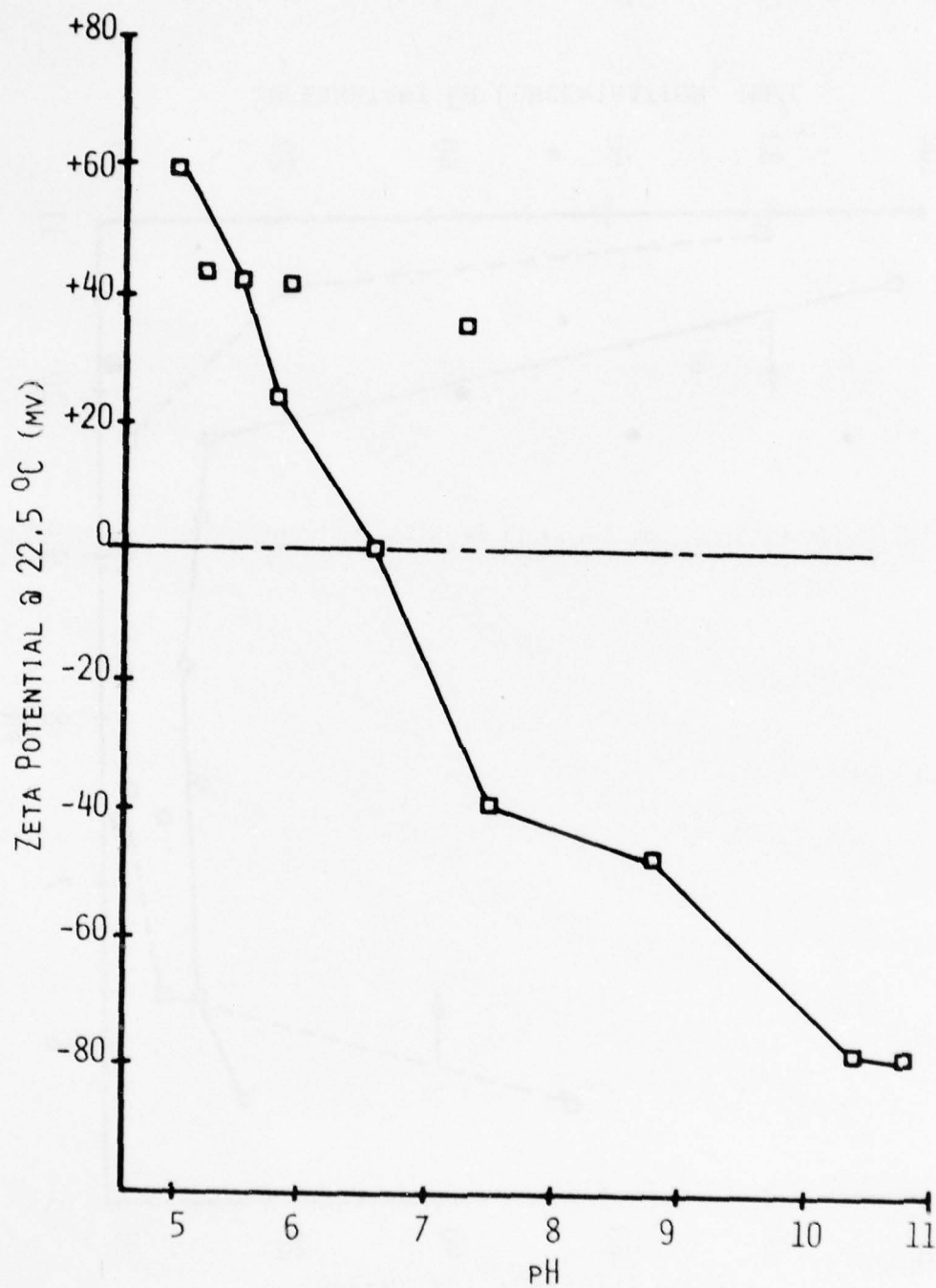


Figure (27). The characteristic surface potential of chromium hydroxide flocs as a function of pH. (Sulfates present in solution)

of sulfate ions for charge neutralization. Finally, Figure 28 shows the fate of sulfates during the removal of chromium from solution. In this case, the data presented is for a chromium-zinc mixed-metal system. At pH values below the characteristic isoelectric point of $\text{Cr}(\text{OH})_3(\text{s})$, sulfate ions are being removed from solution. However, at pH values above the IEP, the sulfate concentration is not affected by the precipitation of $\text{Cr}(\text{OH})_3$. These data support the conclusion that sulfate ions are removed from solution through adsorption to the chromium hydroxide surface.

3. Chromium Mixed-Metal Systems

Thomas and Theis (20) investigated the effect of several cations on the removal of chromium from solution. In general, nickel, zinc, copper and cadmium were found to effect the stability of chromium hydroxide most significantly by destabilizing the chromium suspension at high pH. Also, metals such as nickel were found to affect the stability of chromium at lower pH values. For example, Thomas and Theis reported that the presence of nickel would produce stable chromium suspensions up to pH 8.5. Thus, it is obvious that some form of interaction between chromium and these other metals is occurring. Thomas and Theis attributed this effect to complexing between the various divalent cations and chromium. However, they did not investigate fully the fate of these divalent cations during the insolubilization and precipitation of chromium hydroxide.

In this study, the role of each divalent cation in the precipitation of chromium from solution was evaluated by measuring the residual concentration of each metal after chromium precipitation. Figures 28 through 30 show representative results from chromium mixed-metal system, namely chromium-nickel, chromium-cadmium and chromium-zinc mixtures respectively. Examination of these results shows that both chromium and the added divalent cation are efficiently insolubilized and precipitated from solution. However, these studies also show that the divalent cation present with chromium is removed from solution at pH values far below that predicted necessary by equilibrium chemistry. For example, in Figure 29, nickel is found to be completely insolubilized and precipitated at pH 6.0 to 6.5, showing a measured residual of less than 0.5 mg/l Ni in solution. Equilibrium chemistry calculations, using thermodynamic equilibrium constants, predict that a pH of 8.5 would be necessary to reach this level of nickel remaining in solution.

The data collected from these mixed-metal systems is in conflict with data reported by Thomas and Theis (20). Comparative data from this study and the work of Thomas and Theis are shown in Figure 31. It is difficult to explain this apparent discrepancy in experimental findings. An examination of the experimental methods shows that similar test procedures were utilized in both studies. It should be noted that the results reported by Thomas and Theis present only the total concentration of each metal remaining in the supernatant liquor, with no distinction being made between the soluble and insoluble fractions. Thus, it is possible that, below

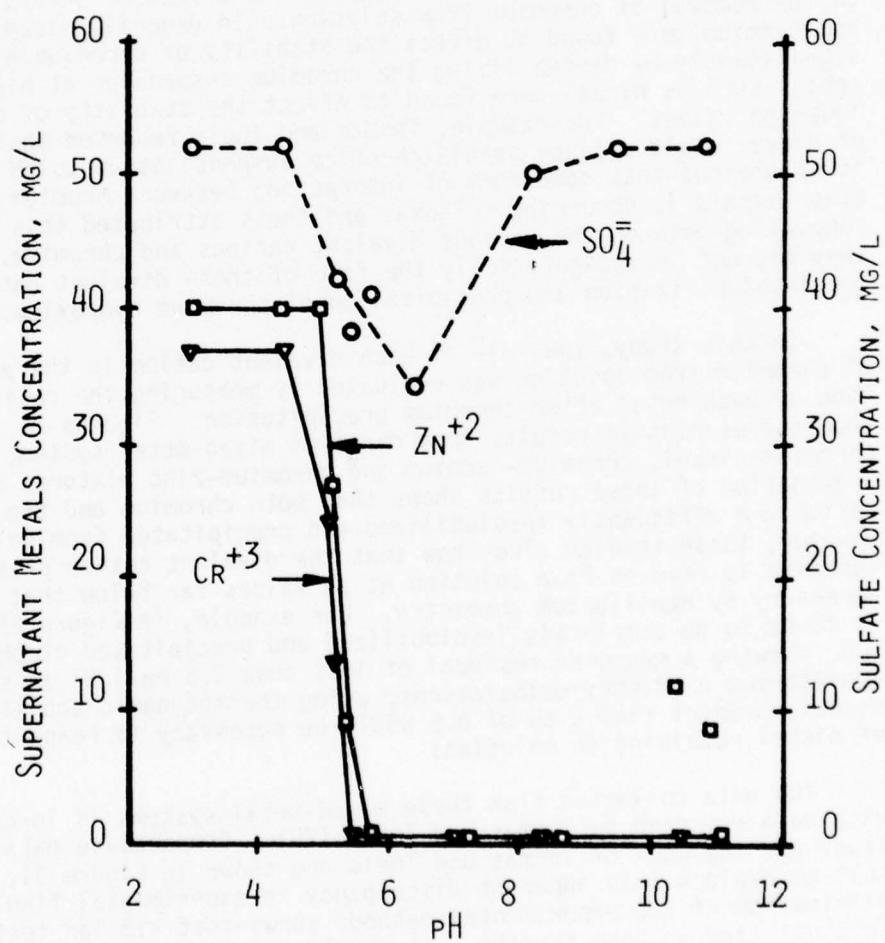


Figure (28). Supernatant Chromium, zinc and sulfate concentrations as a function of pH for a settled sample containing 37 mg/l Cr(III), 40 mg/l Zn(II) and 52 mg/l SO₄ initially.

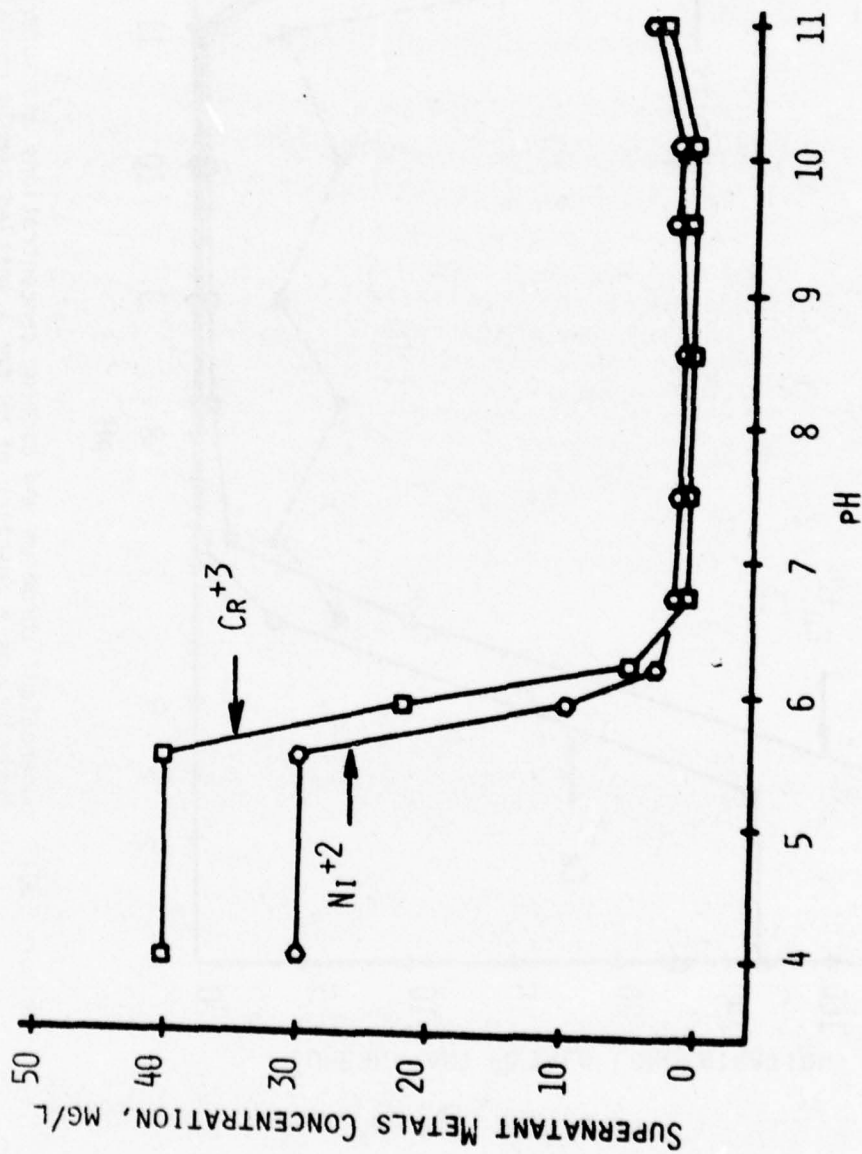


Figure (29). Supernatant chromium and nickel concentrations as a function of pH for a settled sample containing 40mg/l Cr(III) and 30 mg/l Ni(II) initially.

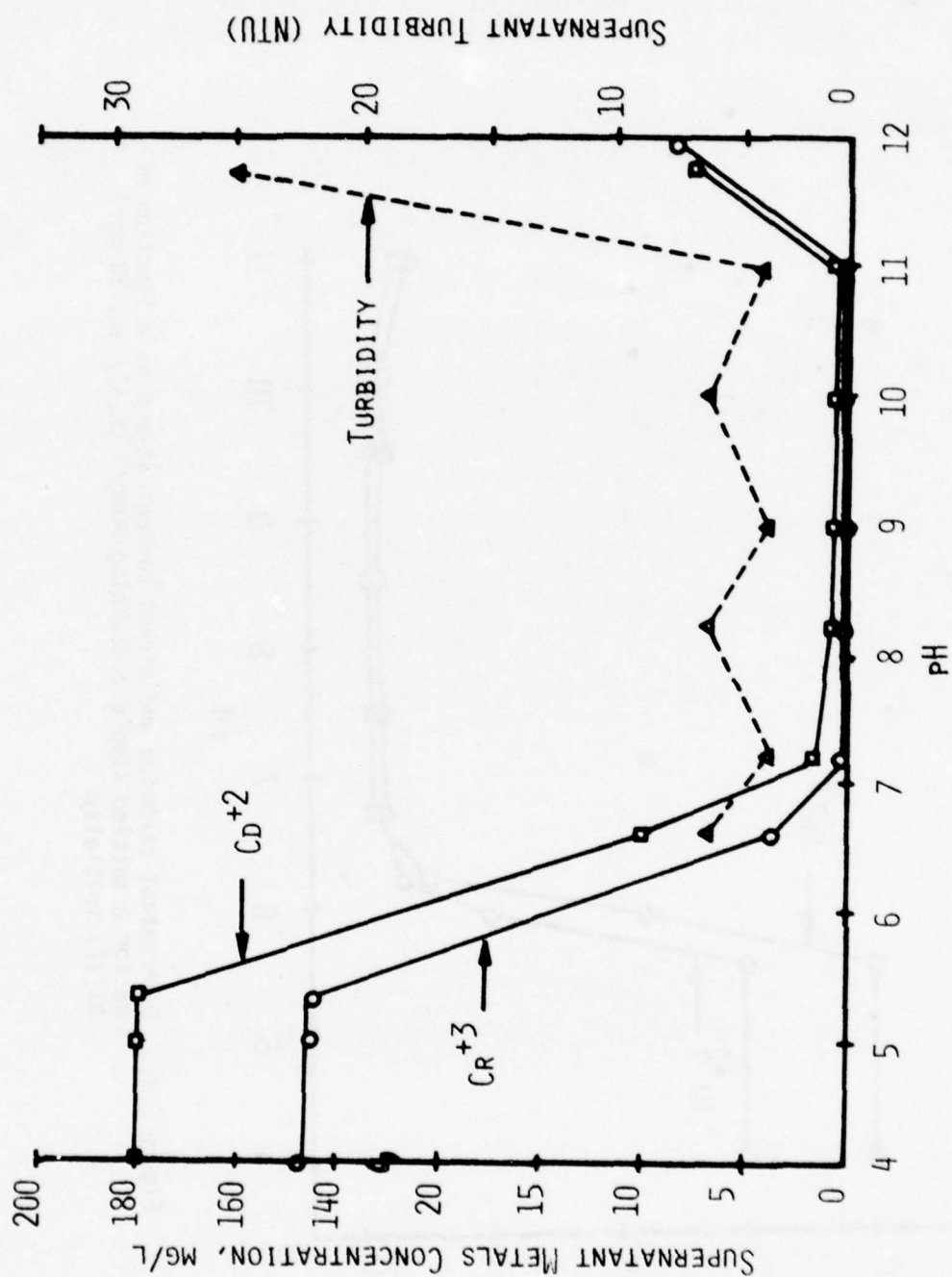


Figure (30). Supernatant chromium and cadmium concentrations and supernatant turbidity as a function of pH for a settled sample containing 147 mg/l Cr(III) and 180 mg/l Cd(II) initially.

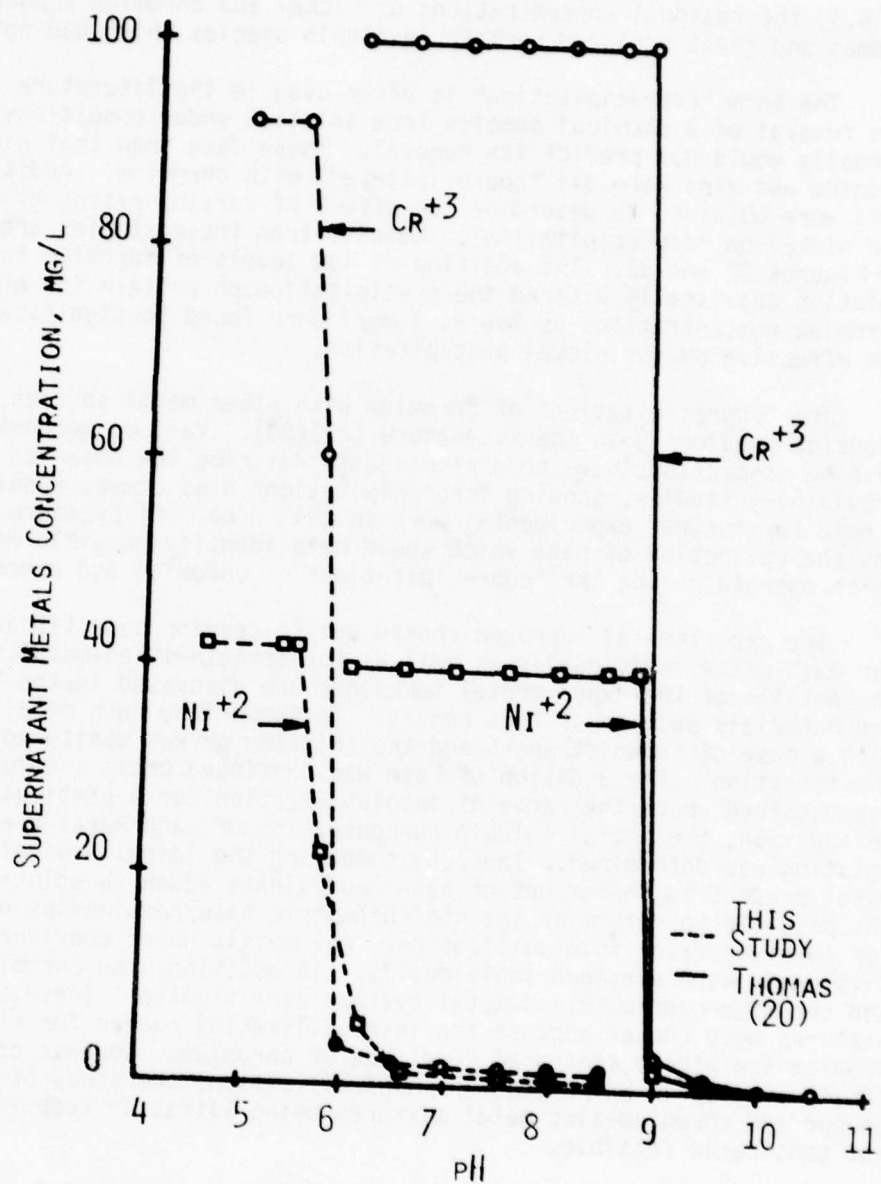


Figure (31). Comparative data from this study and similar studies performed by Thomas and Theis (20).

pH 8.5, the residual concentrations of nickel and chromium reported by Thomas and Theis included certain insoluble species which had not settled.

The term "coprecipitation" is often used in the literature to denote the removal of a chemical species from solution under conditions which normally would not predict its removal. These data show that nickel, cadmium and zinc were all "coprecipitated" with chromium. Additional data were obtained to determine the effect of varying ratios of chromium and nickel on "coprecipitation". Results from these studies are shown in Figures 32 and 33. The addition of low levels of chromium to a nickel solution drastically altered the precipitation:pH pattern for nickel. Chromium concentrations as low as 1 mg/l were found to significantly reduce the effective pH for nickel precipitation.

The "coprecipitation" of chromium with other metal species has been reported previously in the literature (27)(28). Various mechanisms, including adsorption, have been proposed to describe the observed phenomenon. Preliminary studies, showing "coprecipitation" does occur, resulted in a need for further experimental work in this area. Of premiere importance was the collection of data which would help identify possible mechanisms which operate during the "coprecipitation" of chromium and other metals.

The experimental approach chosen was to develop base titration curves for each metal individually as well as for certain mixed-metal systems. The details of the experimental technique are discussed in the Methods and Materials section of this report. To summarize, each metal was titrated with a base of known strength and the solution pH was monitored during the titration. The addition of base was continued until a solution pH was obtained above the range of insolubilization for a particular metal. In addition, the initial soluble concentration of each metal present in solution was determined. Thus, by comparing the initial equivalents of metal present to the amount of base equivalents added to solution, it was possible to determine the stoichiometric base requirement necessary for complete metal insolubilization. All metals under consideration in this study were examined individually. In addition, the chromium-nickel and chromium-cadmium mixed-metal systems were studied. These two metal mixtures were chosen because the insolubilization ranges for nickel and cadmium are widely separated from that of chromium. Because of a significant overlap of pH ranges for insolubilization, the study of chromium-copper and chromium-zinc metal mixtures using titration techniques was not considered feasible.

Representative graphs from the titration of each individual metal are shown in Figures 34 through 37. Analysis of these results show the titration method to be useful and reliable as a research tool. In each experimental study, the stoichiometric amount of base added to solution was approximately equal to the initial amount of metal present on an equivalent basis. The endpoint of each titration curve is defined as the point at which the solution pH begins a rapid rise following the insolubilization "plateau".

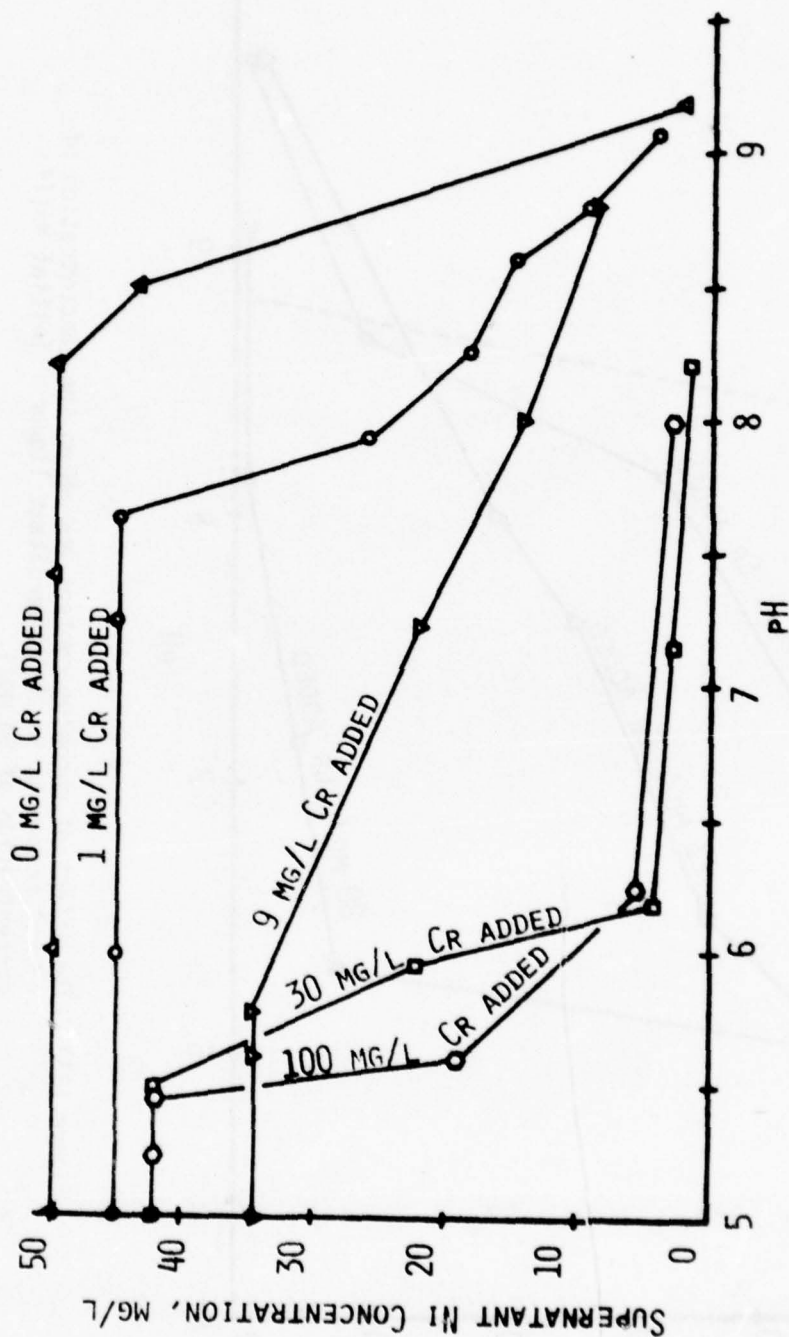


Figure (32). The effect of chromium content and pH on the concentration of nickel remaining in the supernatant liquor. Initial Ni(II) concentration of 50 mg/l.

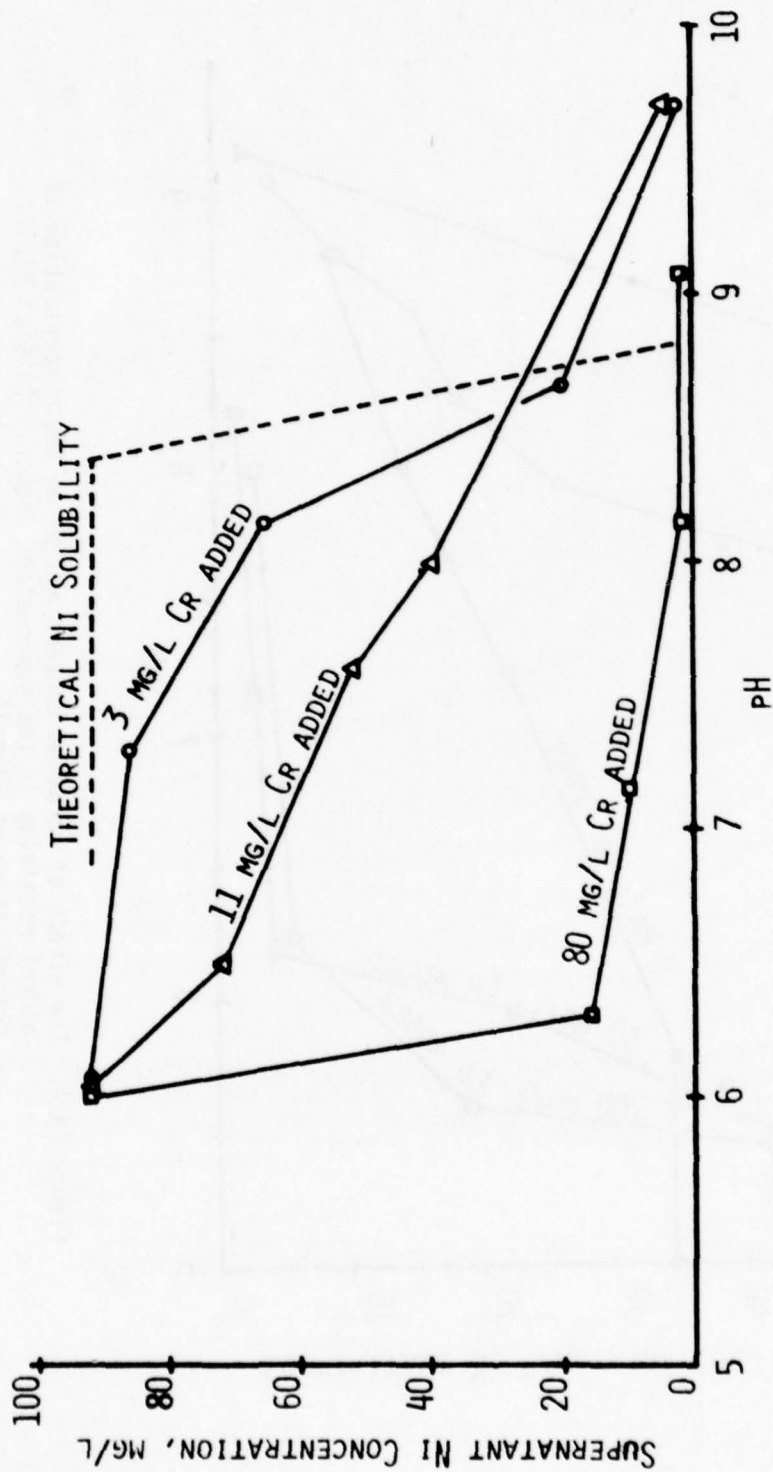


Figure (33). The effect of chromium content and pH on the concentration of nickel remaining in the supernatant liquor. Initial Ni(II) concentration of 90 mg/l.

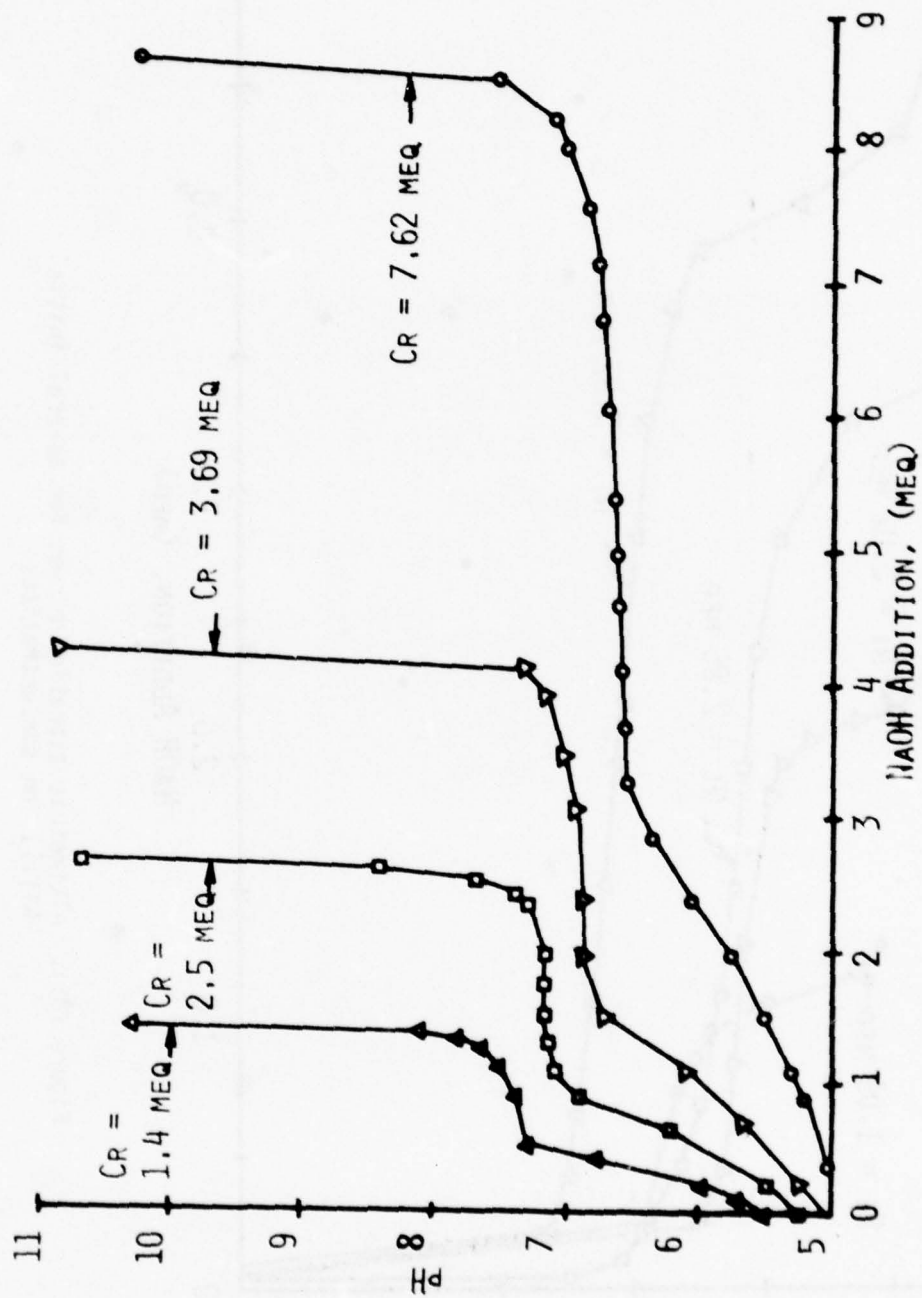


Figure (34). Alkometric titration curves for several initial Cr(III) ion concentrations.

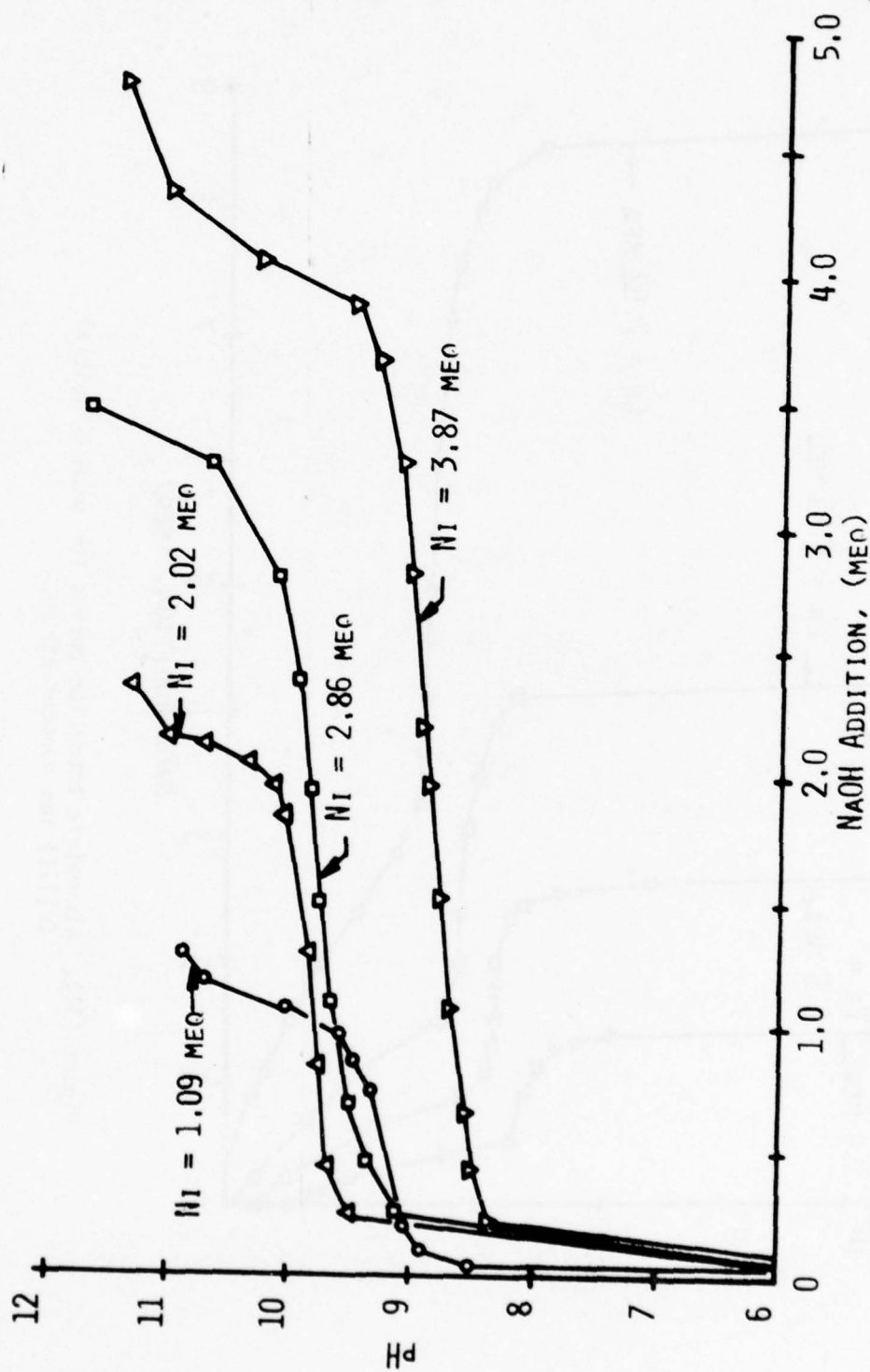


Figure (35). Alklimetric titration curves for several initial $Ni(II)$ ion concentrations.

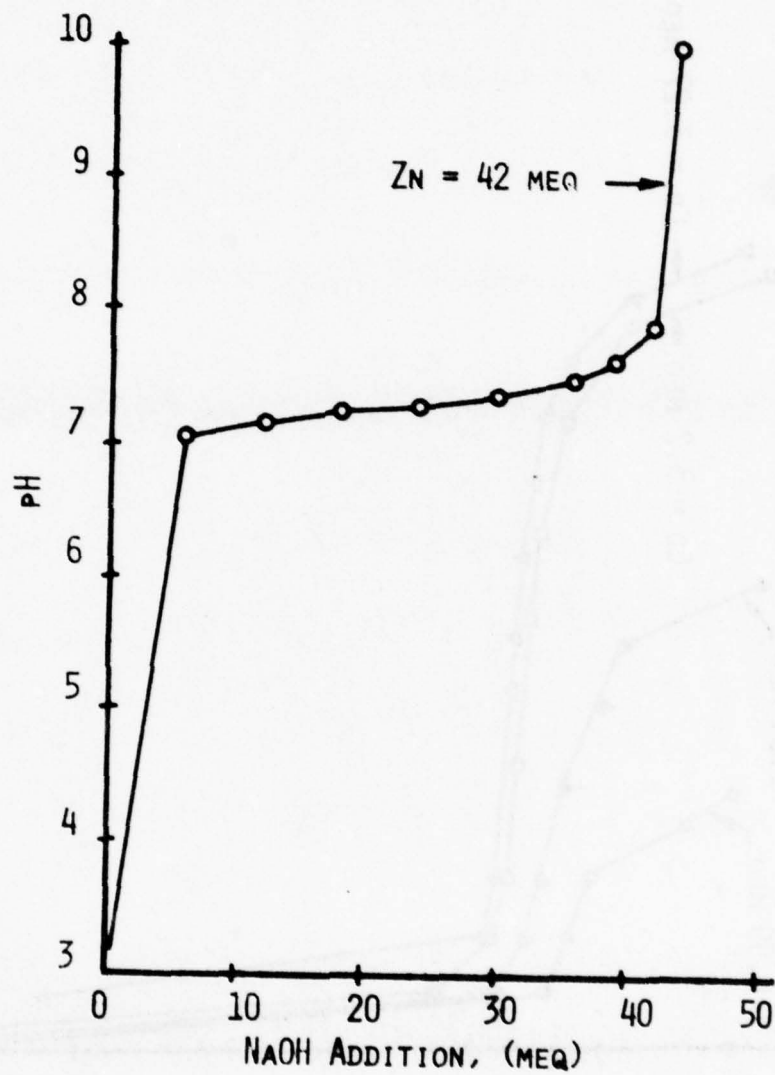


Figure (36). Alkimeric titration curve for zinc.

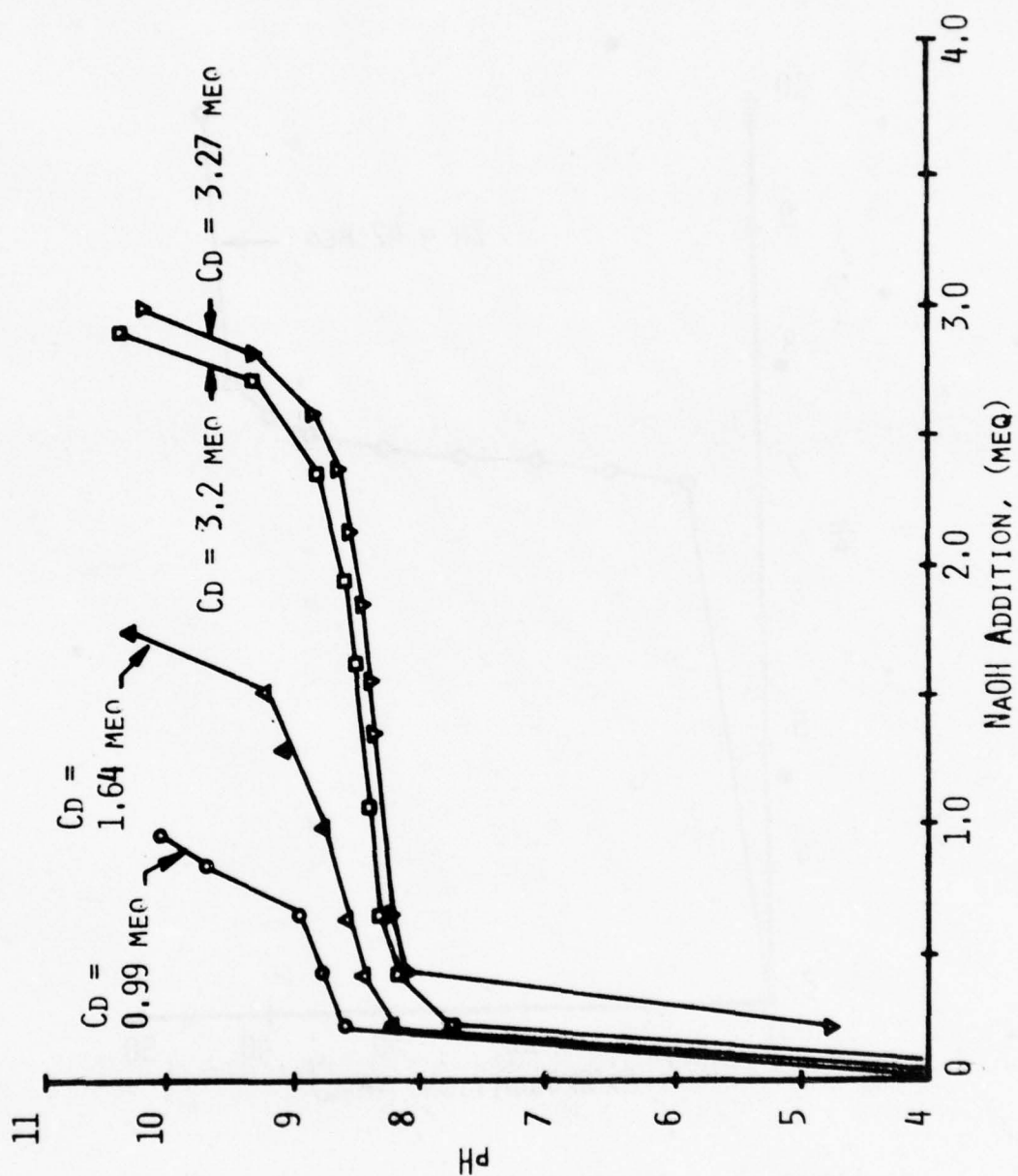


Figure (37). Alkometric titration curves for several initial Cd(II) ion concentrations.

Having completed these initial studies, efforts were made to examine the chromium-nickel mixed-metal system in an in-depth fashion. Titration curves were developed using several initial ratios of chromium to nickel in solution. Representative results from these studies are shown in Figures 38 through 42. Examination of these results leads to the following observations:

(1) In many instances, the solution pH remains below pH 6.5 throughout the titration, corresponding to the pH range of chromium insolubilization. Examples of this behavior are seen in Figure 38. In each case, the pH does not stabilize at any time in the range of 8.0 to 9.0, corresponding to the insolubilization of nickel. Rather, it rises rapidly from 6.5 to 10.5 or 11.0. Thus, all metals present are insolubilized at the pH 5.0 to 6.5 "plateau". This result is different than would be predicted by equilibrium chemistry considerations. Figure 42 shows this difference between theoretical predictions and experimental observations for one set of experimental results. In this study, the initial chromium and nickel amounts were 18.2 and 35.6 milliequivalents respectively. Theoretically, equilibrium chemistry would predict that, following base addition roughly equal to the initial amount of chromium present, a distinct rise in pH should be noted. The pH should progress to near pH 8.0, into the range of nickel insolubilization. In this pH range, the insolubilization of nickel hydroxide would serve to produce a second pH "plateau" which would continue until approximately 35.6 meq of base had been added. At this point, all metals present would be insolubilized and further base additions would produce a rapid rise in solution pH. Comparing the theoretical curve to that determined experimentally shows clearly that this is not occurring.

(2) Figures 39 through 41 show cases where two pH "plateaus" have been established, corresponding to the regions of chromium and nickel insolubilization. However, the base equivalents added to the inflection point of the titration curve are always much larger than the initial amount of chromium present. Thus, a mass balance of the system shows that any additional base added to reach the inflection point must be utilized in the insolubilization of nickel. For example, Figure 40 shows that 100 meq of base were added during the low pH "plateau" before the inflection point was reached. The initial chromium present in this titration corresponded to 20 meq. Thus, since no appreciable rise in pH is noted over this pH "plateau", it can be concluded that the additional 80 meq of base were utilized in the insolubilization of nickel from solution.

(3) A summary of the initial metals concentrations and the total required base equivalents determined experimentally from each mixed-metal test are listed in Table 6. By comparing the amount of initial metals present to the amount of base required for complete insolubilization, it can be seen that, within the confines of experimental error, the equivalents of base added compares well with the equivalents of metals present initially. This is an important finding since it provides some insight into possible explanations for the "coprecipitation" phenomenon. Owing

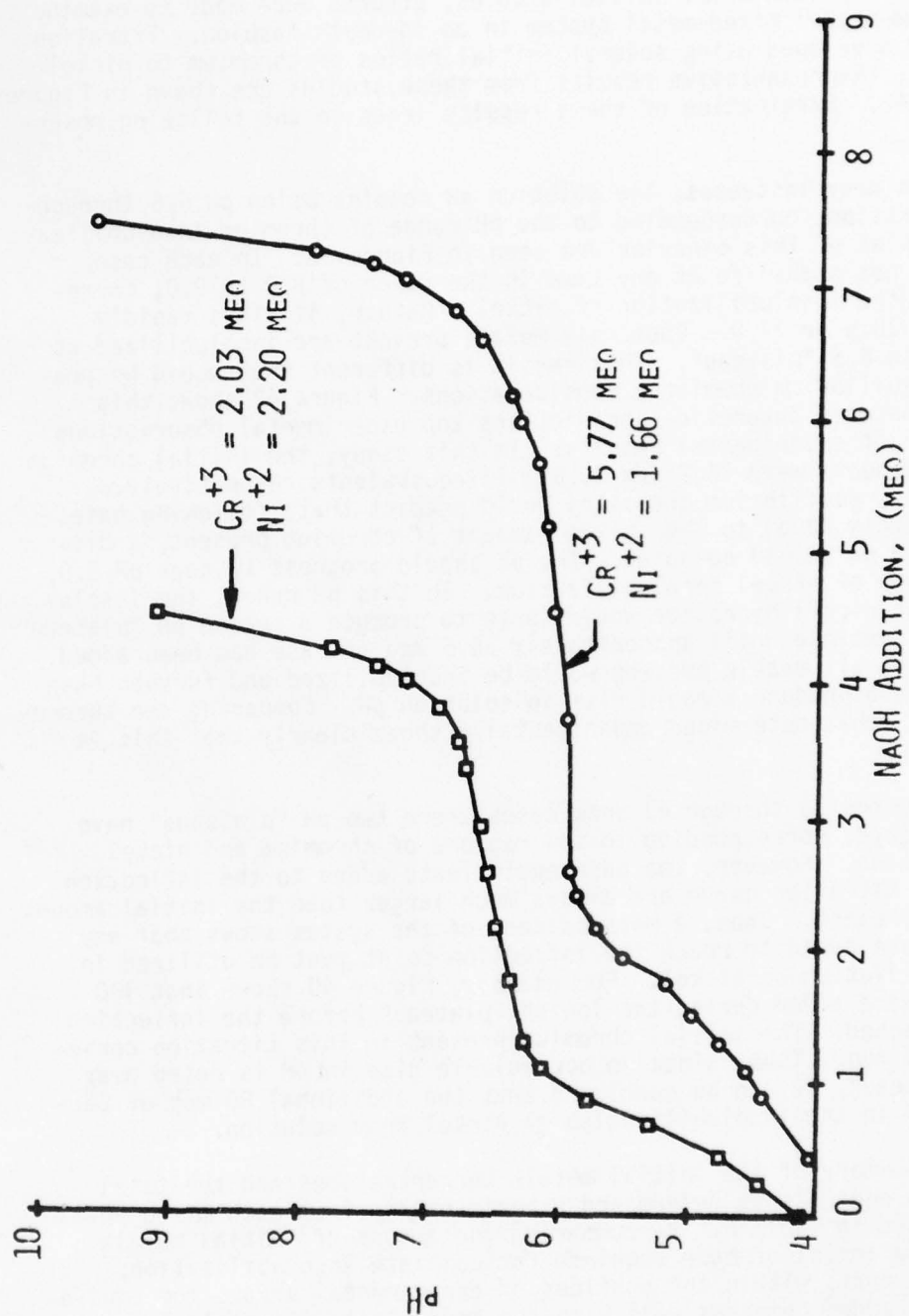


Figure (38). An alklimetric titration curve for a Cr(III) - Ni(II) metal mixture.

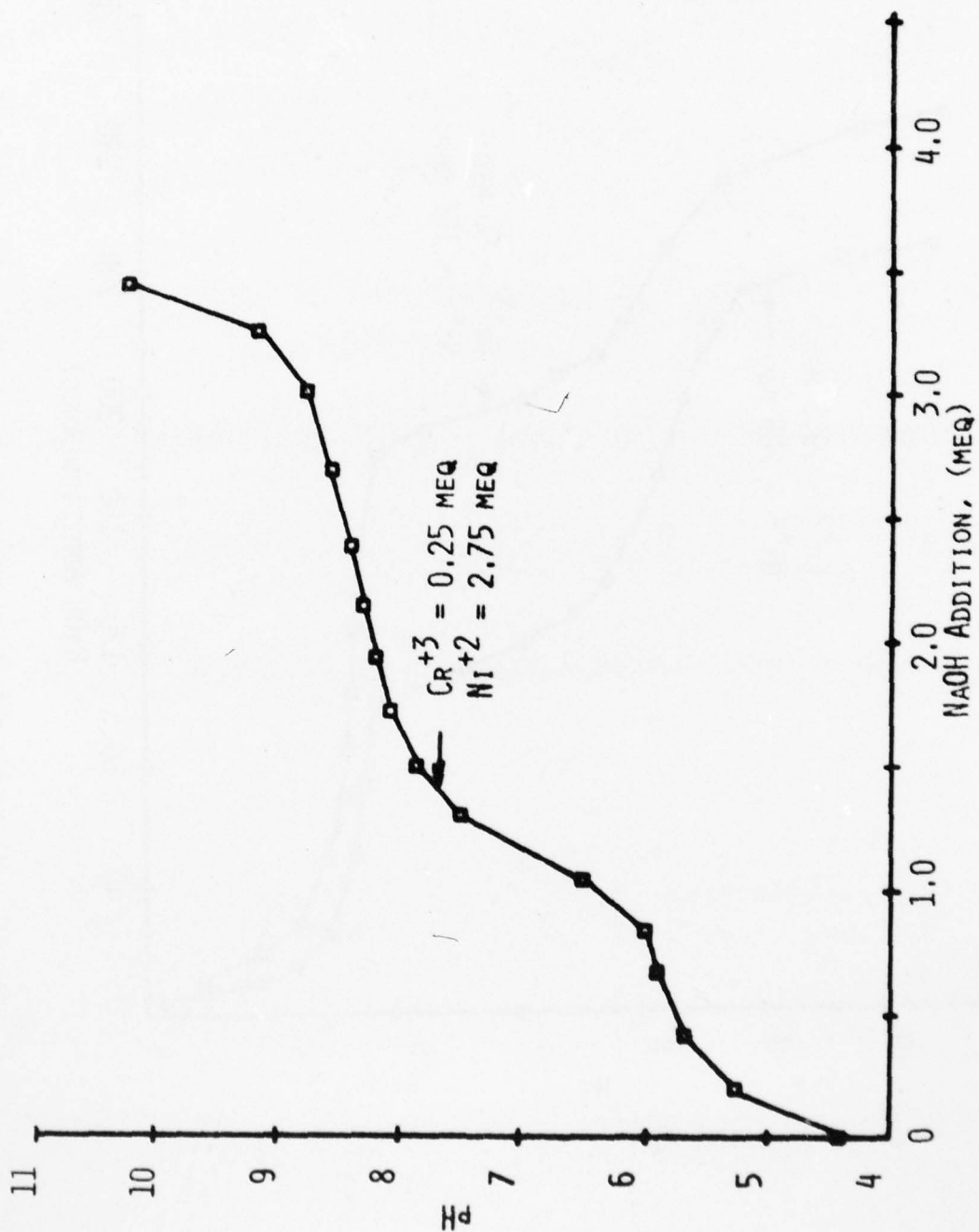


Figure (39). An alkometric titration curve for a Cr(III) - Ni(II) metal mixture.

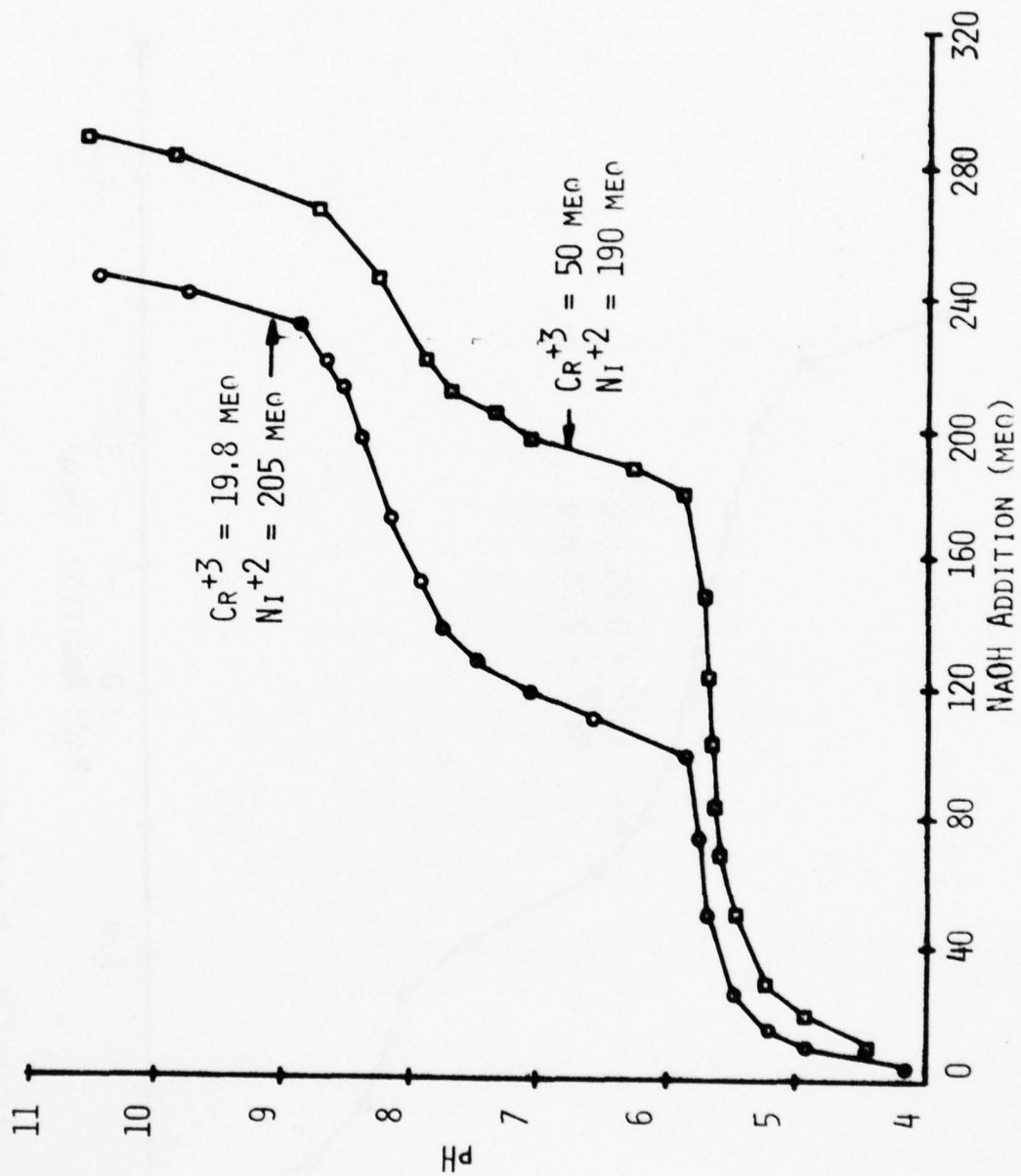


Figure (40). Alkometric titration curves for two Cr(III) - Ni(II) metal mixtures.

TABLE 6. RESULTS OF CHROMIUM - NICKEL
"COPRECIPITATION" STUDIES

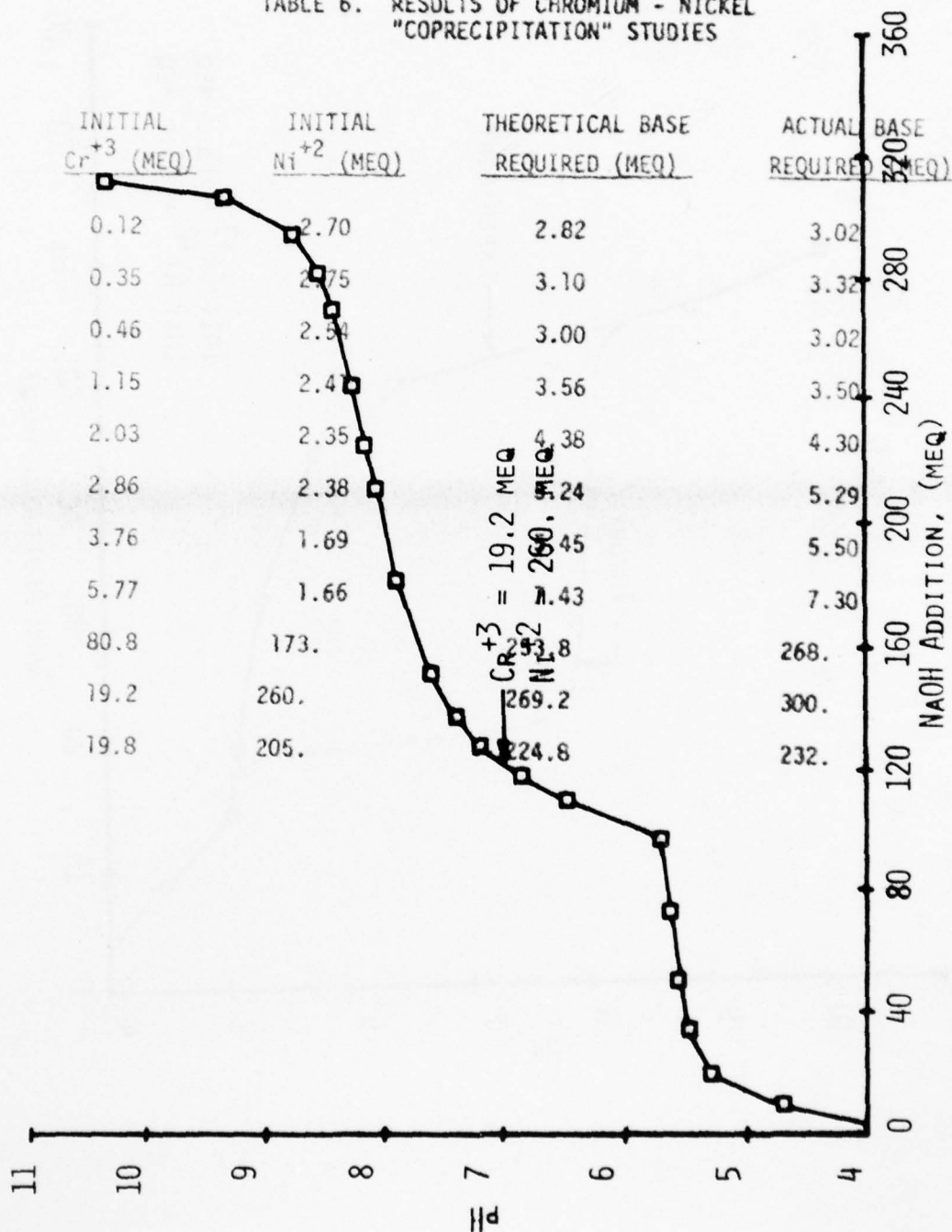


Figure (41). An alkimetric titration curve for a $Cr(III)$ - $Ni(II)$ metal mixture.

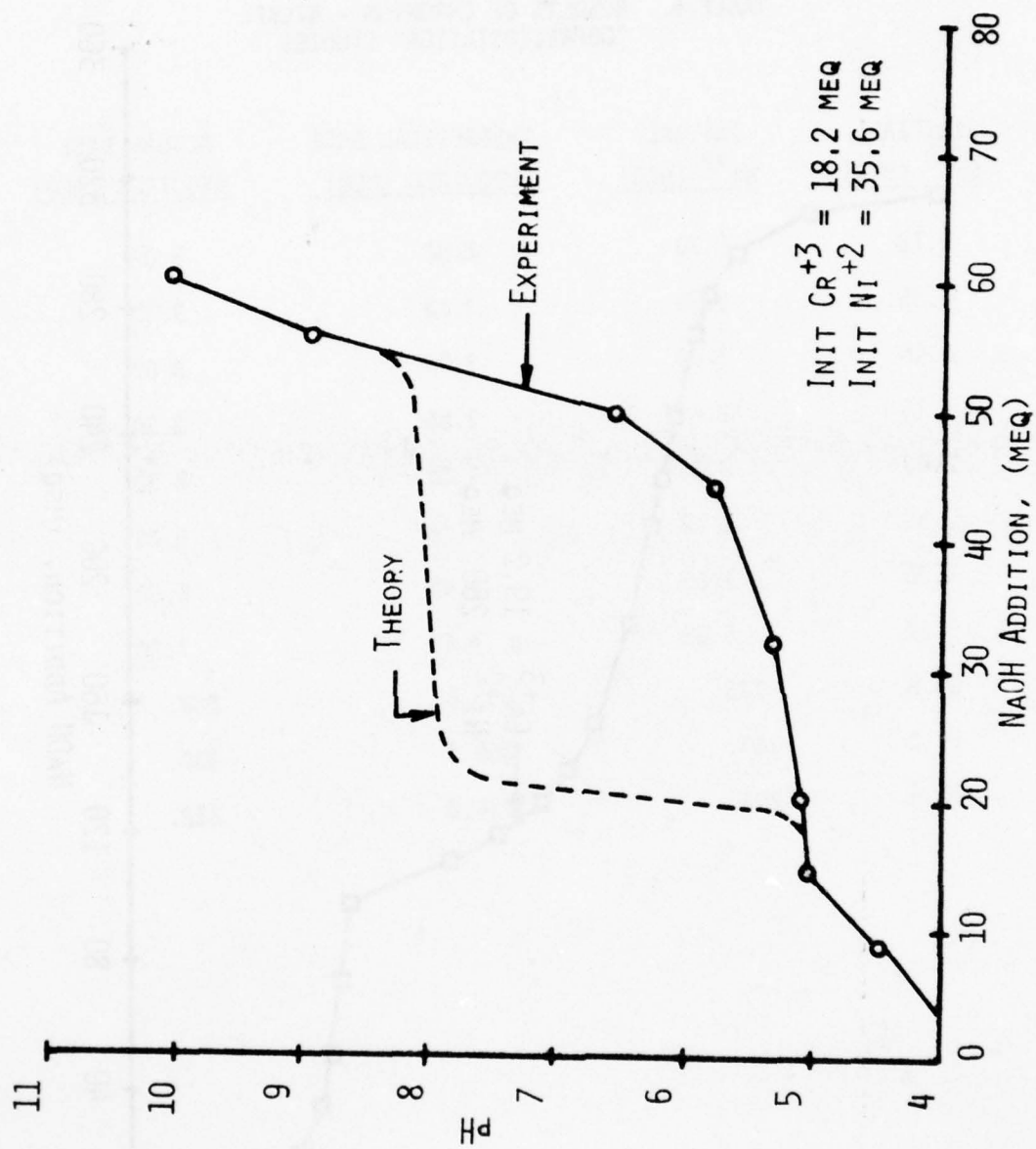


Figure (42). Alkimeric titration curves (theoretical and experimental) for a $\text{Cr(III)} - \text{Ni(II)}$ metal mixture.

TABLE 6. RESULTS OF CHROMIUM - NICKEL
"COPRECIPITATION" STUDIES

<u>INITIAL Cr⁺³ (MEQ)</u>	<u>INITIAL Ni⁺² (MEQ)</u>	<u>THEORETICAL BASE REQUIRED (MEQ)</u>	<u>ACTUAL BASE REQUIRED (MEQ)</u>
0.12	2.70	2.82	3.02
0.35	2.75	3.10	3.32
0.46	2.54	3.00	3.02
1.15	2.41	3.56	3.50
2.03	2.35	4.38	4.30
2.86	2.38	5.24	5.29
3.76	1.69	5.45	5.50
5.77	1.66	7.43	7.30
80.8	173.	253.8	268.
19.2	260.	269.2	300.
19.8	205.	224.8	232.

to the close agreement between base requirements and initial metals present, it appears that adsorption of nickel to the chromium surface is not a likely mechanism; rather, the data show that both metals are being completely insolubilized as metal hydroxide species.

The possibility of a reversible adsorption reaction involving nickel and the chromium hydroxide surface was investigated. The hypothesis tested is as follows:

Initially, in the pH range favoring chromium insolubilization, nickel ions may be adsorbed to the chromium surface. However, upon continued base addition, the nickel ions may desorb from the particle surface and insolubilize as nickel hydroxide. Thus, the adsorption of nickel would result in the production of a "metastable" chromium-nickel species from which nickel could desorb at high pH values.

To test this hypothesis, experimental test procedures were devised. Insolubilization studies were performed using a chromium-nickel mixture. The solution pH was raised through base addition to the range of pH 7 to 7.3, a range which would produce complete chromium insolubilization but would leave nickel in solution. After achieving this pH range, the suspension was flocculated and settled for one hour. After settling, the soluble concentration of metals remaining in the supernatant liquor was determined. By comparing the amount of metals removed at this pH value with the amount of base added to solution, it should be possible to examine the possibilities for nickel adsorption. If adsorption is a viable phenomenon, the total amount of metals removed from solution would be much higher than the equivalent amount of base added.

Results of these experiments are shown in Table. 7. In all cases, the amount of chromium and nickel removed at pH 7.0 to 7.3 could be roughly accounted for by the number of base equivalents added to solution. Thus, one may conclude that adsorption does not play a major role in the "coprecipitation" of chromium and nickel.

After eliminating adsorption as a possible mechanism for "coprecipitation", other alternatives were considered. One possible mechanism was that nickel was involved in an "inclusion reaction" where nickel ions could be incorporated in the insolubilization of chromium ions. Throughout the study, it had been experimentally observed that, during the initial additions of a base to a chromium-bearing wastewater, the solution color would turn from a violet-blue to a blue-green in the pH range 4.0 to 4.5. Examination of chromium speciation diagrams such as those shown in Figures 43 and 44 for 10^{-2} and 10^{-3} molar chromium solutions show this pH range to correspond to the production of certain polynuclear chromium species. Thus, it was felt that nickel may be incorporated into the production of these chemical species. To test this hypothesis, a series of three experimental tests were undertaken. In the first test, both nickel and chromium were initially present in solution and base added

TABLE 7. RESULTS OF Cr - Ni "COPRECIPITATION" STUDIES

TEST #	pH	SOLUBLE Ni (mg/l)	SOLUBLE Ni (meq)	SOLUBLE Cr (mg/l)	SOLUBLE Cr (meq)	METALS REMOVED (meq)	BASE ADDED (meq)*
1	2.4	184	2.51	150	3.46	--	--
	7.3	18.6	0.25	0.5	--	5.72	5.84
	10.1	0.5	--	0.5	--	5.97	6.39
2	2.5	294	4.01	60	1.38	--	--
	7.3	46	0.63	0.5	--	4.76	4.34
	10.4	0.5	--	0.5	--	5.39	5.86
3	2.3	720	9.81	60	1.38	--	--
	7.3	485	6.61	0.5	--	4.58	4.00
	10.2	0.5	--	0.5	--	11.19	11.43
4	2.3	585	7.97	105	2.42	--	--
	7.3	220	3.00	0.5	--	7.39	6.72
	10.2	0.5	--	0.5	--	10.39	10.65

* Corrected for pH changes.

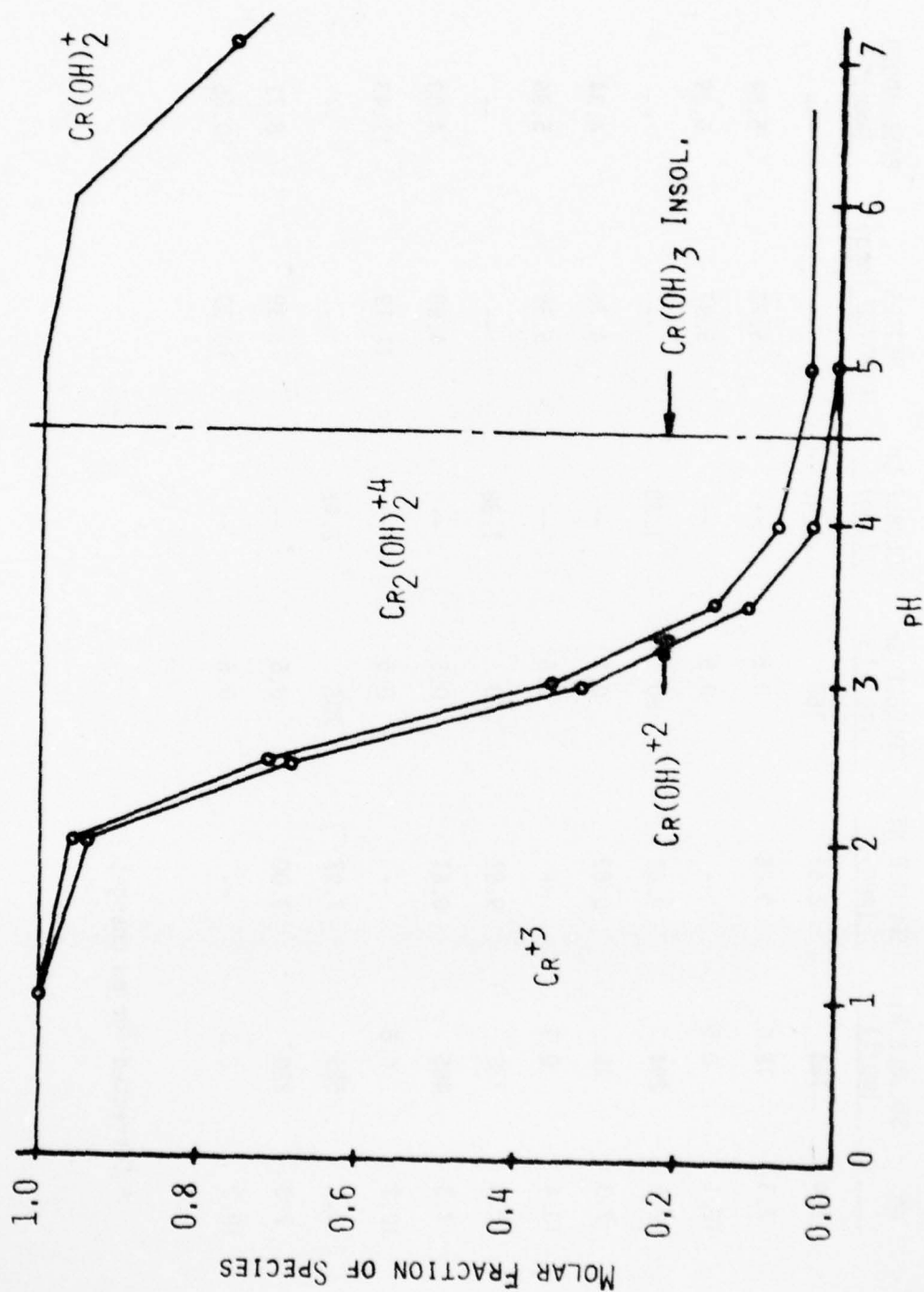


Figure (43). Distribution of Cr(III) species as a function of pH
($\text{Cr}_T = 10^{-2}\text{M}$).

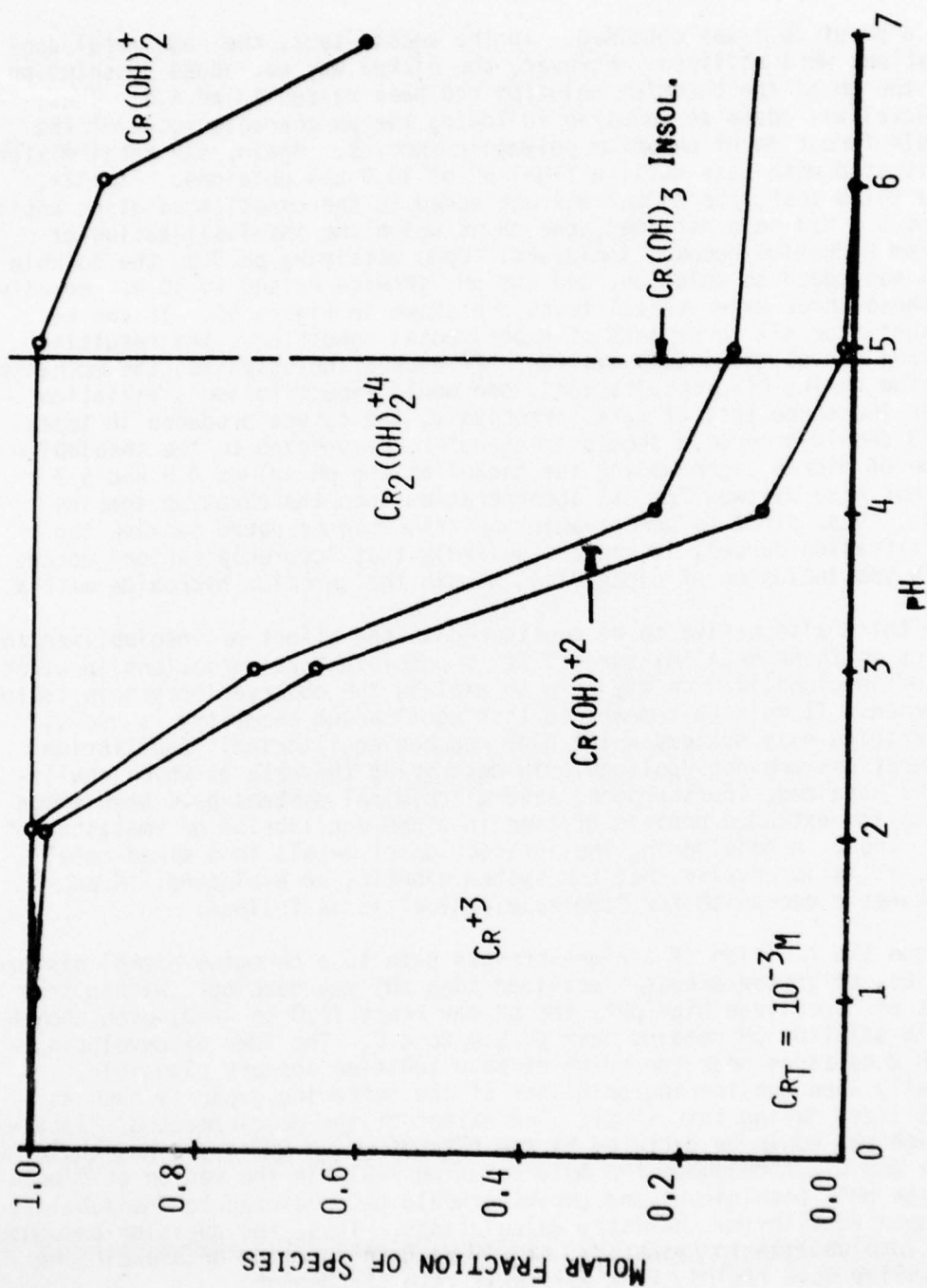


Figure (44). Distribution of Cr(III) species as a function of pH
($C_{Cr} = 10^{-3}M$).

until a pH of 10.1 was obtained. In the second test, the same metal concentrations were utilized. However, the nickel was not added to solution until the pH of the chromium solution had been raised to pH 4.5. Thus, the nickel was added to solution following the pH characteristic of the possible formation of chromium polymeric species. Again, the metal mixture was titrated with base until a final pH of 10.0 was obtained. Finally, in the third test, the nickel was not added to the chromium solution until a pH of 5.3 had been attained, the pH at which the insolubilization of chromium hydroxide becomes incipient. Upon attaining pH 5.3, the soluble nickel was added to solution, and the pH likewise raised to 10.0. Results from these three experimental tests are shown in Figure 45. It can be seen that, for all three sets of experimental conditions, the resulting titration curves are indeed similar. If nickel inclusion was the mechanism occurring during "coprecipitation", one would expect to see a variation between the three sets of data. Precisely, the curves produced in tests 2 and 3 should produce a second "plateau" corresponding to the insolubilization of nickel since adding the nickel at the pH values 4.5 and 5.3 would not have allowed for its incorporation into the chromium species formed. Thus, since no perceivable variation can be noted between the three titration curves, it appears unlikely that "coprecipitation" occurs through the inclusion of nickel ions within the chromium hydroxide matrix.

A third alternative to be considered is the effect of insolubilization kinetics on these metal mixtures. It is possible that variations in kinetic rates of insolubilization may help to explain the observed "coprecipitation" phenomenon. It must be remembered that equilibrium chemistry is useful in describing only systems which have reached equilibrium. Equilibrium considerations are not applicable in describing the rate at which equilibrium is attained. Furthermore, several chemical systems have been shown to exist for extended periods of time in a non-equilibrium or "metastable" state. Thus, in considering the interaction of metals in a mixed-metal system, it is imperative that the system kinetics be evaluated. A proposed kinetic mechanism for "coprecipitation" is as follows:

Upon the addition of a high-strength base to a chromium-nickel mixture, conditions of instantaneous "localized high pH" may develop. Within the regions of "localized high pH", the pH may reach 11.0 to 12.0, even though the bulk solution pH remains near pH 5.0 to 6.0. The idea of developing high pH conditions near the point of base addition appears plausible, especially when considering solutions of low buffering capacity such as were utilized during this study. The extent of the development of "localized high pH" would be dictated by the rate at which hydroxyl ions could diffuse and mix throughout the bulk solution. Within the region of "localized high pH", both nickel and chromium would be predicted to insolubilize based upon equilibrium chemistry calculations. Thus, the question becomes one of insolubilization kinetics, namely whether chromium or nickel ions insolubilize more rapidly from a kinetic rate standpoint.

Examination of the literature related to the kinetic rates of chromium and nickel insolubilization show such a mechanism to be feasible. Stumm

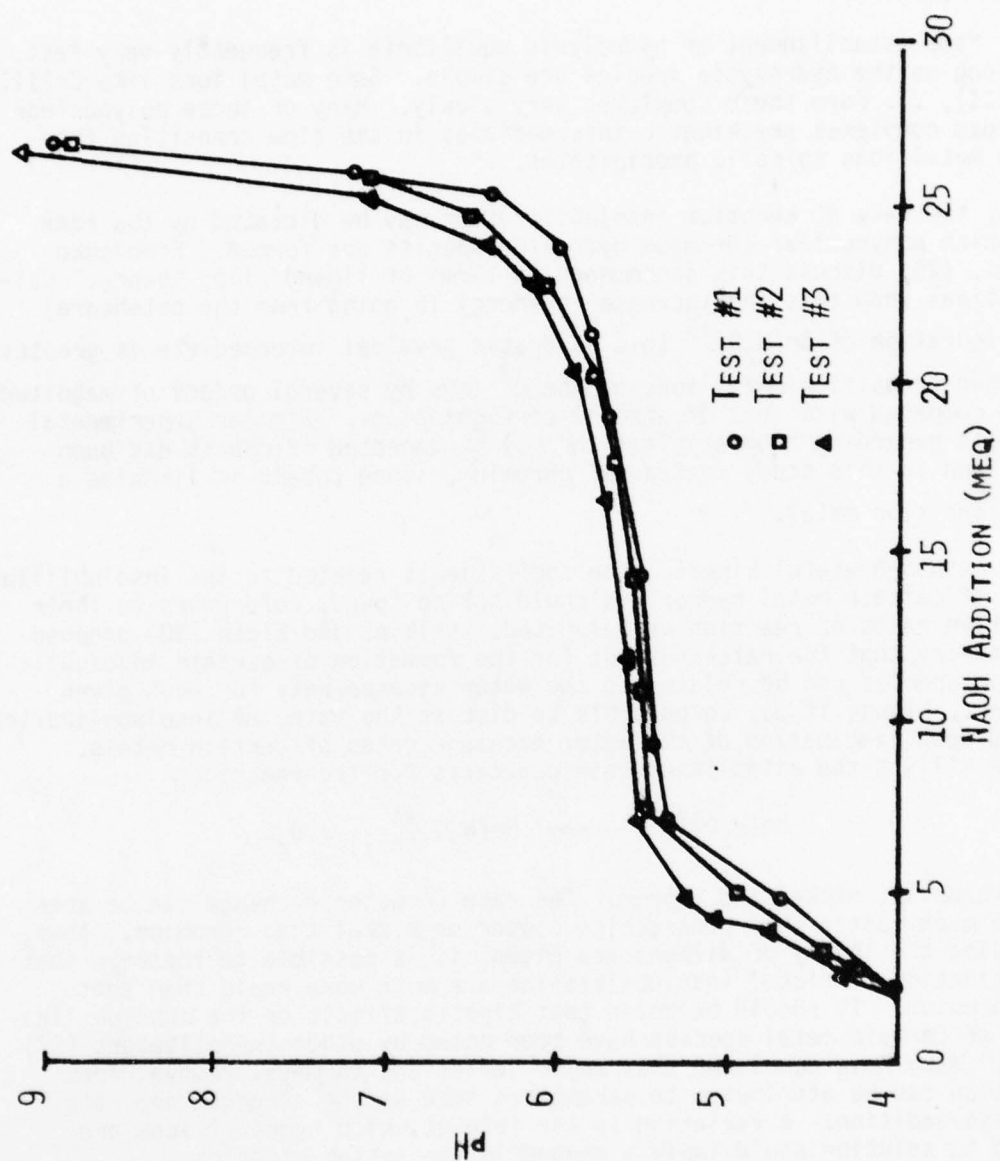


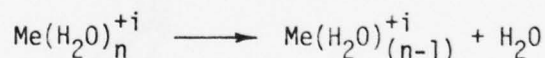
Figure (45). Alkimeric titration curves for a Cr(III) - Ni(II) metal mixture (Cr(III) = 12.2 meq, Ni(II) = 12.2 meq).

and Morgan (16) state

"the establishment of hydrolysis equilibria is frequently very fast, as long as the hydrolysis species are simple. Some metal ions like Cr(III), Co(III), ... form their complexes very slowly. Many of these polynuclear hydroxo complexes are kinetic intermediates in the slow transition from free metal ions to solid precipitates..."

Thus, the rate of chromium insolubilization may be dictated by the rate at which polynuclear chromium hydroxide species are formed. Ermolenko et al. (29) discuss this phenomenon in terms of ligand field theory. Calculations show that the increase in energy in going from the octahedral configuration of $\text{Cr}(\text{H}_2\text{O})^{+3}$ to a quadratic pyramidal intermediate is greatest for the transition metal ions of the d^3 ions by several orders of magnitude when compared with ions of other d configurations. Similar experimental results regarding "coprecipitation" may be expected if cobalt had been utilized in this study instead of chromium, since cobalt is likewise a d^3 transition metal.

Although useful kinetic rate coefficients related to the insolubilization of certain metal hydroxides could not be found, references to their relative rates of reaction were located. Wilkins and Eigen (30) propose the theory that the rate constant for the formation of certain insolubilization species can be related to the water exchange rate for that given element. Thus, it may be possible to discuss the rates of insolubilization based upon examination of the water exchange rates of certain metals. Table 8 lists the established rate constants for the reaction



for chromium, nickel and copper. The rate of water exchange can be seen to be much faster when considering copper or nickel than chromium. Thus, applying the theory of Wilkins and Eigen, it is possible to theorize that the kinetics of nickel insolubilization are much more rapid than that of chromium. It should be noted that kinetic effects on the insolubilization of certain metal species have been noted by other investigators (31) (32). Many have concluded that major variations in metal removal from solution can be attributed to parameters such as the strength and rate of base addition. A variation in the rate at which hydroxyl ions are added to solution would imply a change in the system kinetics.

To summarize, of the proposed mechanisms considered, the only one which appears viable relates to the kinetics of metals insolubilization and how large differences in kinetic rates may override conditions predicted from thermodynamic equilibrium considerations. Mechanisms related to the adsorption or inclusion of other metals during the insolubilization of chromium were found to be inadequate in the description of experimental data collected during this study.

TABLE 8. WATER EXCHANGE RATES FOR CERTAIN METAL IONS

<u>METAL ION</u>	<u>WATER EXCHANGE RATE CONSTANT ($M^{-1} \text{sec}^{-1}$)</u>
Cu^{+2}	$10^{8.3}$
Ni^{+2}	$10^{4.4}$
Cr^{+3}	$10^{-4.7}$
Fe^{+3}	$10^{0.6}$

AD-A070 233

MISSOURI UNIV-COLUMBIA DEPT OF CIVIL ENGINEERING

F/6 13/2

METAL HYDROXIDES FROM ELECTROPLATING: SLUDGE CHARACTERIZATION A--ETC(U)

MAY 79 J T NOVAK, M M GHOSH, W KNOCHE

F08635-77-C-0281

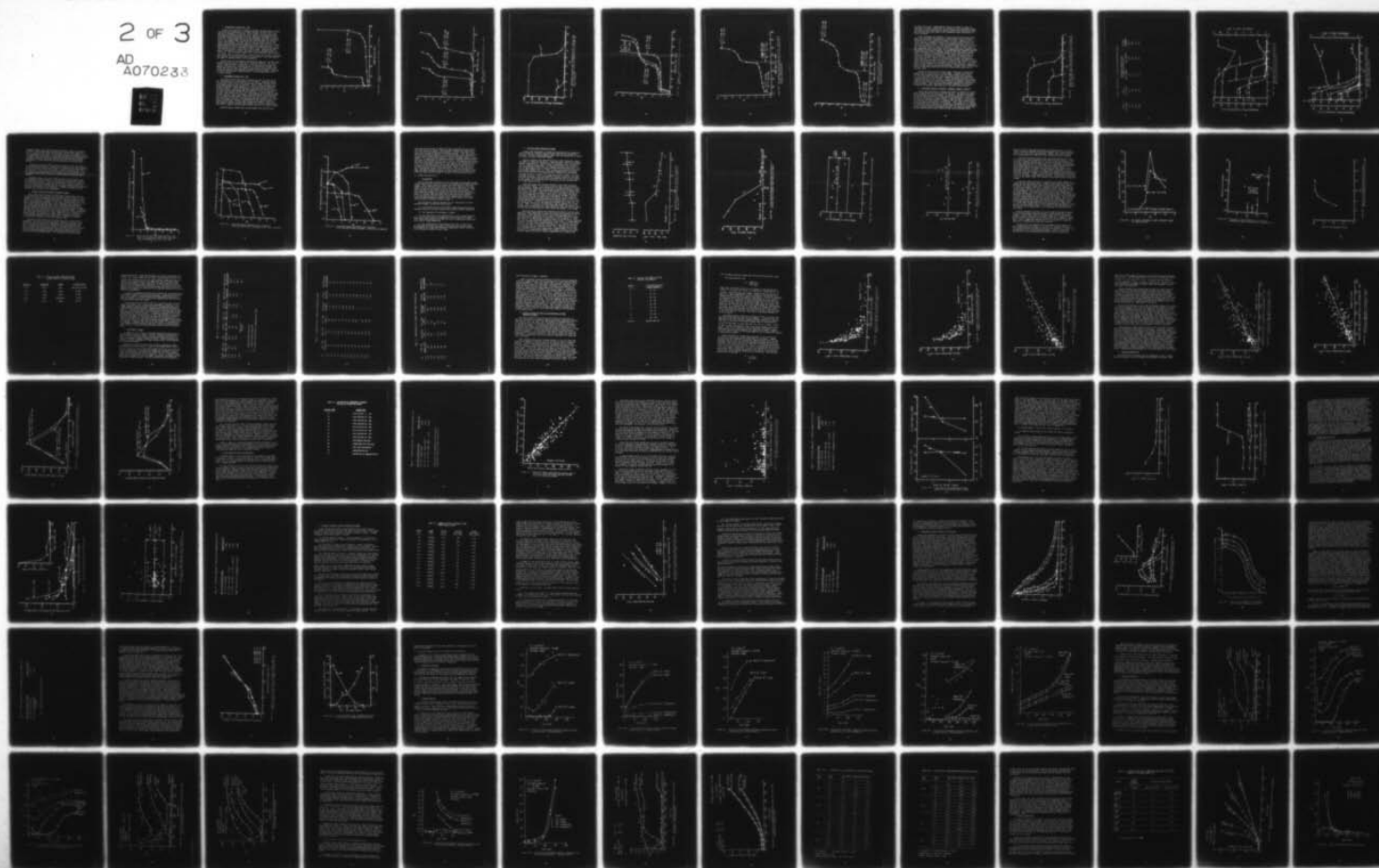
UNCLASSIFIED

AFESC/ESL-TR-79-09

NL

2 OF 3

AD
A070233



4. Mixed-Metal Studies (Fe - Ni)

Studies were undertaken to determine whether the phenomenon of "coprecipitation" was characteristic of other trivalent cations. Since iron was one of the metals of interest in this project, the iron(III)-nickel mixed-metal system was chosen for study. Results of experimental tests using the previously described titration techniques are shown in Figures 46 and 47. Close examination of the data presented shows the coprecipitation is not apparent when considering the insolubilization of iron and nickel from solution. For each ratio of iron and nickel studied, the amount of base added during the lower pH "plateau" (pH 2.8 to 3.5) closely approximates the initial iron concentration on an equivalent basis. Following addition of the stoichiometric amount of base required for complete iron insolubilization, a sharp rise in pH is noted. The solution pH is seen to approach pH 7.5 to 8.0, the range of nickel insolubilization as $\text{Ni}(\text{OH})_2(\text{s})$. After subsequent addition of a base requirement nearly equivalent to the initial nickel present, a second rise in pH is noted, signifying the complete insolubilization of both iron and nickel. Thus, two distinct pH ranges of insolubilization can be determined.

Studies were also performed to determine the amount of iron and nickel removed from solution as a function of insolubilization pH. The results of this study are shown in Figure 48. It can be clearly seen that no apparent interaction or "coprecipitation" is taking place. Rather, both nickel and iron are seen to be removed from solution in pH ranges which correspond closely to the theoretic insolubilization pH ranges. Therefore, it can be concluded that "coprecipitation" is not characteristic of all trivalent cations.

5. Mixed-Metal Studies (Cu - Ni)

The intent of this study was to evaluate the fate of nickel during the insolubilization of other metals such as copper. Copper was chosen for evaluation with nickel since the pH range of copper insolubilization corresponds closely to that of chromium. Various ratios of copper and nickel concentrations were examined in a series of insolubilization and titration studies. Figures 49 through 51 show representative results of these studies. Each graph shows the characteristic titration response that would be predicted by equilibrium chemistry. A low pH "plateau" is seen in the range of pH 5.5 to 6.2, corresponding to the range of copper insolubilization. Once a base amount roughly equivalent to the concentration of copper has been added, a distinct rise in pH is noted, with the pH rising to pH 7.5 to 8.0. Continued base addition results in the formation of a second pH "plateau", corresponding to the insolubilization of nickel from solution. Finally, when an equivalent amount of base has been added to insolubilize the nickel present in solution, a second rapid rise in pH is noted, signifying the insolubilization of all metals present.

Insolubilization studies were also performed using varying ratios

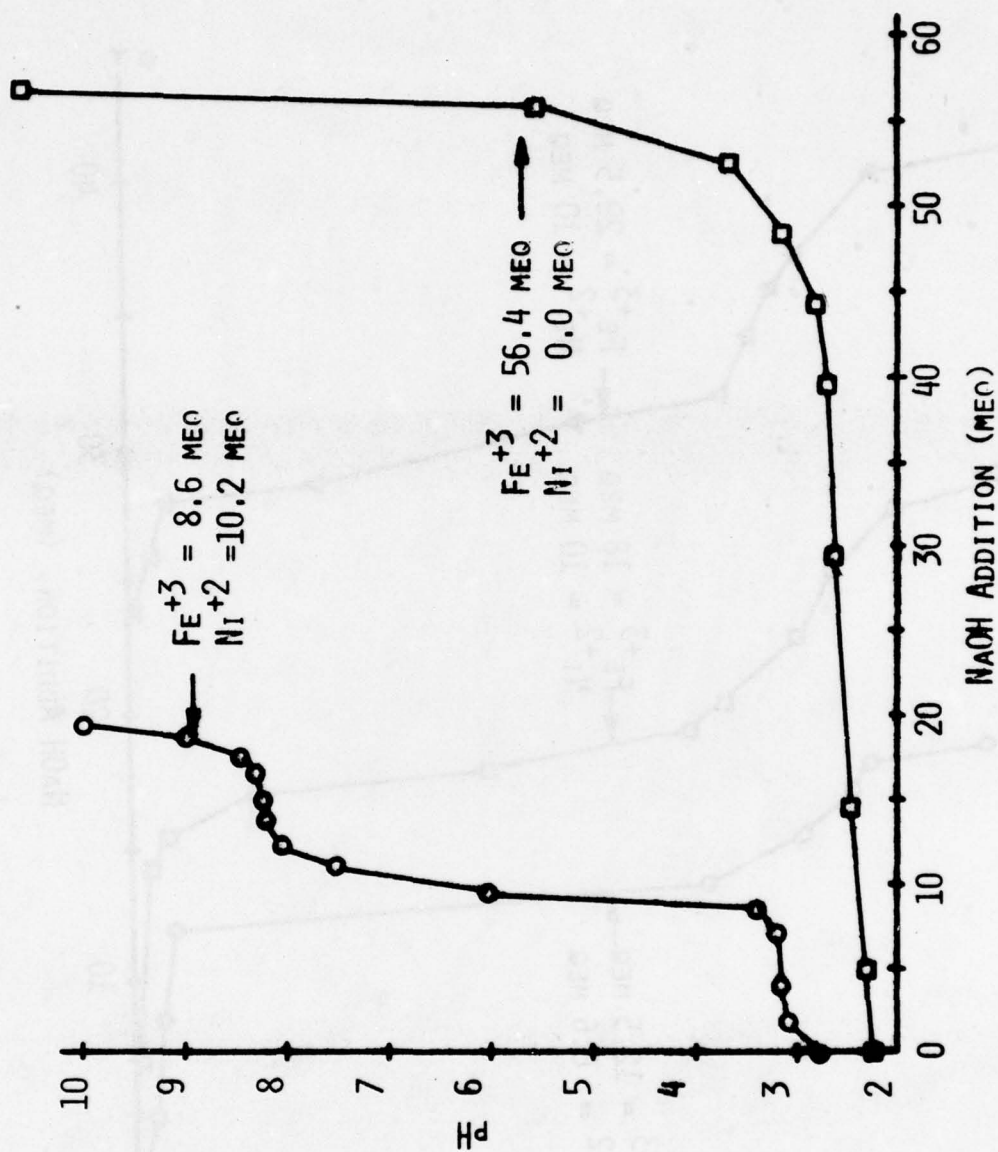


Figure (46). Alkometric titration curves for Fe(III) - Ni(II) metal mixtures.

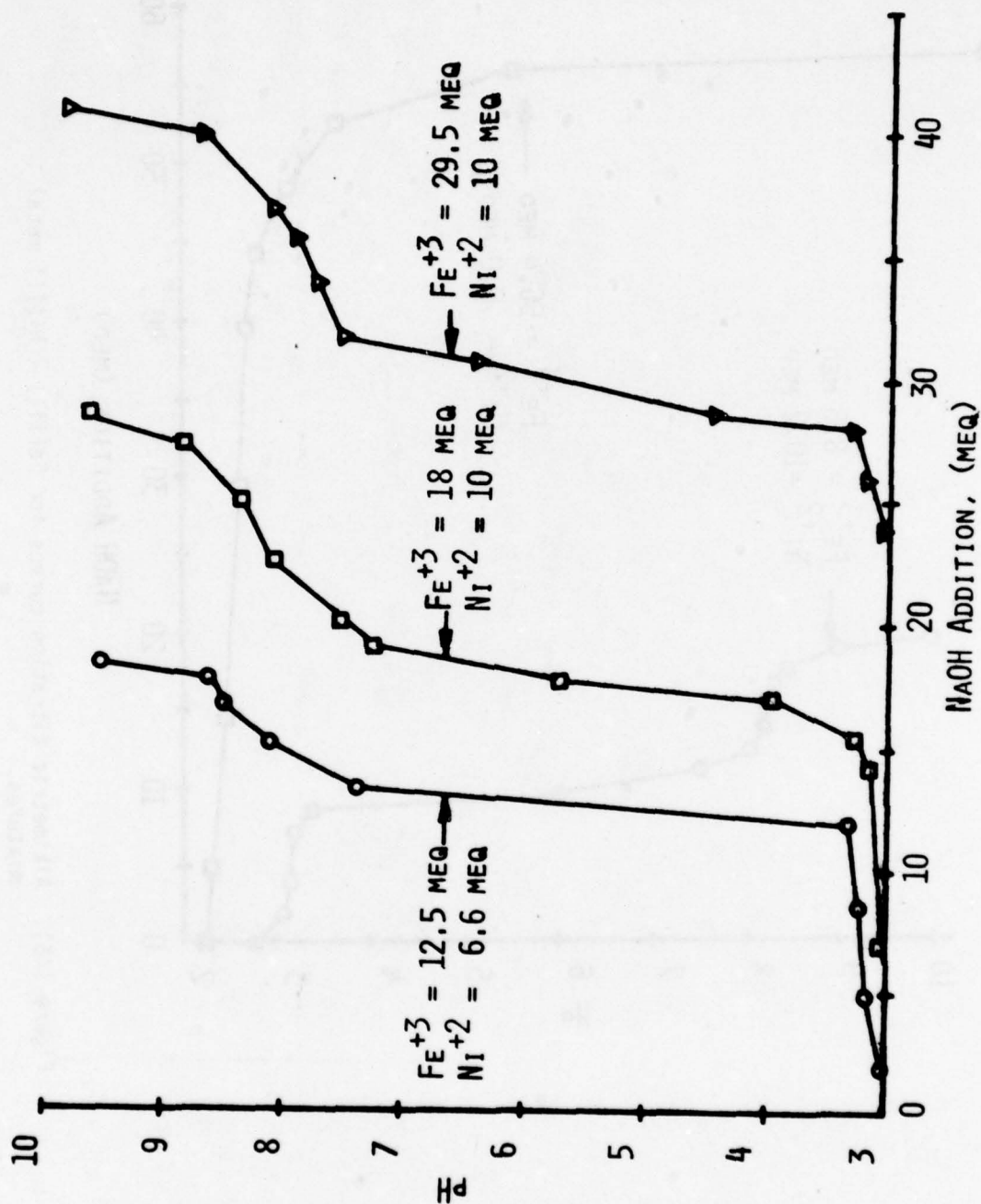


Figure (47). Alkometric titration curves for several Fe(III) - Ni(II) metal mixtures.

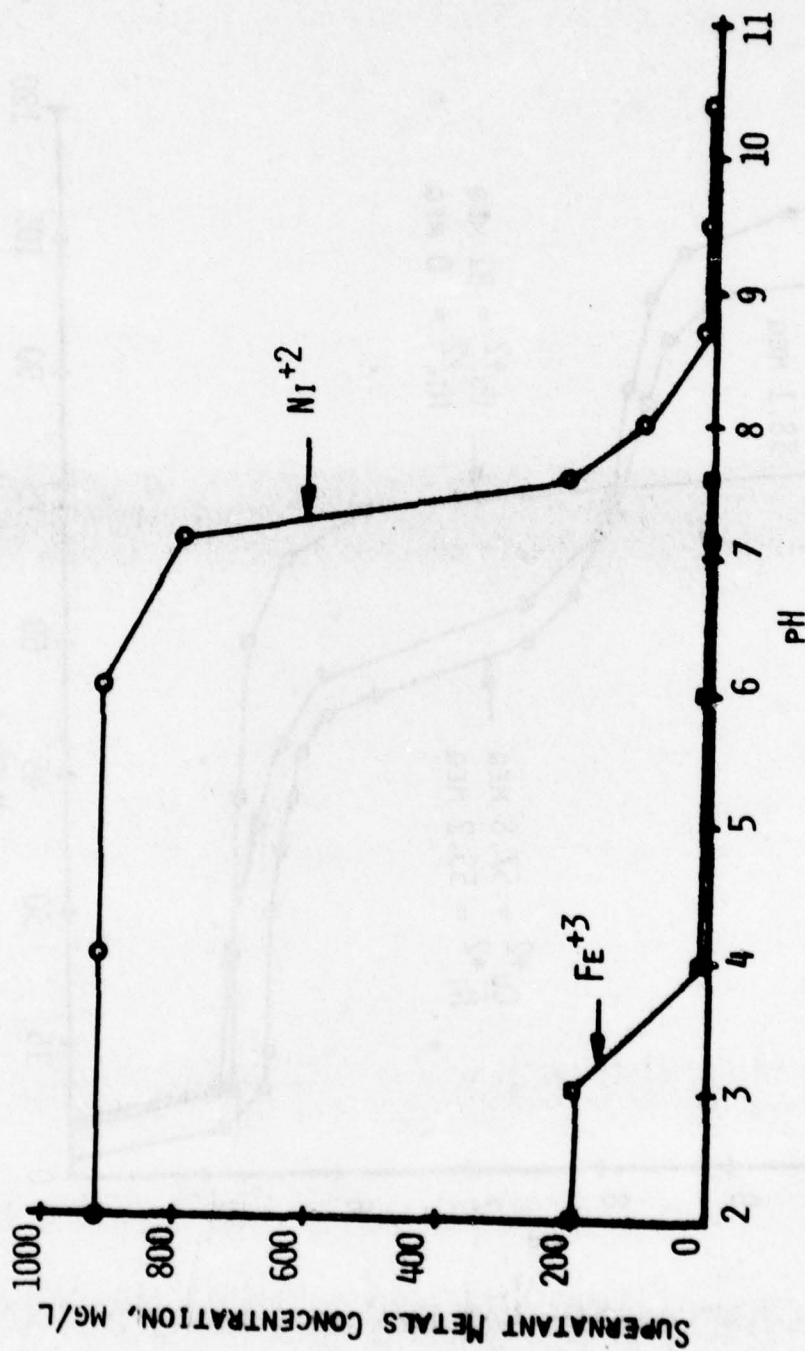


Figure (48). Supernatant iron and nickel concentrations as a function of pH for a settled sample containing 200 mg/l Fe(III) and 900 mg/l Ni(II) initially.

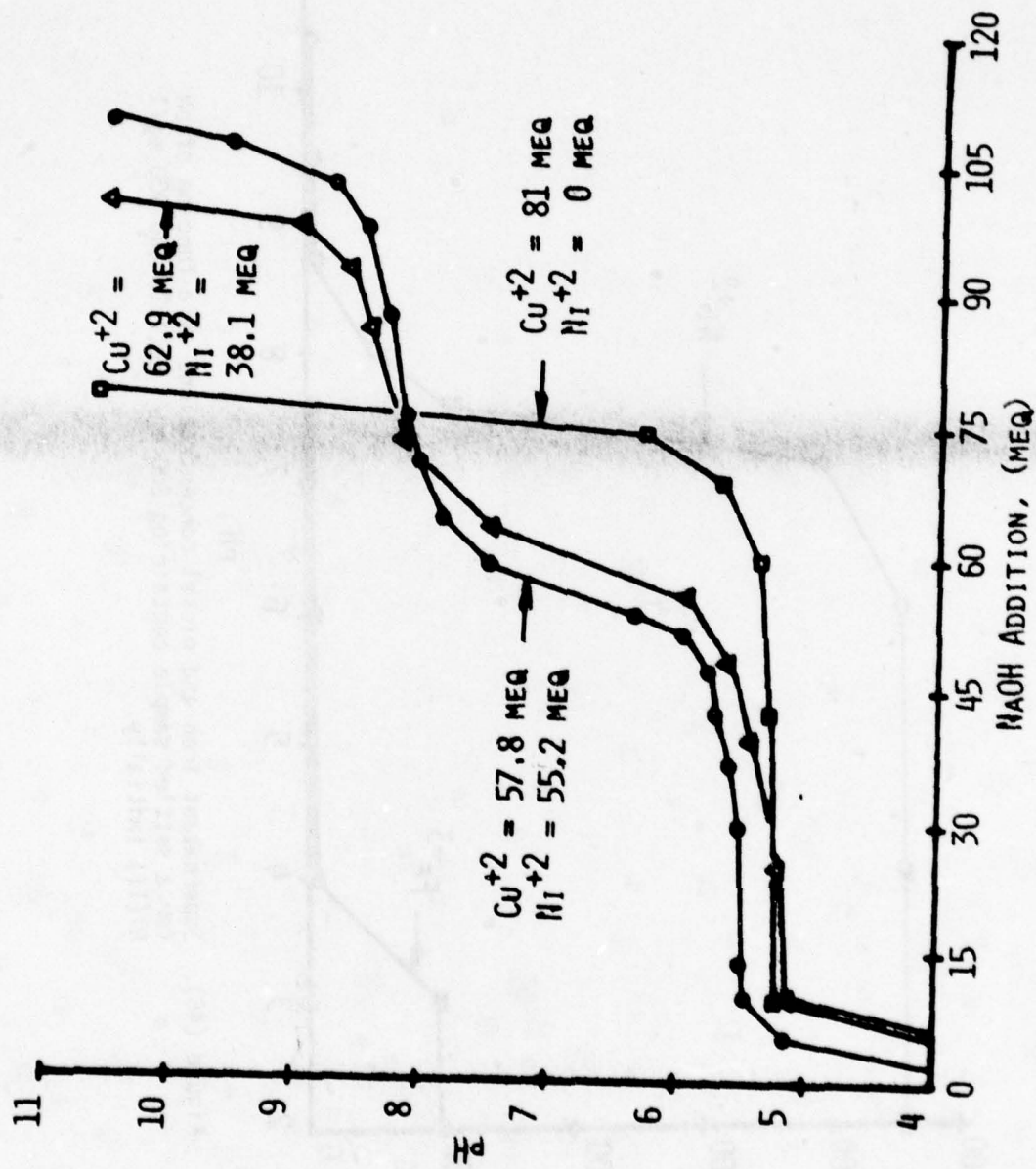


Figure (49). Alkometric titration curves for several Cu(II) - Ni(II) metal mixtures.

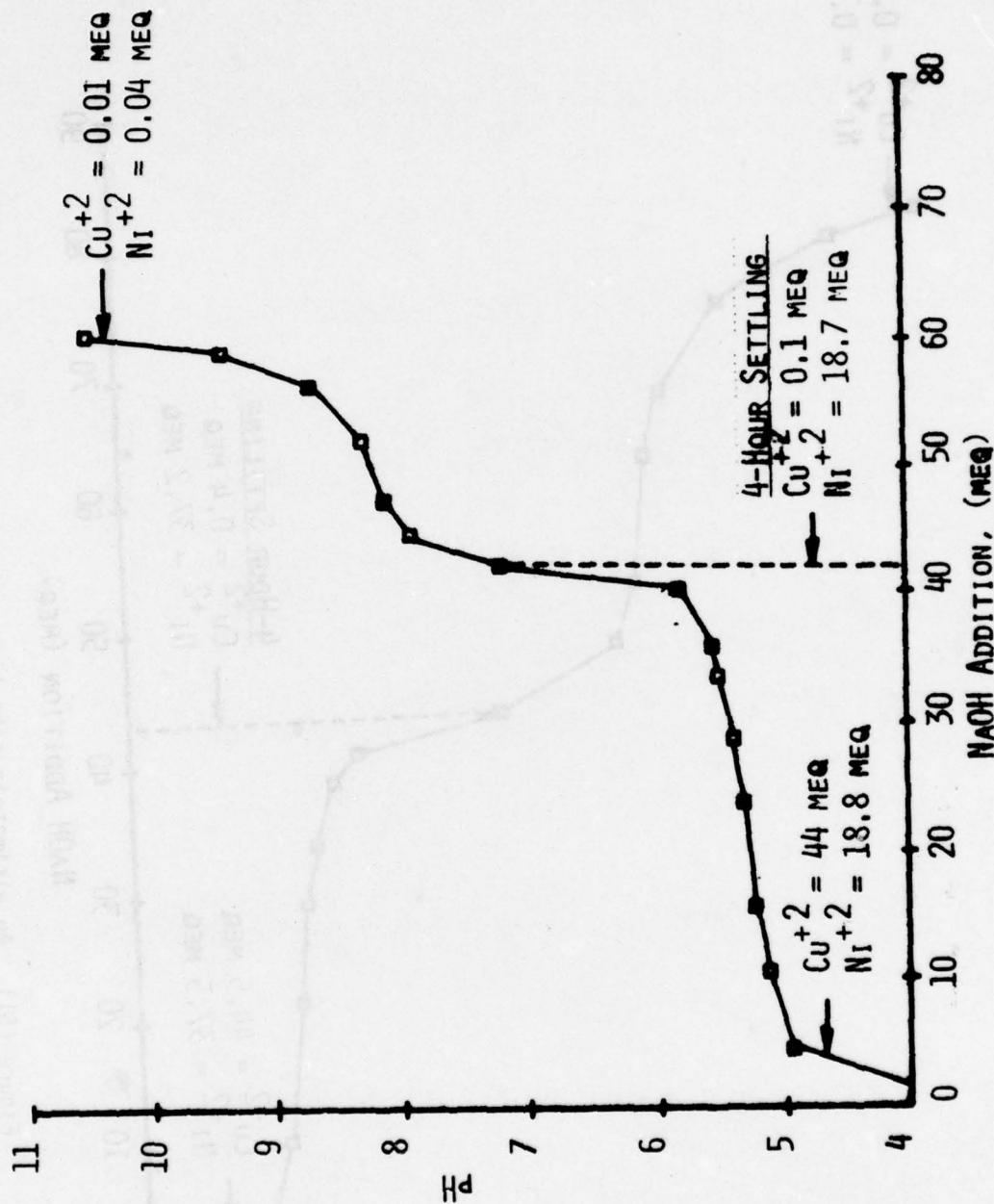


Figure (50). An alkimetric titration curve for a Cu(II) - Ni(II) metal mixture, showing the possibilities for the application of "selective precipitation".

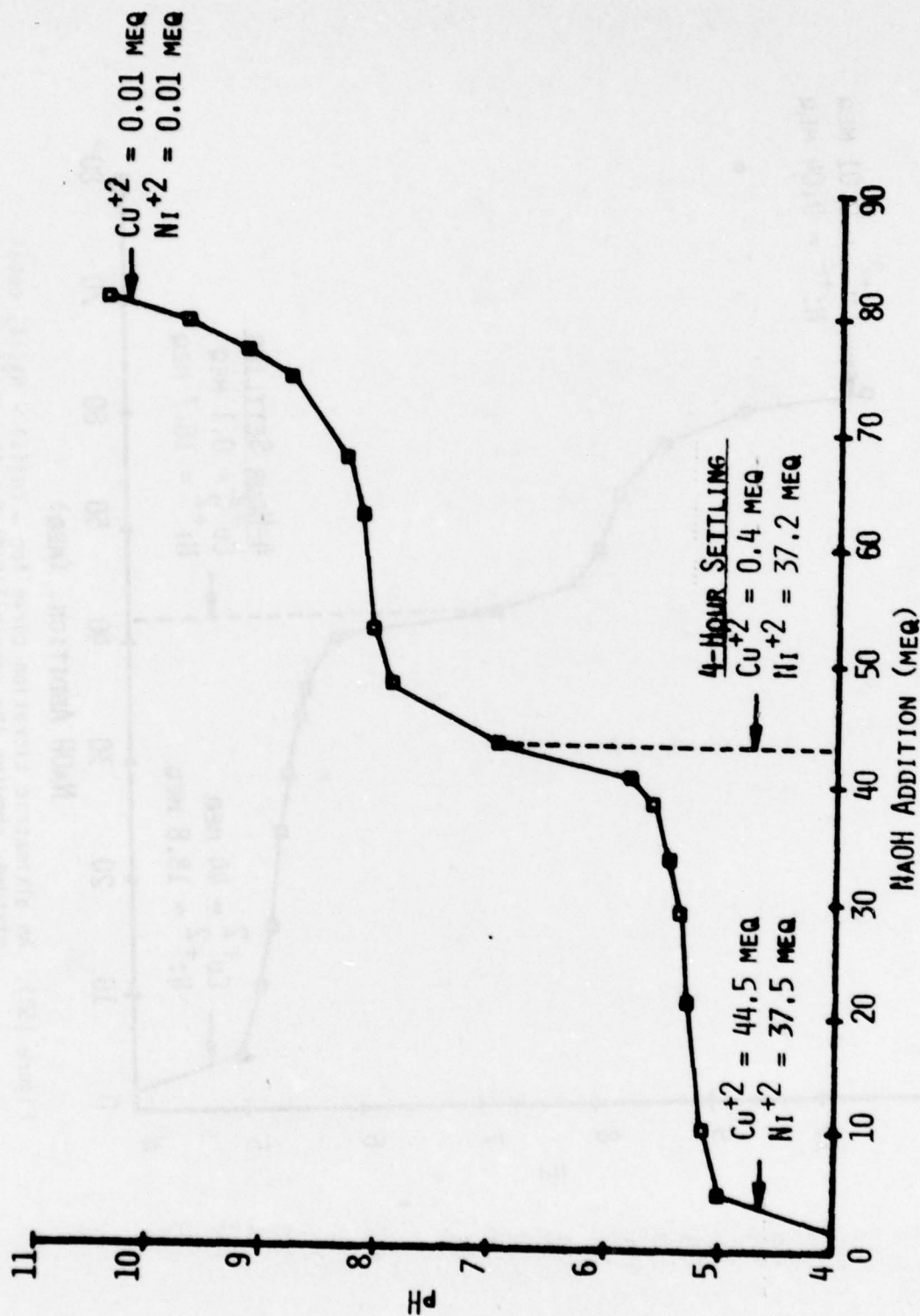


Figure (51). An alkometric titration curve for a Cu(II) - Ni(II) metal mixture, showing the possibilities for the application of "selective precipitation".

of copper and nickel. Representative results are shown in Figure 52. Examination of these results show no interaction occurring between copper and nickel; rather, each metal is seen to insolubilize from solution under pH conditions which would predict the formation of metal hydroxides for these two metals.

From an engineering standpoint, studies such as these provide useful data since they point the way toward a possible metal recovery method. Analyzing the distinct separation ranges for nickel, copper and iron insolubilization, it appears plausible that "selective precipitation" may be a viable recovery method. Selective precipitation would involve increasing the solution pH to a value which would render one metal insoluble, yet allow other metals to remain in solution. Studies of this nature were undertaken utilizing various initial copper and nickel concentrations. The results are listed in Table 9. It can be seen that "selective precipitation" would be a viable treatment method for this mixed-metal system since it is possible to separate and recover both nickel and copper in relatively pure hydroxide suspensions. The method of separation would involve the insolubilization and precipitation of cupric hydroxide at a pH value near 7.0. After a sufficient settling time, the supernatant liquor laden with soluble nickel would be drawn off and treated in a second basin with additional base to produce a solution pH near 10.0. This would result in the formation of a relatively pure nickel hydroxide suspension which likewise could be settled and collected. In each case, a concentrated slurry of each metal hydroxide could be collected which would have an economic value.

"Selective precipitation" systems appear promising for mixed-metal systems such as iron-nickel and nickel-copper. However, referring to the previously-reported results for the chromium mixed-metal systems, it can be seen that efficient metals separation cannot be achieved when "coprecipitation" is seen to occur. Studies performed during this investigation have shown it is relatively impossible to separate chromium from nickel or other divalent metal cations through conventional insolubilization techniques. Each individual mixed-metal system must be analyzed related to the economic applicability of "selective precipitation".

6. Mixed Metal Studies (Chromium - Cadmium - Copper - Nickel)

Studies were undertaken to examine the effect of chromium on a mixed-metal system containing several divalent cations. The metals considered included copper, nickel and cadmium. In addition, the fate of sulfates during the insolubilization of these metals was determined. Figures 53 and 54 are the results of these studies. Figure 53 shows, in the absence of chromium, each metal species is removed from solution as would be predicted by equilibrium chemistry calculations. Also, there is no evidence of "coprecipitation" occurring. Furthermore, a disappearance in sulfates from solution can be detected over the pH range 6.5 to 10.5, corresponding to the insolubilization of the metals present. At higher pH values, the sulfate concentrations remain similar to the initial sulfate levels.

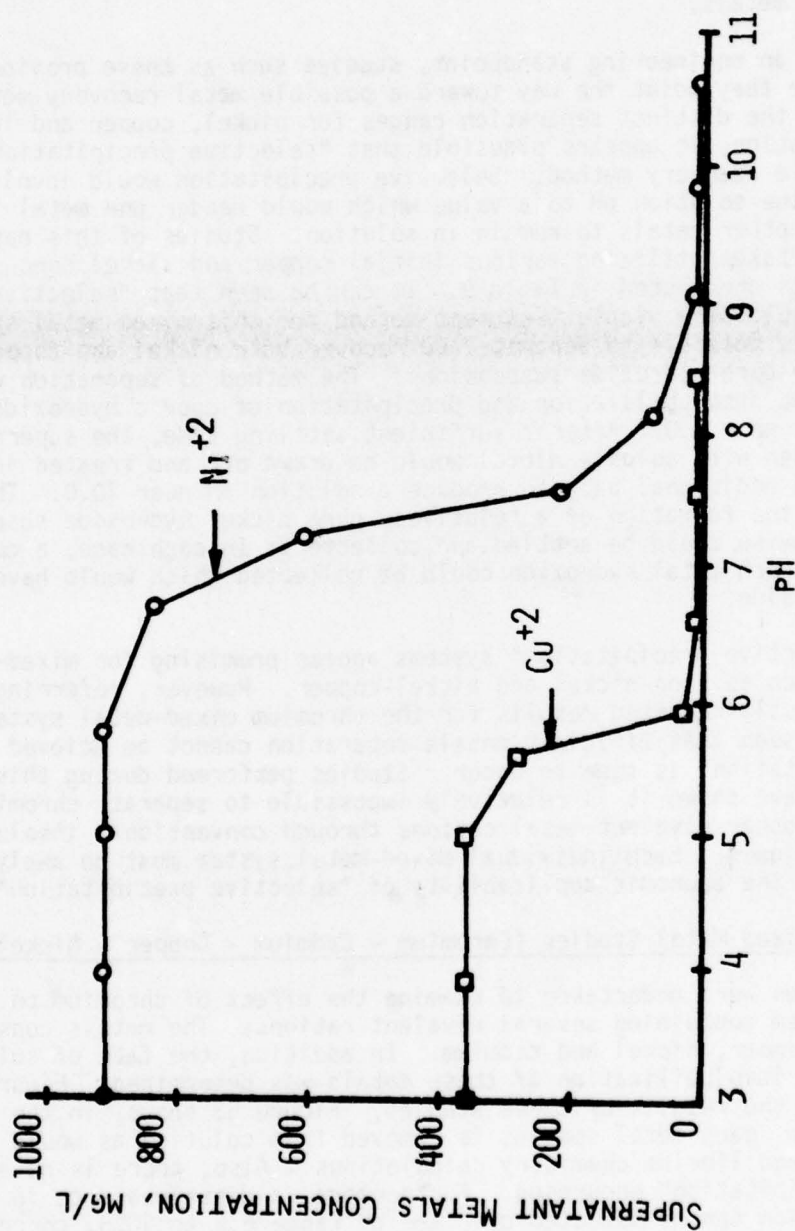


Figure (52). Supernatant copper and nickel concentrations as a function of pH for a settled sample containing 350 mg/l $Cu(II)$ and 900 mg/l $Ni(II)$ initially.

TABLE 9. RESULTS OF Cu - Ni "SELECTIVE PRECIPITATION" STUDIES

INITIAL Cu ⁺² (mg/l)	INITIAL Ni ⁺² (mg/l)	SUPERNATANT CONCENTRATIONS FOLLOWING SETTLING AT pH 7		% NICKEL RECOVERED
		Cu (mg/l)	Ni (mg/l)	
720.	1120.	6.8	1100.	98.2
720.	560.	5.0	550.	98.2
1350.	700.	7.7	680.	97.1
1000.	560.	4.2	535.	95.6

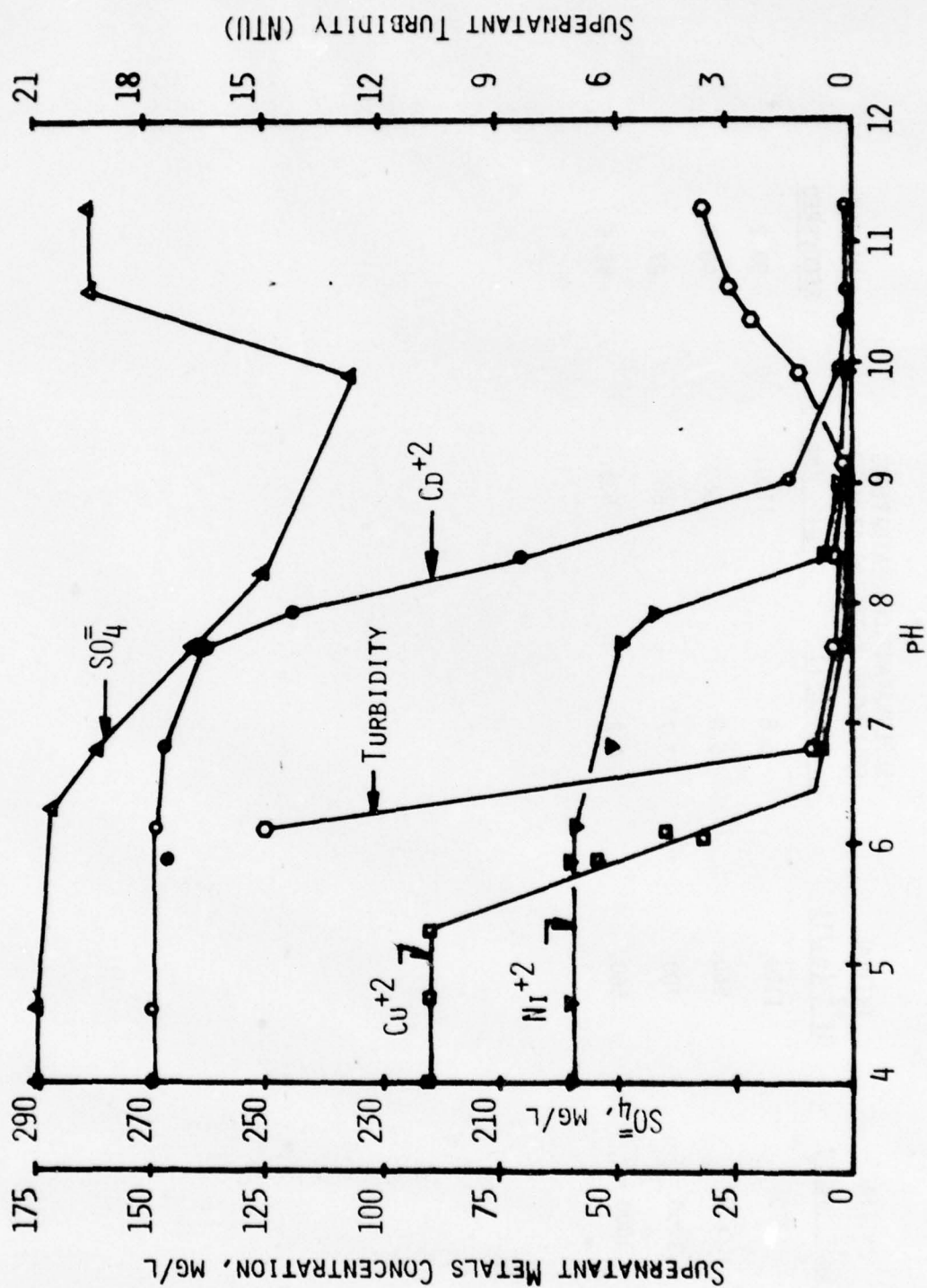


Figure (53). Supernatant metals and sulfate concentrations and supernatant turbidity as a function of pH (mixed-metal system containing no Cr(III)).

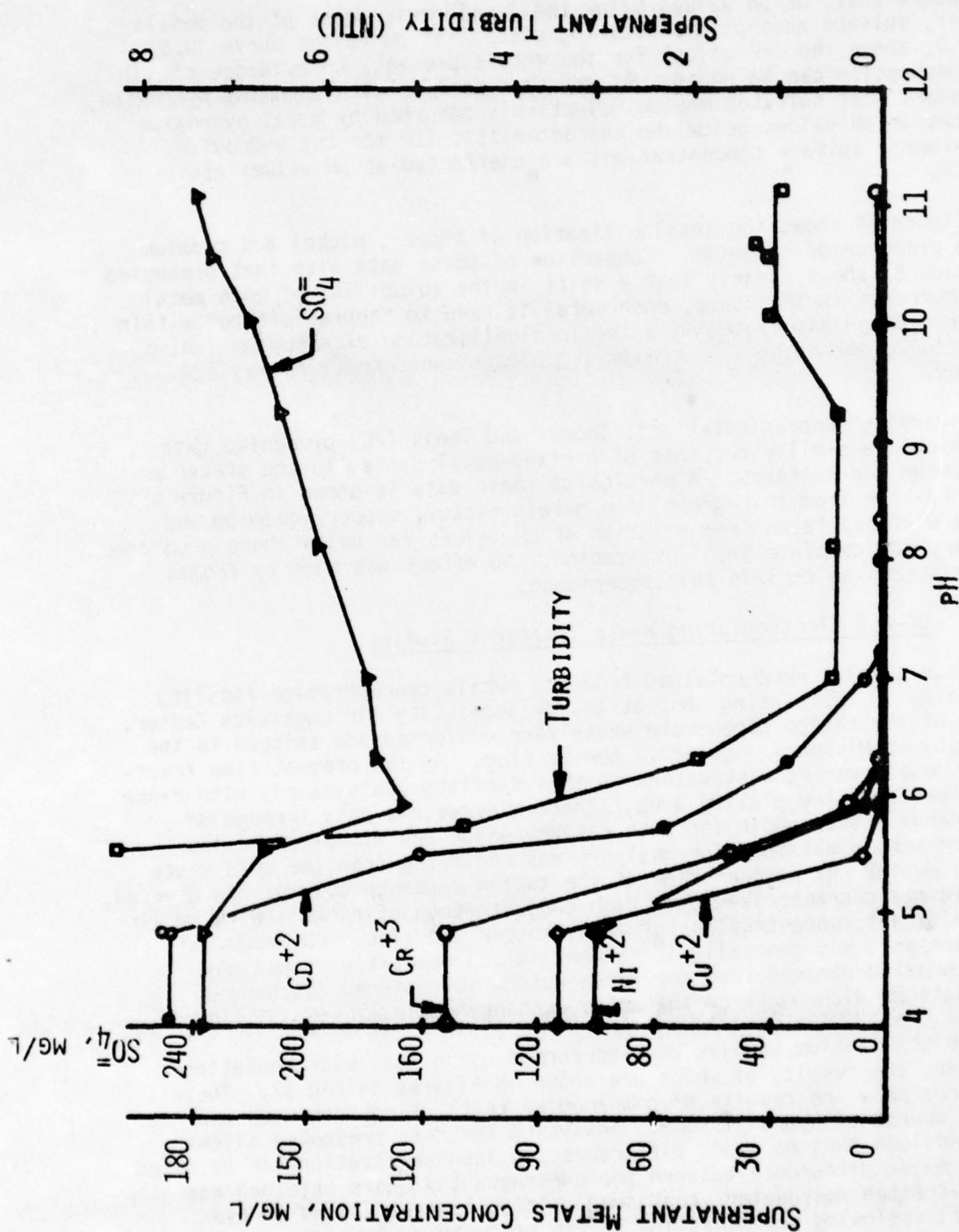


Figure (54). Supernatant metal and sulfate concentrations and supernatant turbidity as a function of pH (mixed-metal system containing Cr(III)).

It appears that, at pH values below the isoelectric point of the metals present, sulfate adsorption is taking place. At pH values above 10.5 to 11.0, above the IEP values for the metals present, no evidence of sulfate adsorption can be noted. As was seen earlier with chromium hydroxide, it appears that sulfates may be selectively adsorbed by metal hydroxide surfaces at pH values below the characteristic IEP for the hydroxide. Furthermore, sulfate concentrations are unaffected at pH values above the IEP.

Figure 54 shows the insolubilization of copper, nickel and cadmium in the presence of chromium. Comparison of these data with that presented in Figure 53 shows clearly that a shift in the solubility of each metal has occurred. In this case, each metal is seen to "coprecipitate" within the range of pH associated with the insolubilization of chromium. Also, it should be noted that a decrease in sulfate concentrations was again observed.

Regarding "coprecipitation", Thomas and Theis (20) presented data which showed a similar response of a mixed-metal system to the presence of chromium and sulfates. A portion of these data is shown in Figure 55. As can be seen from this graph, the metals nickel, copper, cadmium and zinc were precipitated from solution at pH values far below those predicted necessary for complete insolubilization. No effort was made by Thomas and Theis (20) to explain this phenomenon.

7. OC-ALC Electroplating Waste Treatment Studies

Waste samples were obtained from the metals concentration facility as operated in the plating shop at the Oklahoma City Air Logistics Center. Samples of the cation regenerate waste were collected and shipped to the University of Missouri - Columbia for testing. At the present time treatment of metal-bearing wastewaters at this facility deals mainly with rinse water flows from the plating shop. These rinsewaters pass through an ion exchange system employing both cation, anion and mixed-bed resins. The waste sample obtained for analysis was collected from the acid waste produced during the regeneration of the cation exchange column. In general, the waste was characterized by a high concentration of nickel, with smaller but significant concentrations of iron, copper and zinc. Chromium, although present, was generally in rather limited quantities since most of the chromium removed from the rinse waters is captured (exchanged) as chromate or dichromate on the anion exchange resin.

Insolubilization studies were performed using this electroplating wastewater, the results of which are shown in Figures 56 and 57. These two figures show the results of comparative tests using both NaOH and CaO as a source of hydroxyl ions. Analyzing the data presented allows one to conclude that no major differences in insolubilization can be noted. The only major difference between the supernatant liquors obtained was the lime-treated wastewaters contained calcium concentrations of over 2,500 mg/l following sedimentation. This produced a rinse water which

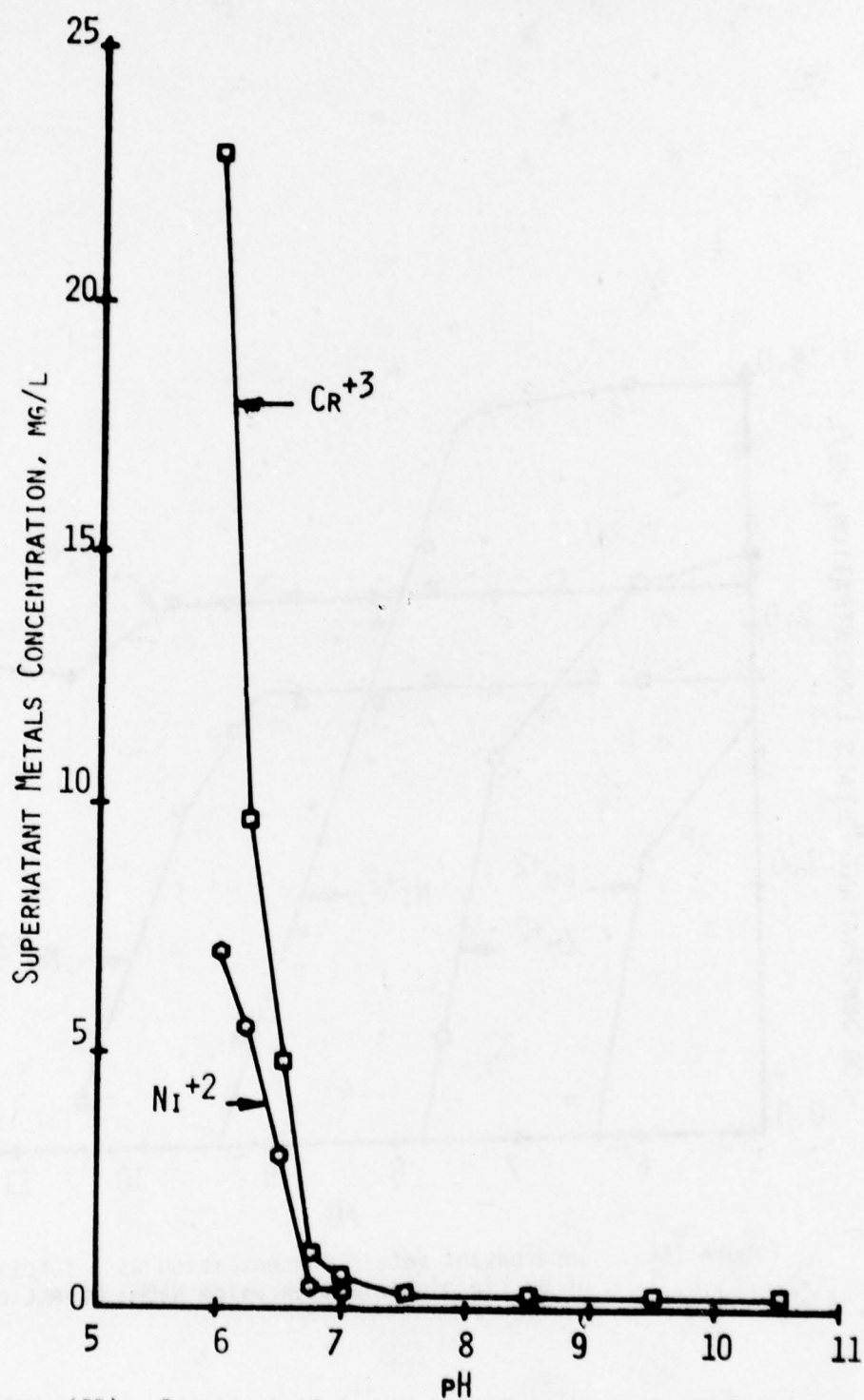


Figure (55). Representative data from Thomas and Theis (20).
Note: All supernatant $\text{Cu}(\text{II})$, $\text{Cd}(\text{II})$ and $\text{Zn}(\text{II})$ concentrations were less than 1 to 2 mg/l.

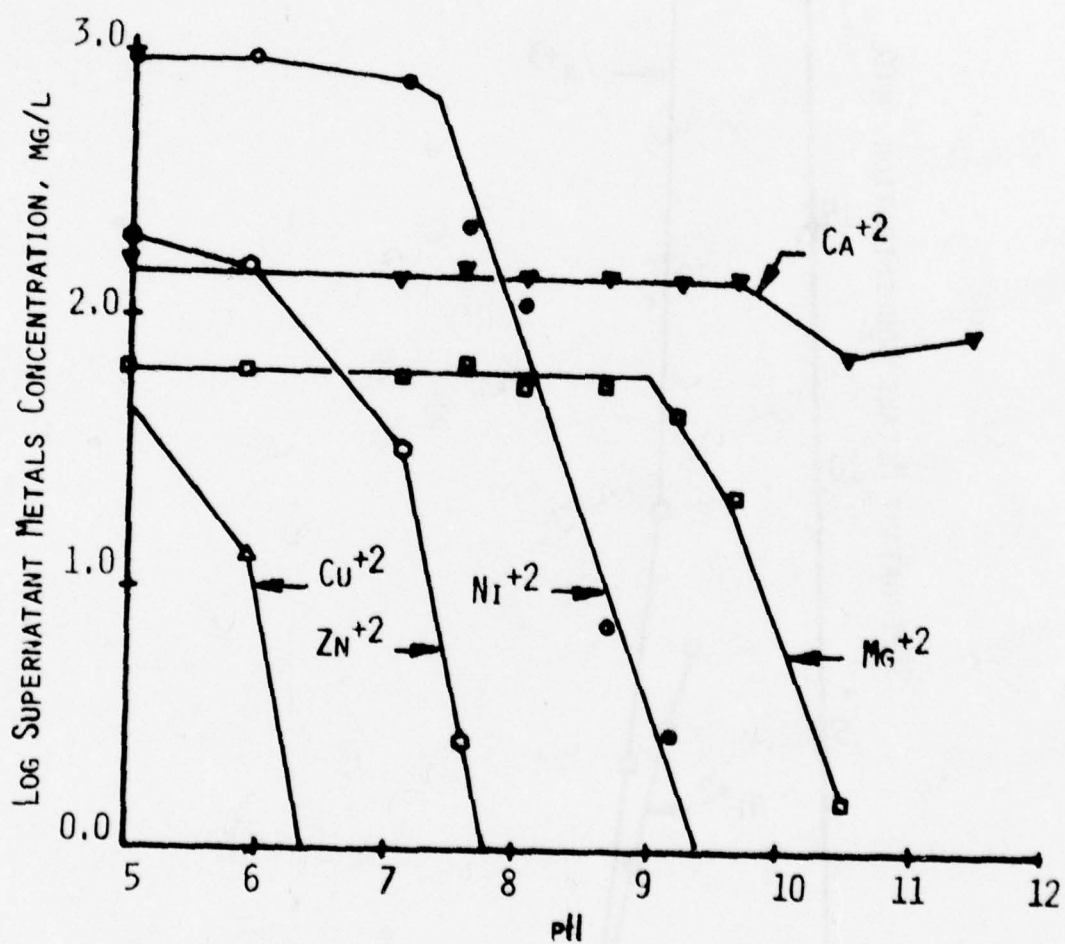


Figure (56). Supernatant metals concentration as a function of pH (insolubilization using NaOH) UC-ALC cation regenerant.

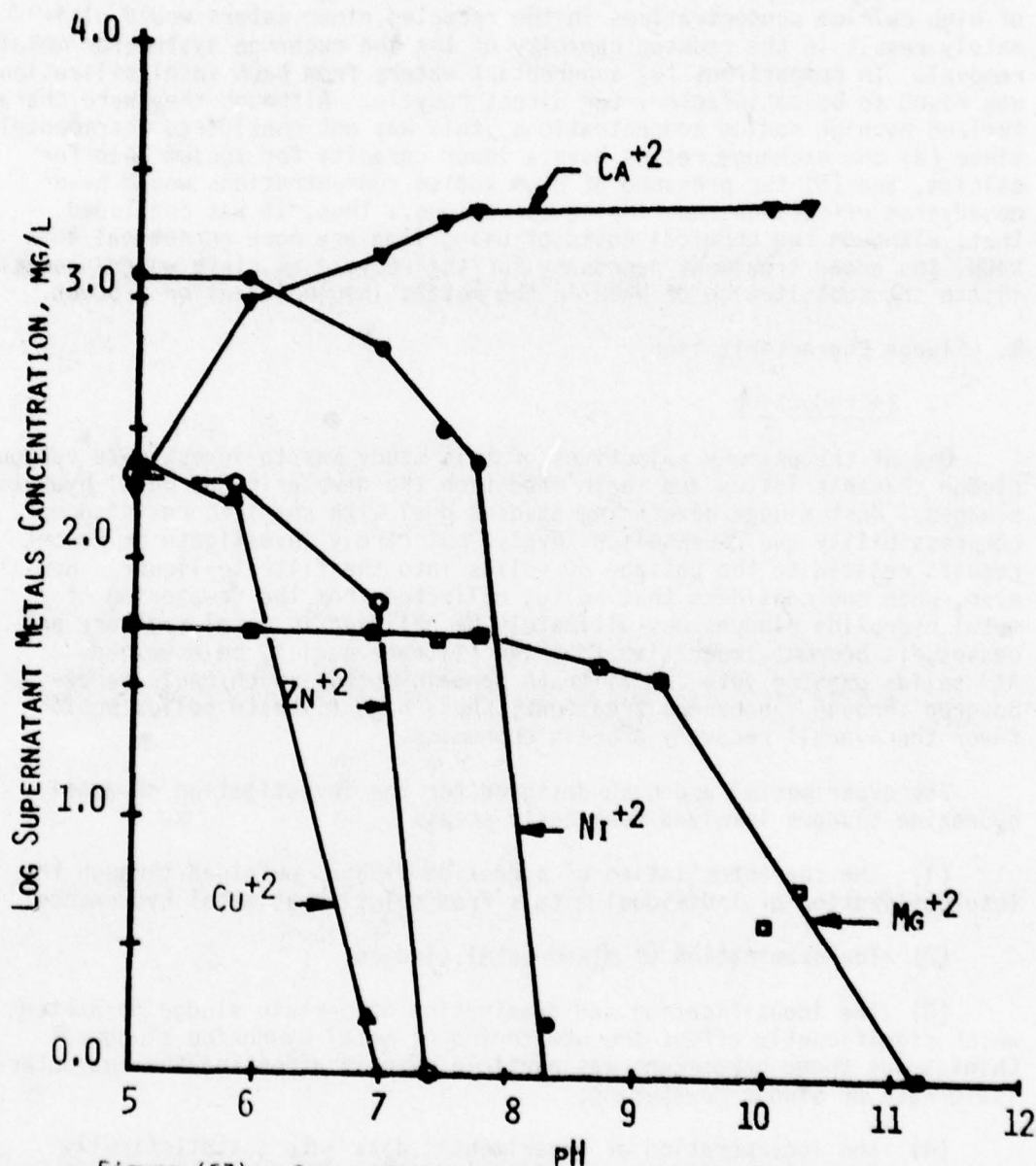


Figure (57). Supernatant metals concentration as a function of pH (insolubilization using CaO). OC-ALC cation regenerant.

would necessitate further treatment for water softening prior to recycle into the rinse water system. The additional treatment was deemed necessary since the ion exchange resin presently utilized in the waste treatment facility showed a capacity for calcium exchange. Thus, the presence of high calcium concentrations in the recycled rinse waters would ultimately result in the reduced capacity of the ion exchange system for metals removal. In comparison, the supernatant waters from NaOH insolubilization was found to be satisfactory for direct recycle. Although they were characterized by high sodium concentrations, this was not considered detrimental since (a) the exchange resins have a lower capacity for sodium than for calcium, and (b) the presence of high sodium concentrations would have no adverse effects on the rinsing operations. Thus, it was concluded that, although the chemical costs of using lime are more economical than NaOH, the added treatment necessary for the recycle of rinse waters necessitate the substitution of NaOH in the metals insolubilization process.

B. Sludge Characterization

1. Introduction

One of the primary objectives of this study was to investigate various sludge characteristics and their effect on the dewatering of metal hydroxide sludges. Most sludge dewatering studies deal with specific resistance, compressibility and cake solids levels, but rarely investigate or report results related to the passage of solids into the filtrate liquor. However, when one considers that solids collected from the dewatering of metal hydroxide sludges may ultimately be utilized in metal recovery processes, it becomes imperative that the filtrate quality be examined. All solids passing into the filtrate contain metals which could be recovered through subsequent treatment; thus, high filtrate solids would favor the overall recovery process economics.

The experimental approach designed for the investigation of metal hydroxide sludges involved four basic steps:

- (1) The characterization of hydroxide sludges obtained through the insolubilization of individual metals from solution as metal hydroxides;
- (2) The examination of mixed-metal sludges;
- (3) The identification and examination of certain sludge parameters which significantly affect the dewatering of metal hydroxide sludges. Chief among these parameters was particle size in affecting the characteristic rate of sludge dewatering;
- (4) The incorporation of experimental data into a statistically derived model which would be useful in predicting the rate and extent of dewatering of a given metal hydroxide sludge given certain characteristic information related to that sludge.

2. Individual Metal Hydroxide Sludges

Studies were undertaken to examine and characterize the sludges produced through the insolubilization of metals from solution as metal hydroxides. The main research emphasis dealt with the examination of chromium, nickel and cupric hydroxide sludges.

Results related to the characterization of nickel hydroxide sludges are shown in Figures 58 through 61. Figure 58 shows a direct relationship between sludge particle size and specific resistance; also, the indirect role of sludge pH can be noted. As the insolubilization pH increases, the resultant mean sludge floc size likewise increases, going from a low size of approximately 9 to 11 microns at pH 8-9 to a high near 20 microns at pH values greater than 11.5. Also, as the particle size increases, the resultant specific resistance decreases substantially, decreasing from high values of $175-200 \times 10^{11}$ m/kg near pH 8-9 to $75-80 \times 10^{11}$ m/kg at higher pH values. Thus, pH indirectly relates to specific resistance since the insolubilization pH affects the resulting size of flocs present in the sludge. This resulting size distribution in turn characterizes the sludge dewatering rate.

Figure 59 relates the filtrate turbidity to the nickel hydroxide pH of insolubilization. At pH values near 8-9, high filtrate turbidity can be observed. Referring to the particle size data presented in Figure 58 shows this pH range to be characterized by particles of extremely small size (9 to 11 microns). Since the filter medium utilized in these filtration studies was near 8 microns in pore size, a relatively high amount of solids passage may be related to the passage of extremely fine particles through the cake and supporting filter medium. As the sludge pH increases, the amount of solids passing into the filtrate is seen to decrease dramatically, approaching filtrate turbidity levels of 2 to 5 FTU at high pH values. In this pH range, the characteristic sludge floc size has increased, resulting in the presence of smaller amounts of fine particles. Thus, in reference to nickel hydroxide sludges, pH plays an important role in determining the sludge dewatering rate and filtrate quality by affecting the characteristic size of particles present in the sludge.

Figures 60 and 61 present data related to the effect of pH on nickel hydroxide sludge compressibility and cake solids levels obtained following dewatering. Figure 60 shows no direct relationship between pH and "s", the coefficient of compressibility; rather, all nickel hydroxide sludges were found to be compressible to some extent, with an average "s" value near 0.9-1.0. By placing 90% confidence limits on the "s" values determined, it can be concluded that the sludge pH has little effect on sludge compressibility. For the nickel sludges examined, this is a logical conclusion since, as was shown in Figure 58, the changes in particle size observed as a function of pH are relatively small. Thus, although the floc mean size increases from 9-11u at low pH values to approximately 20u at high pH values, it is questionable whether this change in particle size would produce a marked variation in particle compressibility, assuming that

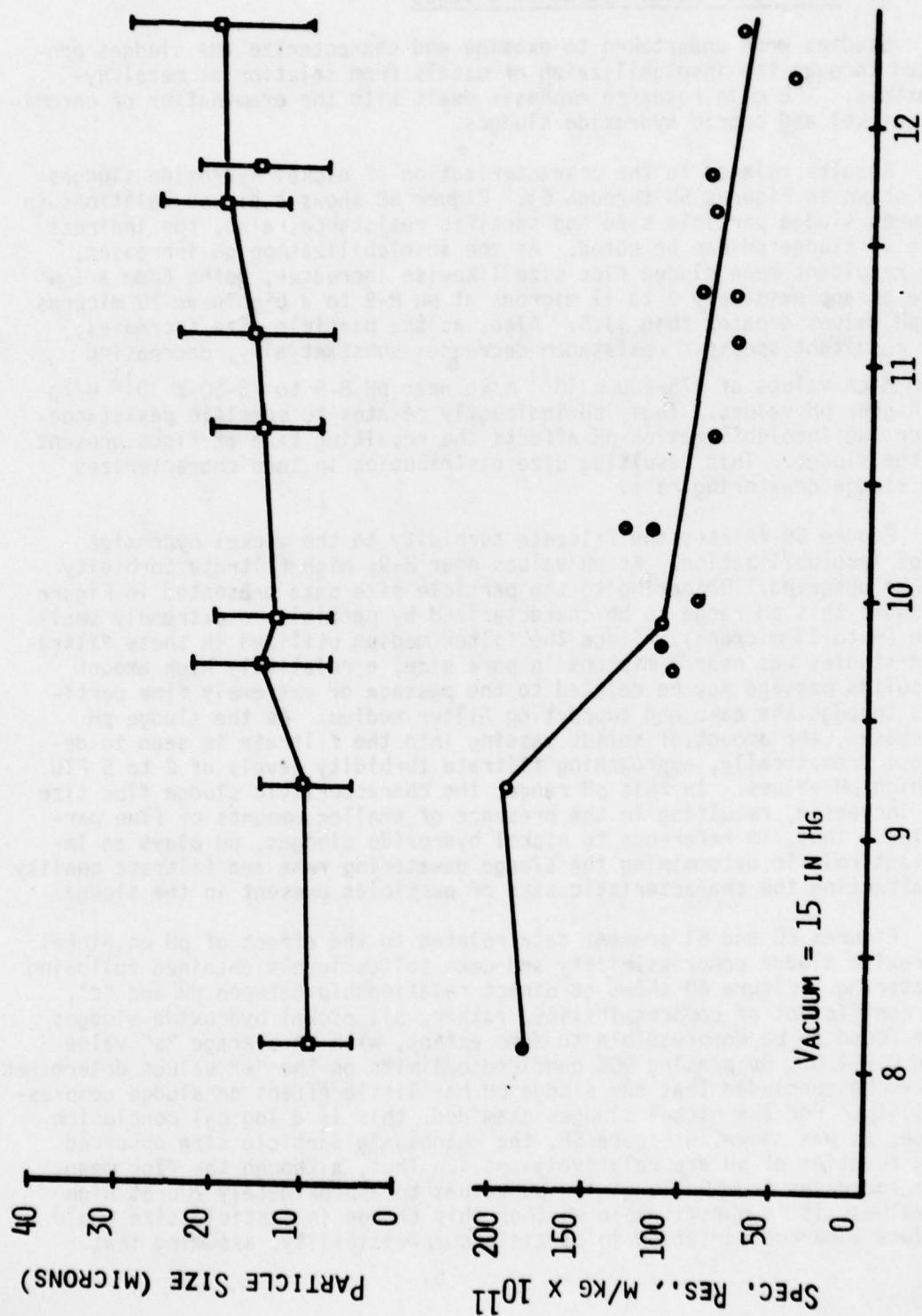


Figure (58). The characteristic sludge floc size and corresponding specific resistance of nickel hydroxide sludges as a function of pH.

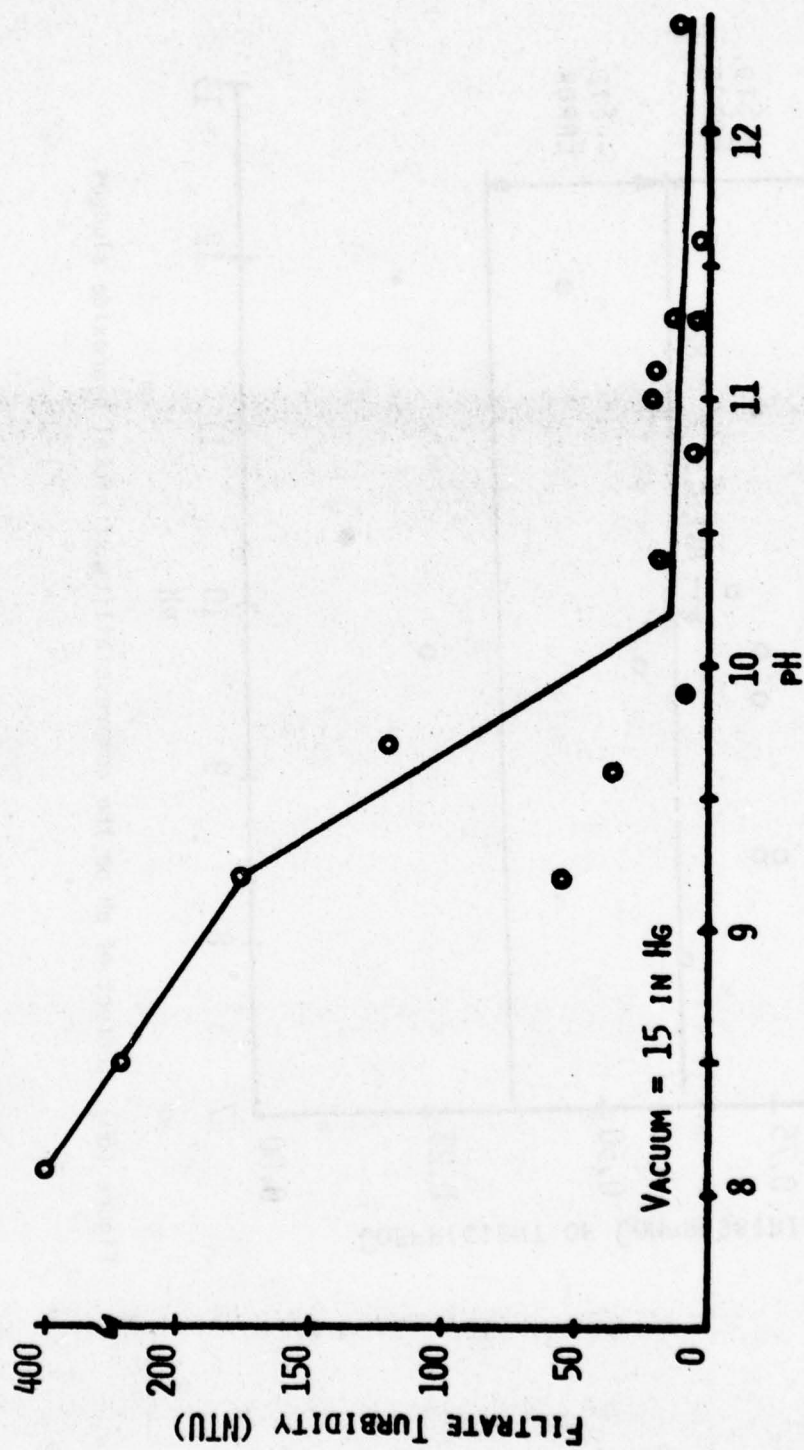


Figure (59). Filtrate quality obtained during vacuum filtration as a function of pH for several nickel hydroxide sludges.

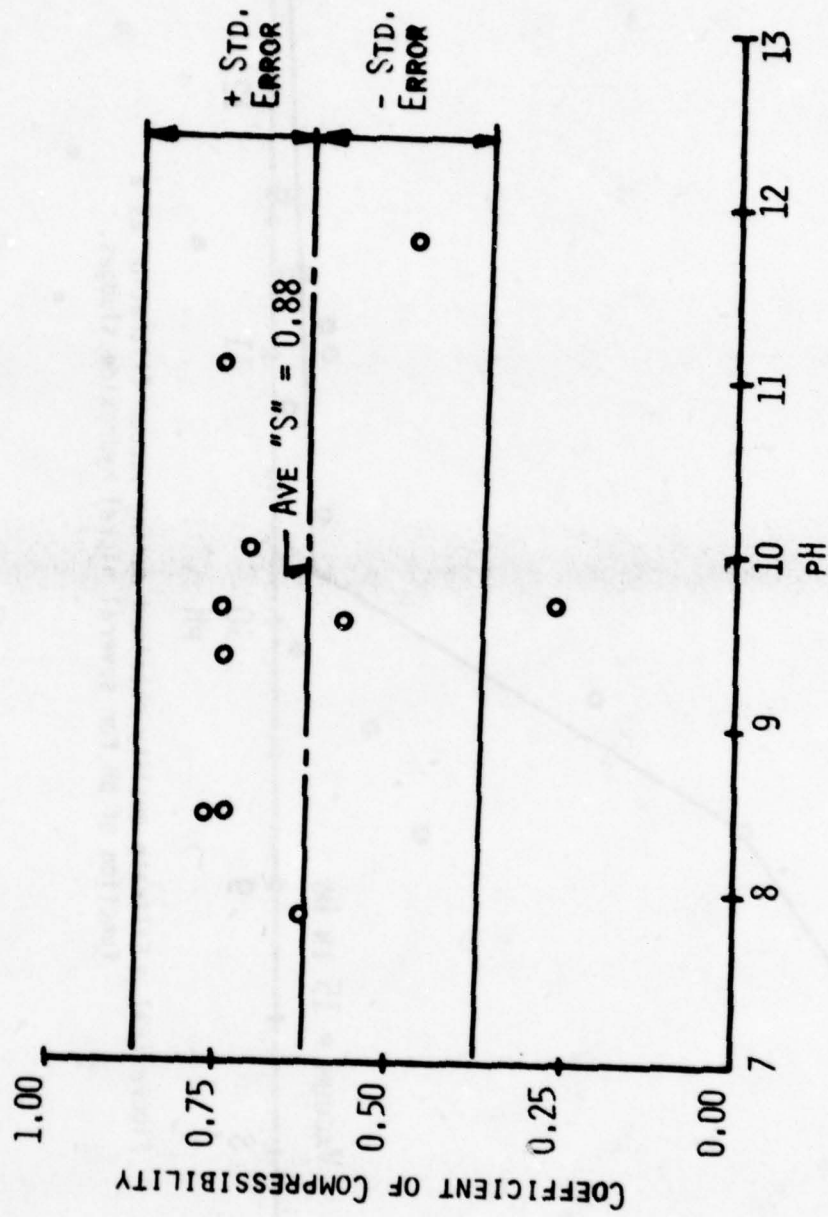


Figure (60). Effect of pH on the compressibility of nickel hydroxide sludges.

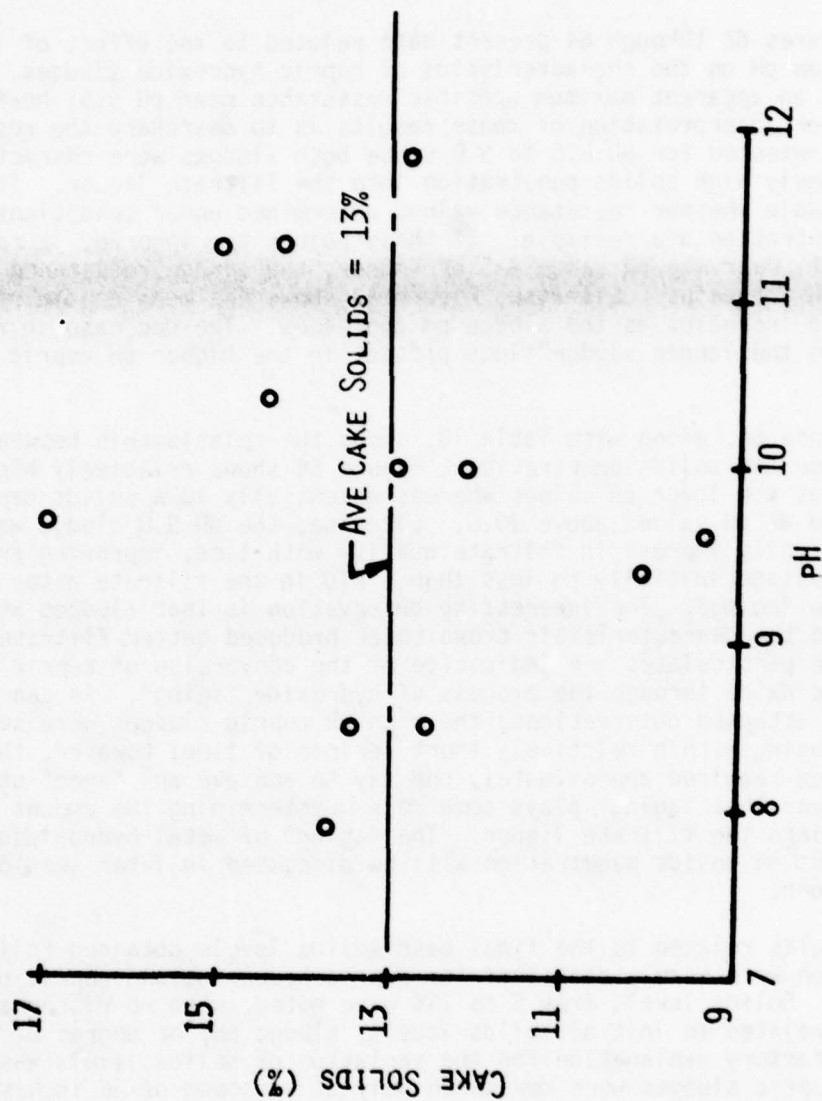


Figure (61). Effect of pH on the cake solids concentration obtained following vacuum filtration (nickel hydroxide sludges).

particle size has any discernable effect on compressibility. Finally, Figure 61 shows no apparent relationship between nickel hydroxide sludge pH and final cake solids concentrations. Rather, most nickel sludges were characterized by 12-15% cake solids following vacuum filtration.

Figures 62 through 64 present data related to the effect of insolubilization pH on the characteristics of cupric hydroxide sludges. Figure 62 shows an apparent maximum specific resistance near pH 9.5; however, the proper interpretation of these results is to disregard the resistance values presented for pH 8.5 to 9.0 since both sludges were characterized by extremely high solids penetration into the filtrate liquor. It is questionable whether resistance values determined under conditions of high penetration are reliable. If these points are ignored, it can be seen that, over the pH range 9.5 or higher, the sludge resistance decreases as the pH increases. Likewise, Figure 63 shows the mean cupric hydroxide floc size increases as the sludge pH increases. The decrease in resistance is due to the larger sludge flocs present in the higher pH cupric hydroxide sludges.

Figure 64, along with Table 10, shows the relationship between pH, sludge age and solids penetration. Figure 64 shows relatively high solids passage at the lower pH values whereas essentially 100% solids capture was noted at pH values above 10.0. Likewise, the pH 9.0 sludge was seen to drastically improve in filtrate quality with time, improving from 25% solids passage initially to less than 5 FTU in the filtrate after 3 days of sludge "aging". The interesting observation is that sludges which possessed the characteristic brown color produced better filtrate quality. The brown particulates are indicative of the conversion of cupric hydroxide to cupric oxide through the process of hydroxide "aging". As can be seen from the attached observations, the high pH cupric sludges were seen to undergo aging within relatively short periods of time; however, the pH 9.0 sludge required approximately one day to achieve an "aged" state. It is clear that "aging" plays some role in determining the amount of solids passing into the filtrate liquor. The "aging" of metal hydroxides and its effect on solids penetration will be discussed in later sections of this report.

Results related to the final cake solids levels obtained following filtration were widely scattered for cupric hydroxide and cupric oxide sludges. Solids levels from 5 to 25% were noted, with no discernable pattern related to initial solids levels, sludge pH, or degree of "aging". No satisfactory explanation for the variation of solids levels was developed. Cupric sludges were dewatered only at a vacuum of 15 inches Hg, therefore no compressibility data was collected.

Problems of solids penetration during dewatering were observed for pure chromium hydroxide sludges at all levels of insolubilization pH. The problem could not be directly related to the presence of sludge "fines" as noted earlier for nickel hydroxide sludges. Figure 19 shows the characteristic size of chromium hydroxide particles as a function of

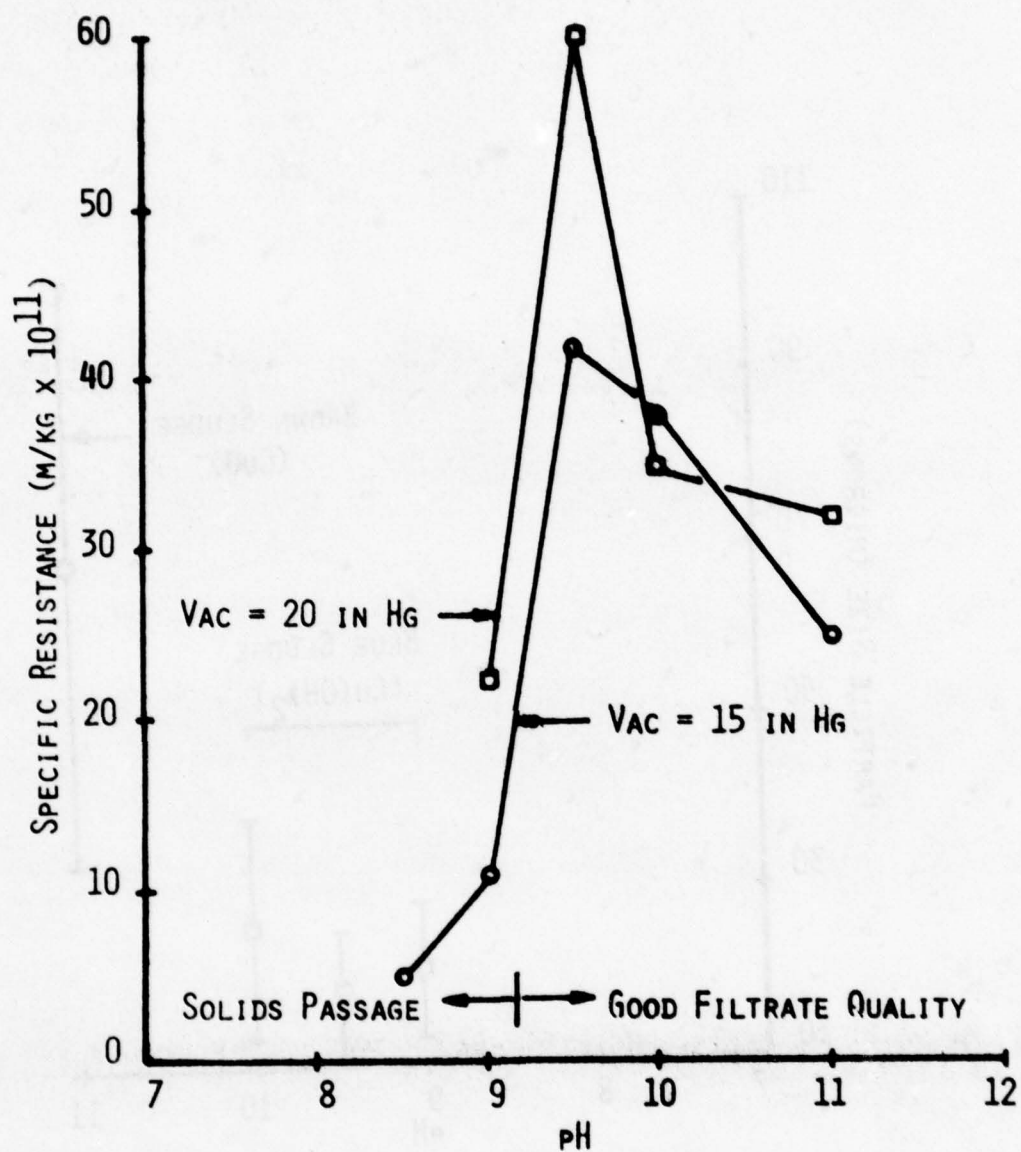


Figure (62). The specific resistance of cupric hydroxide sludges as a function of pH.

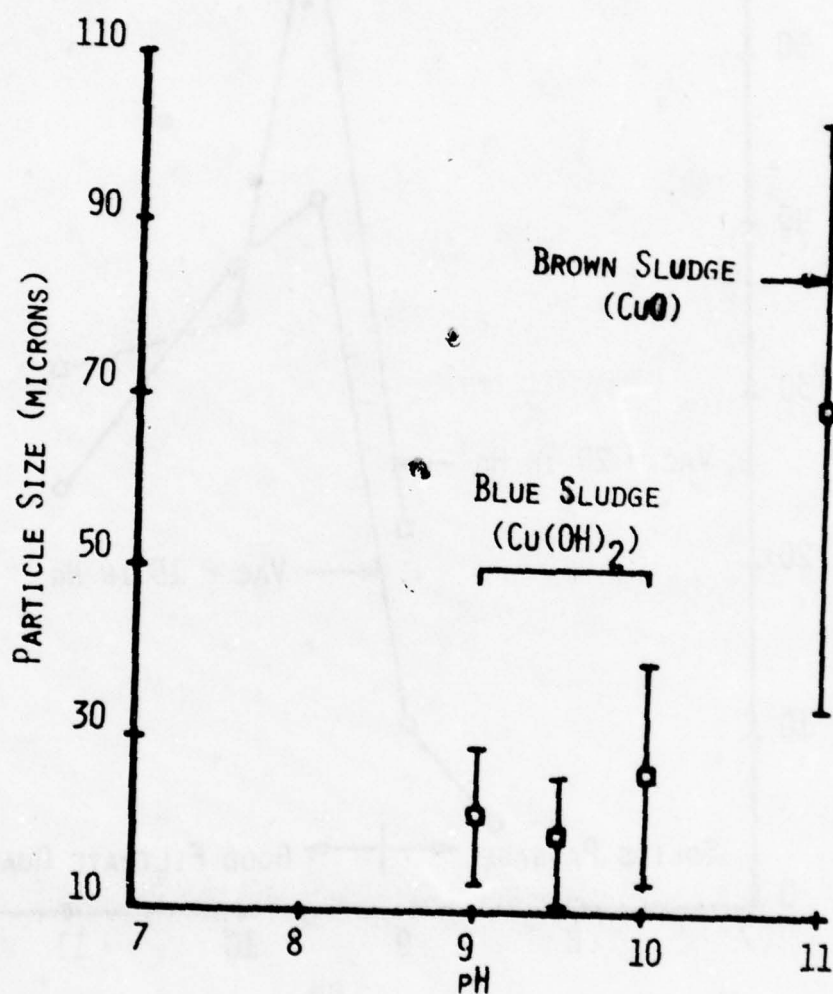


Figure (63). Variations in the characteristic size of cupric hydroxide and cupric oxide flocs as a function of pH.

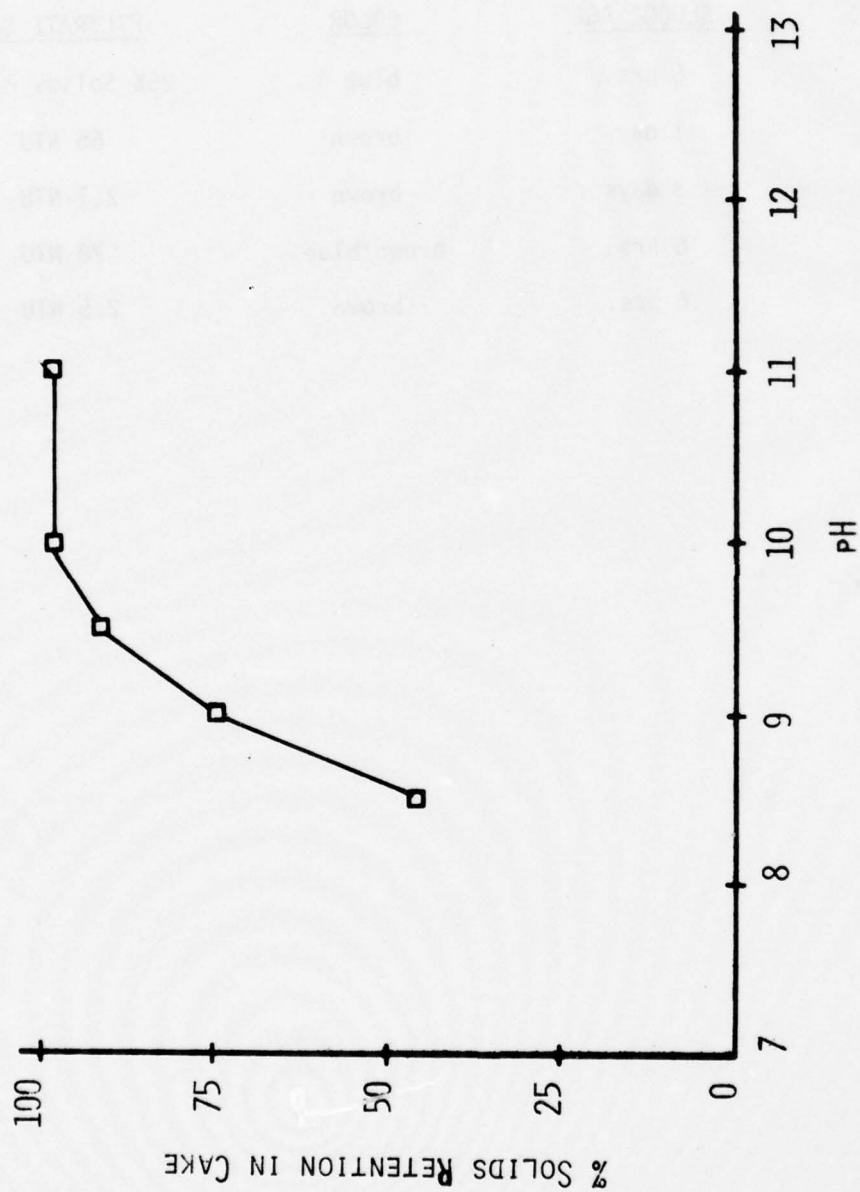


Figure (64). Degree of solids penetration obtained during vacuum filtration as a function of pH for cupric hydroxide sludges.

TABLE 10. EFFECT OF pH AND SLUDGE AGE ON THE
FILTRATE QUALITY OF $\text{Cu}(\text{OH})_2$ SLUDGES

<u>SLUDGE pH</u>	<u>SLUDGE AGE</u>	<u>COLOR</u>	<u>FILTRATE SOLIDS</u>
9.0	6 hrs.	blue	25% Solids Passage
9.0	1 day	brown	65 NTU
9.0	3 days	brown	2.1 NTU
10.0	6 hrs.	brown/blue	78 NTU
11.0	6 hrs.	brown	2.5 NTU

insolubilization pH. Within the pH range 7.0 to 10.0, the characteristic $\text{Cr}(\text{OH})_3$ floc is much larger than 8 microns, the characteristic pore size of the filter medium utilized. Yet, most chromium sludges were seen to produce solids penetration of up to 90% of the initial solids present and all pure chromium sludges, both fresh and aged, produced at least 20% solids breakthrough during dewatering. It is obvious that, since the particle size is characteristically much greater than that of the filter medium, floc "break-up" or shear must be in some way involved in the solids penetration phenomenon.

In order to adequately characterize the dewatering of chromium hydroxide sludges, polymer conditioning was necessary. A more detailed discussion of the results of chromium hydroxide sludge conditioning studies will be presented in Section (H) which deals specifically with the conditioning of metal hydroxide sludges.

Finally, noting the possible effects of calcium and other ions mentioned by Pattengill (33), studies were undertaken to characterize the sludges obtained from the insolubilization of chromium hydroxide using lime instead of sodium hydroxide. Representative results are shown in Table 11. Although the filtrate turbidity levels are high, these sludges were found not to penetrate to near the extent of those obtained through sodium hydroxide insolubilization. In comparing the mean size of flocs obtained from lime insolubilization to floc sizes obtained at equivalent pH values with NaOH, it can be seen that both floc sizes are similar. That is, the addition of lime does not result in the production of particles of much larger size than those produced through NaOH insolubilization of chromium. It appears that the use of lime results in the production of a stronger chromium hydroxide floc which is able to withstand higher shear forces or stresses during dewatering without fracture and penetration.

3. Mixed-Metal Sludges

In Tables 12 and 13 data are presented showing the characteristics of mixed-metal hydroxide sludges. The data collected and presented in Table 12 are for synthetic waste solutions containing varying initial levels of chromium, cadmium, copper and nickel. Table 13 contains the results of studies performed on sludges obtained from a nickel-dominant electroplating wastewater.

Referring to Table 12, most of the synthetic mixed-metal sludges examined were characterized by (1) specific resistance values of 40 to 60×10^{11} m/kg, (2) cake solids levels between 10 to 13%, (3) an initial solids level between 1 to 2% which correspond well with values reported in the literature for metal hydroxide sludges (6), and (4) an average coefficient of compressibility "s" around 1.0. Also, it should be noted that, as the average floc size increased, the specific resistance of the mixed-metal sludges decrease. The role of particle size in affecting

TABLE 11. $\text{Cr}(\text{OH})_3$ INSOLUBILIZATION USING LIME AND NaOH

SLUDGE pH	SPEC. RES. $\text{m/kg} \times 10^{11}$	CAKE SOLIDS (%)	FILTRATE TURB. (NTU)	COEFF. OF COMP. ("S")	SETTLED SOLIDS (%)	MEAN FLOC SIZE (USING LIME)	MEAN FLOC SIZE (USING NaOH)***
8.5*	73.6	27.6	120.	--	1.72	34 u	36 u
9.0*	62.1	28.5	160.	0.97	1.45	37 u	41 u
9.5*	50.1	25.3	250.	0.97	1.03	43 u	38 u
9.9**	--	--	100% solids passage	--	--	--	32 u

* Insolubilization using lime

** Insolubilization using NaOH

*** Particle size for NaOH at comparative pH value

TABLE 12. CHARACTERISTICS OF SYNTHETIC MIXED-METAL SLUDGES

pH	SPEC. RES. (m/kg x 10 ¹¹)	CAKE SOLIDS (%)	FILT. TURB. (NTU)	COEFFICIENT OF COMP.	SETTLED SOLIDS (%)	MEAN PARTICLE SIZE (MICRONS)
9.5	29	9.3	160	1.13	1.11	27
9.5	15	12.3	200	1.69	2.12	29
9.7	63	12.3	43	1.18	1.32	19
9.7	52	10.6	28	1.04	1.26	20
10.0	62	11.4	32	0.94	0.90	25
10.5	52	11.2	36	0.96	1.14	22
11.0	47	10.5	47	1.05	1.53	22
11.0	54	13.5	100	3.36	1.42	22
11.0	38	13.7	250	--	1.88	29
11.0	38	12.2	9	--	1.81	33
11.0	43	11.2	100	--	1.42	22
11.0	26	13.5	187	--	2.12	35
11.0	46	12.3	94	--	1.45	25

TABLE 13. CHARACTERISTICS OF SLUDGES FROM TINKER AIR FORCE BASE

PH	SPEC. RES. (m/kg x 10 ¹¹)	CAKE SOLIDS (%)	FILT. TURB. (NTU)	COEFFICIENT OF COMP.	SETTLED SOLIDS (%)	MEAN PARTICLE SIZE (MICRONS)
8.5	133	13.5	2.7	0.97	1.18	13
9.0	133	13.7	2.7	1.09	1.40	12.5
9.7	108	--	120.	1.00	1.54	15
10.0	145	12.9	4.5	1.46	1.06	13
10.0	139	13.6	3.4	0.52	1.35	12
11.0	146	16.6	30.	0.38	1.49	11

the filtration of sludges is apparent.

Table 13 presents the data related to the effect of pH in characterizing the sludges obtained from the treatment of a nickel-dominant metal-bearing wastewater. These waste samples were obtained from the electroplating shop at Tinker Air Force Base in Oklahoma City, Oklahoma. The waste was characterized by high nickel concentrations and other metals (chromium, copper and zinc approximately 50 to 100 mg/l). Examination of the results presented in Table 13 show these sludges to be characterized by (1) a relatively high resistance to filtration, (2) low filtrate turbidities, and (3) small mean floc sizes. Comparing these results to data presented in Table 12, the major difference noted between these two mixed-metal systems can be seen to be due to the variation in floc sizes obtained during insolubilization. The nickel-dominant system produced a higher resistance to fluid flow. Also, by comparing the data presented in Figure 58 to that listed in Table 13, it can be seen that the nickel dominant mixed-metal system behaves in a fashion similar to pure nickel hydroxide sludges at similar pH values. Thus, one may conclude that a mixed-metal sludge dominated by one metal may respond to dewatering in a manner similar to that of a pure hydroxide sludge of that same metal at the same pH value.

4. Effects of Particle Size on the Dewatering of Metal Hydroxide Sludges

The role of particle size and size distribution in affecting the specific resistance of a sludge to dewatering has been examined by several investigators (34) (35) (36). Karr and Keinath (37) studied the role of various particle size fractions in affecting the specific resistance of wastewater sludges. In analyzing the effect of various size fraction on specific resistance, Karr and Keinath were able to identify one size range which most significantly affected the ultimate resistance of a sludge to vacuum filtration. The relative weight fraction of supracolloidal particles (between 1.2 to 104 microns) was found to affect the resulting sludge specific resistance directly. Particles of larger size fractions were found to contribute little to the overall characteristic sludge specific resistance.

After examining the results of these studies, it was felt that more research was needed to determine the role of particle size in sludge dewatering. Although the identification of the supracolloidal fraction as being crucial in sludge dewatering was noteworthy, the range of particle sizes contained within this size fraction, 1.2 to 104 microns, is rather large. It was the intent of this study to divide this size range into smaller size subsets and investigate the effect of each size subset on sludge dewatering, with particular reference to metal hydroxide sludges. Through the use of the HIAC Particle Counter, it was possible to divide the supracolloidal size range into numerous size subsets, as listed in Table 14. The relative fraction of particles in each of these size ranges was determined for each sludge investigated during this study. In all,

TABLE 14. PARTICLE SIZE RANGES UTILIZED
FOR HIAC SIZE ANALYSIS

<u>RANGE #</u>	<u>SIZE FRACTION WITHIN RANGE (MICRONS)</u>
1	5 - 10
2	10 - 20
3	20 - 30
4	30 - 40
5	40 - 50
6	50 - 60
7	60 - 70
8	70 - 80
9	80 - 100
10,11,12	greater than 100

over 175 metal hydroxide sludges were characterized during this study.

The Kozeny equation (38):

$$R^* = \frac{36K(1-e)}{e^3(p_p)(D_e)^2}$$

shows that, at constant porosity e , an increase in the characteristic sludge floc size (D_e) will result in a reduction in sludge specific resistance. For metal hydroxide sludges, Figures 65 and 66 show clearly the role of mean sludge particle size in affecting the characteristic dewatering rate as measured by specific resistance. The results presented in these two figures are for pressure differentials of 15 in. and 20 in. Hg respectively. Examination of each figure shows the sludge specific resistance is very sensitive to the mean sludge floc size in the range of 8 to 20 microns, and less sensitive at higher mean size values. Remembering that the mean pore size of the filter medium was approximately 8 microns, it is possible that, at lower mean size values, the increased resistance may be partially due to the blinding of the filter medium. With larger mean size particles, the fraction of flocs in the size range of the filter medium is smaller, resulting in a decreased tendency to blind the medium.

The Kozeny equation states the resistance to flow is inversely proportional to the square of the particle diameter. In order to test the applicability of this equation in explaining metal hydroxide sludge dewatering, a statistical relationship between specific resistance and $(1/d_p)^2$ was developed, d_p being the mean floc size of a sludge. Figure 67 shows a rather well-defined linear relationship between the two parameters. This is an interesting finding since many investigators have questioned the use of this equation for compressible sludges. However, as can be seen by Figure 67, the Kozeny equation can be successfully applied to compressible sludges.

Another parameter of interest was the effect of the distribution of particle sizes present on the sludge specific resistance. Simmons and Dahlstrom (39) reported that certain sludge characteristics are more dependent upon particle size distribution than on average particle size and shape. Two sludges may have the same mean size floc and yet possess widely differing size distributions. Thus, it is conceivable that variations in size distribution could play a role in determining the resistance of a given sludge to dewatering. To check this possibility, statistical methods were used to examine the effect of both mean floc size and size distribution on the observed sludge specific resistance. The resulting equation was of the form:

$$r^* = \frac{1}{(d_p)^2(SD)}$$

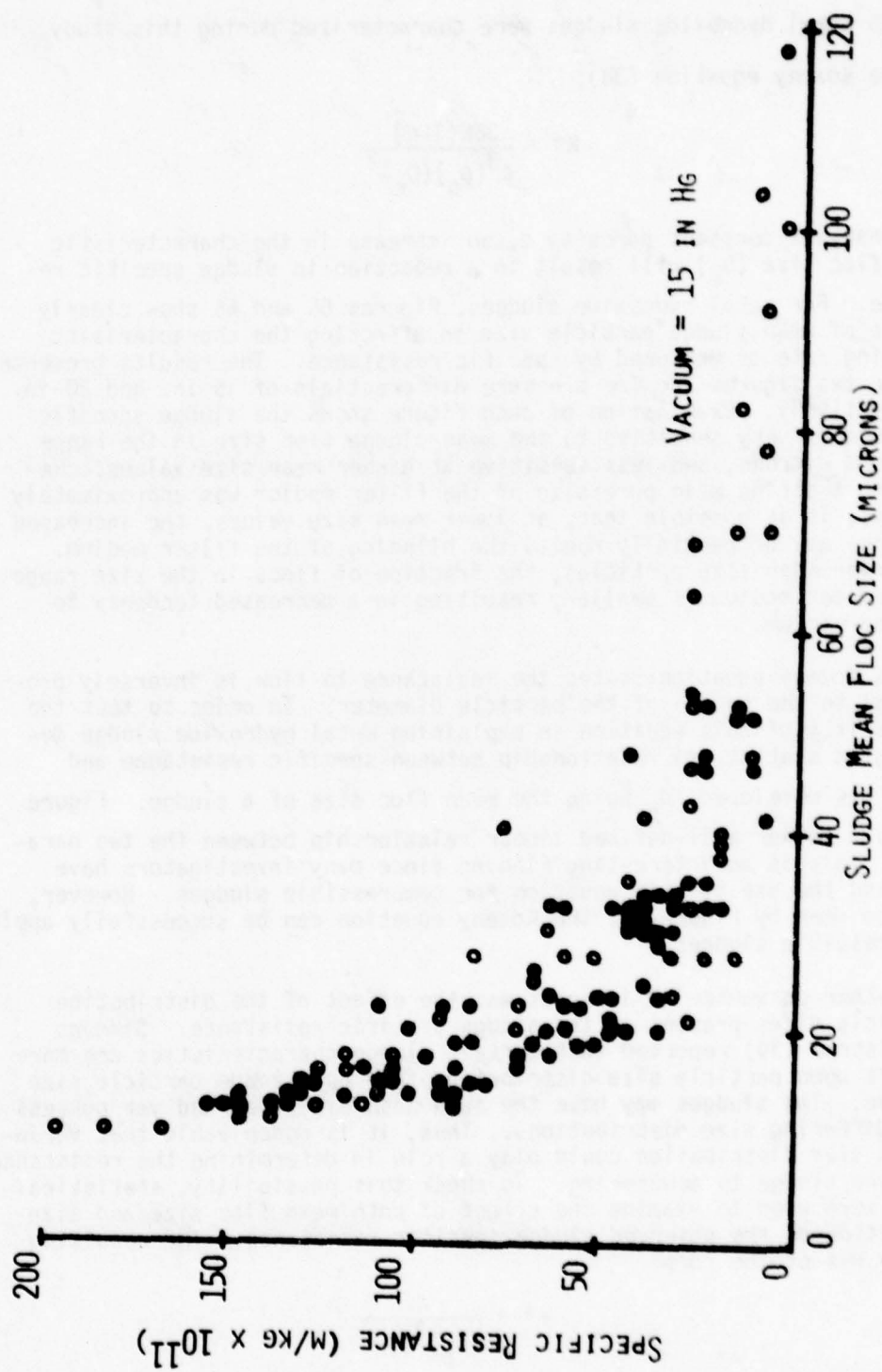


Figure (65). Variations in the specific resistance of metal hydroxide sludges as a function of the size of sludge flocs.

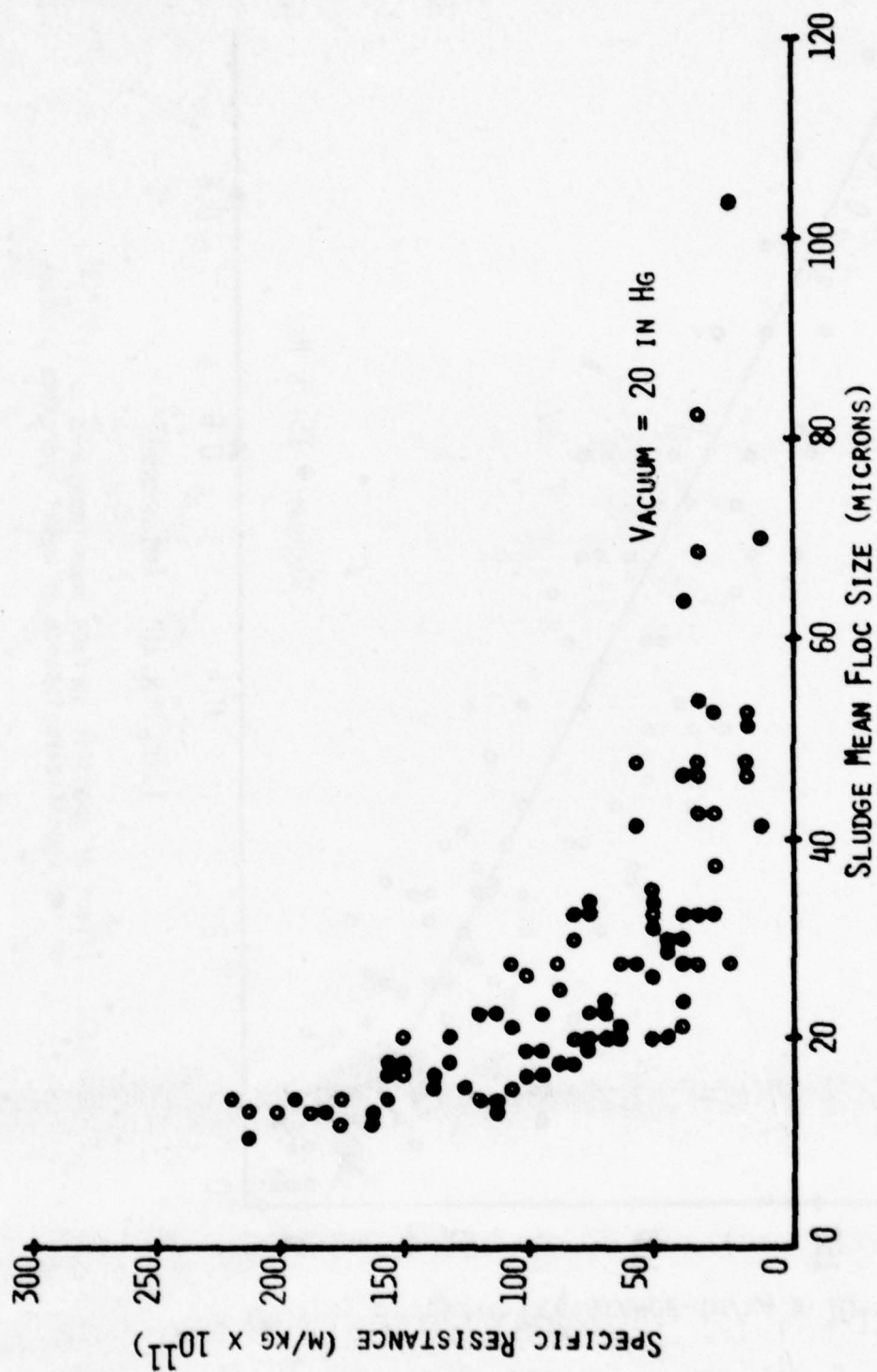


Figure (66). Variations in the specific resistance of metal hydroxide sludges as a function of the size of sludge flocs.

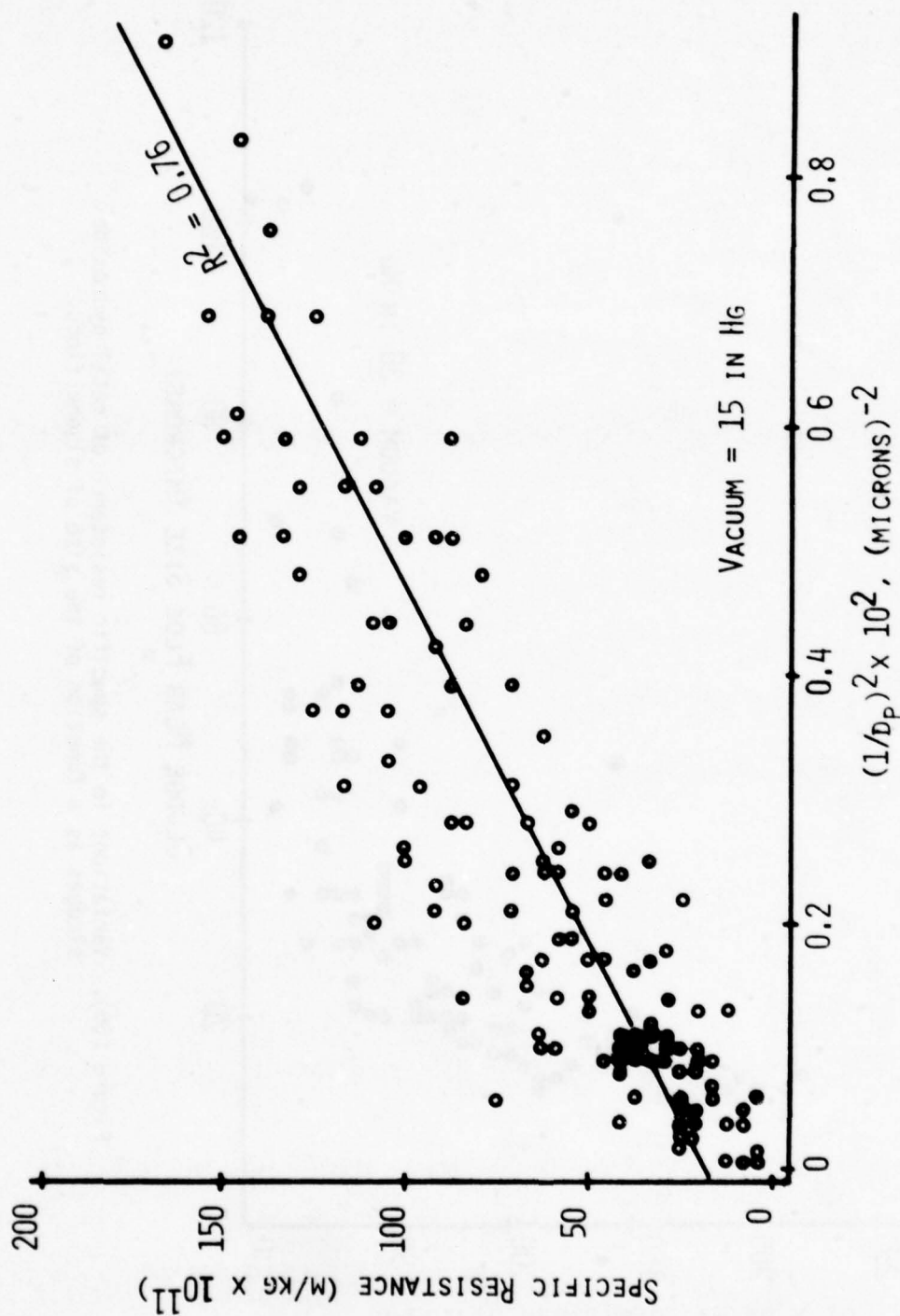


Figure (67). Effect of specific surface area (measured as $(1/d_p)^2$) on the specific resistance of metal hydroxide sludges.

where SD was the standard deviation of size distribution around the mean particle size. The correlation coefficient for this relation was similar to that for $(1/d_p)^2$ alone ($R^2 = 0.78$). It appears that the effect of size distribution is minimal, and tends to be such that sludges of widely varying particle sizes appear to dewater better than sludges of uniform size (small size deviation).

Another variable to be examined was the effect of various particle size fractions on the specific resistance of metal hydroxide sludges. Table 14 lists the size fraction ranges utilized in this investigation. In general, a vast majority of the flocs produced during the insolubilization and precipitation of metal hydroxides fell within the size range of 5 to 60 microns; some form of sludge conditioning was often found necessary to produce significant numbers of particles of characteristic size greater than 60 microns. Figures 68 and 69 show the effect of the 5-10 μ and 10-20 μ fractions on sludge specific resistance.

Figures 68 and 69 show a significant relationship between the relative fraction of fine particles (5-10 μ and 10-20 μ) and the specific resistance. This would be expected since (a) larger amounts of fine particles result in an increase in the surface area to volume ratio characteristic of a given sludge, resulting in an increase in the resistant drag forces developed during fluid flow through the sludge cake. (b) The presence of "fines" may also result in the blockage of pores either within the cake itself or the supporting filter medium. The possibility of filter medium blockage is extremely significant since the mean pore size of the filter medium is very similar to the size of particles in this size range. If blinding (blockage of pores) does occur, it reduces the available cross-section available for fluid flow, causing an increase in specific resistance.

Figures 70 and 71 show clearly the role of floc size and size distribution in determining sludge specific resistance. In general, sludges with similar particle size fractions will produce similar dewatering characteristics, regardless of the chemical composition of the sludge. Although exceptions to this were noted where two sludges of like size did not produce similar resistance values, the typical result between two sludges of similar size fractions was to produce similar specific resistance values. This is extremely important since it again shows the dramatic effect of floc size in characterizing sludge specific resistance. Of the parameters investigated during this study, size was by far the most crucial factor in determining most aspects of the dewatering characteristics of metal hydroxide sludges. Sludge pH and variations in metal content were found to be secondary or indirect parameters in that they would have a greater effect in determining the characteristic size distribution of flocs present.

5. Statistical Modelling

Using the results collected from the examination of over 175 metal hydroxide sludges, statistical methods were employed to develop a model

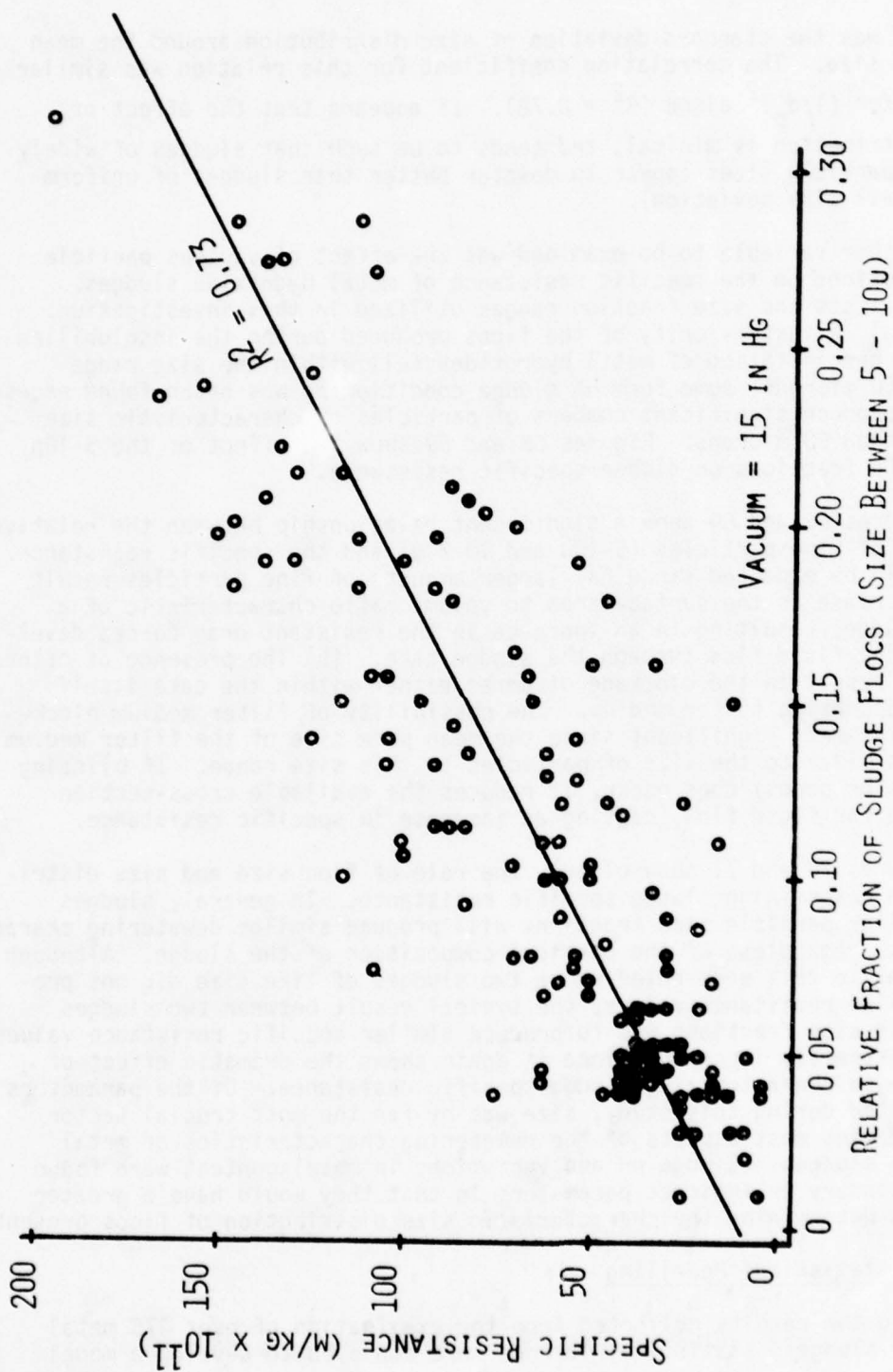


Figure (68). Variations in sludge specific resistance as a function of the stated sludge particle size range (5 - 10u).

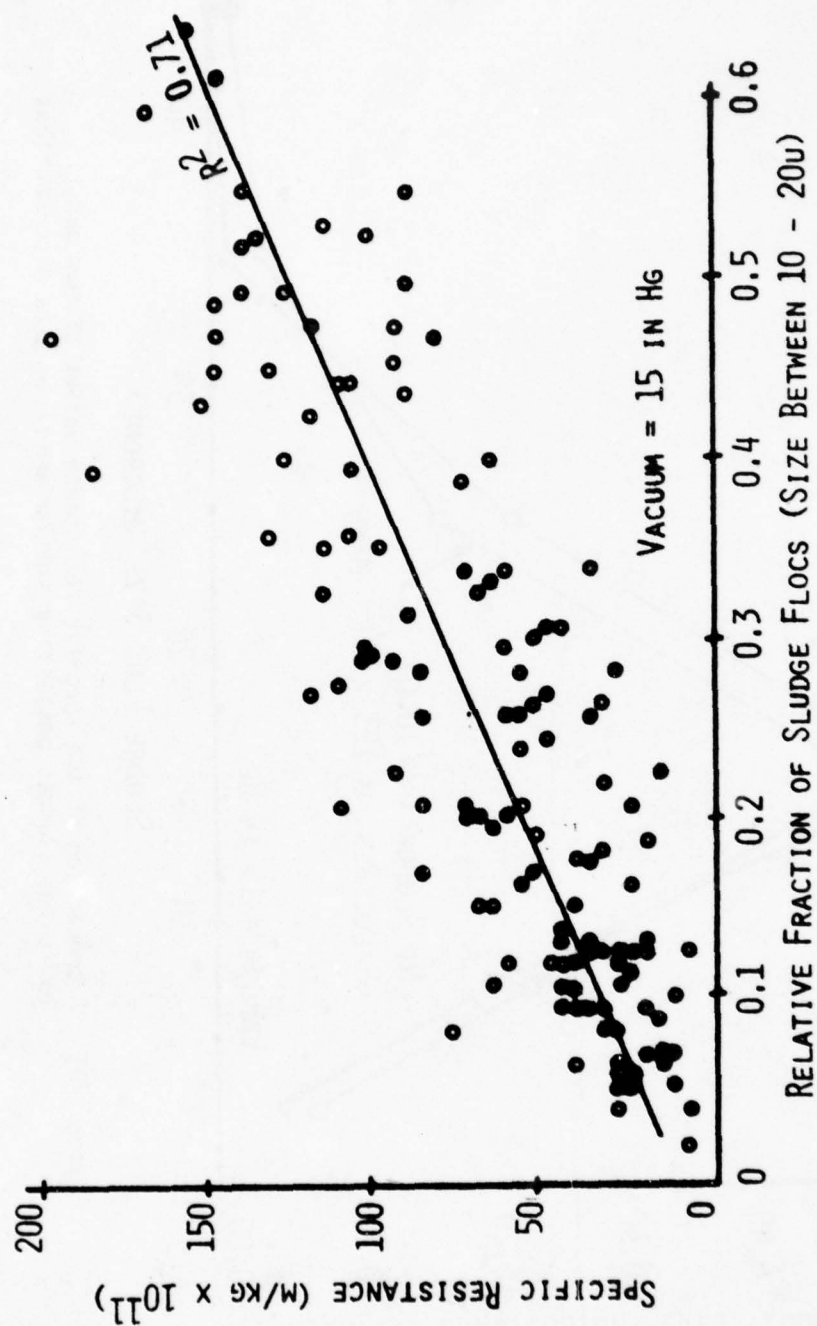


Figure (69). Variations in sludge specific resistance as a function of the stated sludge particle size range (10 - 20u).

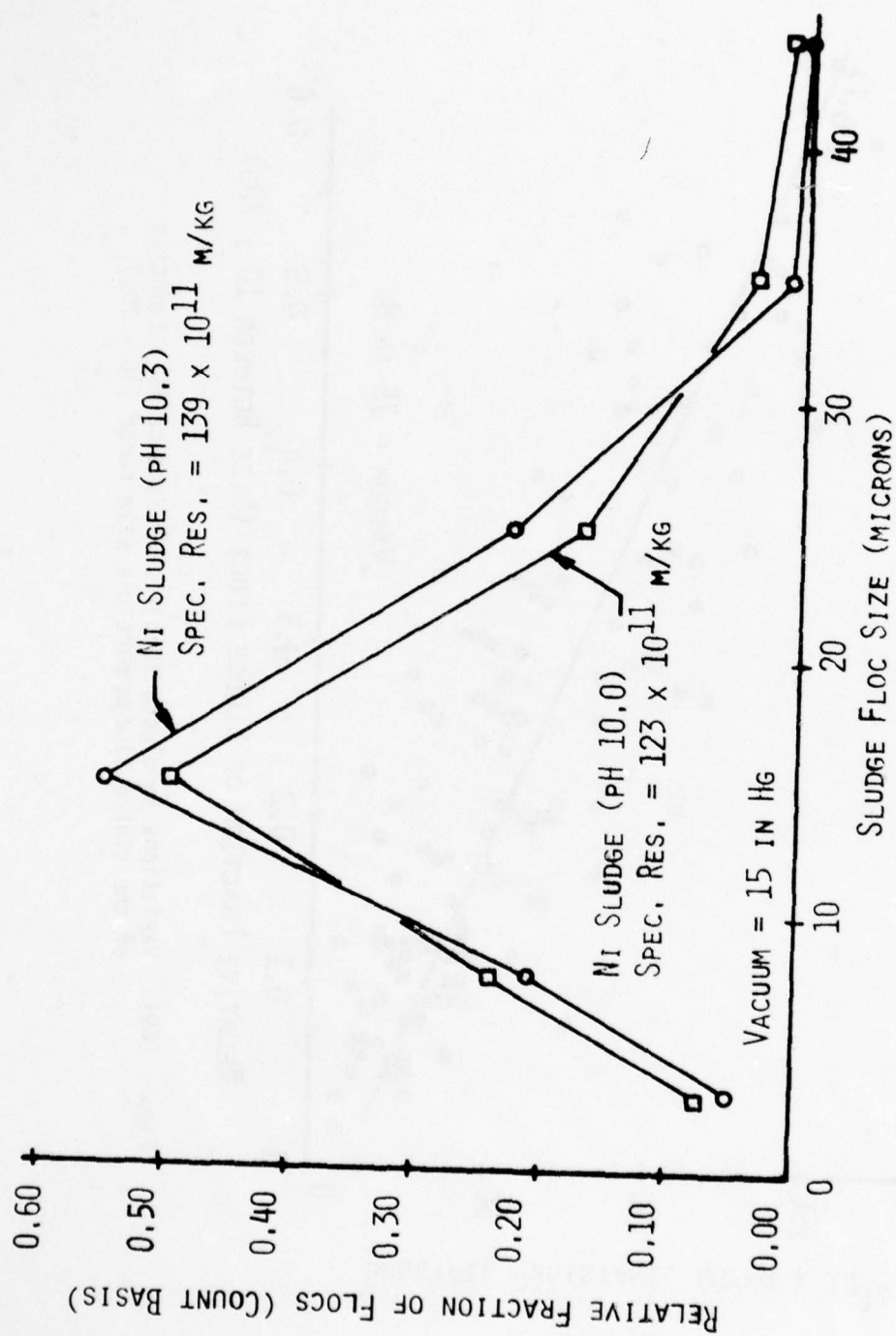


Figure (70). A comparison of the specific resistance values of two metal hydroxide sludges possessing similar particle size distributions.

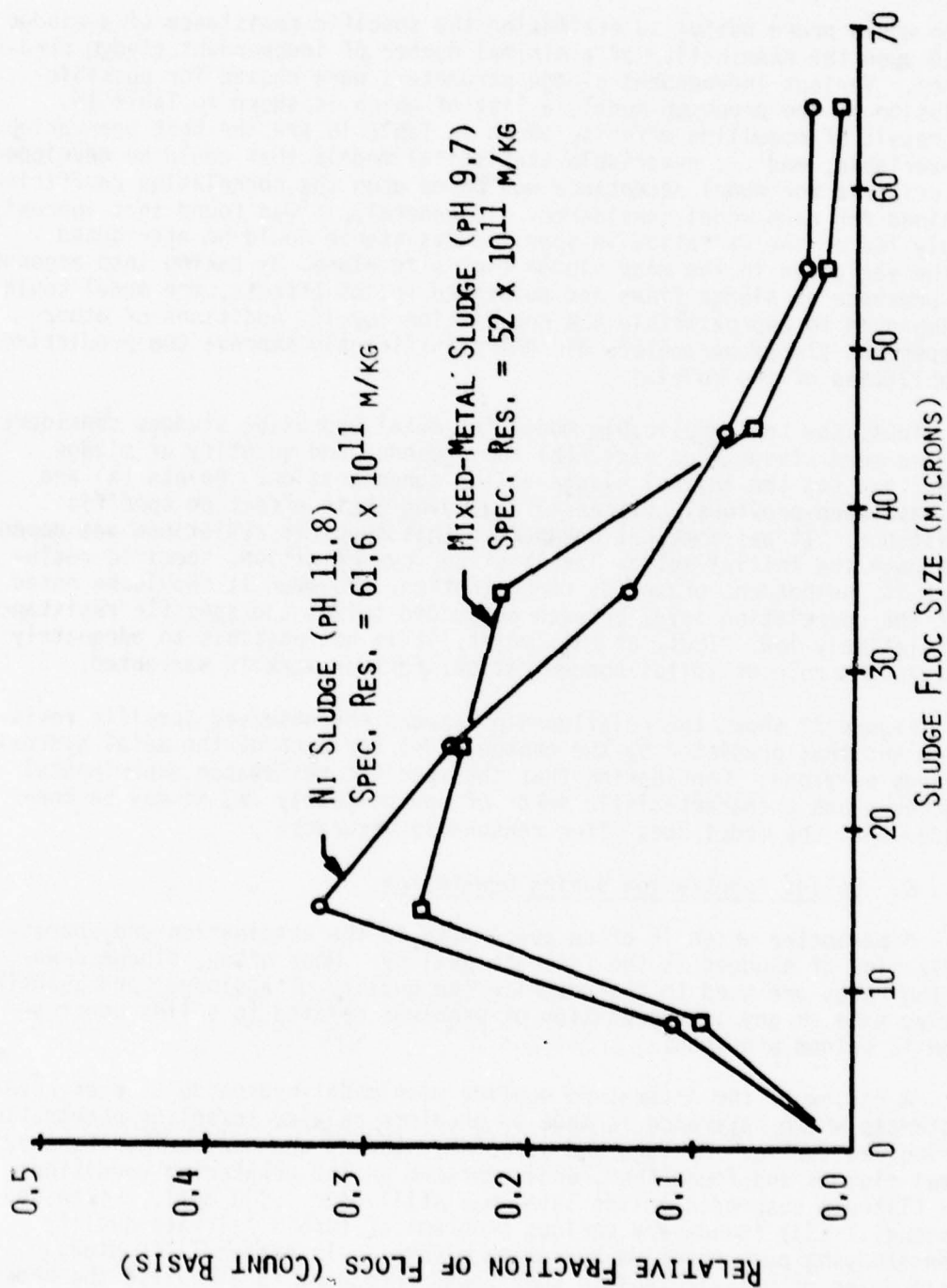


Figure (71). A comparison of the specific resistance values of two metal hydroxide sludges possessing similar particle size distributions.

which would prove useful in estimating the specific resistance of a sludge based upon the examination of a minimal number of independent sludge parameters. Various independent sludge parameters were chosen for possible inclusion in the proposed model, a list of which is shown in Table 15. The result of modelling efforts, shown in Table 16 are the best one-variable, two-variable, and ... n-variable statistical models that could be developed. The criteria for model acceptance was based upon the correlation coefficient obtained for each model considered. In general, it was found that approximately 76% of the variation in specific resistance could be attributed to the variation in the mean sludge floc size alone. By taking into account the presence of sludge fines and suspended solids effects, the model could be improved to approximately 82% correlation level. Additions of other independent sludge parameters did not significantly improve the predictive capabilities of the model.

Thus, the best applicable model for metal hydroxide sludges considers (a) the mean sludge floc size, (b) the presence and quantity of sludge fines, and (c) the initial sludge solids concentration. Points (a) and (b) have been previously discussed regarding their effect on specific resistance. It was somewhat unexpected that specific resistance was dependent upon the initial solids levels since, by definition, specific resistance is independent of solids concentration. However it should be noted that the correlation level between suspended solids and specific resistance is relatively low. Thus, at this point, it is not possible to adequately explain the role of solids concentration; further work is warranted.

Figure 72 shows the relationship between the observed specific resistance and that predicted by the chosen model for each of the metal hydroxide sludges examined. Considering that the specific resistance experimental procedure has a characteristic error of approximately 7%, it may be concluded that the model does offer reasonable accuracy.

6. Solids Penetration During Dewatering

A parameter which is often overlooked in the examination and characterization of sludges is the filtrate quality. Most often, sludge dewatering rates are used to characterize the quality of a sludge, and quantitative data or any interpretation of problems related to solids penetration is seldom provided.

A review of the literature dealing with metal hydroxide sludges reveals instances where reference is made to problems related to solids penetration during dewatering. McVaugh and Wall (40) studied the dewatering of heavy metal sludges and found that, under optimum pH and dewatering conditions, the filtrate suspended solids level was still near 1,500 mg/l. Likewise, Pattengill (33) found very serious problems of turbid filtrate quality when studying pure chromium hydroxide sludges. In Pattengill's study small doses of polyelectrolyte were found necessary to alleviate the problem.

TABLE 15. DESCRIPTION OF INDEPENDENT VARIABLES
UTILIZED IN STATISTICAL MODELS

<u>VARIABLE NAME</u>	<u>DESCRIPTION</u>
X1	Size Fraction 5 - 10u
X2	Size Fraction 10 - 20u
X3	Size Fraction 20 - 30u
X4	Size Fraction 30 - 40u
X5	Size Fraction 40 - 50u
X6	Size Fraction 50 - 60u
X7	Size Fraction 60 - 70u
X8	Size Fraction 70 - 80u
X9	Size Greater Than 80u
ME	Sludge Mean Floc Size (d_p)
SD	Floc Size Distribution
SS	Settled Solids (%)
CC	Coefficient of Compressibility

TABLE 16. STATISTICAL MODELLING - SLUDGE SPECIFIC RESISTANCE (SR)

<u>MULTILINEAR REGRESSION MODEL</u>	<u>CORRELATION (R²)</u>
SR = 22.4 + 16080 (1/ME) ²	0.763
SR = 14 + 92 (X2) + 10575 (1/ME) ²	0.790
SR = 25 + 116 (X2) + 9048 (1/ME) ² - 7 (SS)	0.818

(Addition of other independent variables did not significantly improve the model correlation.)

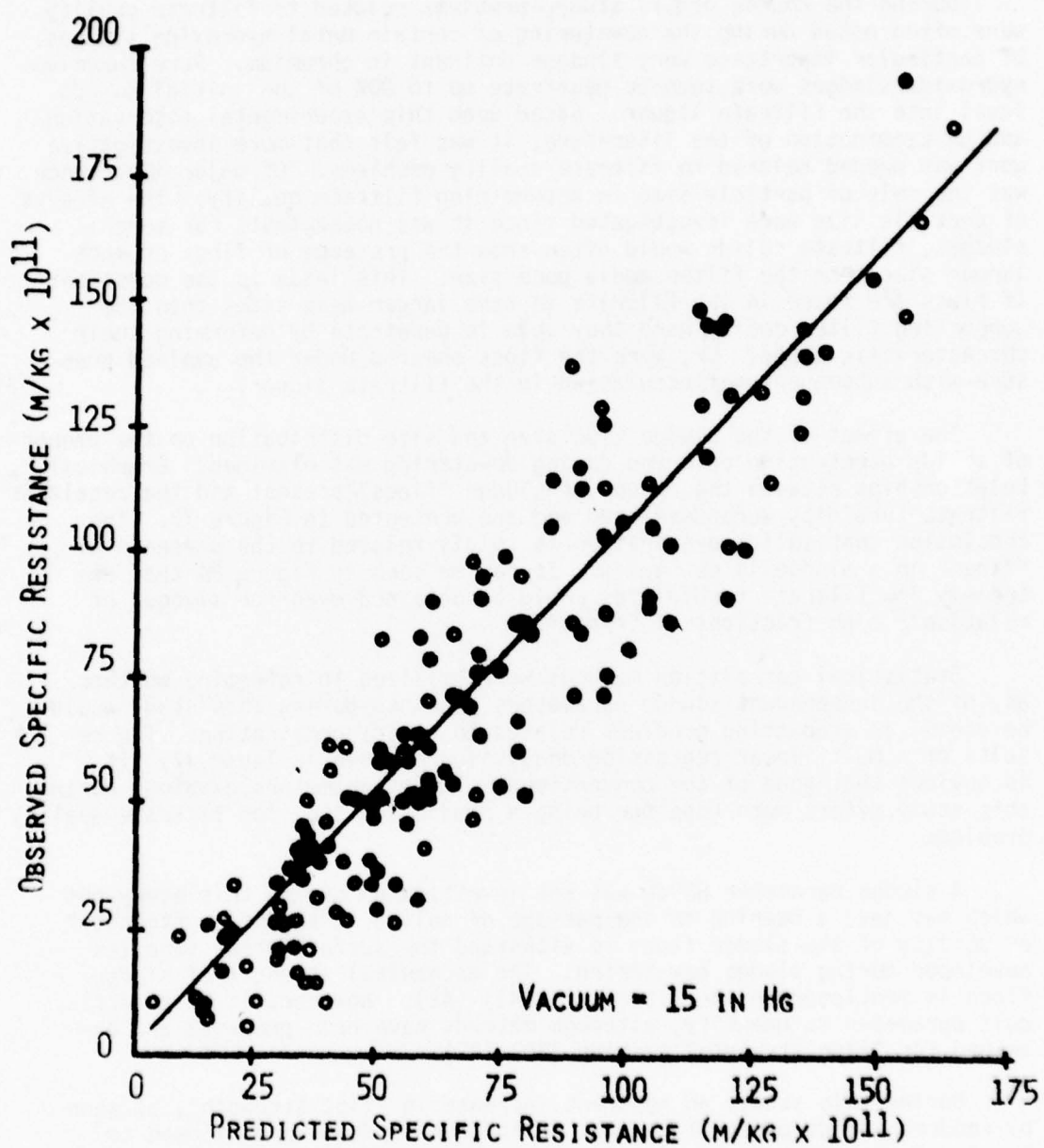


Figure (72). Comparison between experimentally observed specific resistance values and values predicted through the use of statistical models.

During the course of this study, problems related to filtrate quality were often noted during the dewatering of certain metal hydroxide sludges. Of particular importance were sludges dominant in chromium. Pure chromium hydroxide sludges were seen to penetrate up to 90% of the initial solids level into the filtrate liquor. Based upon this experimental observation and an examination of the literature, it was felt that more investigative work was needed related to filtrate quality problems. Of major importance was the role of particle size in determining filtrate quality. The effects of particle size were investigated since it was noted that, for several sludges, filtrate solids would often show the presence of flocs of much larger size than the filter media pore size. This leads to the question: If flocs are found in the filtrate to have larger mean sizes than the supporting filter media, were they able to penetrate by deforming their characteristic shape? Or, were the flocs sheared under the applied pressure with subsequent reflocculation in the filtrate liquor?

The effect of the sludge floc size and size distribution on the amount of solids penetration observed during dewatering was examined. Graphical relationships between the amount of sludge "fines" present and the resultant filtrate turbidity were developed and are presented in Figure 73. The conclusion that solids penetration is solely related to the presence of "fines" in a sludge is not valid. It can be seen in Figure 84 that extremely low filtrate turbidities could be obtained even for sludges of relatively high fractions of "fines".

Statistical correlation methods were utilized to determine whether any of the independent sludge parameters examined during this study would be useful in predicting problems related to solids penetration. The results of a multilinear regression analysis are shown in Table 17. It is obvious that none of the conventional sludge parameters examined during this study offers much hope for being a predictive tool for filtrate quality problems.

A sludge parameter which was not investigated during this study but which may have a bearing on the passage of solids is the "floc strength" or ability of the sludge flocs to withstand the surface shear stresses developed during sludge dewatering. The mechanical strength of sludge flocs is mentioned in the literature (41) (42). However, it is a difficult parameter to quantify, although methods have been proposed and examined for "floc strength" testing (38) (42).

During this study, an apparent increase in "floc strength", as seen by reduced solids penetration, was noted when sludges were allowed to "age". Representative results for the dewatering of certain mixed-metal hydroxide sludges are seen in Figure 74. In all cases, the filtrate quality was seen to improve dramatically with time. No dramatic improvement in the specific resistance was noted with time. Specific resistance values held roughly constant or improved only slightly. If the sludge specific resistance is indicative of particle size changes, it appears that very little change in particle size occurred with aging. Changes in floc size

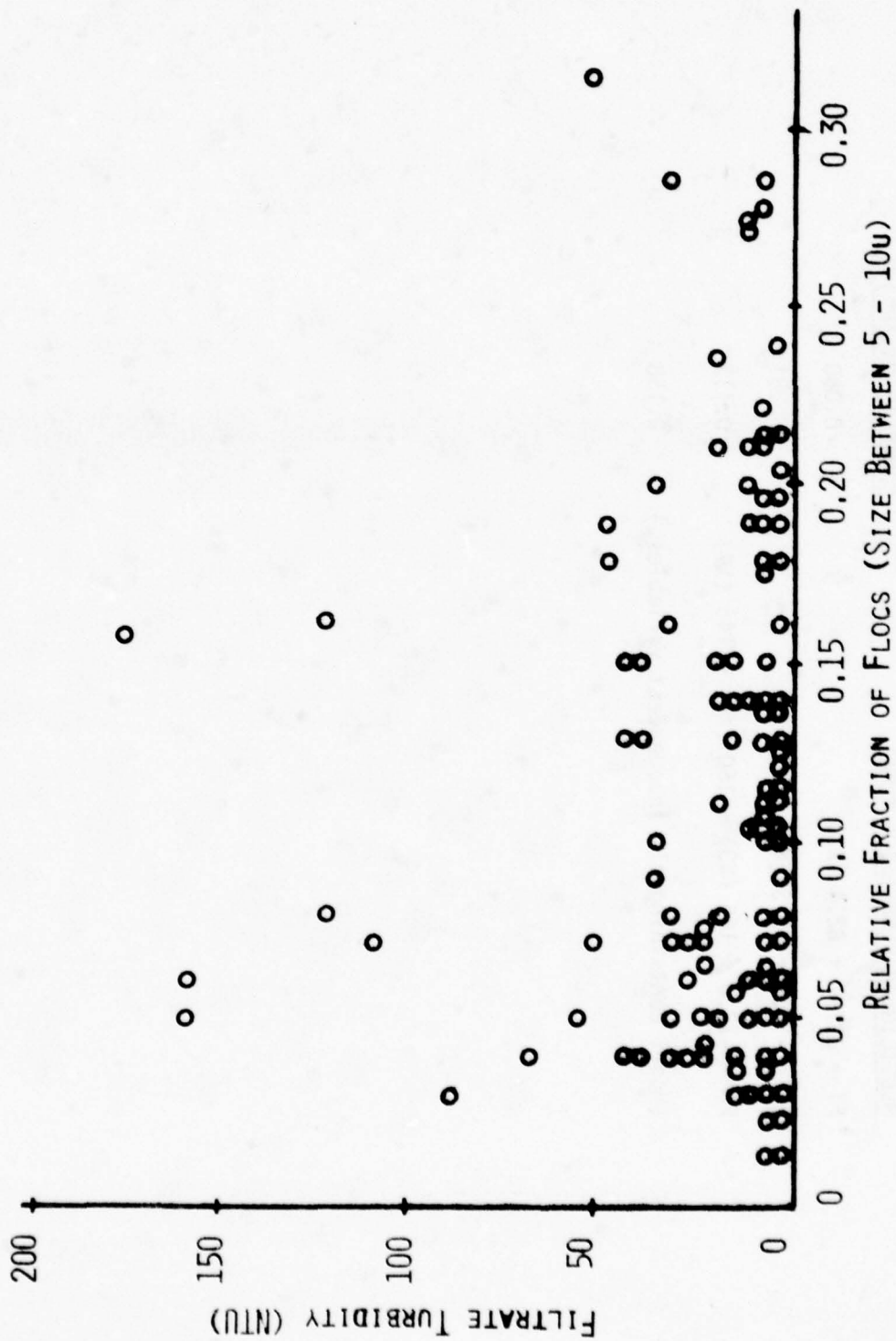


Figure (73). The effect of sludge "fines" on the filtrate turbidity obtained during vacuum filtration.

TABLE 17. STATISTICAL MODELLING - FILTRATE TURBIDITY (FT) IN NTU

<u>MULTILINEAR REGRESSION MODEL</u>	<u>CORRELATION (R²)</u>
FT = 01.97 + 82.4 (X3)	0.060
FT = -11.8 + 99.3 (X3) + 62 (X5)	0.081
FT = -17.0 + 166 (X3) + 160 (X5) - 146 (X4)	0.117
(Model containing all independent variables.)	0.158

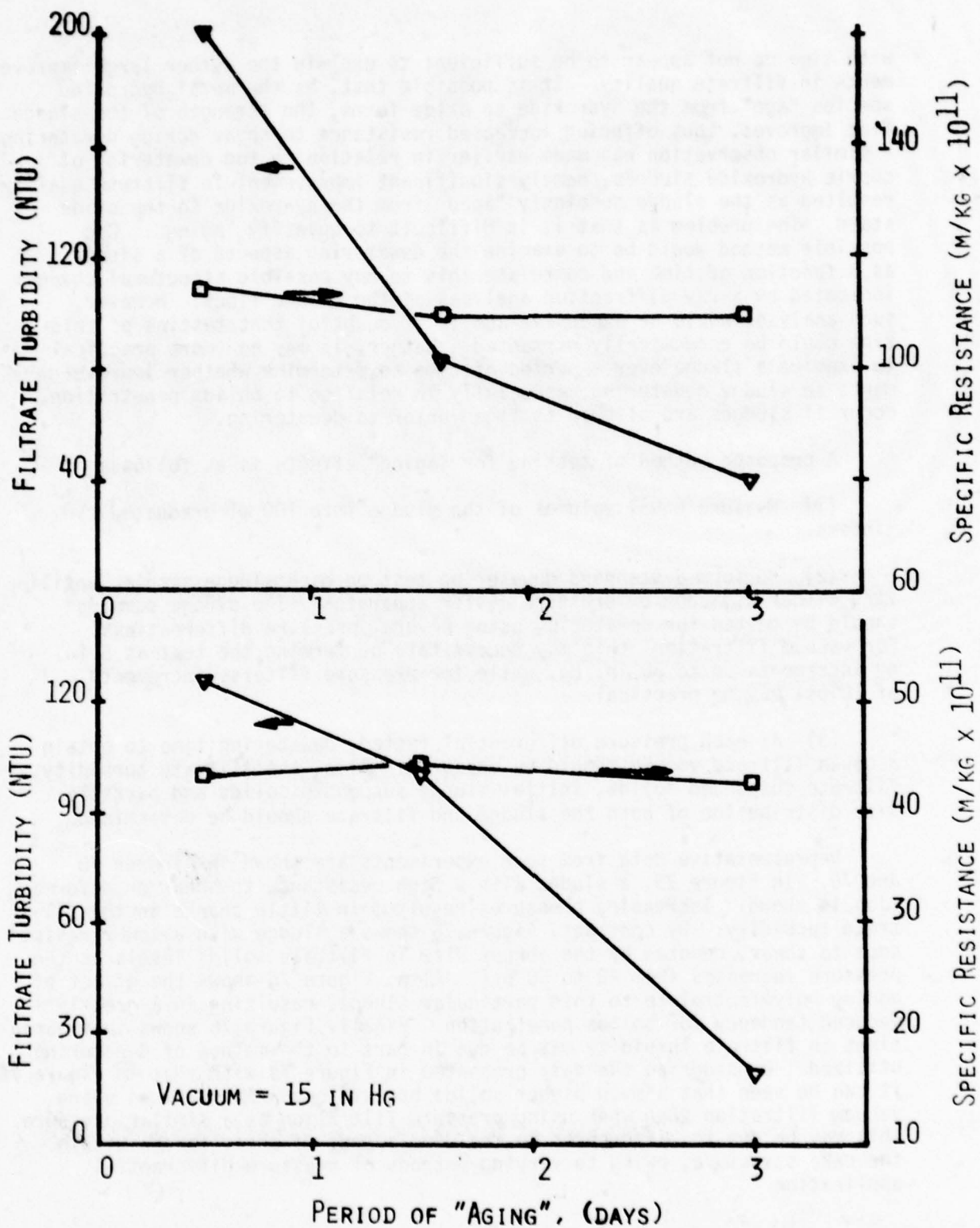


Figure (74). Sludge specific resistance and filtrate quality as a function of time of "aging".

with time do not appear to be sufficient to explain the rather large improvements in filtrate quality. It is possible that, as the metal hydroxide species "age" from the hydroxide to oxide forms, the strength of the sludge floc improves, thus offering increased resistance to shear during dewatering. A similar observation was made earlier in relation to the dewatering of cupric hydroxide sludges, namely significant improvement in filtrate quality resulted as the sludge seemingly "aged" from the hydroxide to the oxide state. The problem is that it is difficult to quantify "aging". One possible method would be to examine the dewatering aspects of a sludge as a function of time and correlate this to any possible structural changes indicated by x-ray diffraction analyses of the sludge flocs. However, such analyses would be expensive and it is doubtful that testing of this type could be economically warranted. Rather, it may be more practical to examine a sludge over a period of time to determine whether improvements in sludge dewatering, especially in relation to solids penetration, occur if sludges are allowed to "age" prior to dewatering.

A proposed method of testing for "aging" effects is as follows:

- (1) Measure equal volumes of the sludge into 100 ml graduated cylinders.
- (2) Perform a standard dewatering test on each sludge sample, utilizing either a vacuum or pressure filter apparatus. The sludge samples should be tested for dewatering using several pressure differentials. For vacuum filtration, this may necessitate performing the test at 5 in. Hg increments up to 30 in. Hg, while for pressure filters, increments of 10 psi may be practical.
- (3) At each pressure differential tested, dewatering time to obtain a given filtrate volume should be measured. Also, the filtrate turbidity, filtrate suspended solids, initial sludge suspended solids and particle size distribution of both the sludge and filtrate should be determined.

Representative data from such experiments are shown in Figures 75 and 76. In Figure 75, a sludge with a high resistance to shear or deformation is shown. Increasing pressures resulted in little change in the filtrate turbidity. By contrast, Figure 76 shows a sludge with a lower resistance to shear, denoted by the abrupt rise in filtrate solids levels as the pressure increases from 40 to 50 psi. Also, Figure 76 shows the effect of adding polyelectrolyte to this particular sludge, resulting in a greatly reduced tendency for solids penetration. Finally Figure 76 shows that variations in filtrate turbidity may be due in part to the method of dewatering utilized. Considering the data presented in Figure 74 with that in Figure 76, it can be seen that a much higher solids breakthrough occurred when using vacuum filtration than when using pressure filtration at a similar pressure. This may be due to differences in the development of shear forces within the cake structure, owing to varying methods of pressure differential application.

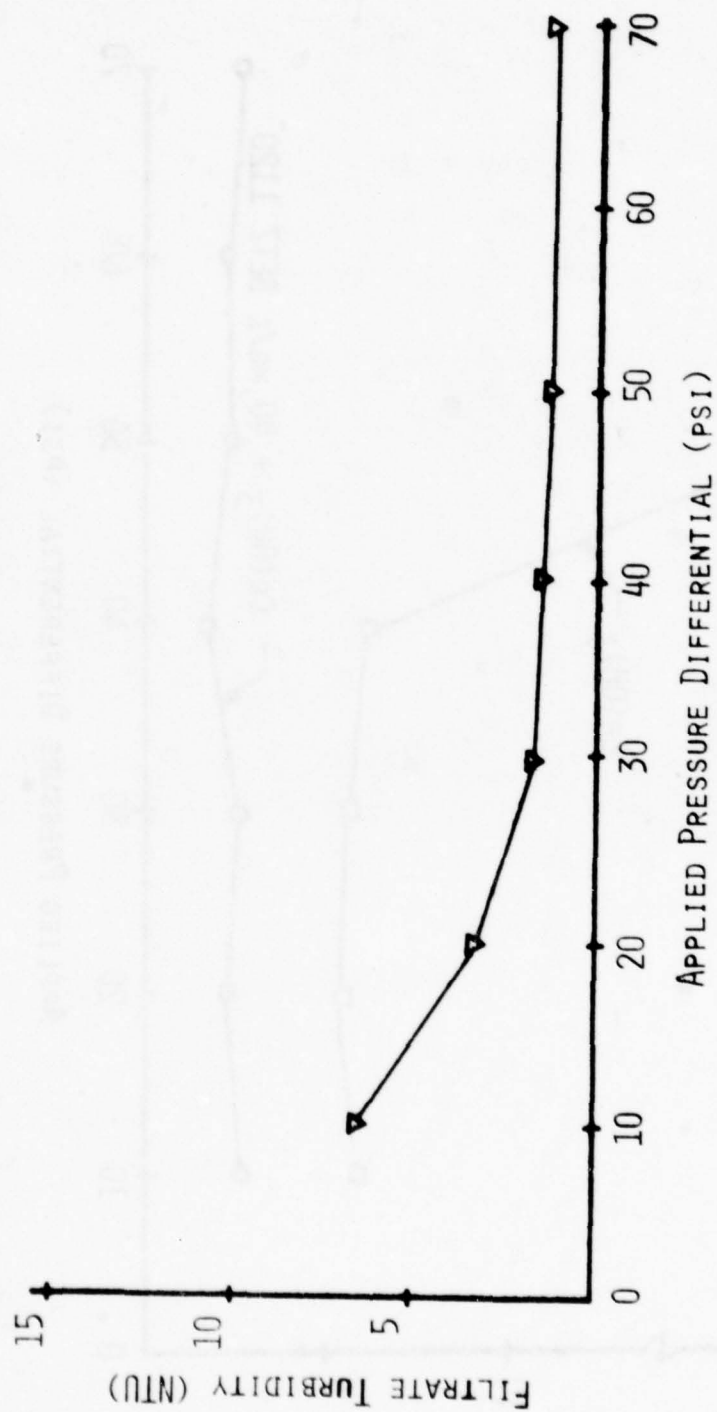


Figure (75). Vacuum filtrate quality as a function of applied pressure differential.

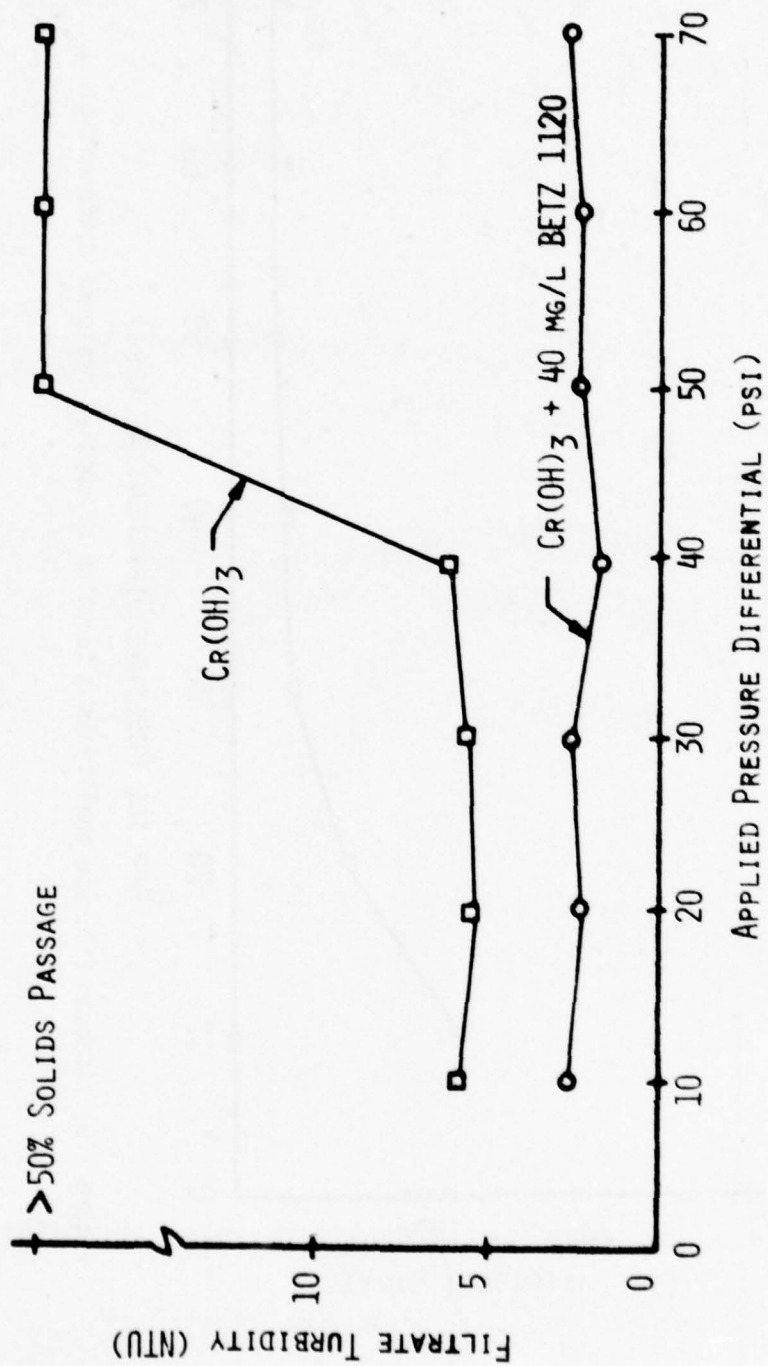


Figure (76). Filtrate quality as a function of applied pressure differential using a laboratory filter press.

Studies of the dewatering of metal hydroxide sludges have shown polyelectrolytes to be beneficial in minimizing filtrate quality problems. Pattengill's work on chromium hydroxide sludges showed that polymer doses as low as 0.5 mg/gr (0.05%) could effectively reduce the quantity of solids passing into the filtrate (33). Representative data obtained in this study for polymer use is shown in Figure 77. This figure is especially noteworthy since it shows the variation in size fractions which pass into the filtrate as a function of conditioning dose. One can see that improved filtrate quality is marked by the capture within the sludge cake of all but the finest particulates. One possible explanation for the role of polyelectrolytes is in improving the structural integrity or "floc strength" of the sludge particles, with polymer "bridging" playing a major role. This would account for the fact that only high molecular weight polyelectrolytes (greater than 10^6) were found to be beneficial. Studies employing lower weight polyelectrolytes did not prove successful. Thus, it would be recommended that, if filtrate quality were a significant problem at a sludge dewatering facility, sludge conditioning studies should be undertaken utilizing several high molecular weight polyelectrolytes. A polymer would then be chosen for application based upon its reduction of specific resistance as well as its improvement in filtrate quality.

7. Sludge Compressibility

Using the data collected during the dewatering portion of this study, it was possible to evaluate the effect of floc size and size distribution on sludge compressibility. Also, the effect of each size fraction was examined. Figure 78 shows the effect of increasing the mean sludge floc size on the coefficient of compressibility. An examination of this figure shows no apparent relationship exists between these two parameters; rather, most of the sludges examined were characterized by "s" values in the range 0.5 to 1.5. Applying the 90% confidence limit on "s" of $\pm 42\%$, as was previously determined in the methods and materials section, it is possible to conclude that no distinct relationship exists between the mean sludge floc size and "s", at least when considering the size range of 1 to 100 microns. Sludges with larger floc sizes were not included in this study since it was difficult to properly evaluate their size distribution using the HIAC counter.

The results of a multilinear regression analysis to evaluate the effect of certain sludge parameters on the coefficient of compressibility "s" are listed in Table 18. Examining these results shows that no single sludge parameter or combination of sludge parameters proves worthwhile for predicting variations in sludge compressibility. This is noteworthy since it shows no significant trend between either the presence of small or large size flocs and "s". Given the results of this analysis, coupled with the determined experimental error associated with the determination of "s", it becomes obvious that the determinations of "s" are unreliable and cannot be used in design of dewatering equipment.

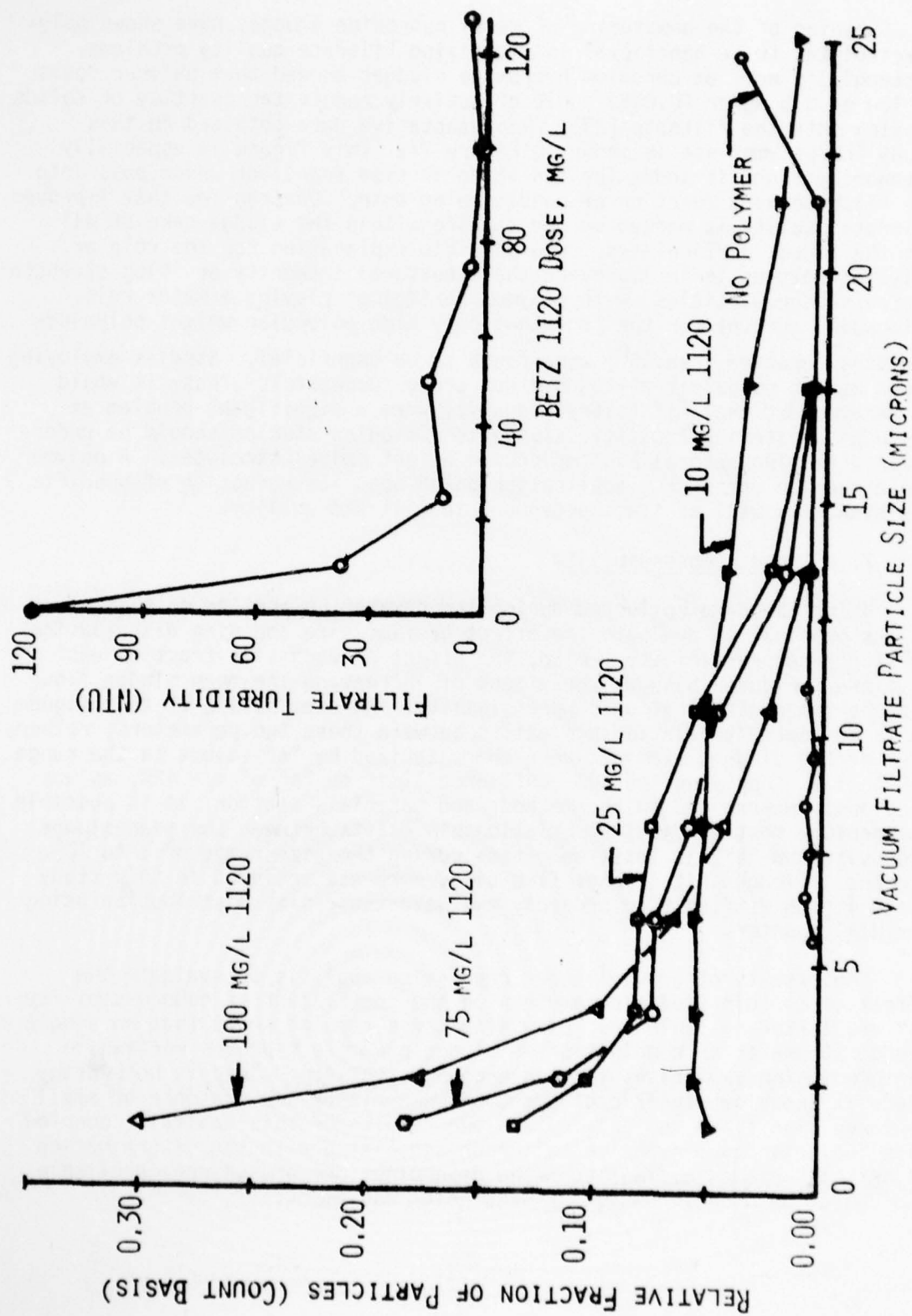


Figure (77). Effects of polymer conditioning on filtrate quality.

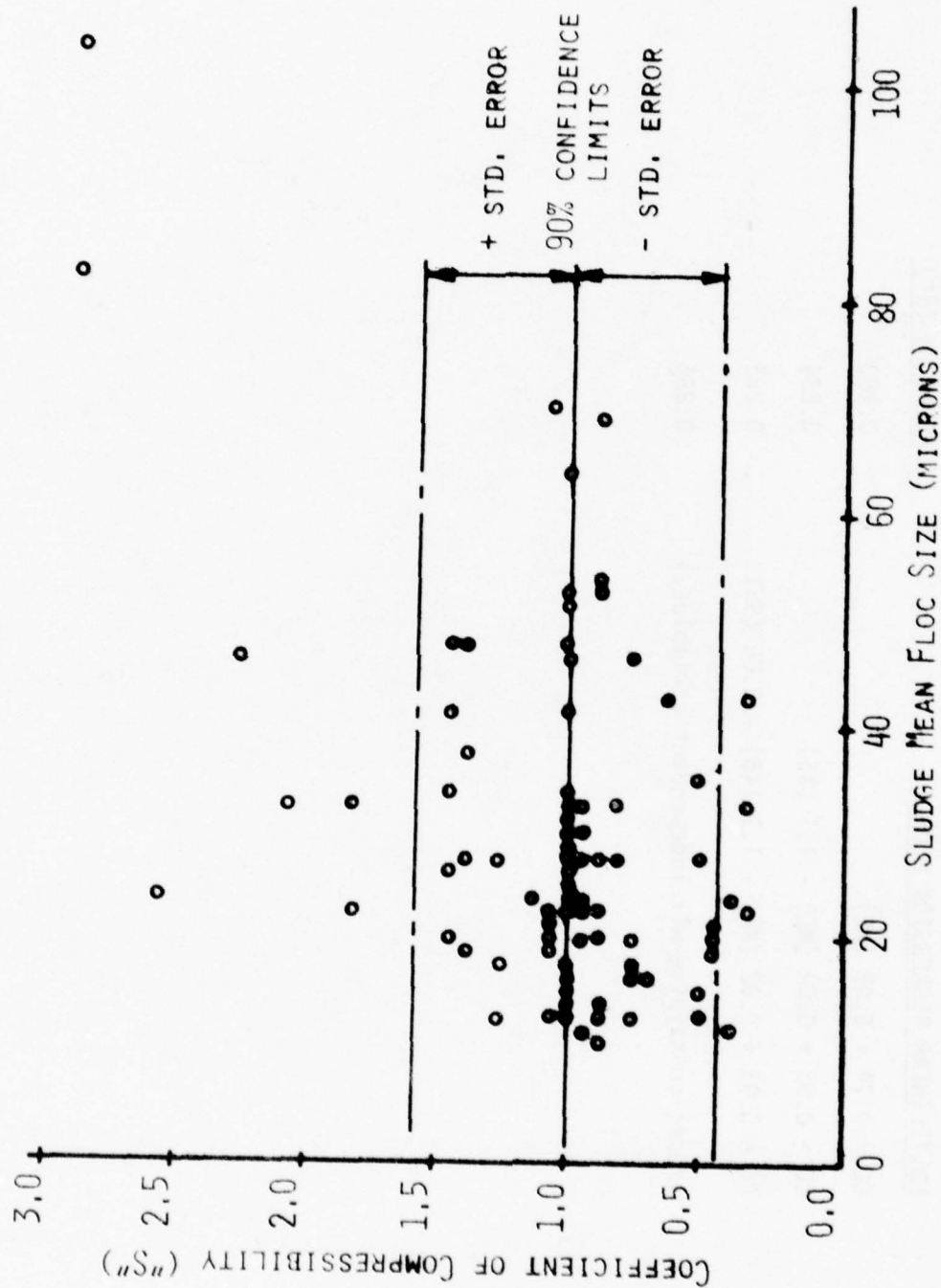


Figure (78). Variations in sludge compressibility as a function of the sludge mean floc size (data for metal hydroxide sludges).

TABLE 18. STATISTICAL MODELLING - COEFFICIENT OF COMPRESSIBILITY (CC)

<u>MULTILINEAR REGRESSION MODEL</u>	<u>CORRELATION (R²)</u>
CC = 0.74 + 0.02 (ME)	0.180
CC = 0.83 + 0.02 (ME) - 1.1 (X5)	0.234
CC = 0.95 + 0.02 (ME) - 1.1 (X5) - 0.06 (SS)	0.253
(Model containing all independent variables.)	0.286

8. Polymer Treatment of Metal Hydroxide Sludges

Sludge conditioning studies using high molecular weight cationic and anionic polyelectrolytes were undertaken to examine their useful application for improving the dewatering of metal hydroxide sludges. Sludges considered during these studies included:

(1) Nickel Hydroxide Sludges - the main emphasis in considering these sludges was the use of conditioning agents for improvements in the sludge dewatering rate;

(2) Mixed-Metal Sludges (Nickel Dominant) - again, the emphasis was conditioning for the reduction of sludge specific resistance. Mixed-metal sludges that were low in nickel content were not examined since they were often characterized by relatively low specific resistance values;

(3) Chromium Hydroxide Sludges - chromium sludges were often characterized by low specific resistance values; thus, conditioning for improvements in the sludge dewatering rate alone was not considered necessary. Instead, the main emphasis in dealing with chromium sludges was the minimization of problems related to solids penetration. Filtrate quality was the standard criteria for the useful application of polymers.

Other sludges, such as the cupric hydroxide and cupric oxide sludges, were not examined for conditioning since no sludge dewatering problems occurred with these sludges if they were allowed to age at least one day prior to dewatering.

Results from the polymer conditioning studies are summarized in Table 19. Certain generalizations can be made in reference to the application of high molecular weight polyelectrolytes for metal hydroxide sludge conditioning:

(1) In all cases examined, the application of either cationic or anionic polyelectrolytes produced a decrease in the characteristic sludge specific resistance. Both types of polyelectrolytes were found to work efficiently for all sludge types over the pH range 7.5 to 11.0. Also, the improvement in sludge dewatering rates was found to be directly related to increases in the size of sludge flocs produced during conditioning.

(2) Little variation was noted in cake solids concentration as a function of conditioning dose. Rather, most of the nickel sludges were characterized by final solids concentrations in the range of 10 to 13%, with a few instances of higher solids concentrations occurring in the range of 16 to 18%. For chromium sludges, the final cake solids concentration was often in the range of 21 to 25% solids, corresponding well with the work of Pattengill (33).

(3) The role of polyelectrolytes in influencing filtrate turbidity can be dramatically seen through the results of these studies. In all

TABLE 19. SUMMARY OF METAL HYDROXIDE SLUDGE
CONDITIONING STUDIES

SLUDGE pH	SLUDGE TYPE	INITIAL C ₀ (%)	OPTIMAL DOSE (ppm)	OPTIMAL DOSE (mg/gr)
7.5	Cr(OH) ₃	3.10	60	1.94
5.9	Ni(OH) ₂	1.77	200	11.30
8.5	Ni(OH) ₂	0.50	40	8.00
9.0	Cr(OH) ₃	2.52	33	1.31
9.1	Cr(OH) ₃	3.10	50	1.61
9.4	Ni(OH) ₂	0.90	33	3.67
9.6	Ni(OH) ₂	1.00	30	3.00
9.7	Ni(OH) ₂	1.54	90	5.84
9.7	Ni(OH) ₂	2.50	150	6.00
10.0	Ni(OH) ₂	1.33	75	5.64
11.1	Ni(OH) ₂	0.81	12	1.48
11.3	Ni(OH) ₂	2.31	90	3.90
11.5	Ni(OH) ₂	1.35	41	3.04
11.8	Ni(OH) ₂	2.75	120	4.36
11.8	Ni(OH) ₂	4.68	225	4.81

cases, especially those where significant solids penetration occurred, small polymer doses resulted in a drastic decrease in the amount of solids passing into the filtrate liquor. Often filtrate turbidities of 1 to 3 NTU or less were noted for the dewatering of conditioned sludges. Also, Figure 77 shows the effect of conditioning on the size distribution of particles passing into the vacuum filtrate. As the polymer dose increases, the characteristic floc size of the filtrate decreases. At high polymer doses, the filtrate particles are in the range of 1 to 2 microns, approaching the colloidal range.

The addition of polyelectrolytes appears to serve two functions: (1) the coagulation of sludge "fines", resulting in a decrease in the relative fraction of fines which could conceivably pass into the filtrate. (2) Improvements in floc strength may also be realized through conditioning. This is especially important for chromium sludges which, upon insolubilization and precipitation, are characterized by large flocs with an apparent low resistance to shear. Polymer conditioning appears to provide added mechanical strength to these flocs, resulting in their increased ability to withstand the forces developed during sludge dewatering. Thus, polymer treatment should be considered for cases where solids penetration is a major problem. The added cost of conditioning may be weighed against both an improvement in dewatering and a reduction in solids penetration.

A summary of the conditioning data is listed in Table 19 with representative results related to the conditioning of nickel hydroxide sludges also shown in Figure 79. During this study, the optimum polymer dose was defined as the amount of polymer necessary to produce a specific resistance value of 20×10^{11} m/kg. This value was chosen as representing the specific resistance of a good dewatering sludge. Normally, optimum polymer doses correspond to minimum specific resistance values; however, these conditioning studies did not utilize polymer doses of the large amounts necessary to reach a minimum resistance value. In general, large polymer doses produced a particle size distribution which was too large to be adequately tested using the HIAC particle counter. Thus, for the results of this study, the resistance value of 20×10^{11} m/kg was chosen to correspond to an optimum polymer dose.

Examination of the results presented leads to the following observations:

(1) The polymer requirements for conditioning chromium hydroxide sludges (in mg polymer/gr solids) are significantly less than that required to condition nickel hydroxide sludges.

(2) The optimum polymer dose is dependent upon the initial sludge solids concentration, as shown in Figure 79. This result is similar to that observed by King *et al.*, (43) who showed a similar dependence on sludge solids concentration when considering the polymer conditioning of water treatment plant sludges.

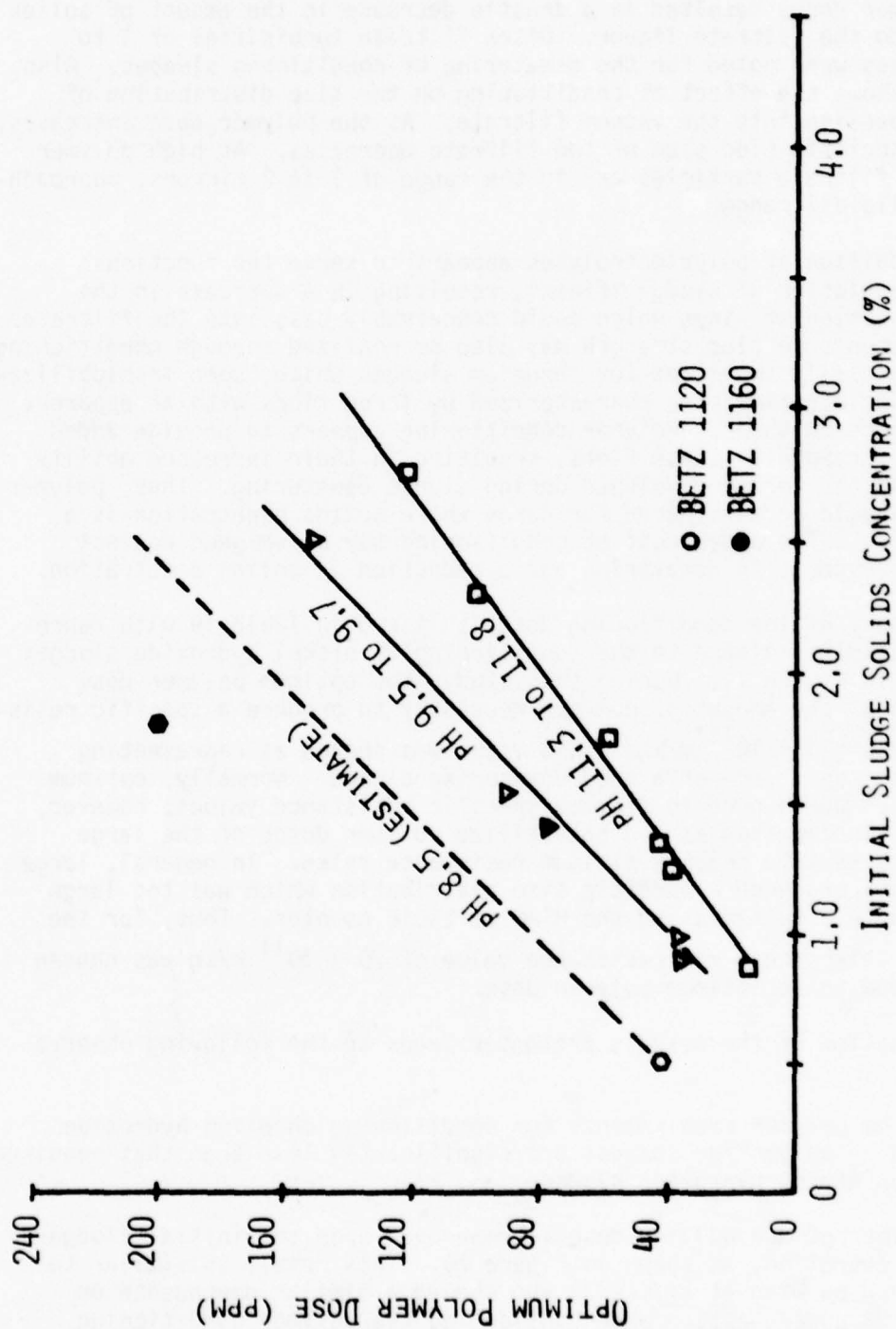


Figure (79). The effect of pH on the polymer dose required for effective conditioning of metal hydroxide sludges (nickel dominant sludges).

(3) The conditioning requirement of nickel hydroxide sludges decreases as the sludge pH increases.

(4) Finally, Figure 79 shows that both cationic and anionic polymers work well for the same type of sludge within the pH ranges listed. Both polymers, having similar molecular weights ($3-5 \times 10^6$), have relatively similar conditioning doses required to produce optimum dewatering rates.

Statistical methods were utilized in an attempt to relate the optimum polymer dosage (in mg polymer/gr solids) to the initial mean size of the sludge to be conditioned. This evaluation could help to explain the role of surface area in determining the necessary polymer dosage for effective sludge conditioning. Data from all three sludge types, using both cationic and anionic polyelectrolytes, were considered within the statistical analysis.

Results from statistical modelling efforts are listed in Table 20. It is obvious that particle size and the corresponding specific surface play an important role in determining the optimum polymer dosage. This observation is similar to that put forth by other investigators. Stumm and O'Melia (44), in discussing the "bridging" action of polyelectrolytes during coagulation, state that

"a direct relationship exists between the available surface area in the colloidal system and the amount of polymer required to produce optimum destabilization."

The analogy between coagulation and sludge conditioning is proper since the main action of polyelectrolytes during sludge conditioning is through the coagulation of sludge particles. Also, La Mer and Healey (45), in reaching this same conclusion, stated that approximately 50% surface coverage of flocs with polyelectrolyte is necessary to produce optimum aggregation by chemical "bridging".

In relation to metal hydroxide sludge conditioning, it may be concluded that such a linear relationship exists, as evidenced by the high correlation between optimum polymer dose and specific surface area (as $1/ME)^2$ in Table 20. Furthermore, it is felt that these results show chemical "bridging" is the mechanism occurring during the conditioning of these sludges. Noval and O'Brien (19) reached the same conclusion from studies related to the polymer conditioning of water treatment sludges. The mechanism of interparticle "bridging" would help to explain the inadequacy of low-molecular weight polymers for metal hydroxide sludge conditioning. Experiments using low-molecular weight cationic polymers were conducted and, in general, produced no significant benefits related to sludge conditioning.

In summary, organic polyelectrolytes can be efficiently utilized for the conditioning metal hydroxide sludges. Their addition to a metal hydroxide sludge promotes coagulation of the particles through the mechanism

TABLE 20. OPTIMUM POLYMER DOSE FOR SLUDGE CONDITIONING (OP)

<u>MULTILINEAR REGRESSION MODEL</u>	<u>CORRELATION (R²)</u>
OP = 4.93 - 0.2 (SS)	0.009
OP = 17.1 - 0.81 (ME)	0.663
OP = -1.04 + 1231 (1/ME) ²	0.761
OP = Optimum Polymer Dose (mg polymer/gr solid)	

of interparticle "bridging", producing a significant increase in floc size and a corresponding decrease in sludge specific resistance. Also, polymer conditioning may work to improve the mechanical strength of flocs, as evidenced by a decreased tendency for floc shear and the reduction of solids penetration into the vacuum filtrate.

9. Thickening of Metal Hydroxide Suspensions

Studies were undertaken to examine in detail the thickening characteristics of metal hydroxide suspensions. Of prime importance was an evaluation of the effect of floc size in determining the interfacial settling rate of a metal hydroxide suspension. Coagulation/flocculation studies were performed using a standard six-place jar test apparatus. Synthetic polyelectrolytes of various characteristic charge were employed as flocculant aids. Two types of metal hydroxide suspensions were examined: (1) pure nickel hydroxide suspensions in the pH range 10.0 to 11.0, and (2) a synthetic mixed-metal hydroxide suspension near pH 10.0. Solids concentrations from 0.42% to 1.92% were examined. Each suspension, after polymer addition and adequate flocculation, was analyzed for its characteristic particle size distribution. Also, samples of each suspension were placed into with 250 ml or 1 liter graduated cylinders. Thickening studies were performed by monitoring the height of the solid-liquid interface as a function of time. The effects of using small-size cylinders on thickening rates were ignored, citing the results of Schaefer (46). In his examination of the settling characteristic of chemical sludges, Schaefer concluded the diameter of settling column had a minimal effect on the observed settling behavior.

Representative results from the examination of metal hydroxide suspensions are shown in Figure 80. Increased doses of polyelectrolytes produce a distinct increase in the observed interfacial settling velocity. Likewise, Figure 81, presenting the variation in the floc size distribution as a function of polyelectrolyte dose, shows a similar increase in the mean sludge floc size. Thus, the improvement in settling velocity noted is due principally to increases in the size of flocs present in suspension.

The relationship between floc size and suspension thickening velocity was observed repeatedly with every initial solids concentration examined for both types of metal hydroxide suspensions. Also, Figure 80 shows each suspension settled to the same ultimate sludge depth. That is, the addition of polyelectrolytes appeared to have no effect on the ultimate solids concentration achieved by gravity thickening. It may be concluded that polymer conditioning increases the characteristic size of flocs present, resulting in an increase in the interfacial settling velocity but producing no perceivable effect on the ultimate solids concentration obtained.

In Figure 82 representative settling data is used to show the relationship which exists between the mean suspension floc size and the interfacial settling velocity. A series of parallel lines corresponding to

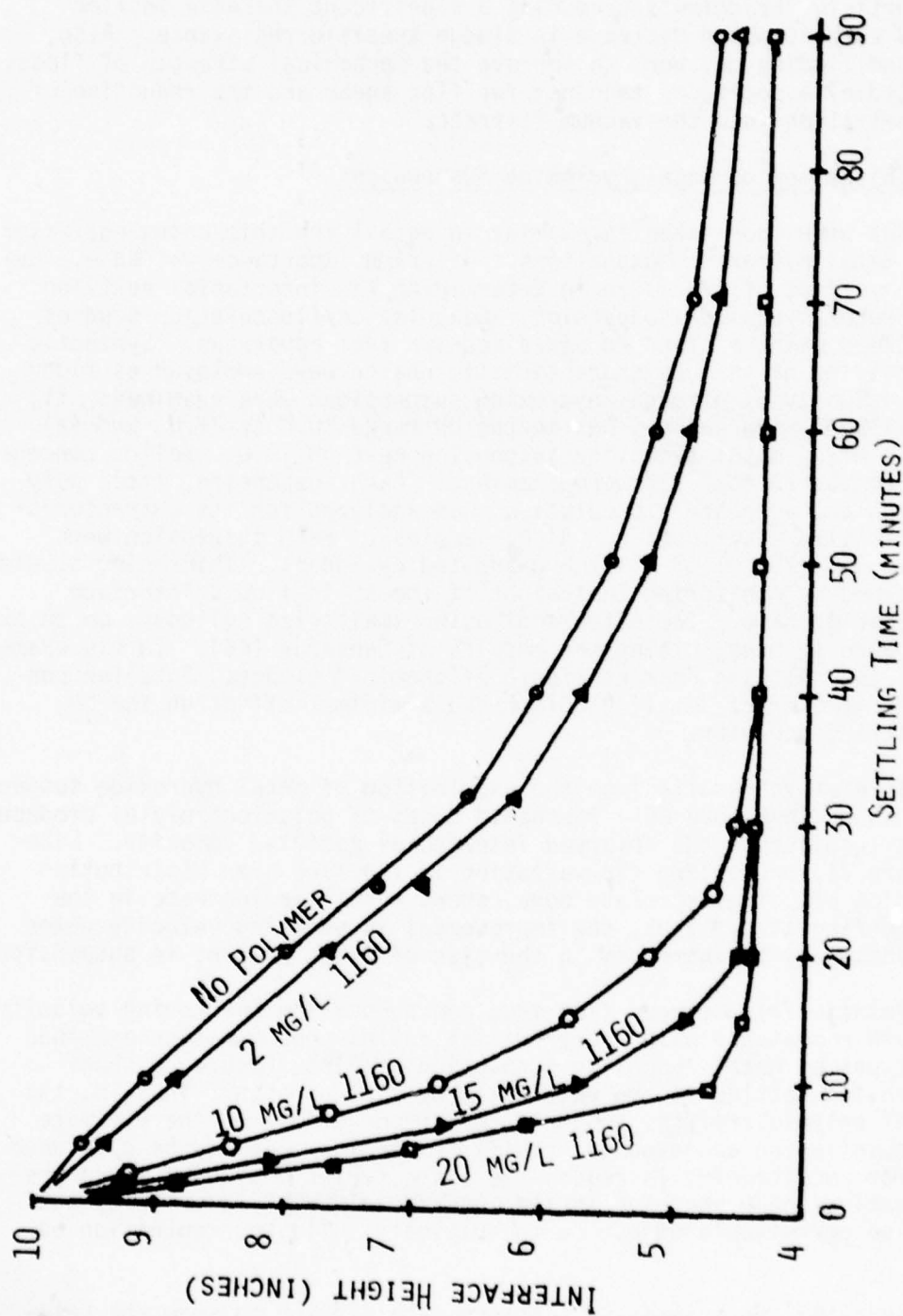


Figure (80). Effects of polymer conditioning dosage on the rate of thickening of metal hydroxide suspensions.

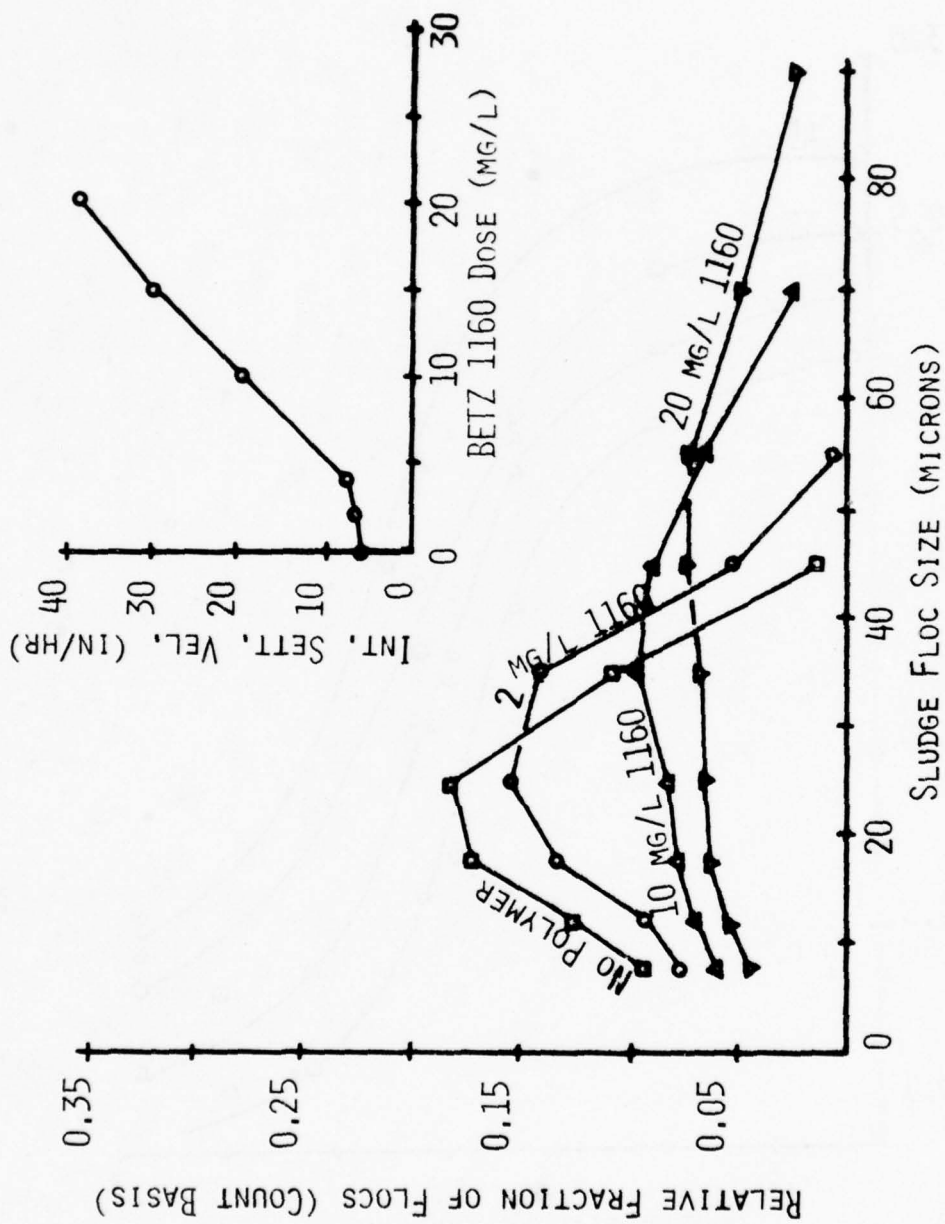


Figure (81). Effects of polymer conditioning dosage on the size of flocs present in metal hydroxide suspensions.

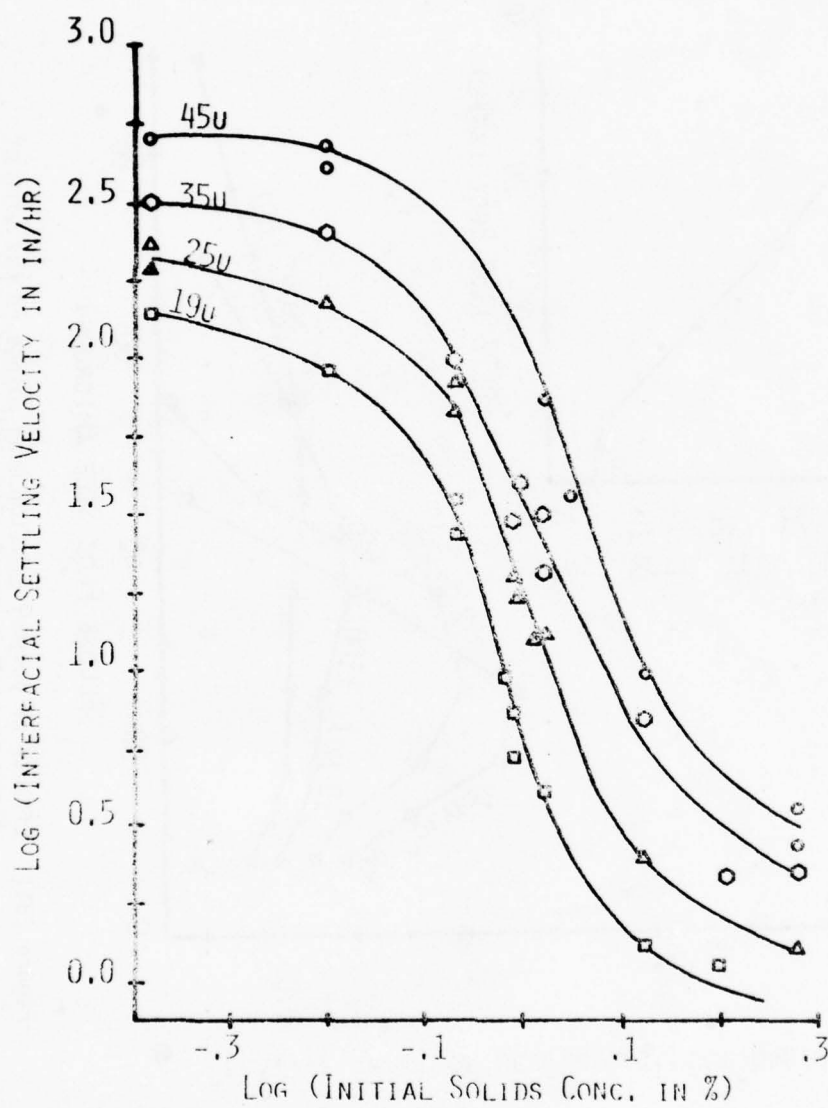


Figure (82). Particle size effects on the thickening rates of metal hydroxide suspensions.

increases in the mean floc size are noted. For a given solids concentration, an increase in size produces a corresponding increase in the thickening velocity. It is important to note that the lines corresponding to similar floc sizes are roughly parallel, implying that conditioning has produced no major change in the floc density. Results presented by Schaefer (46) have shown that changes in the floc density produce a shift in the characteristic slope of a log settling velocity versus solids concentration plot. As the floc density increases, the slope decreases, implying a decreased dependency of settling velocity on the solid concentration. Pattengill (33) presented similar results for the settling of chromium hydroxide suspensions. As the chromium floc density increased, the slope of the log (v) versus solids concentration plot was seen to decrease. Thus, since the data shown in Figure 82 presents no evidence of a variation in slope, it may be concluded that conditioning results in an increase in the metal hydroxide floc size but has little effect on the floc density.

Numerous investigators have developed empirical equations showing the effect of sludge solids concentration on the settling velocity (47). Several of these relationships contain empirical constants. It was the intent of this study to examine how parameters such as sludge floc size were accounted for in these models. Using data from the analysis of metal hydroxide suspensions, an empirical relationship was developed to account for the effects of solids concentration and particle size on the observed interfacial settling velocity. Table 21 presents the two models which show the highest levels of statistical significance. Examining the two relationships presented allows one to conclude that the initial solids concentration plays the most dramatic role in determining the observed interfacial settling velocity. Equation (a) shows that a small increase in the initial solids concentration will produce a dramatic decrease in the rate of interface settling. However, the inclusion of particle size in the empirical model can be seen to produce a significant improvement, increasing the correlation coefficient of the model to $R^2 = 0.92$. Roughly 92% of the variation in observed interfacial settling velocities can be accounted for strictly by the solids concentration and the mean suspension floc size. Also, it is important to note that, in Equation (b)

$$(ISV) \propto k(ME)^{1.833}$$

for a given solids concentration. This relationship is similar to that provided by Stokes Law for the settling of discrete particles

$$(V_c) = k(d_p)^2.$$

Finally, Equation (b) can be seen to be indeed similar to the model presented by Vesilind (47).

It may be concluded that zone settling can be characterized by flocs which appear to settle independently, though hindered by fluid flow around neighboring particles. Likewise, if adequate dilution of the suspension

TABLE 21. STATISTICAL MODELLING - INTERFACIAL SETTLING VELOCITY (ISV)

<u>MULTILINEAR REGRESSION MODEL</u>	<u>CORRELATION (R²)</u>
(a) $ISV = 15.24 (1/SS)^4$	0.823
(b) $ISV = \frac{0.029 (ME)^{1.833}}{(SS)^{4.45}}$	0.918

ISV = Interfacial Settling Velocity (in/hr).

was provided, the flocs would settle as discrete particles. Finally, it should be noted that the models presented in Table 21 must be modified to account for possible variations in floc density before they may be applied to other suspensions.

Figure 83 presents the results of comparative thickening tests using cationic, anionic and nonionic polyelectrolytes as flocculant aids. No appreciable difference can be noted between the use of any of the three polyelectrolytes; rather, all are seen to produce similar improvements in the interface settling velocity. For the polymers examined, it can be concluded that polymer charge does not affect the applicability of a given polyelectrolyte to this mixed-metal suspension, at least when considering pH values near 10.0. The mechanism of polymer action appears to involve "bridging", a characteristic response to the use of high molecular weight polymers. It should be noted that the only polymers studied were characterized by molecular weight values in excess of 2×10^6 . No studies were performed to evaluate the applicability of low-molecular weight polymers for coagulating metal hydroxide suspensions.

Finally, attempts were made to determine whether a correlation between settling rates and dewatering rates could be observed for metal hydroxide suspensions. Two separate thickening studies using nickel hydroxide suspensions were performed using cationic and anionic polyelectrolytes respectively. In each study, the original nickel suspension was dosed with increasing polymer concentrations. Each sample was then placed into a one-liter graduated cylinder, and a thickening test was performed to determine the characteristic interfacial settling velocity for each polyelectrolyte dosage. Following a twelve-hour thickening period, the concentrated solids slurry was removed from the bottom of each settling column. Filtration studies were then performed on 100 ml samples of each slurry to determine the time necessary to obtain a filtrate volume of 60 ml.

Representative results from each study are shown in Figure 84. The addition of polymer produced an increase in the settling velocity and a corresponding increase in the dewatering rate during filtration. This is a reasonable observation, owing to the previous discussion related to the effects of particle size on both the interfacial settling velocity as well as in relation to the characteristic resistance to dewatering. One may conclude that, for metal hydroxide sludges, the rate of thickening and the filtration rate correlate and are both dependent on particle size.

In summary, the results presented in Sections (8) and (9) have shown the beneficial aspects of polyelectrolyte additions for the conditioning of metal hydroxide suspensions. Improvements related both to thickening and dewatering have been documented for several metal hydroxide sludges. Also, the results of this study have shown that a significant correlation exists between the thickening and filtering rates of hydroxide sludges. Finally, in all cases, the action of polyelectrolytes was through the

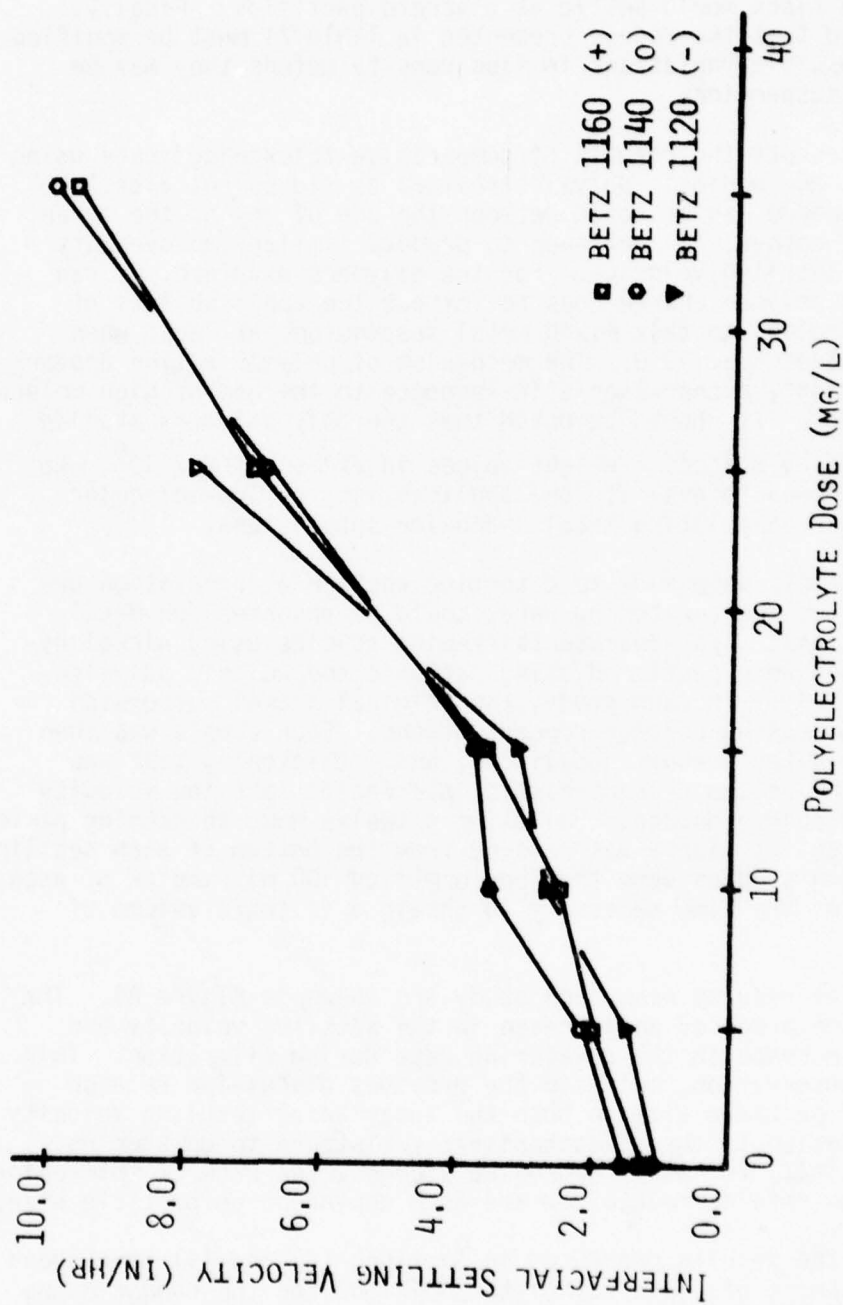


Figure (83). Comparative results from the use of several polymer types for the improvement of metal hydroxide suspension thickening rates.

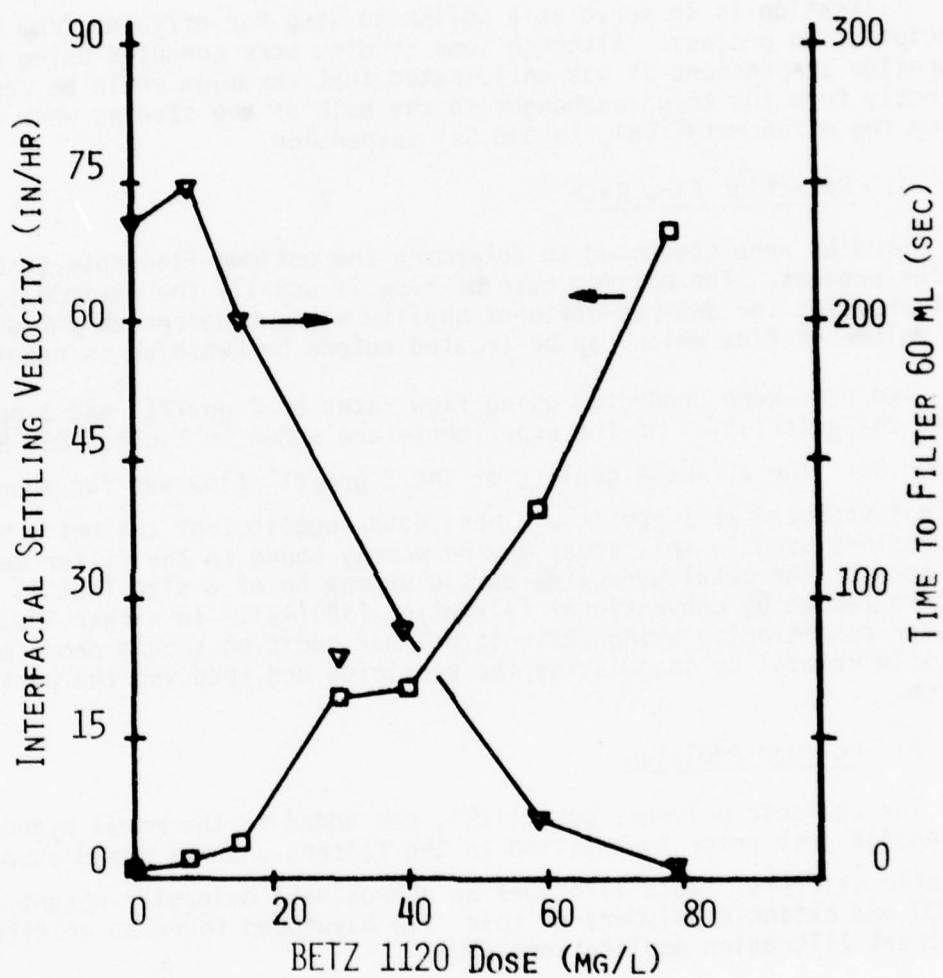


Figure (84). Sludge thickening rates and dewatering rates as a function of polymer conditioning dose.

coagulation of hydroxide flocs, most probably by the mechanism of inter-particle "bridging".

C. Gravity Dual Media Filtration of Metal Oxide Suspensions

Filtration is to serve as a polishing step for effluent from the precipitation process. Although some studies were conducted using chromium hydroxide suspensions it was anticipated that chromium would be recovered directly from the anion exchanger so the bulk of the studies were conducted using the mixed metal (Ni, Zn and Cu) suspension.

1. Effect of Flow Rate

Studies were conducted to determine the optimum flow rate to be used in the process. The optimum rate of flow is usually the maximum loading that provides the desired effluent quality without appreciably reducing the volume of flow which can be treated before backwashing is required.

Two runs were conducted using flow rates of 2 gpm/ft² and 3 gpm/ft². Other characteristics of the experiments are shown in Figures 85, 86, 87 and 88. The effluent quality of the 2 gpm/ft² flow was far superior to that produced at 3 gpm/ft². These data suggest that the metal hydroxide suspensions used in this study may be poorly bound to the filter media surfaces or the metal hydroxide particles may be of a size that is difficult to remove by conventional filtration (48)(49). In either instance, polymer conditioning using cationic polymer addition should produce better particle removal by coagulating the particles and reducing the particle charge.

2. Polymer Addition

The cationic polymer, Betz 1175[•], was added to the metal hydroxide suspension just prior to addition to the filters and was mixed using two magnetic stirrers. Betz 1175[•] has an approximate molecular weight of 10,000 and cationic polymers of this size have been found to be effective in direct filtration applications (50).

A comparison of the removal efficiency obtained without polymer, shown in Figure 85, to that obtained when polymer was used, shown in Figure 89, provides evidence that polymer addition can greatly increase particle removal efficiency in a filter. Head loss data for the two runs, with and without polymer addition, are shown in Figure 86 and 90. As shown earlier, almost all of the turbidity removal occurs in the upper layer of the sand bed when no polymer is used, the 18 inch anthracite layer playing only a minor role in the particle removal process. The addition of polymer results in better utilization of the bed such that particle removal appears to be distributed well throughout the bed. Overall, polymer addition results in improved particle removal and reduced head loss through the filter bed.

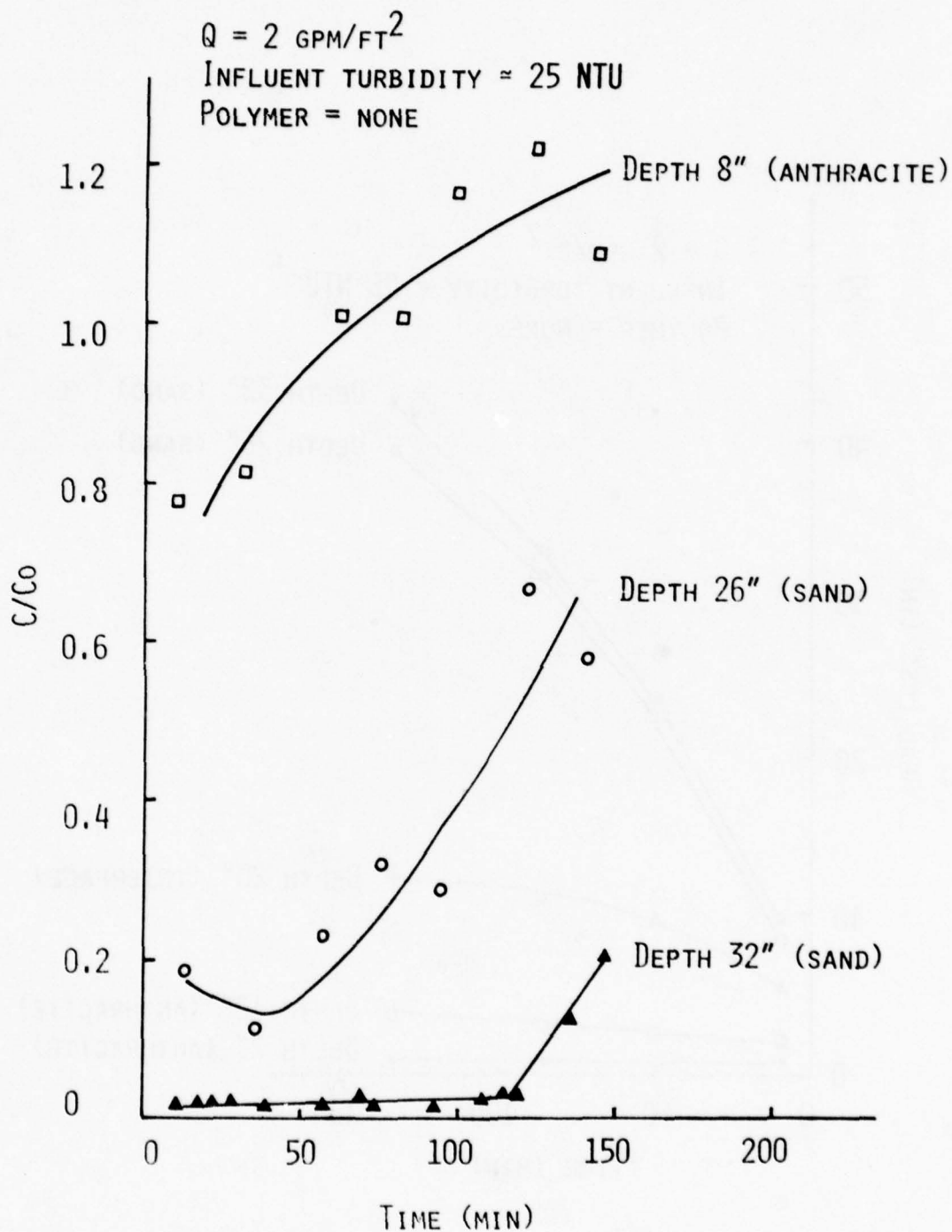


Figure (85). Filtration of mixed-metal hydroxide suspension without polymer addition - effluent profile.

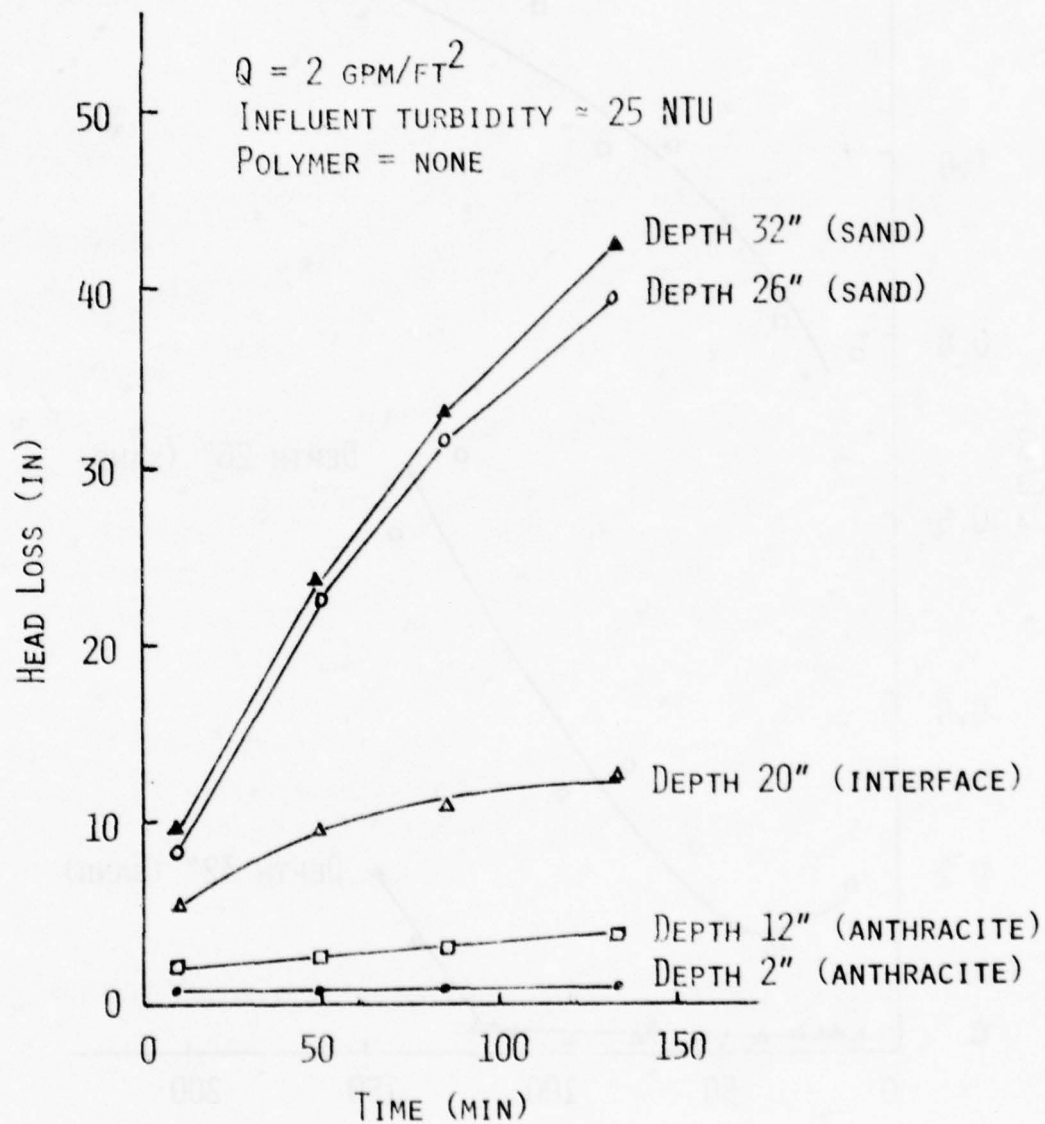


Figure (86). Filtration of mixed-metal hydroxide suspension without polymer addition - headloss profile.

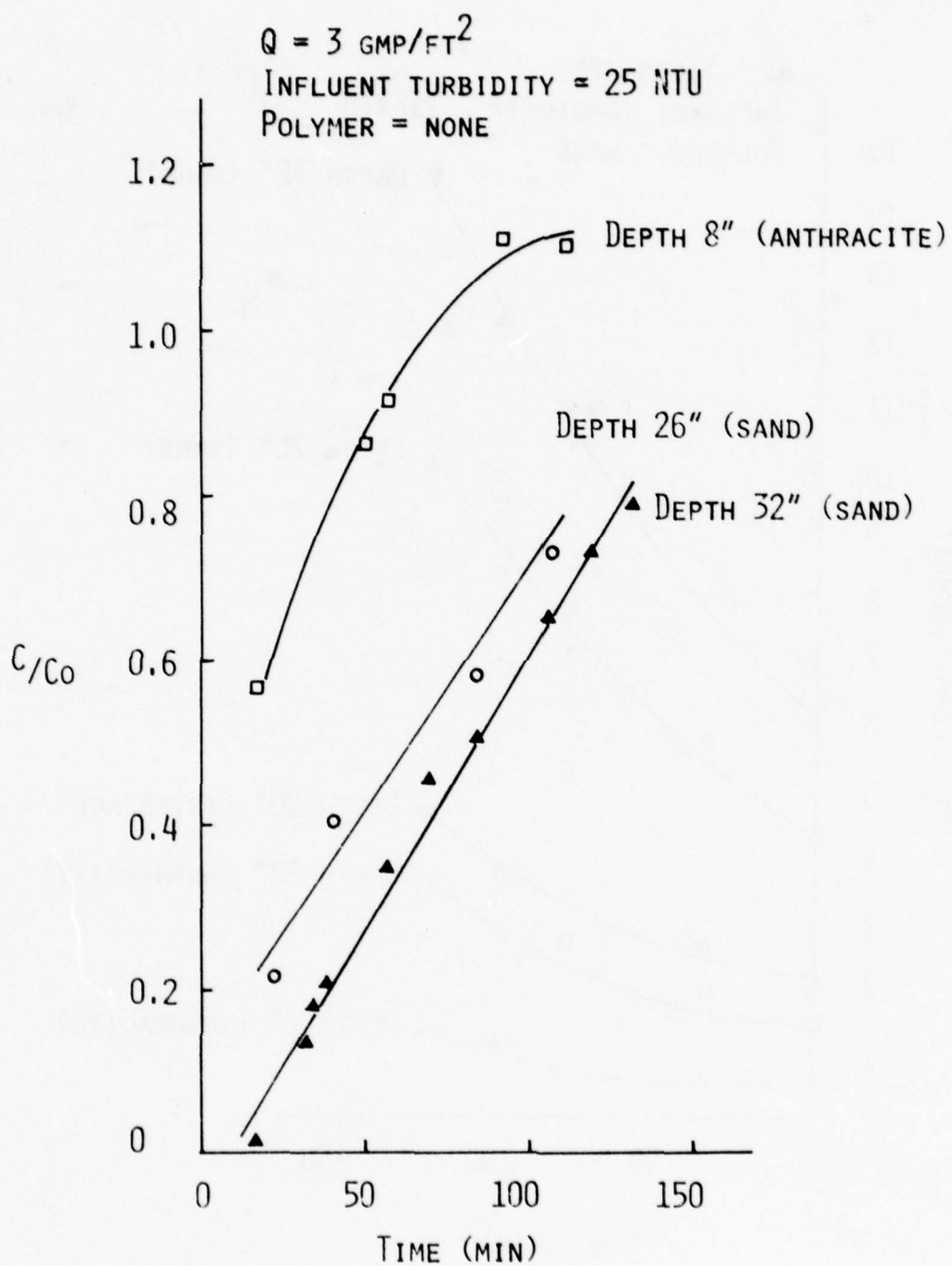


Figure (87). Filtration of mixed-metal hydroxide suspensions without polymer addition - effluent profile.

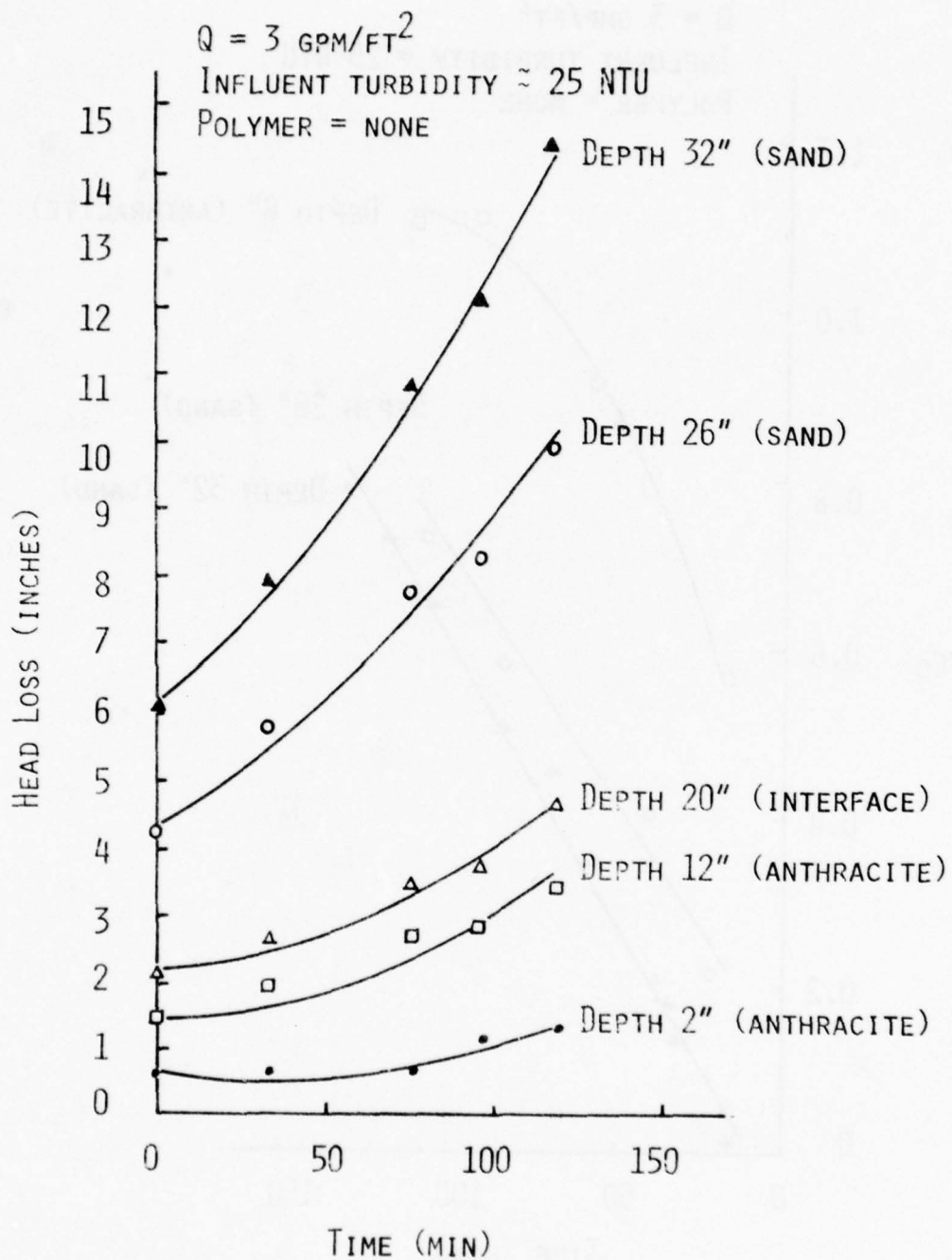


Figure (88). Filtration of mixed-metal hydroxide suspension without polymer addition - headloss profile.

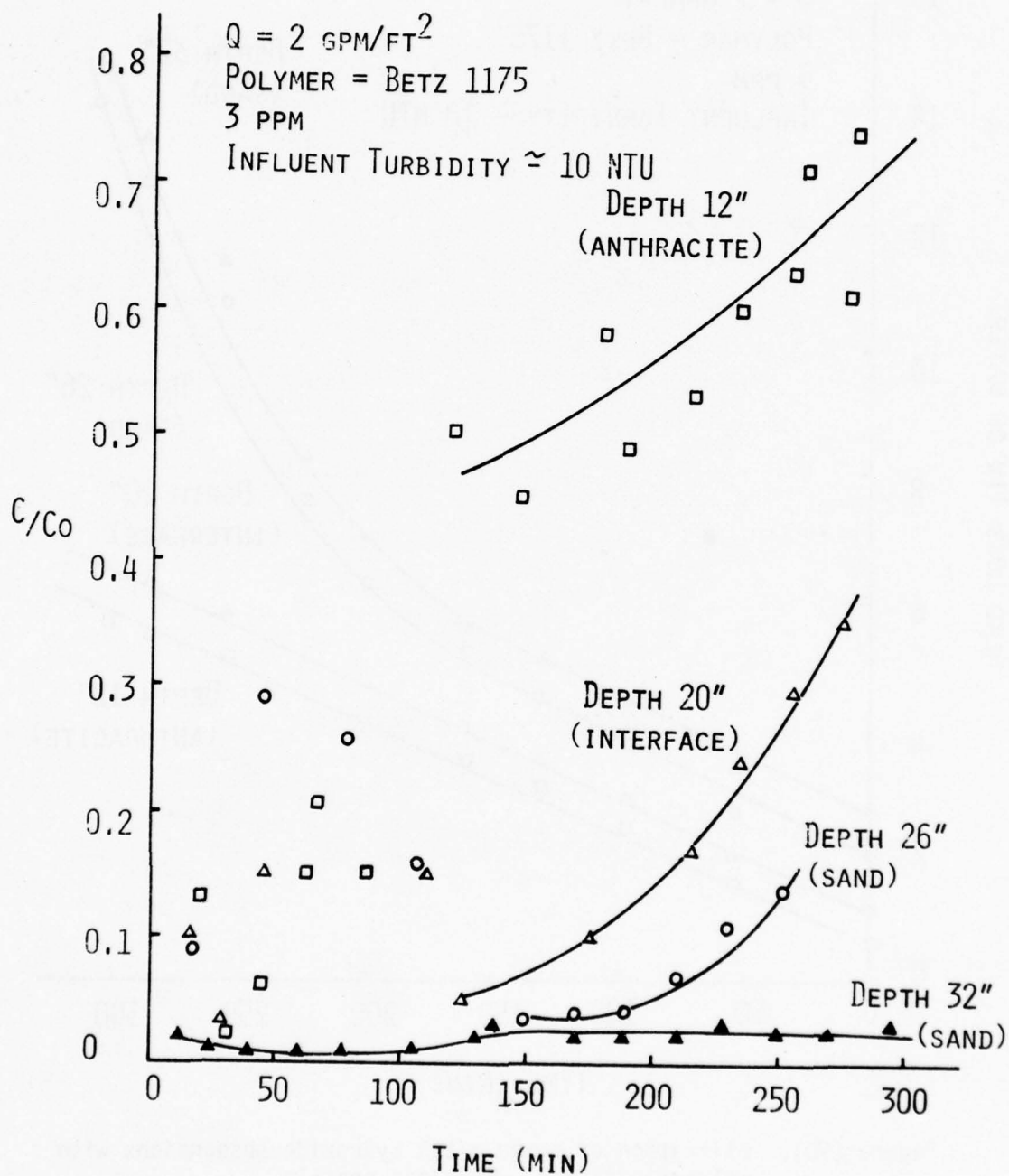


Figure (89). Filtration of mixed-metal hydroxide suspensions with polymer addition - effluent profile.

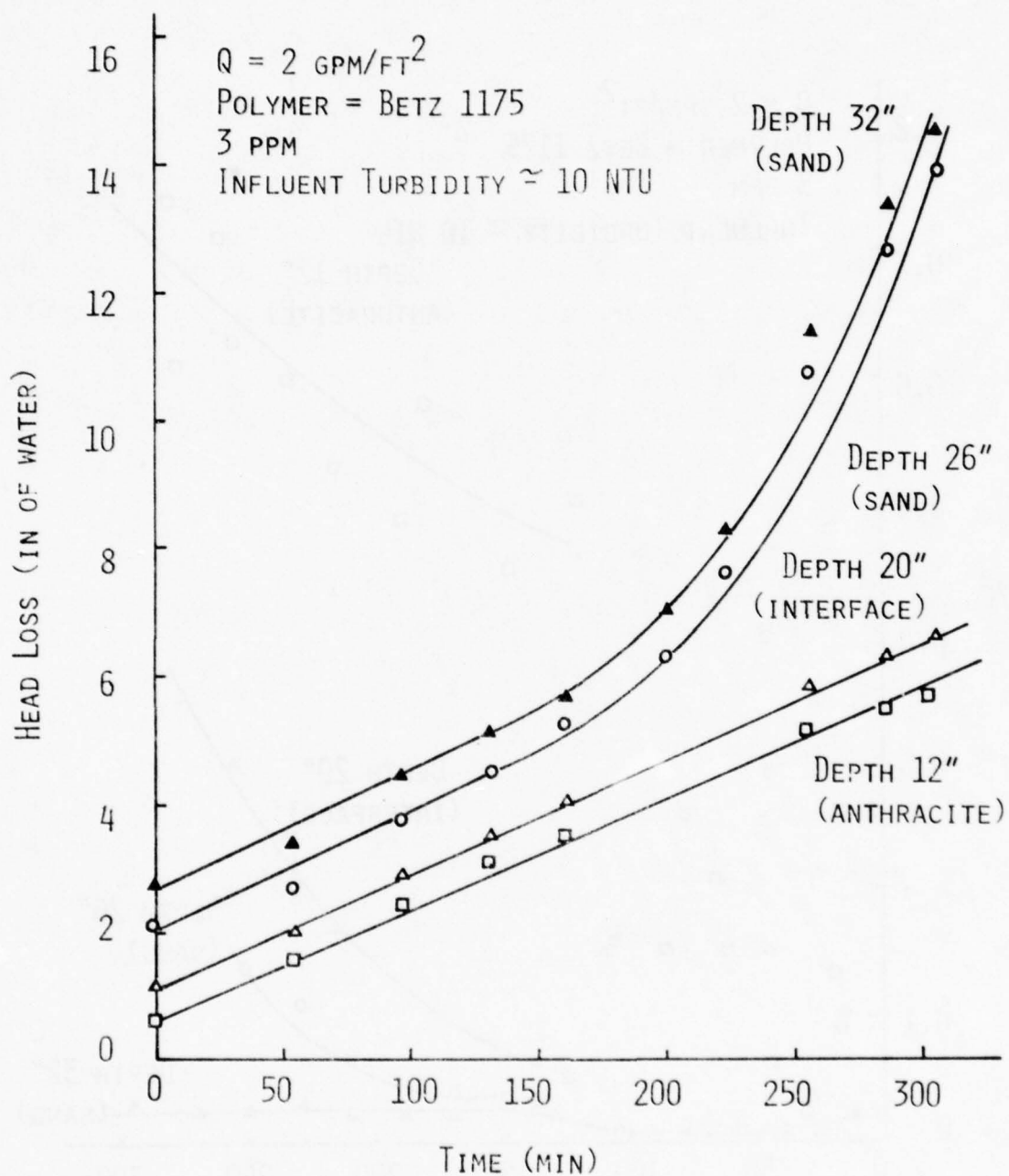


Figure (90). Filtration of mixed-metal hydroxide suspensions with polymer addition - headloss profile.

Additional studies conducted using the 10 NTU turbidity suspension show that the amount of polymer needed for improved filter performance is quite small. In Figure 91 the turbidity removal using 0.5 mg/l Betz 1175* is shown to be equal or superior to that obtained using 3 mg/l, shown in Figure 89. Both doses perform well and head losses are minimal.

Increasing the filter rate from 2 to 4 gpm/ft² resulted in a marked deterioration in filter performance. The filter data for 4 gpm/ft² using 3 mg/l Betz 1175* is shown in Figure 92. Comparison of the data in Figure 89 (2 gpm/ft²) with that in Figure 92 (4 gpm/ft²) suggests that at the higher flow rates the anthracite media is not effectively used, possibly because insufficient time is being allotted for particles to make contact with the surface of the media. This results in heavy particle application to the sand layer, producing high head losses and rapid particle breakthrough. Increased polymer addition did not improve filter performance at this flow rate as indicated in Figure 93.

3. Precoat Filtration

An alternative to adding polymer to the metal suspension is polymer precoating of the filter media. If particle removal is inefficient because of charge repulsion between the particle and filter media surface or if particles are poorly retained, media precoating can offer advantages over polymer addition directly to the suspension. These advantages are a reduction in material, handling, elimination of a polymer influent mixing unit and elimination of operational problems associated with trying to constantly alter polymer feeding as flow rates and particle concentrations vary.

Precoating was accomplished by bottom feeding a concentrated polymer solution into the bed until it completely covered the media and permitting it to remain in contact for two hours.

The results of one such experiment are shown in Figure 94. These data indicate that precoating provides results comparable to those obtained by direct polymer addition to the suspension solution when flow rates are low (2 gpm/ft²). Precoating followed by operation at 4 gpm/ft² produces results nearly identical to those obtained using polymer addition to the suspension. These data are presented in Figure 95.

Overall, it appears that cationic polymers can effectively be used to aid in the filtration of metal hydroxide suspensions using a mixed media filter. The polymers make the anthracite layer much more effective for particle removal and reduce the overall head loss in the bed by distributing the particle deposition uniformly throughout the bed. The concentration of polymer appeared not to be critical; the lower dose used (0.5 mg/l) worked as well as doses much higher.

Polymer precoating produced results nearly identical to direct polymer

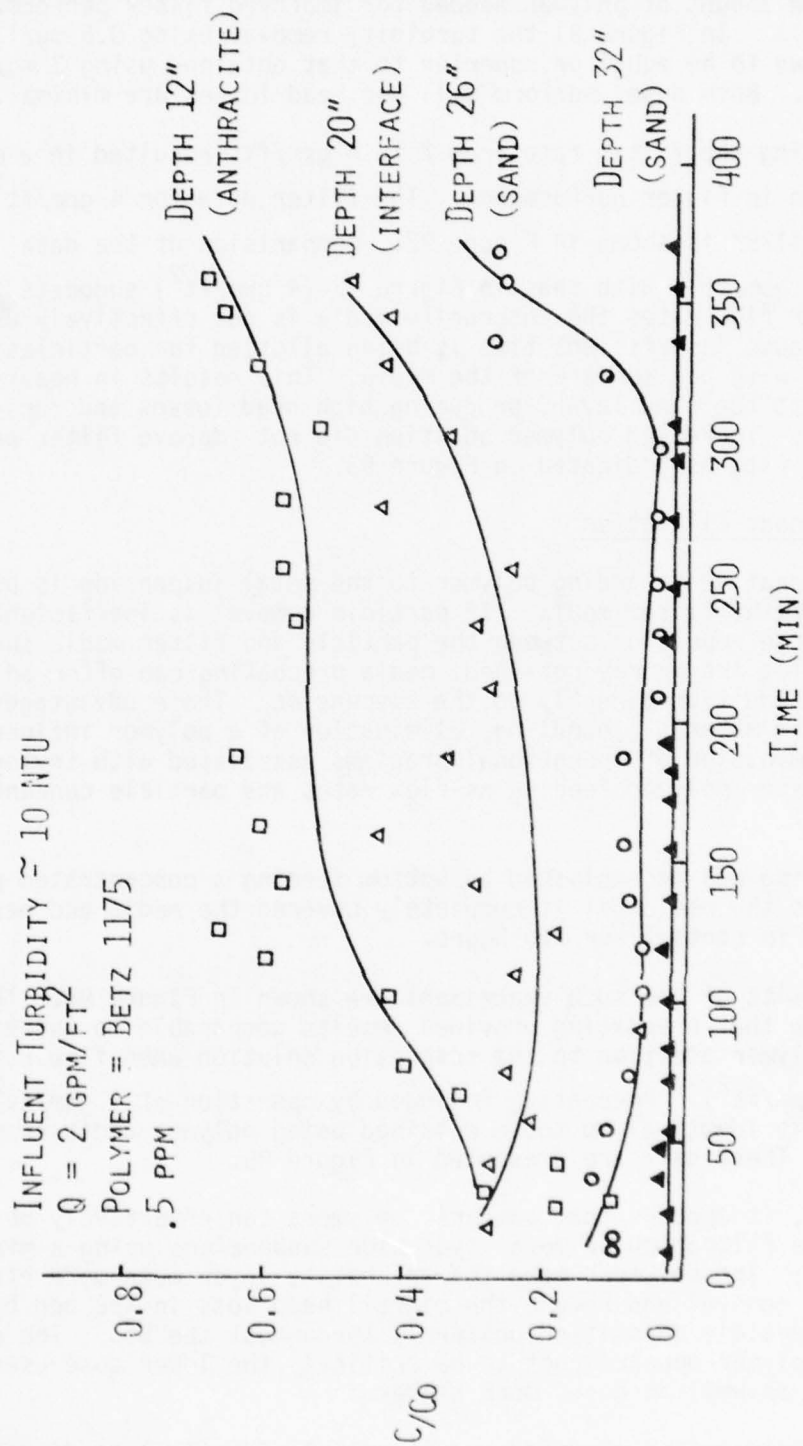


Figure (91). Filtration of mixed-metal hydroxide suspensions with polymer addition - effluent profile.

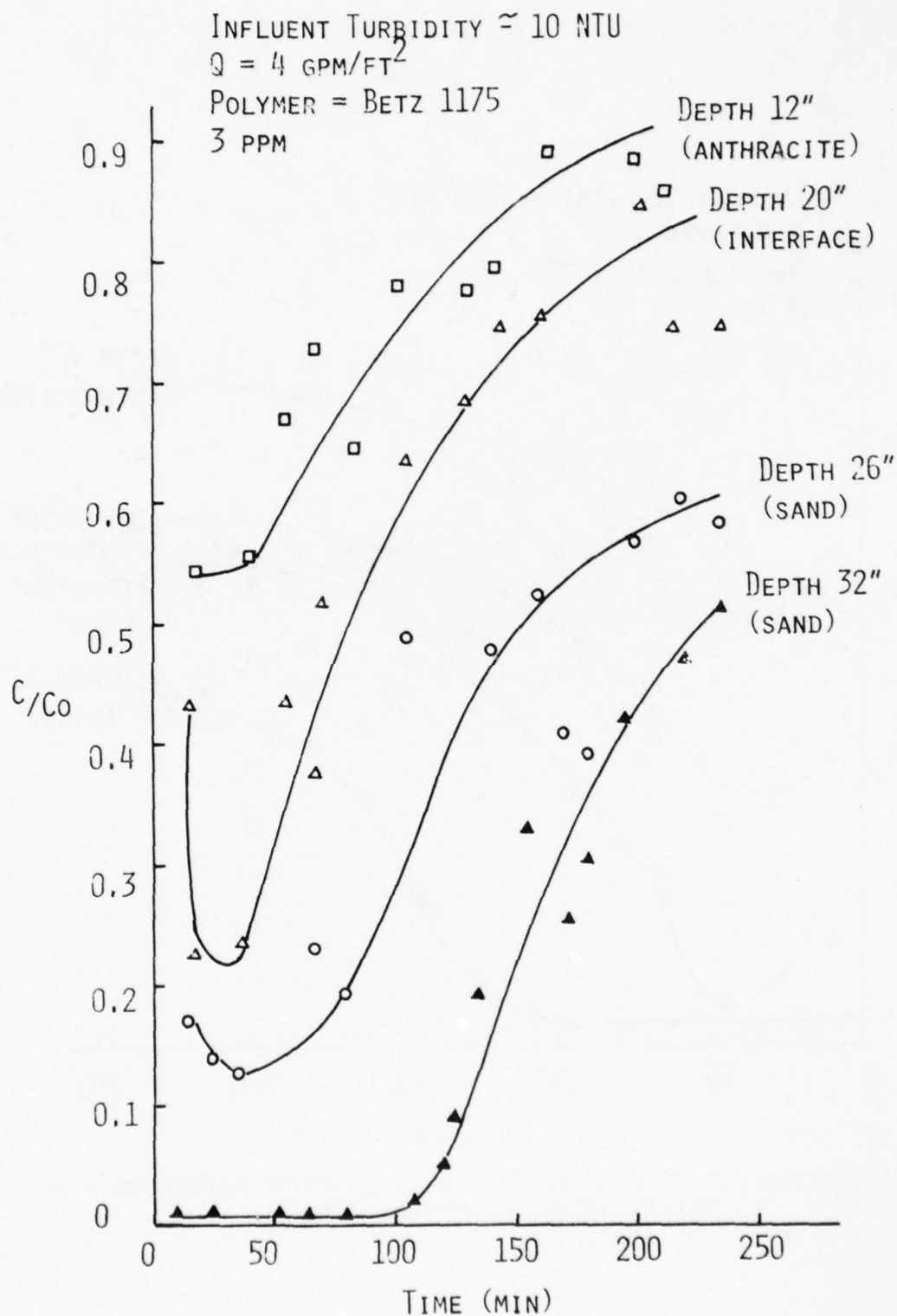


Figure (92). Filtration of mixed-metal hydroxide suspensions with polymer addition - effluent profile.

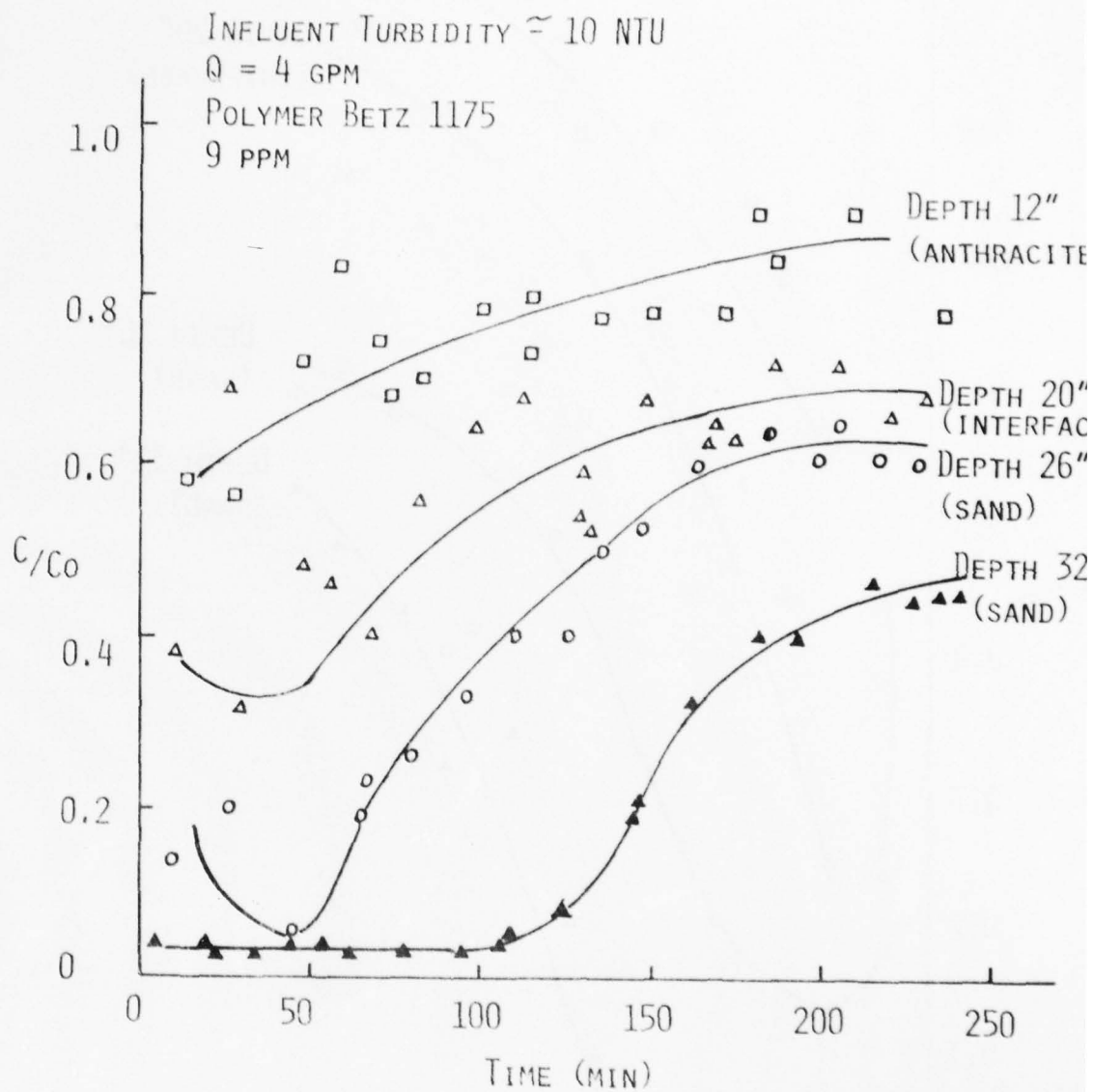


Figure (93). Filtration of mixed-metal hydroxide suspensions with polymer addition - effluent profile.

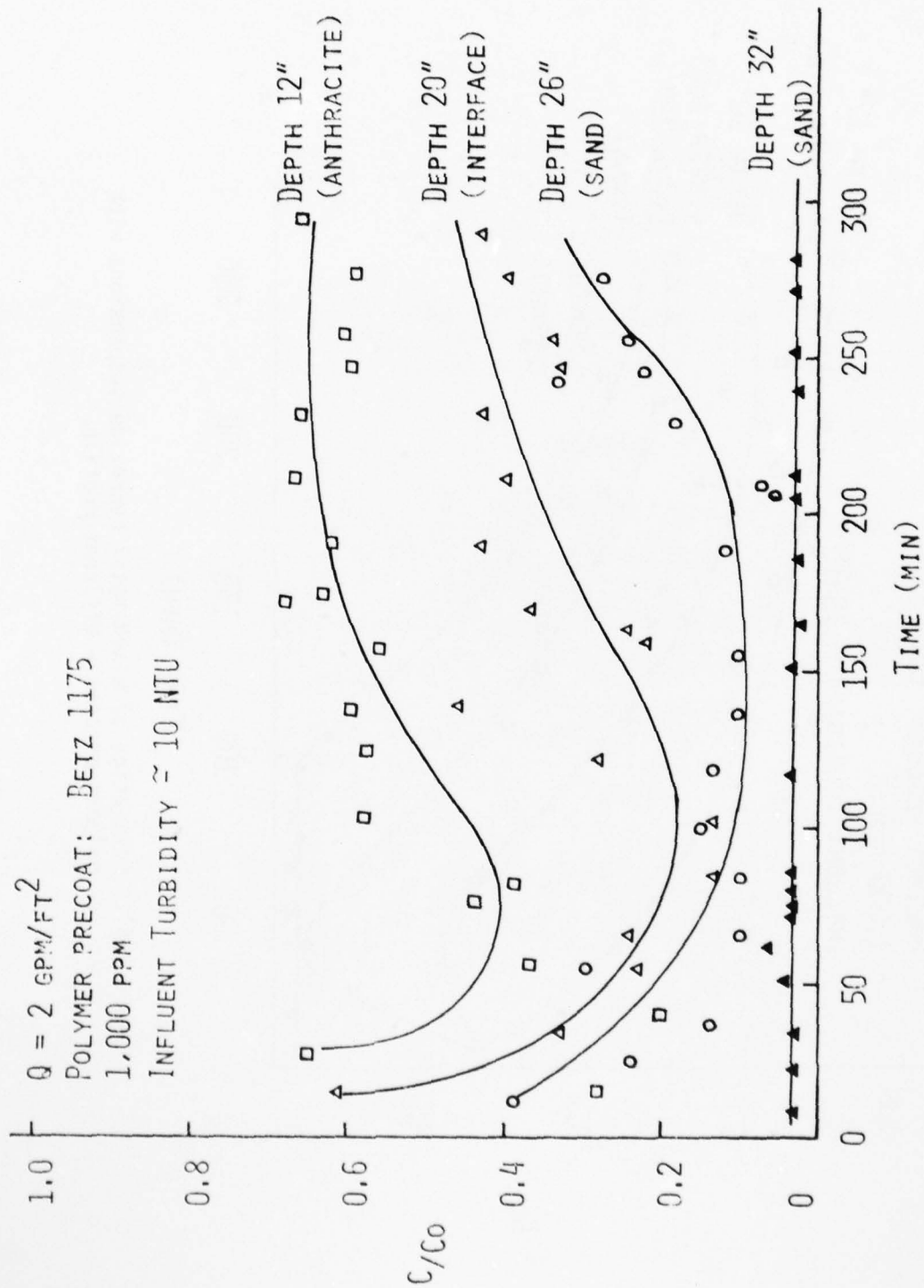


Figure (94). Filtration of mixed-metal hydroxide suspensions with polymer precoat - effluent profile.

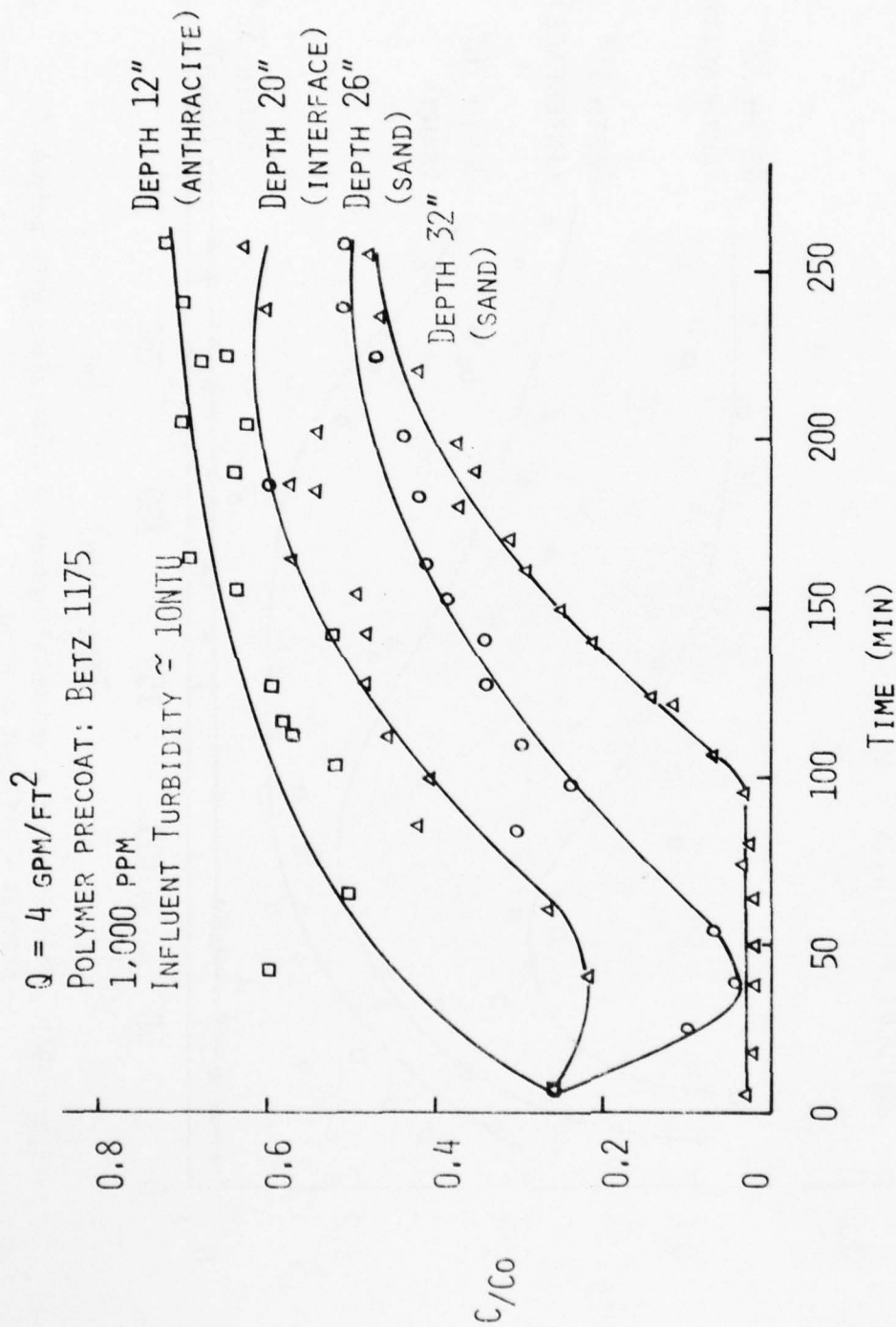


Figure (95). Filtration of mixed-metal hydroxide suspensions with polymer precoat - effluent profile.

application to the suspending medium. Either method can be used and economics and ease of operation should decide the best method of application.

A few filter runs were conducted using anionic polymers. Stump and Novak (50) have shown that anionic polymers have limited application to dual media filters because they cause high head losses at the top surface of the filter. Similar results were obtained in this study using the anionic polymer, Betz 1100*, a 5×10^6 molecular weight polyamine. Data presented in Figures 96 and 97 indicate that even at very small doses, 0.5 mg/l, head losses occur rapidly and at the filter surface. In addition, turbidity removal is not as effective as with cationic polymers.

A preliminary study was conducted to determine if anionic polymer performance could be improved by using a coarser media. Although this study was not meant to be exhaustive, it could provide a direction for future study. Because the lower doses of anionic polymer would result in less chemical cost, optimization of anionic polymer application could be beneficial.

Data was collected using a filter which contained a larger anthracite media (E.S. = 1.0, U.C. = 1.4) than the other filter experiments (E.S. = 0.7, U.C. = 1.5). The results of this experimental run, shown in Figures 98 and 99, indicate that the filter effluent quality can be greatly improved and head losses reduced by the addition of a coarser media. Head losses still greatly exceed those obtained using cationic polymers but indicate that some increase in filter performance may still be possible by further media size alterations. Overall, anionic polymers do not provide filter runs that are equal to those obtained using cationic polymers because of excessive head losses.

Summaries of metal removal efficiencies for some of the filter runs are presented in Table 22. These data show that under the best operating conditions, nickel concentrations in the effluent stream will contain greater than 1 mg/l nickel and often exceed 5 mg/l. Although additional optimization of the granular media process is possible, it is unreasonable to expect metal removals to exceed 95%. This level of removal may be acceptable for recycling of the waste stream but will be unacceptable for direct discharge.

D. Pressure Precoat Filtration with Diatomaceous Earth

Precoat filters often find use in industrial applications because of their smaller space requirements, lower capital investment, and decreased need for extensive pretreatment. This final advantage may be especially applicable to the waste stream from the precipitation process because polymers were needed to provide for effective filtration using a granular filter.

If precoat filtration is to be considered, it must be shown that the filtration processes is effective in removing metals from the waste

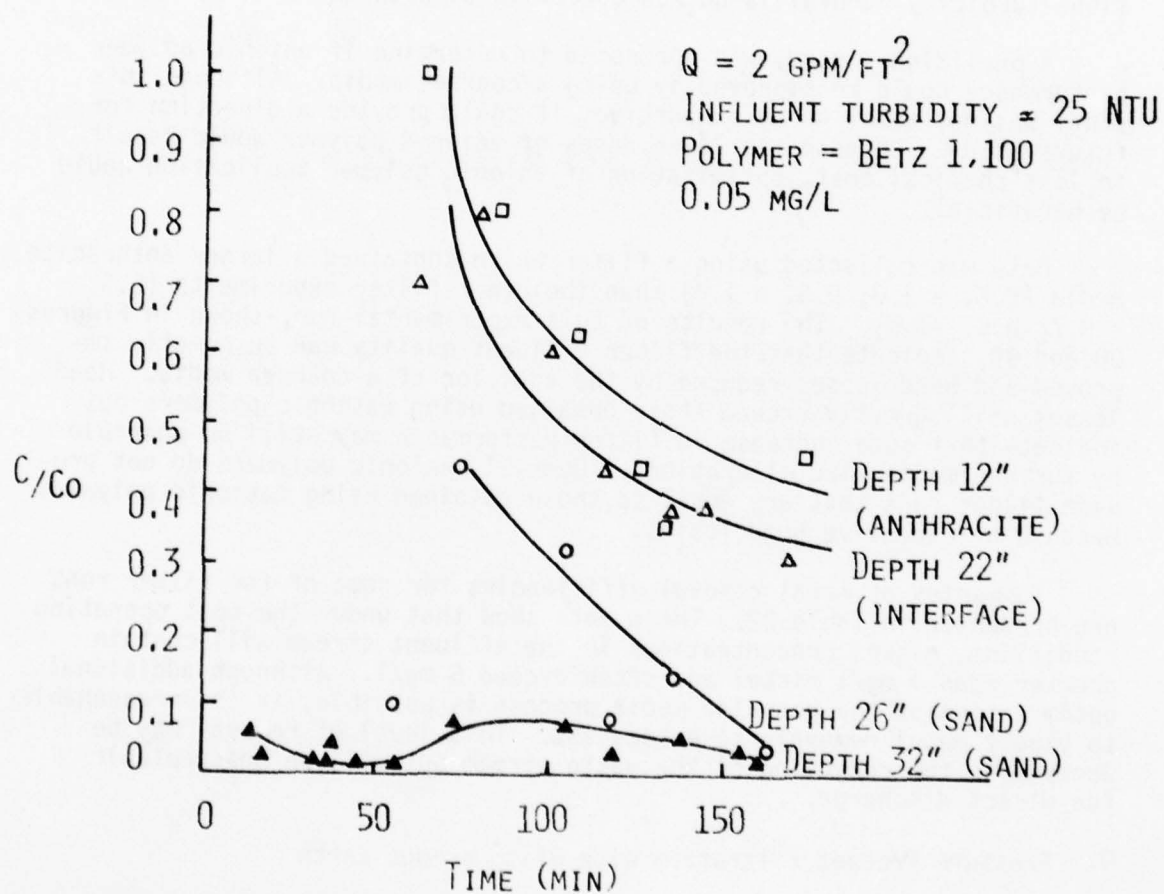


Figure (96). Filtration of mixed-metal hydroxide suspensions with anionic polymer addition - effluent profile.

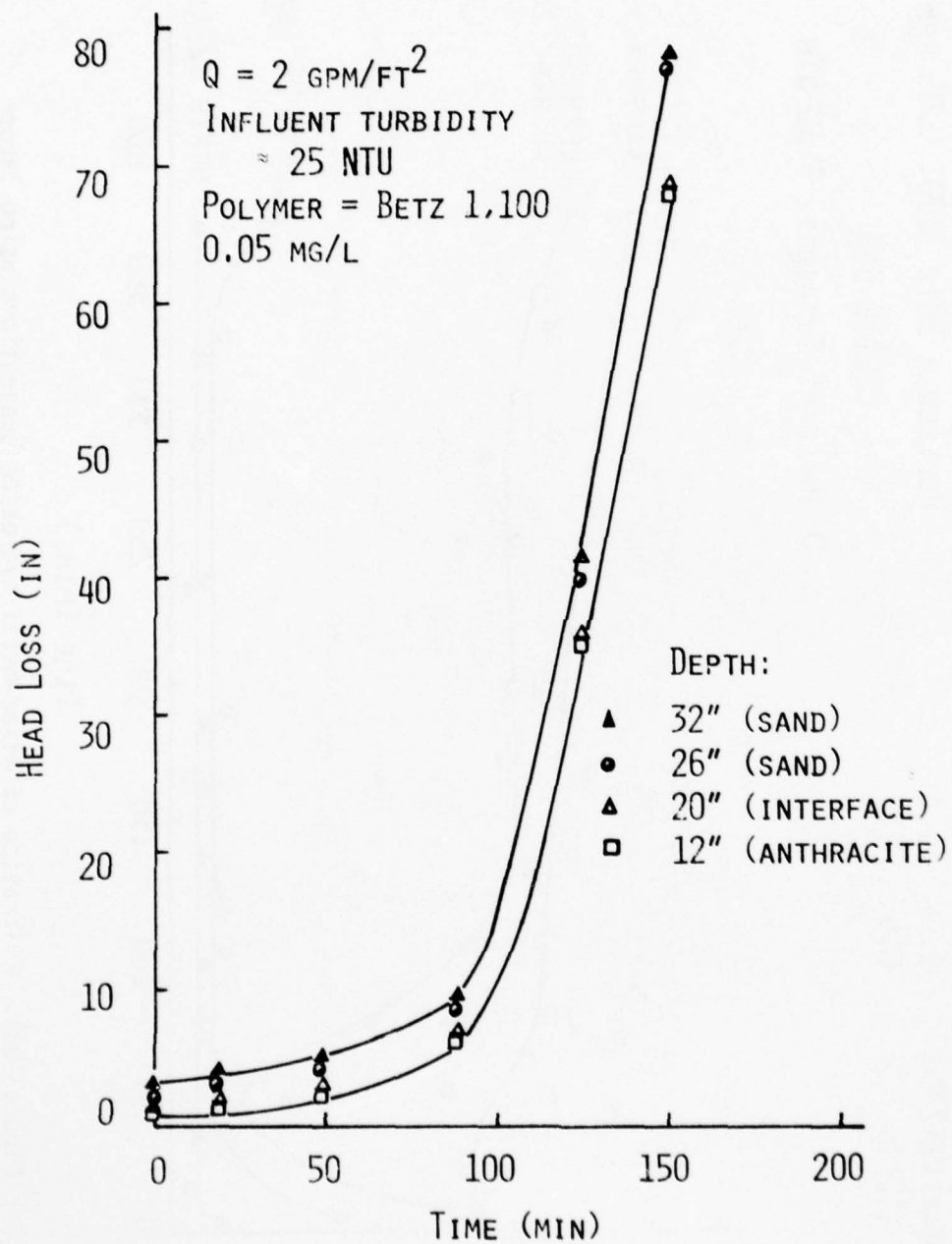


Figure (97). Filtration of mixed-metal hydroxide suspensions with anionic polymer addition - headloss profile.

MEDIA	E.S.	U.C.
ANTHRACITE (20")	1.0	1.4
SAND (12")	0.5	1.2

$Q = 2 \text{ GPM/FT}^2$
 POLYMER = BETZ 1100 0.05 PPM
 CELITE 545

INFLUENT TURBIDITY $\approx 10 \text{ NTU}$

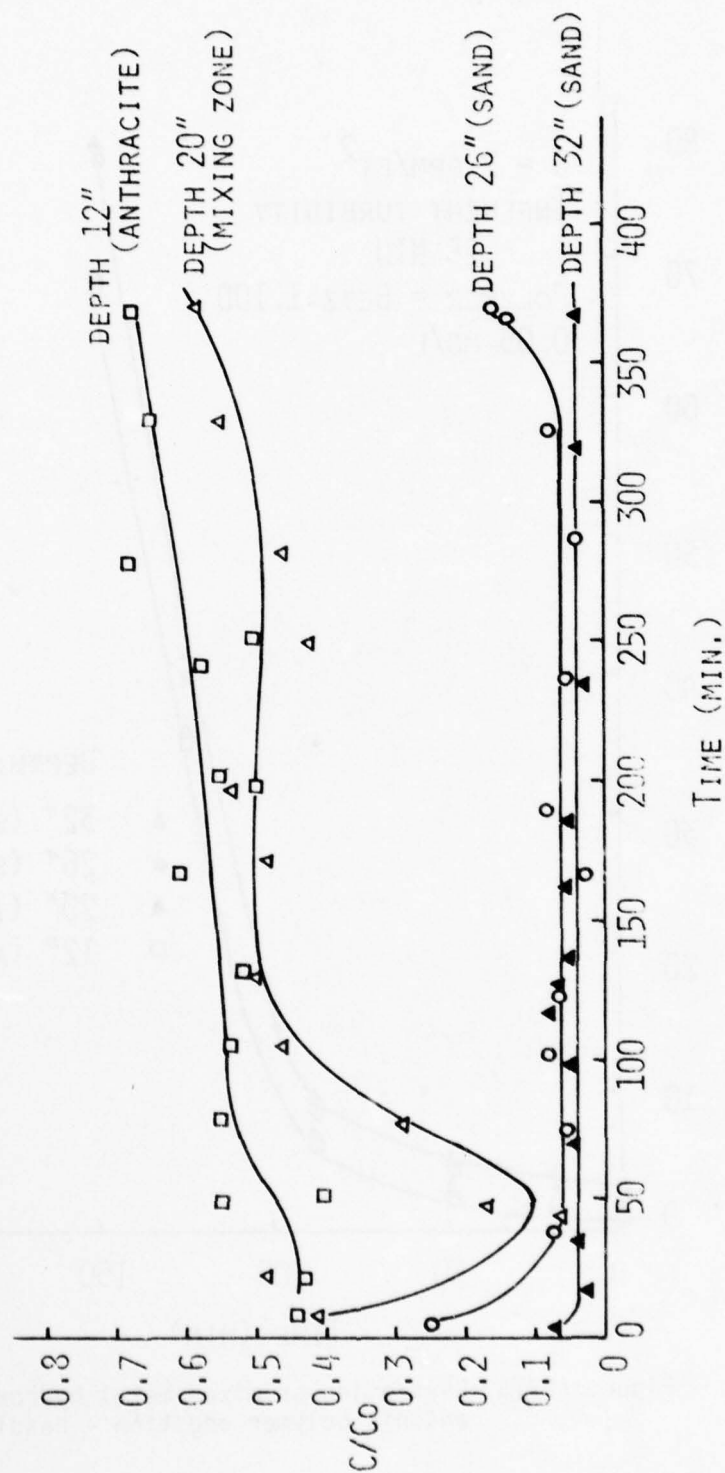


Figure (98). Filtration of mixed-metal hydroxide suspensions using larger graded media - effluent profile.

INFLUENT TURBIDITY ≈ 10 NTU

$Q = 2$ GPM/FT²

POLYMER = BETZ 1100 0.05 PPM

CELITE 545

MEDIA	E.S.	U.C.
ANTHRACITE (20")	1.0	1.4
SAND (12")	0.5	1.2

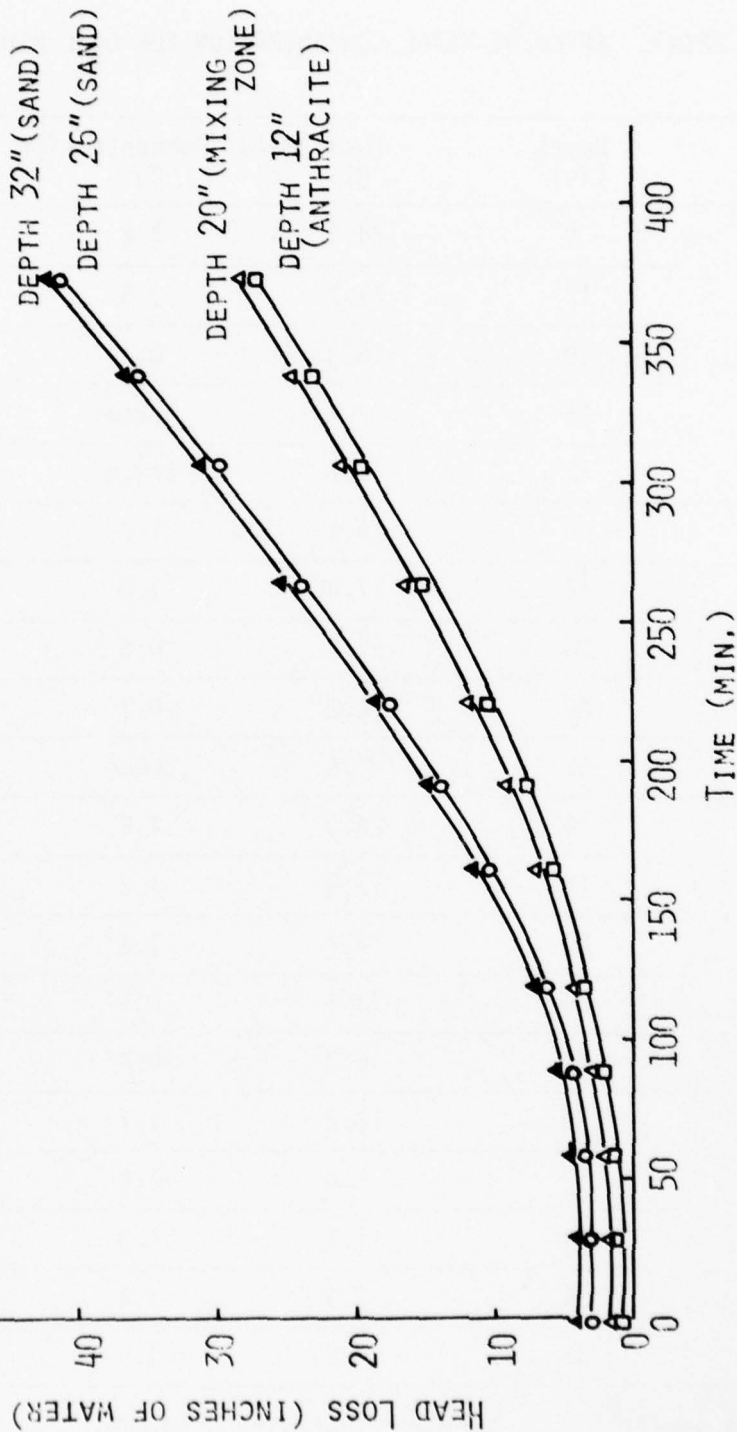


Figure (99). Filtration of mixed-metal hydroxide suspensions using larger graded media - headloss profile.

TABLE 22(a). EFFLUENT METAL CONCENTRATION FOR DUAL MEDIA STUDIES

Time (hr)	Depth (in)	Total Metal Concentration (mg/l)		
		Ni	Cu	Zn
0.25	0	24.3	1.2	6.0
	12	11.7	0.5	2.2
	20	10.3	0.4	2.6
	26	2.2	trace	0.5
	32	1.1	trace	1.1
1.00	0	29.6	1.6	7.9
	12	17.0	1.0	4.8
	20	15.4	0.8	3.8
	26	4.0	0.1	0.4
	32	2.6	trace	0.4
2.25	0	26.0	1.6	8.2
	12	17.8	1.2	5.8
	20	14.7	1.2	5.4
	26	13.1	0.9	4.4
	32	6.3	0.4	2.0
4.00	0	18.2	1.7	7.8
	12	9.6	1.4	6.3
	20	11.1	1.3	6.0
	26	9.3	1.2	5.5
	32	6.2	1.0	4.2

$Q = 4 \text{ gpm/ft}^2$ Influent Turbidity $\approx 10 \text{ NTU}$
 polymer precoat: none
 polymer added to influent: Betz 1175 9 ppm

TABLE 22(b). EFFLUENT METAL CONCENTRATION FOR DUAL MEDIA STUDIES

Time (hr)	Depth (in)	Total Metal Concentration (mg/l)		
		Ni	Cu	Zn
0.30	0	26.2	1.6	9.2
	20	9.4	trace	0.3
	26	8.9	trace	trace
	32	7.2	trace	trace
1.33	0	30.7	1.9	9.1
	12	21.5	1.1	5.3
	20	11.7	0.2	1.4
	26	9.6	trace	trace
	32	5.3	trace	trace
2.25	0	28.9	1.9	8.4
	12	22.8	1.1	4.8
	20	17.6	0.5	2.4
	26	10.2	0.1	0.4
	32	9.5	trace	trace
4.25	0	30.4	1.7	7.6
	12	21.2	1.0	4.6
	20	20.6	0.8	4.2
	26	14.7	0.4	3.0
	32	6.3	0.3	

$Q = 2 \text{ gpm/ft}^2$ Influent Turbidity $\approx 10 \text{ NTU}$

polymer precoat: Betz 1175 1000 ppm

polymer added to influent: none

stream. Once this process has been shown to be feasible, optimum operational conditions must be established. The two operational considerations of importance are the body feed requirements and the optimum flow rate to be used.

Precoat filters operate by first coating a filter medium, called a septum, with diatomaceous earth, then feeding the water to be filtered through the septum supported filter cake. Because the filter cake can rapidly become plugged because of solids buildup and cake compression during the filter cycle, additional cake is usually added continuously by adding diatomaceous earth to the feed suspension throughout the filter cycle. This continuous feed slurry is called body feed. It has been observed that the optimum body feed rate is that which provides for a linear head loss with time. Excess body feeding wastes diatomaceous earth while an insufficient body feed creates rapid head losses and shortened filter runs.

In this study, tests were conducted initially using a buchner funnel apparatus in order to screen various grades of diatomaceous earth. As can be seen in Table 23, little difference in filtrate turbidity was found for the various mesh sizes. Although the buchner funnel screening technique is not accurate because of difficulties in applying a uniform cake, the data in the table indicate that all mesh sizes should perform equally well. For most of the studies, Celite 545* was used because this precoat size represented an approximate average between coarse and fine grades. All experiments were conducted using an influent with a turbidity of 10 NTU.

1. Effect of Body Feed

In Figures 100 and 101 the effect of several body feed rates on head loss and filtrate turbidity are shown. It can be seen in Figure 101 that for all body feed rates above 300 mg/l the filtrate clarity was excellent. The head loss, shown in Figure 100, appeared to become linear with time at or slightly exceeding 700 mg/l so this rate should be near the optimum. Calculations of the volume of water which could be filtered before a specific head loss was exceeded were made and are shown in Figure 102. These data show that a body feed rate of approximately 700 mg/l is optimum for a flow rate of 0.5 gpm/ft².

The head loss values selected for the calculations shown in Figure 102 are well below those actually used in precoat filters. Typical terminal head loss values are 75 to 150 ft. of water. At a head loss of 150 ft., a filter run of nearly 6.5 hrs could be attained under optimum conditions.

It could be expected that body feed rates may require some upward adjustment at high flow rates because the increased flow may cause additional penetration of metal hydroxides into the cake. Data were collected for flow rates of 0.75 and 1.0 gpm/ft² as shown in Figures 103, 104, 105, and 106. At these higher flow rates, filter runs are considerably shortened

TABLE 23. DIFFERENT GRADES OF DIATOMACEOUS EARTH AND THE FILTRATE TURBIDITY OF BUCHNER FUNNEL TEST

Grade	Screen Analysis % Retained	Filtrate Turbidity (NTU)*	
		Cake 0.15 lb/ft ²	Cake 0.10 lb/ft ²
Standard Super-Cel	3.0	1.4	2.6
Celite 512	4.0	1.1	2.3
Hyflo Super-Cel	5.0	1.4	1.8
Celite 503	9.0	1.3	1.2
Celite 545	12.0	1.5	3.4
Celite 550	20.0	1.5	2.6
Celite 560	50.0	1.9	1.5

*Influent Turbidity = 10 NTU

CELITE 545

$Q = 0.5 \text{ GPM/FT}^2$

PRECOAT = 0.15 LB/FT^2

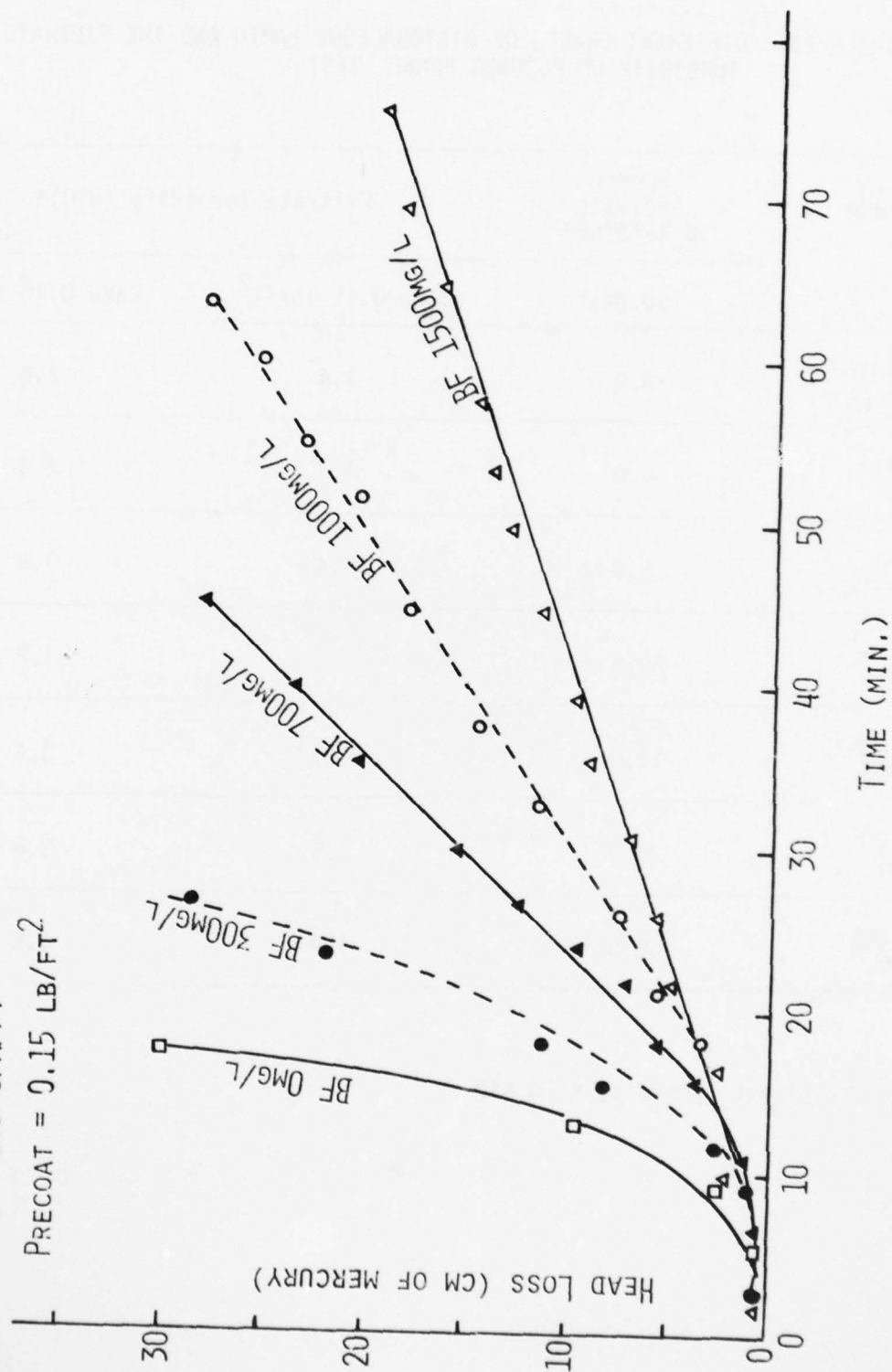


Figure (100). Effect of body feed variations on headloss in a diatomaceous earth filter.

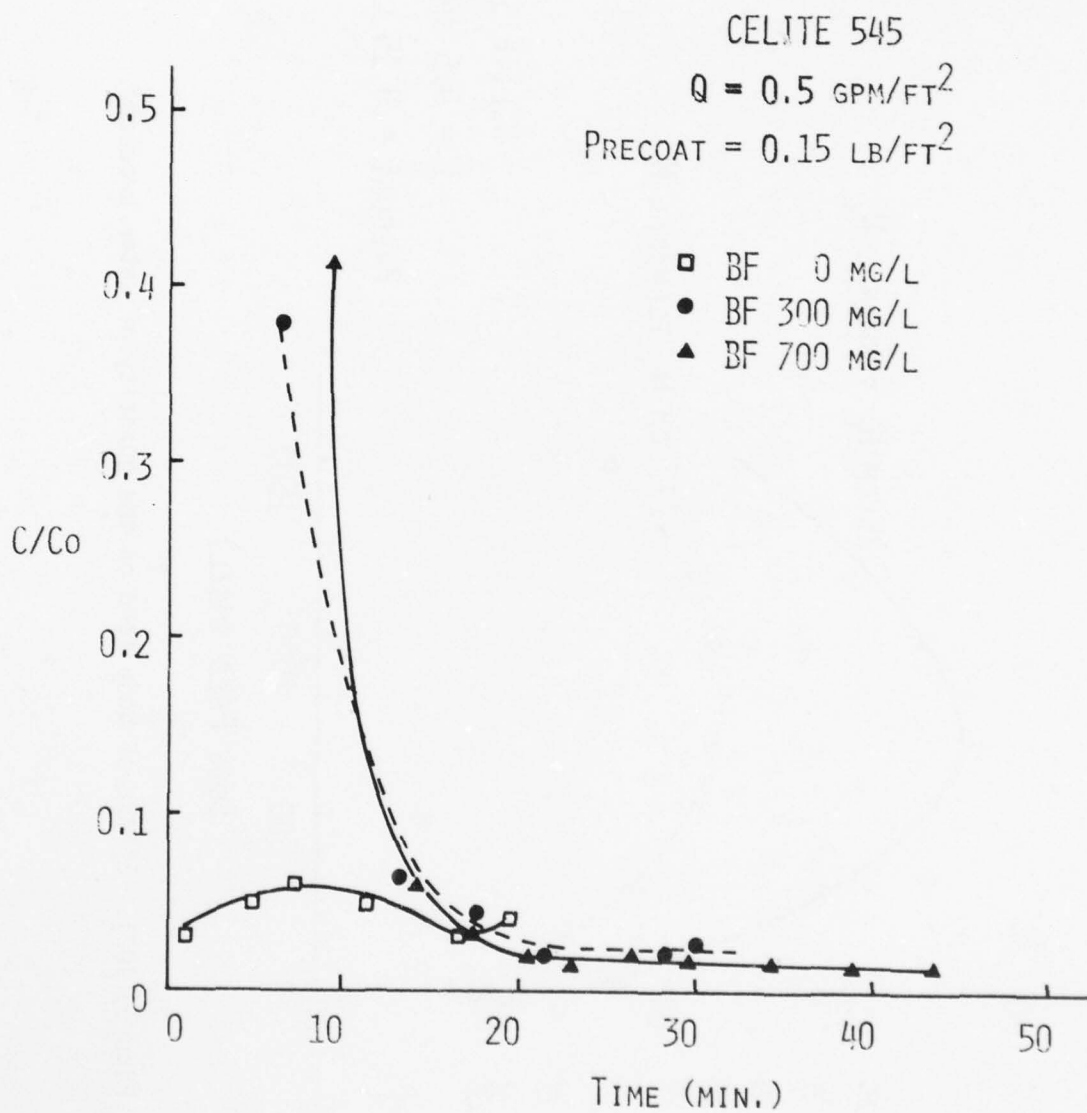


Figure (101). Effect of body feed on filtrate turbidity.

AD-A070 233

MISSOURI UNIV-COLUMBIA DEPT OF CIVIL ENGINEERING

F/6 13/2

METAL HYDROXIDES FROM ELECTROPLATING: SLUDGE CHARACTERIZATION A--ETC(U)

MAY 79 J T NOVAK, M M GHOSH, W KNOCH

F08635-77-C-0281

UNCLASSIFIED

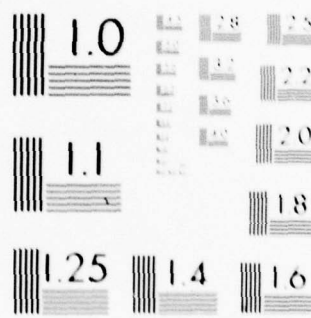
AFESC/ESL-TR-79-09

NL

3 OF 3

AD
A070233





MICROCOPY RESOLUTION TEST CHART
NATIONAL BUREAU OF STANDARDS-1963-A

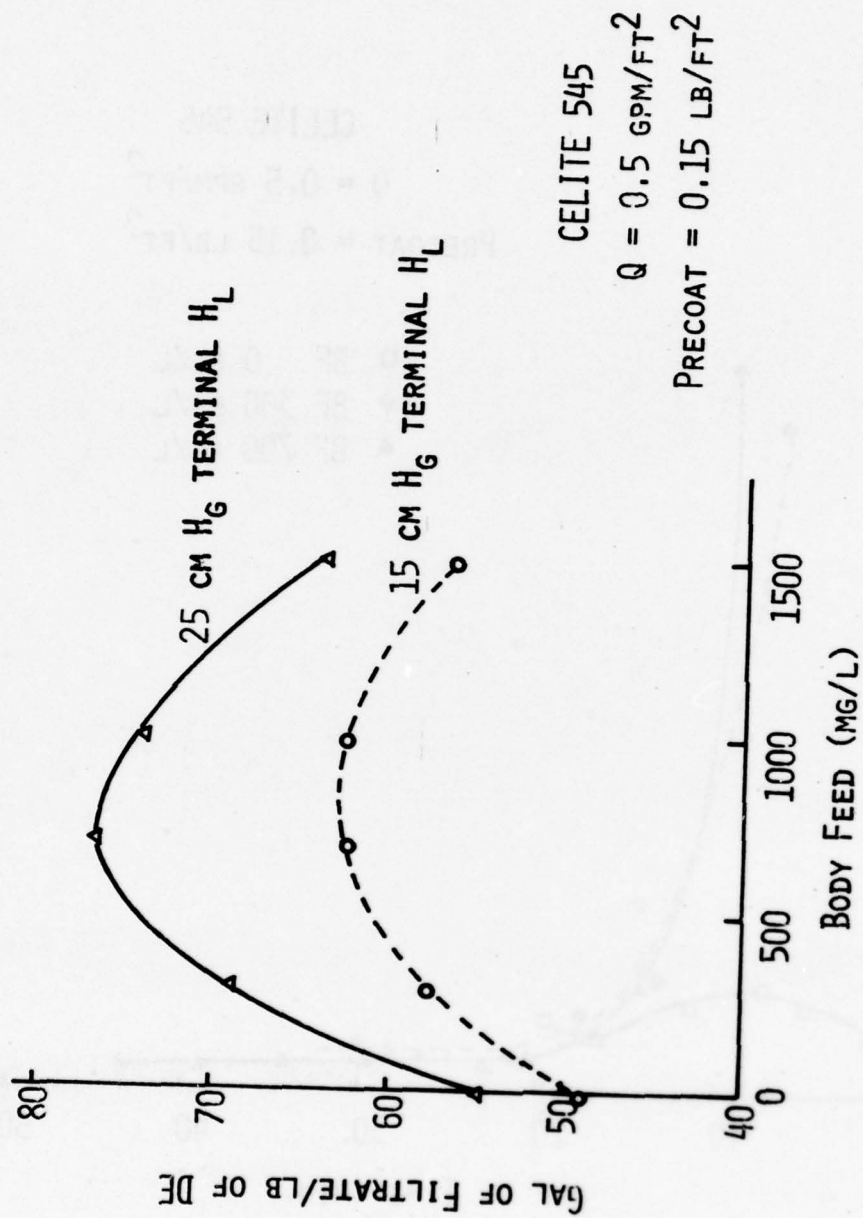


Figure (102). Effect of body feed on the quantity of water produced.

CELITE 545

$$Q = 0.75 \text{ GPM/FT}^2$$

$$\text{PRECOAT} = 0.15 \text{ LB/FT}^2$$

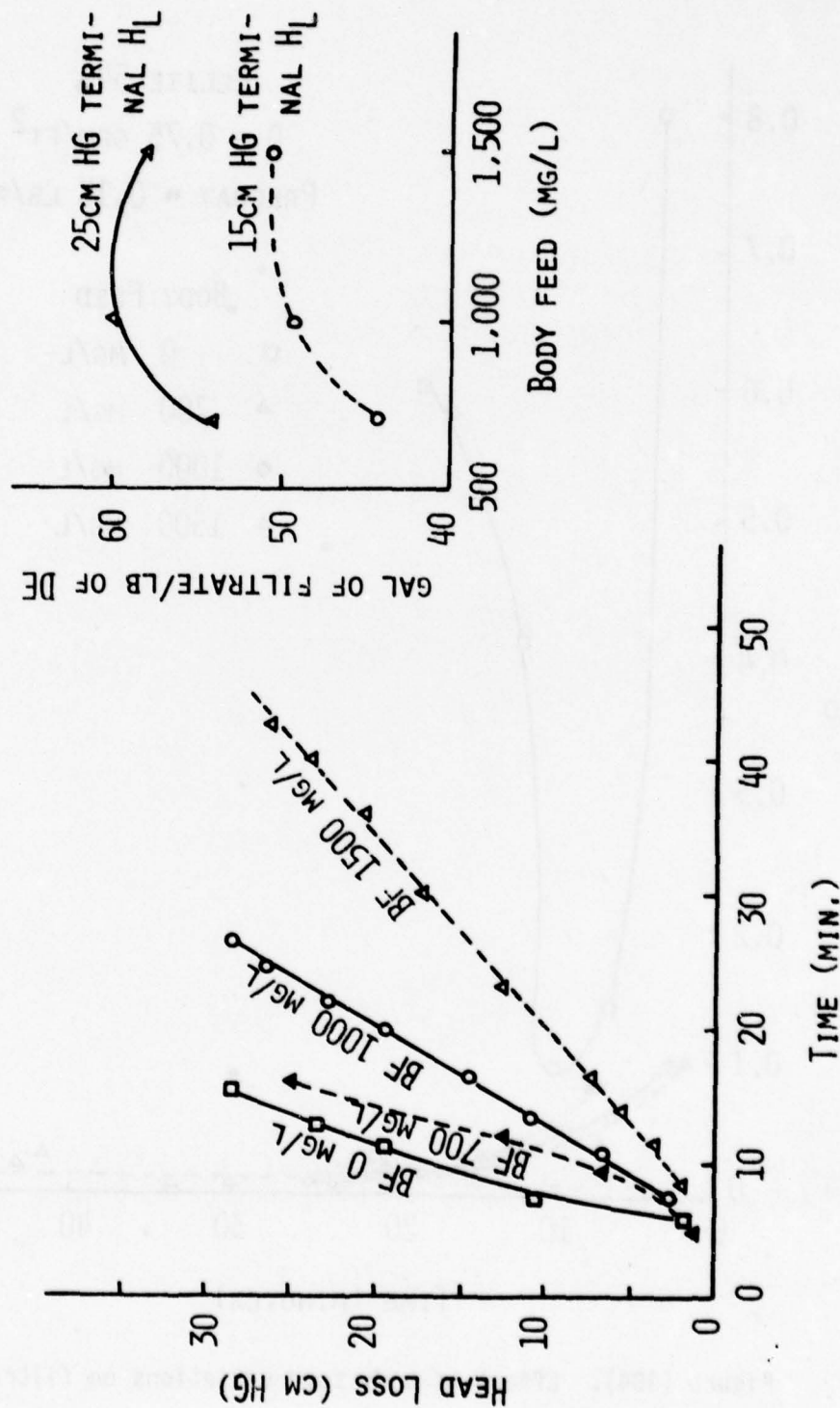


Figure (103). Effect of body feed variations on headloss and water production.

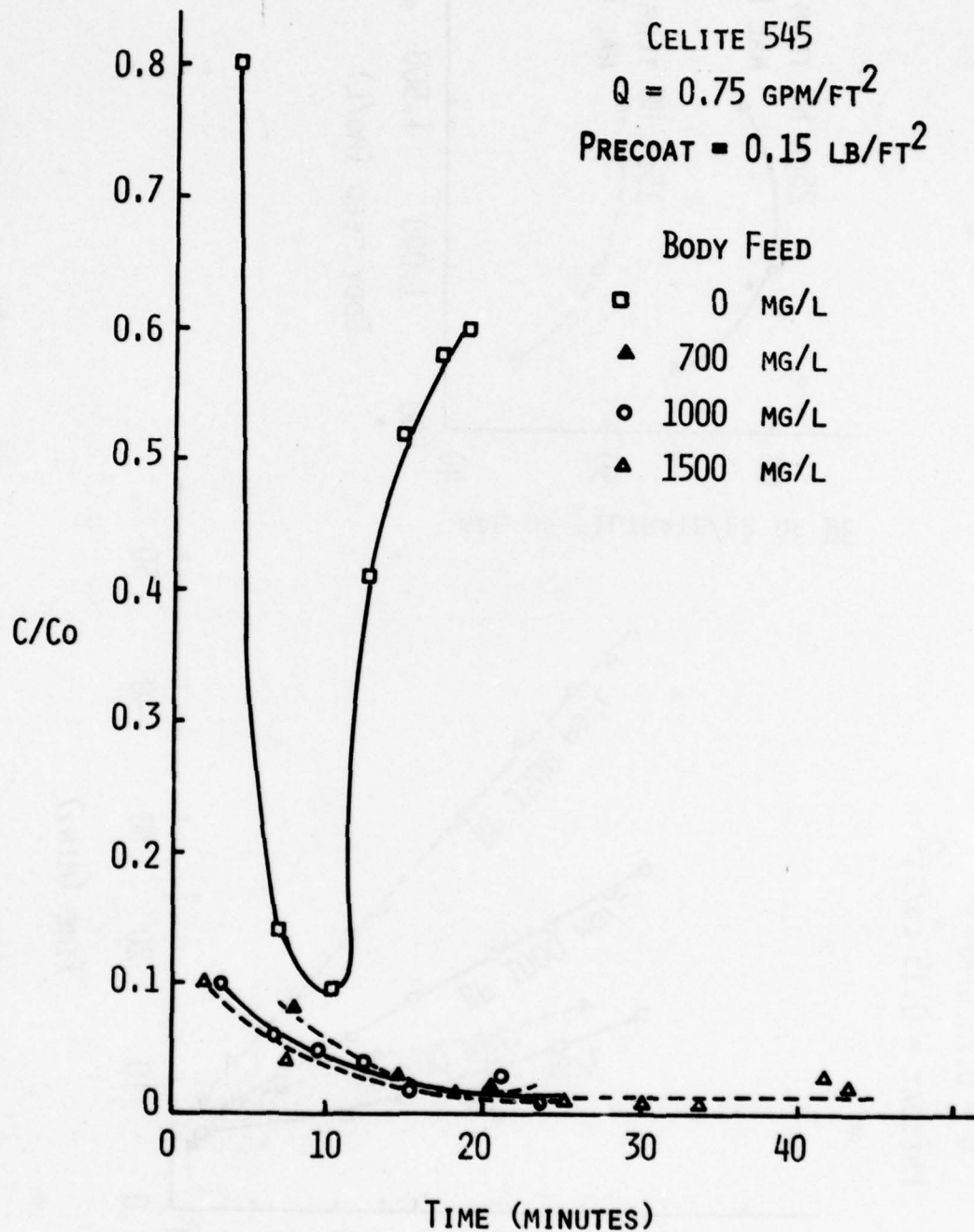


Figure (104). Effect of body feed variations on filtrate turbidity.

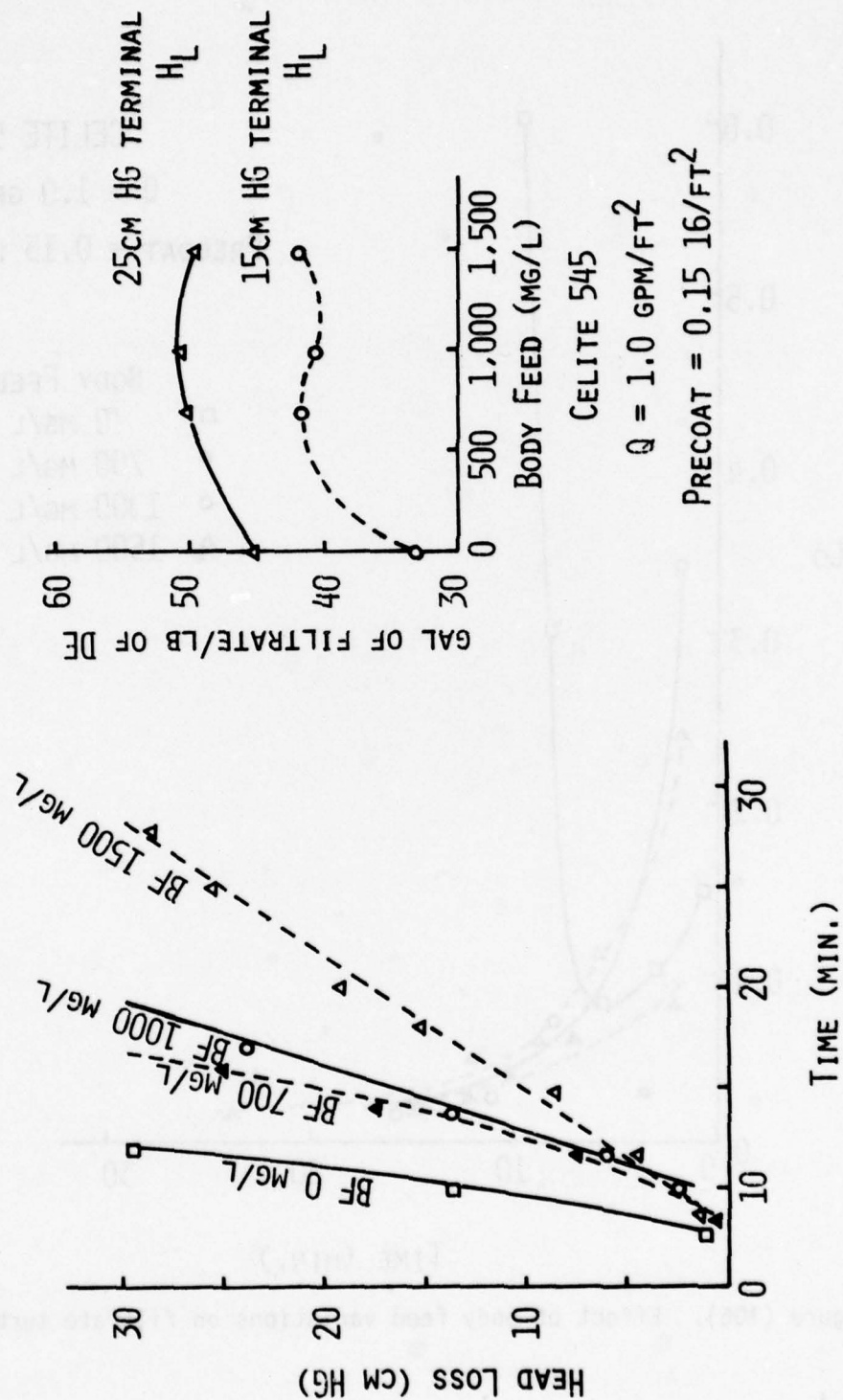


Figure (105). Effect of body feed variations on headloss and water production.

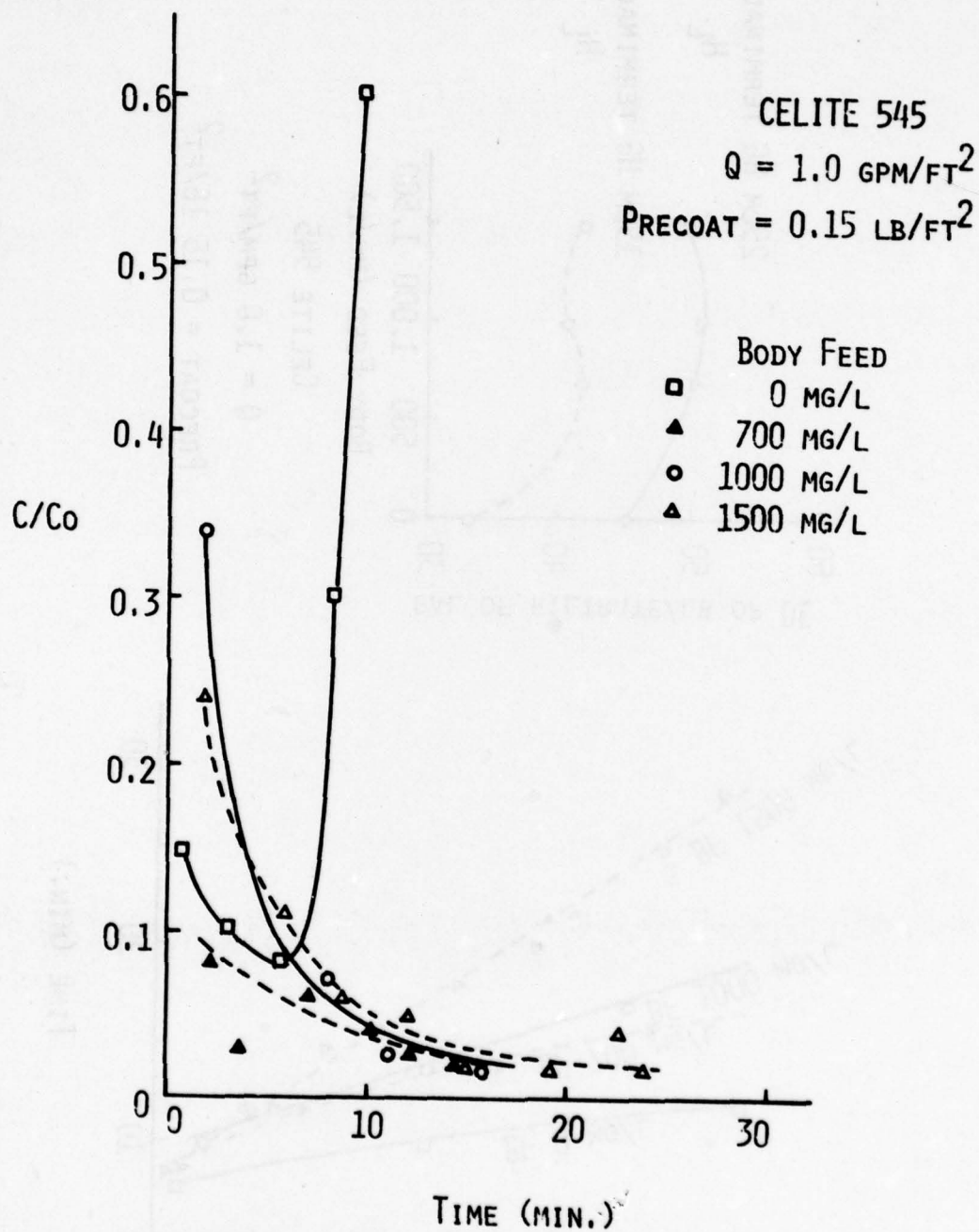


Figure (106). Effect of body feed variations on filtrate turbidity.

and the effectiveness of body feeding is reduced. The systems do, however, continue to produce high quality effluents.

The optimum body feed rate increases somewhat as the flow rate is increased but excess body feeding seems not to be so critical. At a feed rate of 1.0 gpm/ft^2 and applying a body feed of 1000 mg/l which is near optimum, a filter run of 3.8 hours can be attained before a head loss of 150 ft. is reached. This compares with 6.5 hours for a flow of 0.5 gpm/ft^2 and a 700 mg/l body feed.

2. Effect of Precoat Variations

A precoat of 0.15 lb/ft^2 was used for the experiments previously described. This precoat level has been suggested by Cleasby (51) as being near optimum for clay suspensions. Tests were conducted to determine if the 0.15 lb/ft^2 precoat was optimum. Tests were conducted using pre-coats of 0.1 and 0.2 lb/ft^2 and body feeds of 700 and 1000 mg/l at several flow rates. These data, presented in Figures 107 through 110 show that little difference in performance exists for the three cake applications. In general, all of the filter runs produced high quality effluents at comparable head loss values.

In summary (Table 24), diatomaceous earth precoat filtration was found to provide high quality effluents using precoat levels of 0.1 to 0.2 lb/ft^2 and flow rates of 0.5 to 1 gpm/ft^2 . At the lower flow rate the process was slightly more efficient, as measured by the volume of water processes per unit of diatomaceous earth utilized. Higher flow rates were effective but more diatomaceous earth was required. The effluent characteristics were vastly superior to those produced by granular media filtration. If the quality of the filtrate is to be an important consideration, precoat diatomaceous earth filtration should be strongly considered.

E. Liquid-Liquid Extraction

Liquid-liquid extraction, which has long been used in the nuclear field and in analytical chemistry is now becoming used in various recovery processes. In Europe various processes have recently been developed (12): (a) Gullspang process - uses tertiary alkylamine (Alamine 336) in kerosene for extracting Mo, W, Cr, Fe, Co, and Ni from scrap metal and mill shavings, (b) Soderfors process - uses tributylphosphate in kerosene to extract HF, HNO_3 , Mo from stainless steel pickling baths, (c) Valberg process - uses di(2-ethylhexyl) Phosphoric acid (HDEHP) to recover zinc, and (4) MAR process - uses a sequential extraction scheme of first LIX-64N (reagent selective for copper) followed by HDEHP in kerosene (Fe and Zn extracted) and finally MX-200 for Ni and Cr. In the United States naphthenic acid in kerosene to extract metals from electroplating wastewater has been evaluated and found to be unsuccessful (5). The Bureau of Mines uses

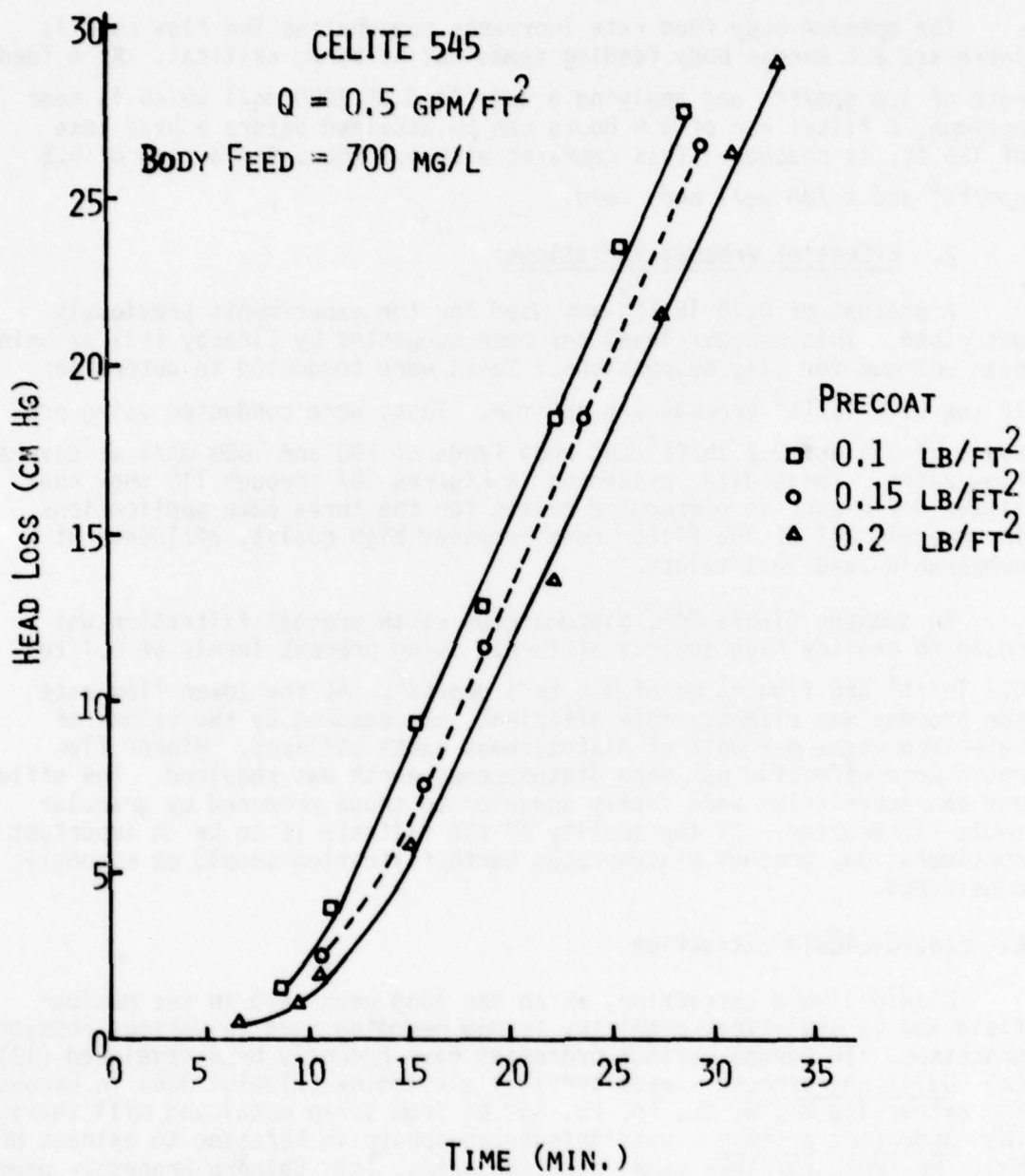


Figure (107). Effect of precoat variations on headloss.

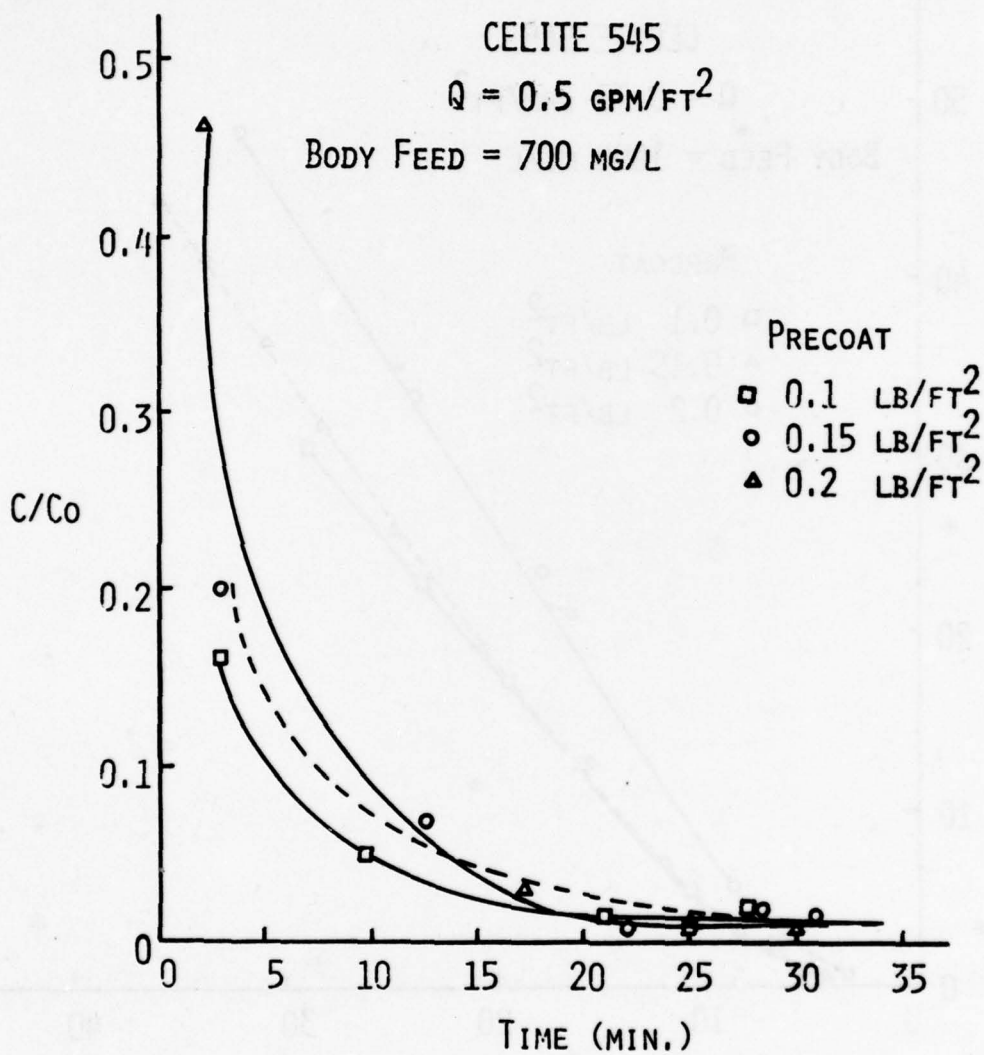


Figure (108). Effect of precoat variations on filtrate turbidity.

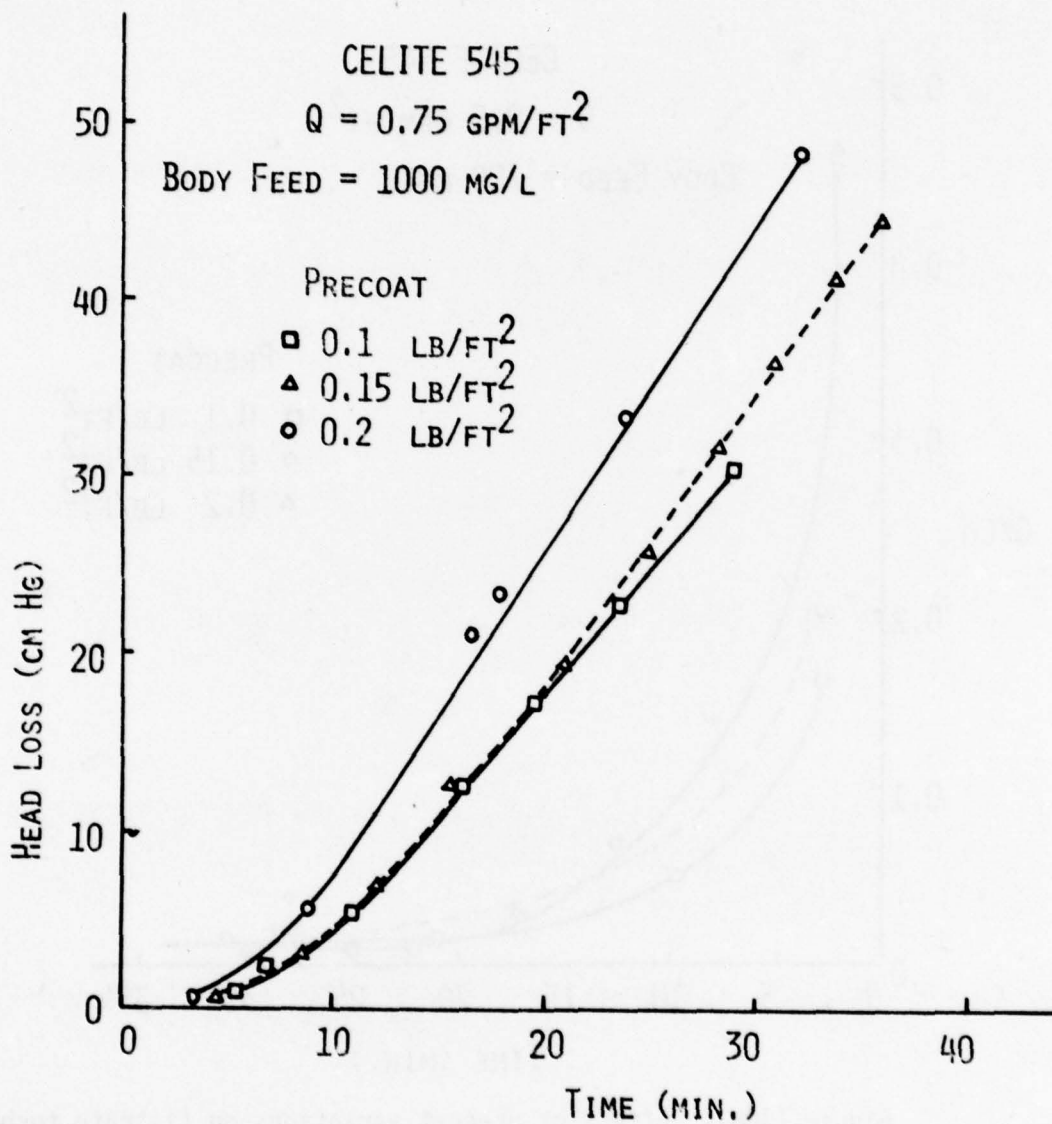


Figure (109). Effect of precoat variations on head loss.

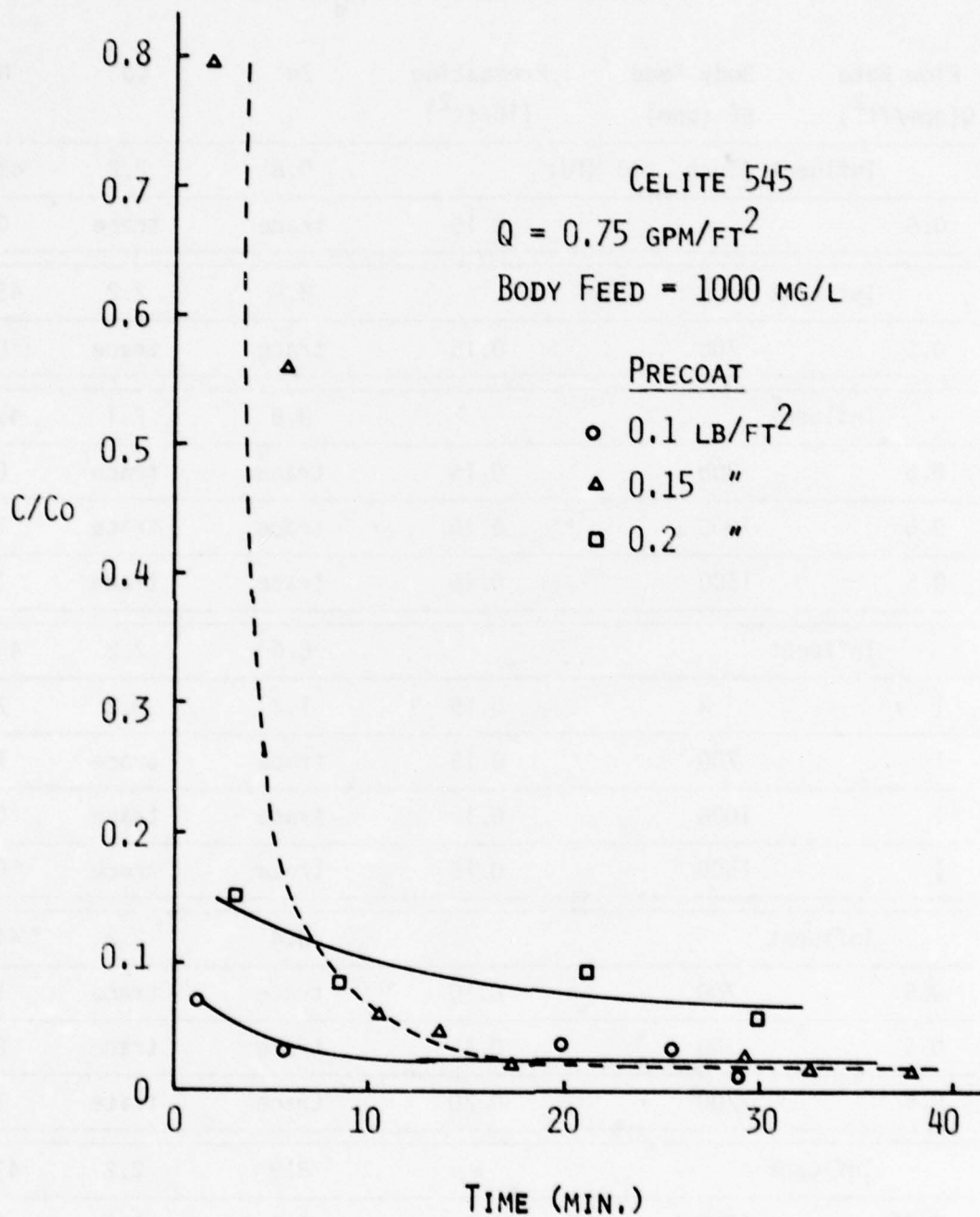


Figure (110). Effect of precoat variations on filtrate turbidity.

TABLE 24. INFLUENT AND EFFLUENT METAL CONCENTRATION
OF DIATOMACEOUS EARTH FILTRATION

Flow Rate Q(gpm/ft ²)	Body Feed BF (ppm)	Precoating (16/ft ²)	Zn	Cu	Ni
Influent (Turb 10 NTU)			9.6	2.2	43.7
0.5	N	0.15	trace	trace	0.9
Influent			8.8	2.2	43.0
0.5	700	0.15	trace	trace	0.2
Influent			8.6	2.1	41.4
0.5	300	0.15	trace	trace	0.2
0.5	1000	0.15	trace	trace	3.1
0.5	1500	0.15	trace	trace	1.1
Influent			8.6	2.2	43.6
1	N	0.15	1.2	0.2	7.2
1	700	0.15	trace	trace	1.4
1	1000	0.15	trace	trace	0.5
1	1500	0.15	trace	trace	0.3
Influent			8.4	2.2	44.9
0.5	700	0.10	trace	trace	1.2
0.5	700	0.15	trace	trace	2.2
0.5	700	0.20	trace	trace	1.4
Influent			8.9	2.2	43.2
0.75	1000	0.1	0.3	0.1	1.7
0.75	1000	0.2	trace	trace	0.3

liquid-liquid extraction to remove Co in the reclaiming of superalloy scrap (11). HDEHP in kerosene has been successfully used to recycle aluminum used for phosphate removal in domestic wastewater treatment. Alamine 336 in xylene has recently been evaluated for removal of toxic metals from metal finishing wastewater (9). It successfully removed the metals which were examined (Cd, Cr, & Zn).

These liquid-liquid extraction studies as well as other methods of metal removal from electroplating wastewater (electrochemical, reverse osmosis, cementation, ion exchange, and neutralization-precipitation) are not completely selective and do not produce a clean metal (5). This is especially true of the methods other than liquid-liquid extraction. However, even the liquid-liquid extraction process has produced a contaminated metal. In the European cases, they found that they were able to use the contaminated recovered metal.

In this work it was attempted to find a very selective liquid-liquid extraction scheme that would produce a clean recovered metal from an electroplating wastewater.

There have been several books written on liquid-liquid extraction and in all cases chelating compounds are given as being the most selective in the extraction process. Therefore, seven chelates which were listed as being the most widely used and known for their selectivity were chosen for this study. These are listed in Table 4.

Before beginning the actual study, the extraction procedure to be used was evaluated.

The first parameter checked was the time necessary to allow for separation of the phases. In this experiment, three chelating compounds were evaluated: (1) Benzoylacetone (0.1M in chloroform), (2) 8-hydroxyquinoline (0.1M in chloroform), and (3) sodium diethyldithio carbamate (0.03M in chloroform). Each was shaken for two minutes with a 100 mg/l solution of Cd, Cu, Zn, Ni and Cr. Aliquots for analysis were then taken periodically to check for variation with settling time. The results are presented in Table 25.

These results indicated that the separations occurred immediately upon separation of the two phases.

TABLE 25
SETTLING EFFECTS ON EXTRACTION EFFICIENCIES OF
THREE DIFFERENT CHELATING COMPOUNDS

Settling Time	% Extraction				
	Cu	Cu	Ni	Zn	Cu
	<u>Benzoylacetone</u>	<u>8-hydroxyquinoline</u>			<u>Sodium Diethyldithiocarbamate</u>
5 sec.	91	98+	98+	47	11
30 sec.	92	98+	98+	47	17
60 sec.	92	98+	98+	47	11
120 sec.	96	98+	98+	47	10
5 min.	96	98+	98+	47	10
15 min.	98+	98+	98+	47	8
30 min.	98+	98+	98+	50	16
60 min.	98+	98+	98+	50	17

The next parameter checked was that of shaking time. In this experiment a metal solution containing 10 mg/l Cd, Cu, Zn, Ni, and Cr was extracted for various shaking times, with aliquots being taken at pre-determined times for analysis. 8-Hydroxyquinoline (0.1 M in chloroform) and sodium diethyldithiocarbamate (0.03M in chloroform) were both checked. The results are given in Table 26. The extracting pH was 5.5.

These results indicated that the metal chelates were being formed very rapidly and that the choice of shaking for two minutes should insure as complete of extraction as will be obtained.

Figure 111 presents data indicating the precision of the method. Figure 111 gives data collected for three different runs on the same day. The results indicate that the precision is acceptable.

In order to check the protocol against reported literature results each of the seven chelates in chloroform were extracted using the "independent batch" method with a metal solution of 100 mg/l Ni, Cr, Cu, Cd, and Zn. The data are plotted versus literature values in Figures 10, 11, 112-116. The overall agreement with the literature is good (10). There are, however, some discrepancies. These were probably caused by problems with precipitation using the above mixed metal solution. At pH's above 5.5, precipitation began to occur. At the high pH's it was difficult to determine if extraction or simply precipitation was the mechanism producing metal removal.

In order for liquid-liquid extraction to be an economically feasible method of metal recovery with today's metal prices, it has to be capable of (1) selectively extracting the metals into an organic layer, (2) stripping the metals from the organic layer into an acid layer, (3) having the chelates remain in the organic layer and still have chelating capabilities. Figure 117 shows these conditions in a flow diagram.

TABLE 26
SHAKING TIME EFFECTS ON EXTRACTION EFFICIENCIES
8HQ and NaDDC

Shaking Time	% Extraction			
	8-Hydroxyquinoline		Sodium Diethyldithiocarbamate	
	Cu	Ni	Cu	Ni
5 sec.	99+	80	99+	99+
30 sec.	99+	99+	99+	99+
1 min.	99+	99+	99+	99+
2 min.	99+	99+	99+	99+
5 min.	99+	99+	99+	99+
15 min.	99+	99+	99+	99+
30 min.	99+	99+	99+	99+
60 min.	99+	99+	99+	99+

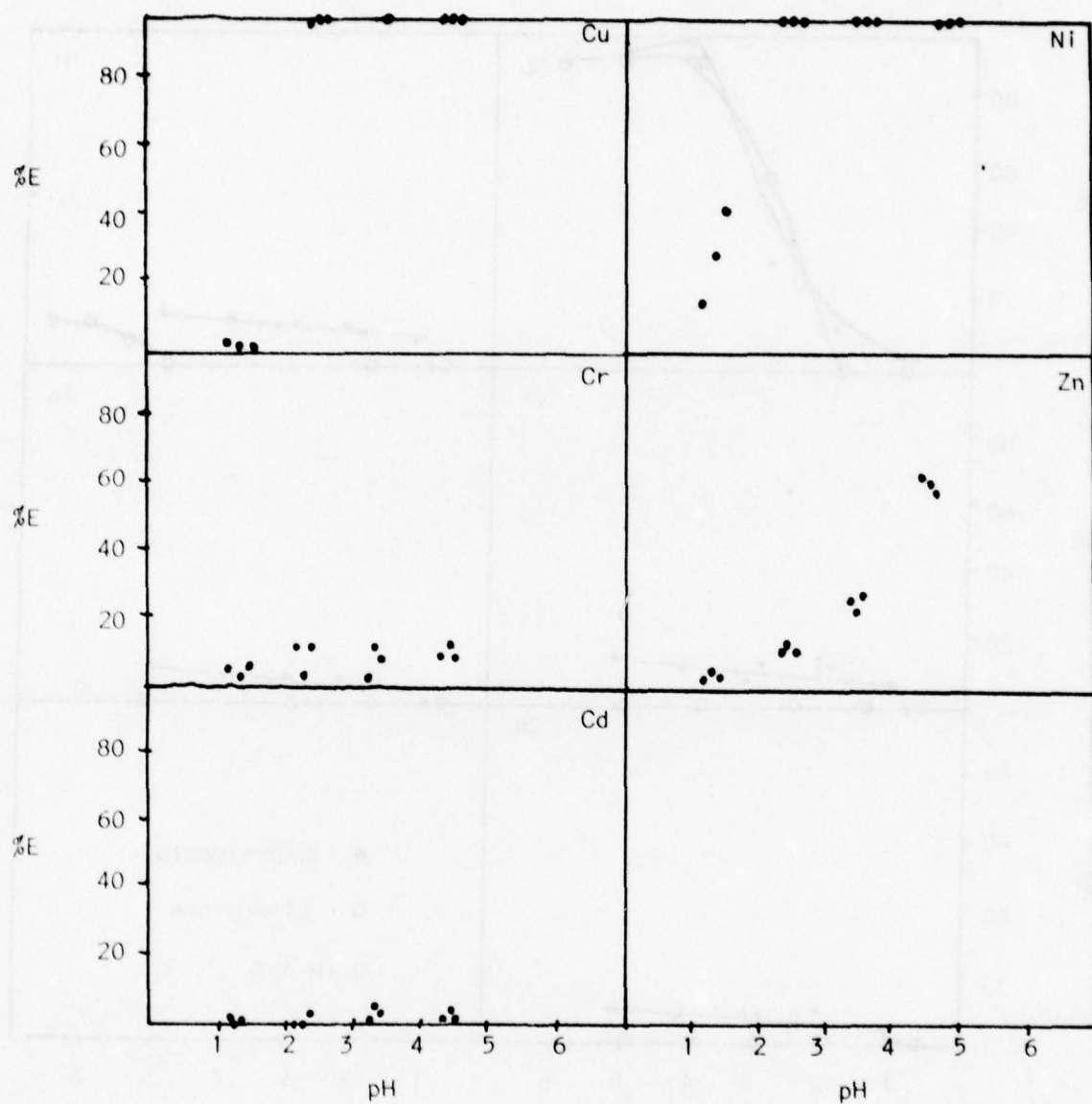


Figure (111). Precision study using 8HQ.

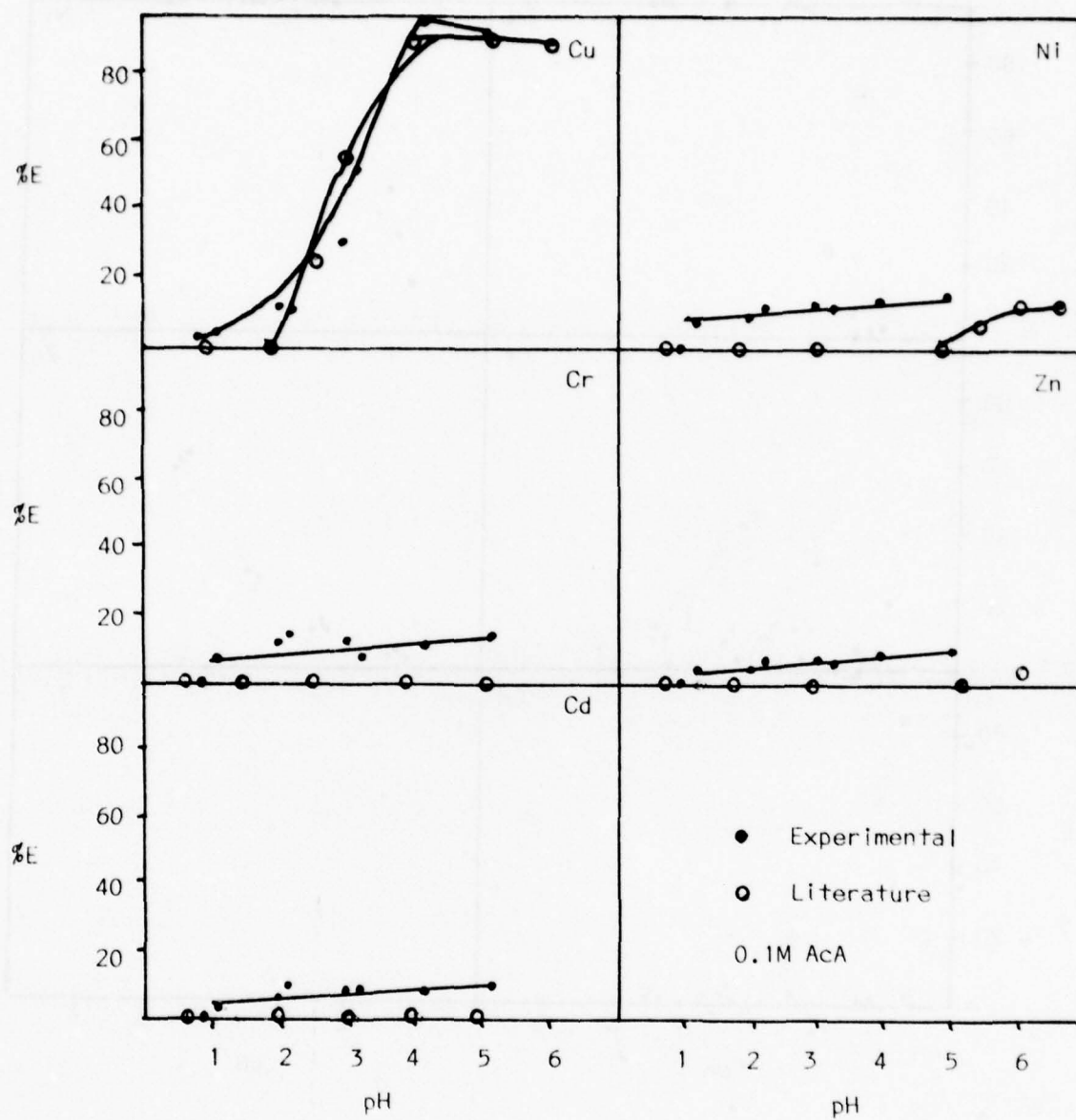


Figure (112). Percent extraction curve for AcA.

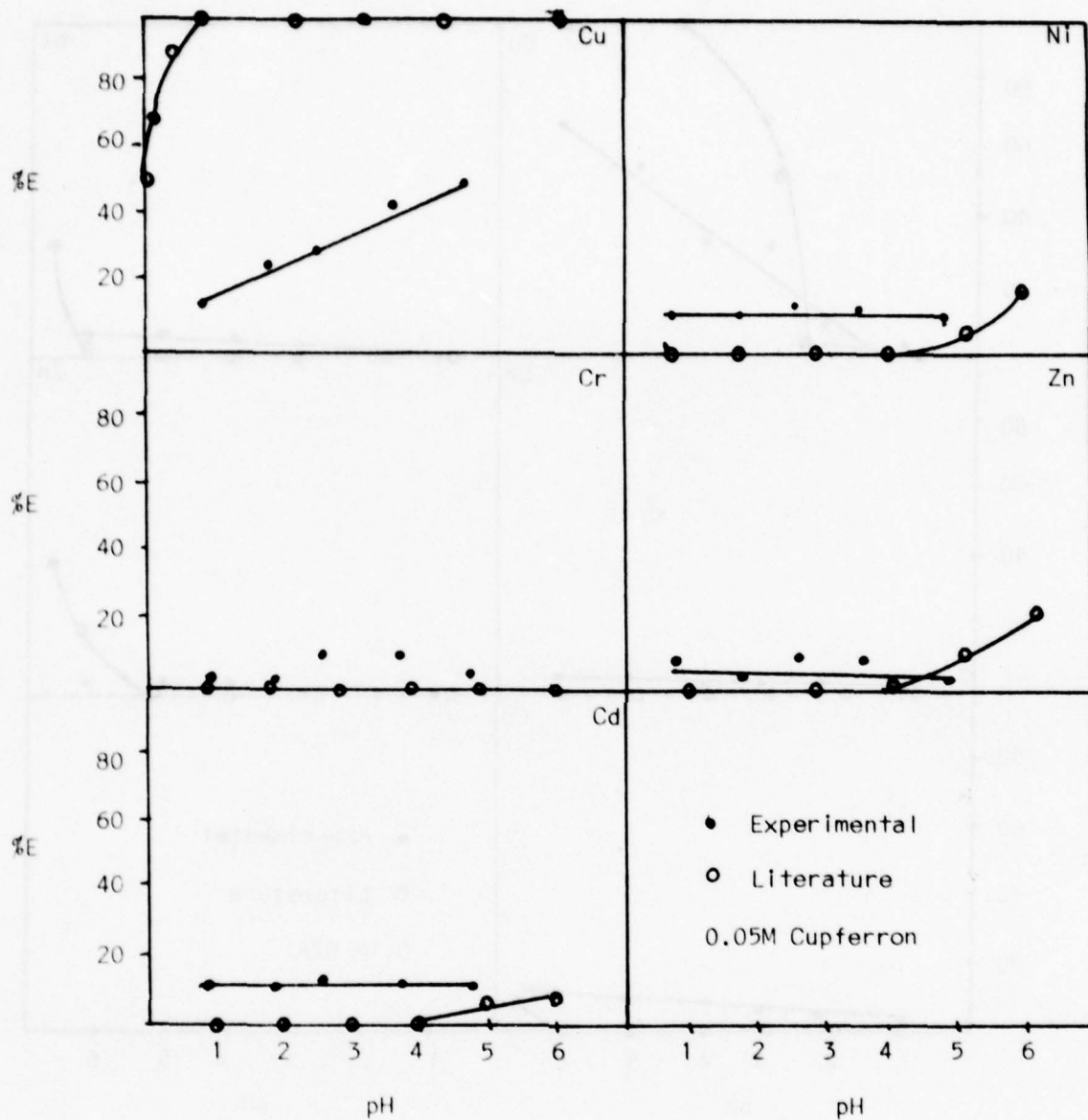


Figure (113). Percent extraction curve for cupferron.

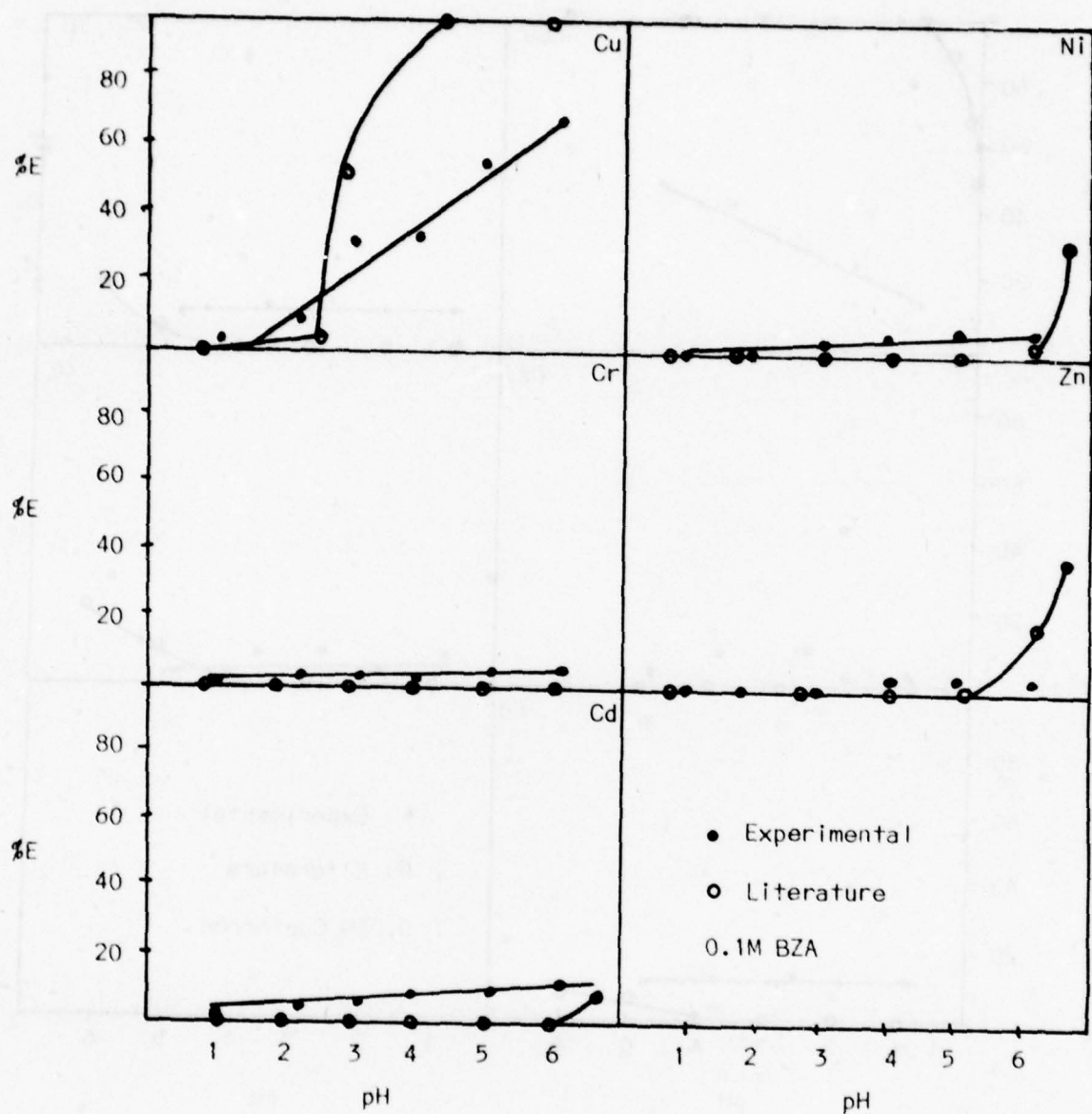


Figure (114). Percent extraction curve for BZA.

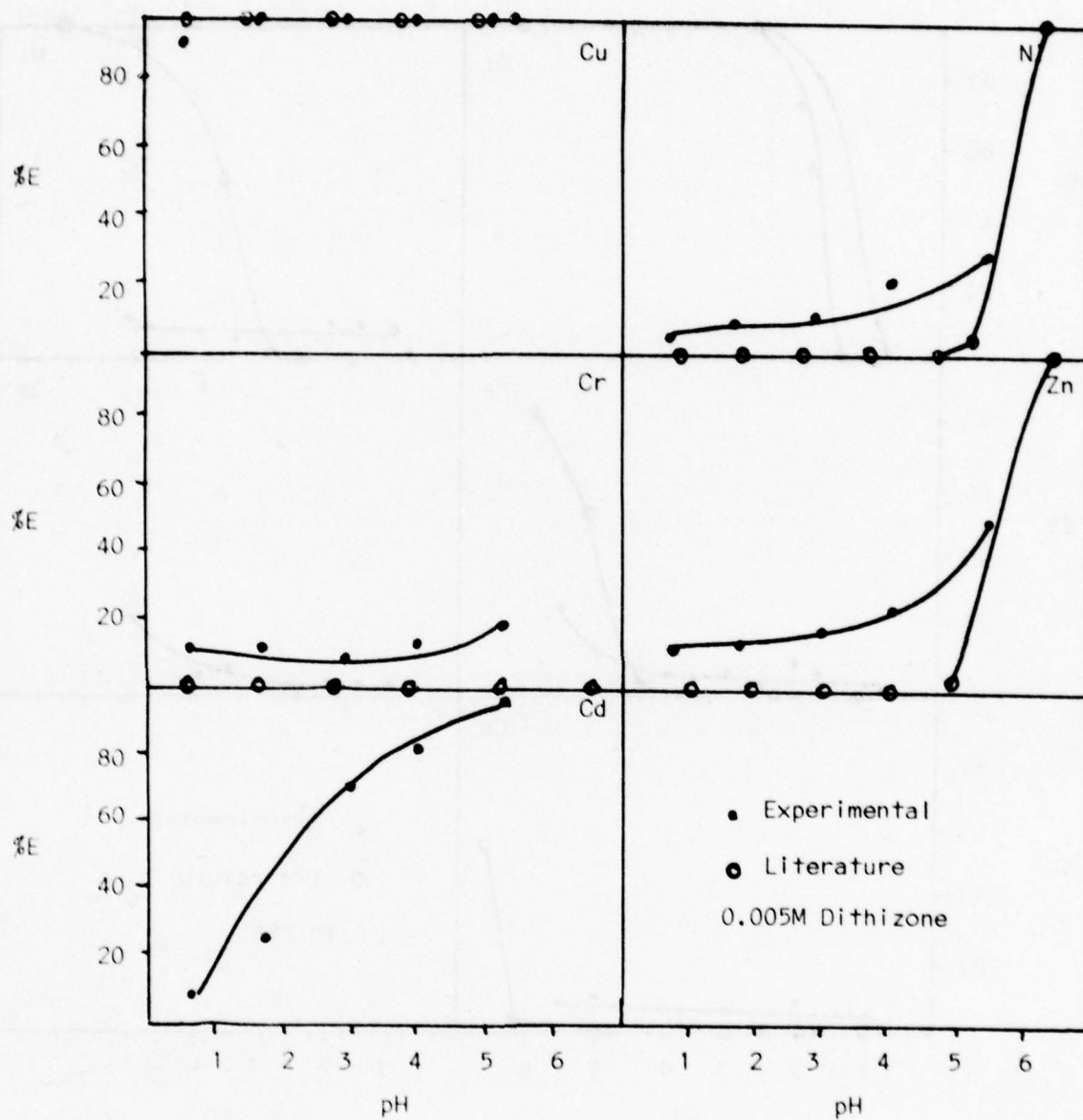


Figure (115). Percent extraction curve for dithizone.

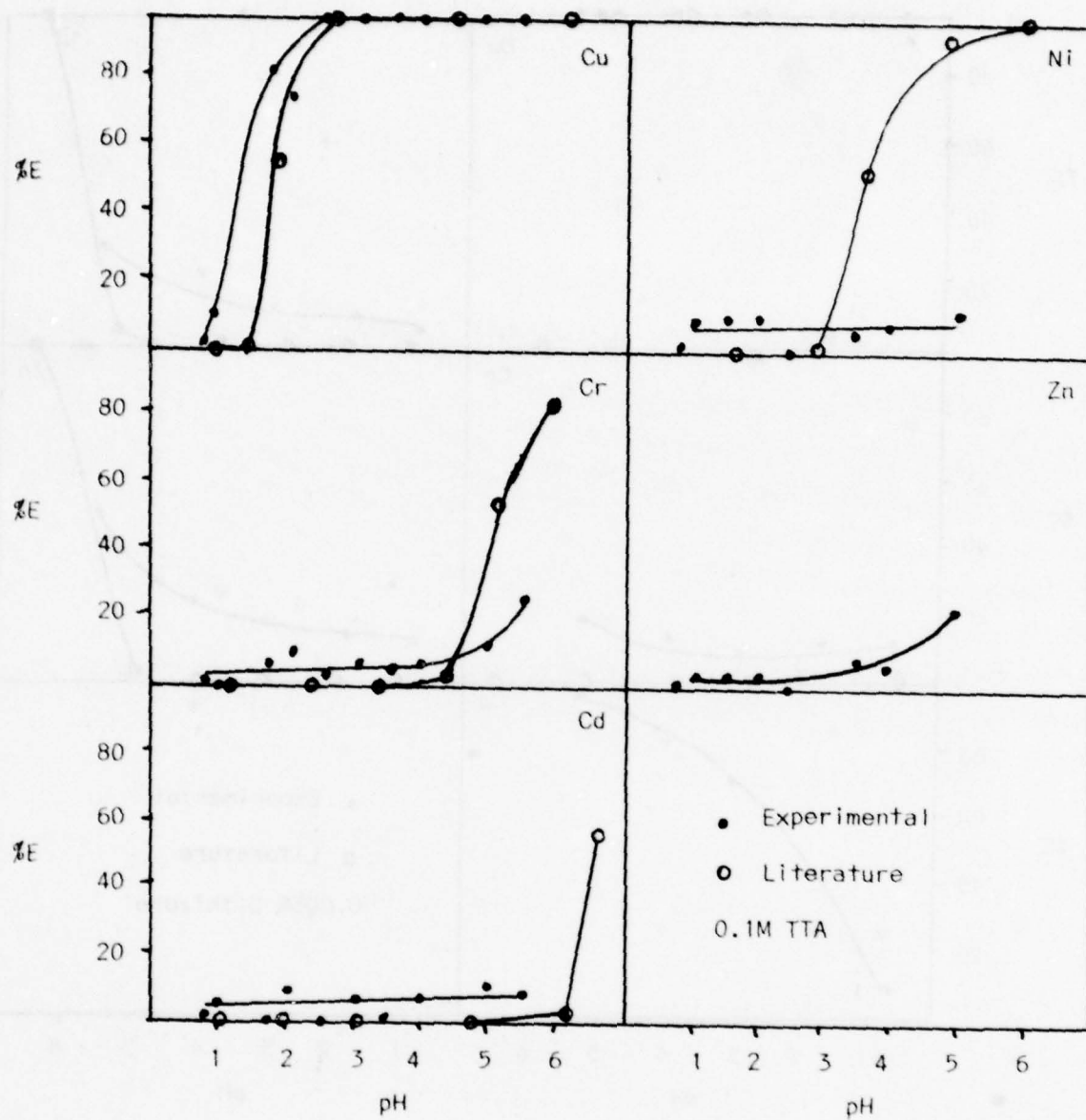


Figure (116). Percent extraction curve for TTA.

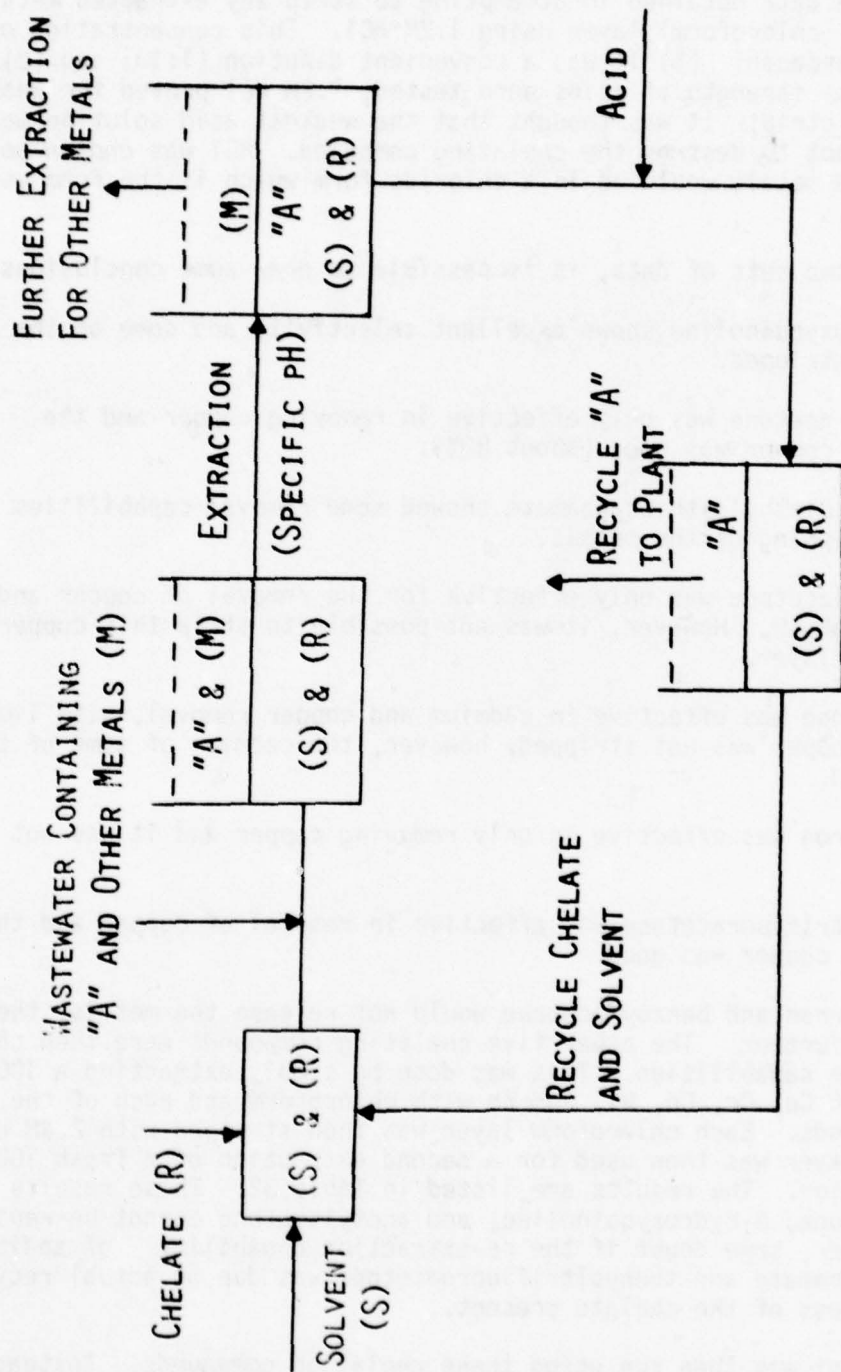


Figure (117). Liquid-liquid extraction flow diagram.

Figures 10, 11, 112-116 show the selectivity that each chelating compound exhibits for a mixed metal solution of Cd, Cu, Cr, Zn and Ni. Tables 27-31 present the data obtained in attempting to strip any extracted metals from the organic (chloroform) layer using 1.2M HCl. This concentration of acid was chosen because: (1) it was a convenient dilution (1:10) and (2) in cases when various strength of acids were tested, 1.2M HCl proved the weakest that would still strip. It was thought that the weakest acid solution would be desirable so not to destroy the chelating compound. HCl was chosen so that the stripped metals would be in a chloride form which is the form used by the Air Force.

From these two sets of data, it is possible to draw some conclusions.

(1) 8-Hydroxyquinoline shows excellent selectivity and some of the metals could be stripped.

(2) Acetyl acetone was only effective in removing copper and the stripping of the copper was good (about 80%).

(3) Sodium Diethyldithiocarbamate showed some removal capabilities with limited stripping of the metals.

(4) Benzoylacetone was only effective for the removal of copper and that was at a high pH. However, it was not possible to strip this copper from the organic layer.

(5) Dithizone was effective in cadmium and copper removal, with limited zinc removal. Copper was not stripped, however, the cadmium of some of the zinc was stripped.

(6) Cupferron was effective in only removing copper and it was not stripped back.

(7) Thenyltrifluoroacetone was effective in removal of copper and the stripping of the copper was good.

Since cupferron and benzoylacetone would not release the metals, they were studied no further. The other five chelating compounds were then checked as to their reuse capabilities. This was done by simply extracting a 100 mg/l metal solution of Cu, Cr, Cd, Ni, and Zn with chloroform and each of the chelating compounds. Each chloroform layer was then stripped with 2.4M HCl. The chloroform layer was then used for a second extraction of a fresh 100 mg/l metal solution. The results are listed in Table 32. These results indicate that dithizone, 8-Hydroxyquinoline, and acetylacetone cannot be reused. There was, however, some doubt if the re-extraction capability of sodium diethyldithiocarbamate and thenyltrifluoroacetone was due to actual recycling or simply an excess of the chelate present.

An experiment was then run using these chelating compounds. Instead of using just the 100 mg/l metal solution, metal solutions also containing 10 and

TABLE 27

PERCENT EXTRACTION AND STRIPPING FOR NaDDC

0.03M Sodium Diethyldithiocarbamate

pH	Cu		Cr		Cd		Ni		Zn	
	%E	%S	%E	%S	%E	%S	%E	%S	%E	%S
0.71	7	17	4	100	12	36	16	9	15	21
2.22	98	71	14	43	19	44	67	2	18	29
3.18	100	57	15	67	20	53	73	2	17	50
4.09	100	32	14	7	20	42	76	1	18	24
5.21	100	27	14	7	21	30	78	3	18	29
6.32	100	--	14	--	20	--	80	--	17	--
7.20	100	36	18	6	27	38	80	4	--	--

TABLE 28

PERCENT EXTRACTION AND STRIPPING FOR BZA

0.1M Benzoylacetone

pH	Cu		Cr		Cd		Ni		Zn	
	%E	%S	%E	%S	%E	%S	%E	%S	%E	%S
0.98	2	0	1	0	1	0	0	0	0	0
2.28	7	0	2	0	3	0	0	0	0	0
3.08	31	0	2	0	6	0	2	0	0	0
4.09	35	0	3	0	10	0	3	0	1	0
5.13	59	0	4	0	11	0	4	0	2	0
6.17	71	0	5	0	13	0	5	0	2	0
7.32	83	0	4	0	13	0	5	0	2	0
8.40	84	0	4	0	14	0	6	0	3	0
9.98	60	0	3	0	13	0	9	0	2	0

TABLE 29
PERCENT EXTRACTION AND STRIPPING FOR CUPFERRON

pH	0.05M Cupferron					
	Cu		Cr		Cd	
	%E	%S	%E	%S	%E	%S
0.90	14	36	2	50	10	55
1.95	24	17	2	50	9	30
2.68	29	10	10	45	14	40
3.82	41	19	9	20	11	42
4.83	56	35	3	67	8	56
5.60	44	27	14	33	17	56
	Ni		Zn			
	%E	%S	%E	%S		
	12	33	7	50		
	13	31	3	100		
	16	19	9	50		
	15	33	7	75		
	10	20	2	167		
	18	18	14	27		

TABLE 30
PERCENT EXTRACTION AND STRIPPING FOR DITHIZONE

pH	<u>0.05M Dithizone</u>									
	Cu		Cr		Cd		Ni		Zn	
	%E	%S	%E	%S	%E	%S	%E	%S	%E	%S
0.85	96	87	12	8	6	57	6	100	12	15
1.80	99	0	12	38	28	90	10	82	16	47
3.06	100	0	8	33	71	91	12	54	20	62
4.08	100	0	16	6	82	85	20	14	27	42
5.36	100	0	19	5	96	80	25	12	43	59
6.38	100	0	19	5	91	85	26	11	34	51

TABLE 31
PERCENT EXTRACTION AND STRIPPING FOR ACA

pH	0.1M Acetylacetone									
	Cu		Cr		Cd		Ni		Zn	
	%E	%S	%E	%S	%E	%S	%E	%S	%E	%S
0.85	2	100	0	0	0	0	0	0	0	0
2.02	13	58	14	0	4	75	7	100	5	0
2.98	33	83	14	0	5	200	11	89	6	117
3.96	36	79	19	0	8	62	11	78	8	14
5.51	71	83	21	0	8	75	10	75	11	40
7.22	62	80	23	0	8	38	9	57	10	0
8.71	61	77	28	0	8	50	9	57	12	10
10.4	86	77	4	0	10	60	5	75	11	40

TABLE 32

RE-EXTRACTION CAPABILITIES OF VARIOUS CHELATING COMPOUNDS

	%E					
<u>0.005M Dithizone</u>	<u>Cd</u>					
1st Extraction (pH = 5.0)	99					
Strip (2.4MHC1)	88					
2nd Extraction (pH = 5.0)	2					
	%E					
<u>0.03M Sodium Diethyldithiocarbamate (NaDDC)</u>	<u>Cr</u>	<u>Cd</u>	<u>Cu</u>	<u>Zn</u>	<u>Ni</u>	
1st Extraction (pH = 3.0)	85	99+	99+	99+	99+	
Strip (2.4MHC1)	38	90	9	88	0	
2nd Extraction (pH = 3.0)	16	95	99	24	30	
	%E					
<u>0.1M Thenylotrifluoroacetone (TTA)</u>	<u>Cr</u>	<u>Ni</u>	<u>Cr</u>	<u>Zn</u>	<u>Cu</u>	
1st Extraction (pH = 4.0)	5	8	4	0	99+	
Strip (2.4MHC1)	--	--	--	--	86	
2nd Extraction (pH = 4.0)	13	13	12	11	99+	
	%E					
<u>0.5M 8-Hydroxyquinoline (BHQ)</u>	<u>Ni</u>					
1st Extraction (pH = 2.0)	99+					
Strip (2.4MHC1)	89					
2nd Extraction (pH = 2.0)	0					
	%E					
<u>0.1M Acetylacetone (AcA)</u>	<u>Cu</u>					
1st Extraction (pH = 5.5)	70					
Strip (2.4MHC1)	83					
2nd Extraction (pH = 5.5)	3					

1000 mg/l Cu, Cd, Cr, Ni, and Zn were used. The results are given in Table 33. The sodium diethyldithiocarbamate results indicate that the re-extraction capabilities may only have been the results of excess chelate present and when high levels of metal were present it was exhausted and no re-extraction was seen. It is difficult to interpret the thenylotrifluoroacetone results. The re-extraction obtained in the previous experiments was not obtained in this one. The compound showed very little ability to be reuseable. The 10 mg/l experiment was rerun with same results.

For 8-Hydroxyquinoline the problem of not obtaining re-extraction is explained by its distribution ratio as a function of pH

<u>pH</u>	<u>Distribution Ratio</u>
0	0.01
1	0.06
2	0.59
3	5.90
4	59.0

The 8-Hydroxyquinoline should, therefore, be in the aqueous layer at low pH's. An experiment was then run to test this hypothesis. Various 10 ml portions of 0.5M 8HQ in chloroform washed with aqueous layers containing different pH's. Each washed chloroform layer was then used to extract a mixed metal solution containing 810 mg/l Ni at pH = 2. The results were as follows:

<u>pH of washing solution</u>	<u>%E</u>
1.0	100
0.6 (0.6M HCl)	77
0.35 (2.4M HCl)	45
Control (water)	100

This seems to confirm that at low pH's 8HQ is transferred to the aqueous layer and, therefore, lost from the chloroform for future extraction.

In another attempt to verify that the 8HQ was lost to the aqueous layer during stripping, UV spectrum was taken to see if increased 8HQ could be seen in the acid solution and decreasing in the organic layer. This was found to be the case.

In order to have recycling for 8HQ, It would be necessary to separate the 8HQ from the aqueous phase or remove the metals from the aqueous phase.

Ion exchange was the first method reviewed. The stripped aqueous layer, containing the 8HQ and metals was eluted through a column containing macroporous cation resin, Bio. Rad. "AG-MP-50", 20-50 mesh, hydrogen form.

TABLE 33

RE-EXTRACTION CAPABILITIES OF THENYOLTRIFLUOROACETONE AND SODIUM
DIETHYLDITHIOCARBAMATE USING DIFFERENT METAL CONCENTRATIONS

<u>0.1M Thenyltrifluoroacetone</u>					
<u>10 mg/l</u>	<u>Cd</u>	<u>Ni</u>	<u>Cr</u>	<u>Cu</u>	<u>Zn</u>
1st Extraction (pH = 4)	0	4	0	78	0
Strip (1.2MHC1)	--	--	--	99+	--
2nd Extraction (pH = 4)	7	10	10	7	9
%E					
<u>100 mg/l</u>	<u>Cd</u>	<u>Ni</u>	<u>Cr</u>	<u>Cu</u>	<u>Zn</u>
1st Extraction (pH = 4)	10	11	11	77	14
Strip (1.2MHC1)	--	--	--	81	61
2nd Extraction (pH = 4)	9	9	9	10	9
%E					
<u>1000 mg/l</u>	<u>Cd</u>	<u>Ni</u>	<u>Cr</u>	<u>Cu</u>	<u>Zn</u>
1st Extraction (pH = 4)	6	8	9	49	28
Strip (1.2 MHC1)	--	--	--	99+	90
2nd Extraction (pH = 4)	8	7	9	4	7
%E					
<u>0.1M Sodium Diethyldithiocarbamate</u>					
<u>10 mg/l</u>	<u>Cd</u>	<u>Ni</u>	<u>Cr</u>	<u>Cu</u>	<u>Zn</u>
1st Extraction (pH = 4)	99+	99+	99+	99+	99+
Strip (2.4MHC1)	80	0	51	0	80
2nd Extraction (pH = 4)	99+	18	2	99+	19

(TABLE 33 cont'd)

100 mg/l

1st Extraction (pH = 4)	99+	99+	86	96	94
Strip (2.4MHC1)	73	0	51	0	70
2nd Extraction (pH = 4)	6	12	7	78	11

1000 mg/l

1st Extraction (pH = 4)	99+	99+	69	99+	99+
Strip (2.4MHC1)	75	0	33	0	34
2nd Extraction (pH = 4)	0	0	5	0	0

Seventy-six percent of the nickel was removed by the cation resin. Nickel was the only metal checked in order to shorten analysis time. The pH of the eluted stripped solution was then adjusted to 4.0 and extracted with clean chloroform. If 8HQ was present, it should extract into the chloroform layer. The chloroform layer was then used to extract a fresh metal solution with 965 mg/l Ni. Only 6% of the Ni was extracted. This indicated that 8HQ did not pass thru the ion exchange column, but was trapped with the metal on the cation resin, probably because the acid destroyed the molecular structure.

A chelating resin, Bio. RAD Chelex 100, 100-200 mesh, sodium form, was also tried. It was thought that the chelating resin might successfully compete for the metals while not reacting with the 8-Hydroxyquinoline. This resin, however, produced the same results as the cation resin discussed previously.

It was, therefore, concluded that at the present time it would be impossible to reuse the chelating compounds. A separation scheme was then planned assuming no reuse of the chelating compounds.

Since the separation scheme was to be used for the regenerate, the selection of a proper scheme should be checked using a real regenerate. The problem of obtaining a proper regenerate sample has been discussed previously. As stated there, it was decided to use a synthetic solution instead. The concentration of metals are listed in Appendix B.

A series of experiments were then done to examine the use of various combinations of chelates in a sequential extraction scheme. In all of these experiments and all future experiments, work was done using a synthetic regenerate solution as described in a previous section. However, in order to test the applicability of this method, in some experiments the regenerate solution was spiked with other metals of interest. In these cases, the added metal concentration will be given.

Figure 118 shows the results of the first experiment. In this run three different 8HQ solutions of the same concentration were used in the sequential scheme.

As can be seen in Figure 118, A (8HQ, pH=0.5), as expected, gave little extraction. B(8HQ, pH=4.0) showed excellent extraction for several elements, in fact, too many to be useful. C(8HQ, pH=5.5) was able to extract the remainder of those elements which B did not. These results indicated that 8HQ would be useful in removing the elements at the higher pH but some elements would need to be removed before its use in order to obtain better selectivity.

In the next run, A(TTA, pH=3) was used expecting to be able to selectively remove Cu. As Figure 119 shows A did selectively remove the Cu with little else being extracted (24% Fe). B(8HQ, pH=5.3), as before had good removal of Cd, Ni, Fe, Zn and any Cu remaining. C(8HQ, pH=7.2) didn't have much left to extract and therefore was not of much benefit.

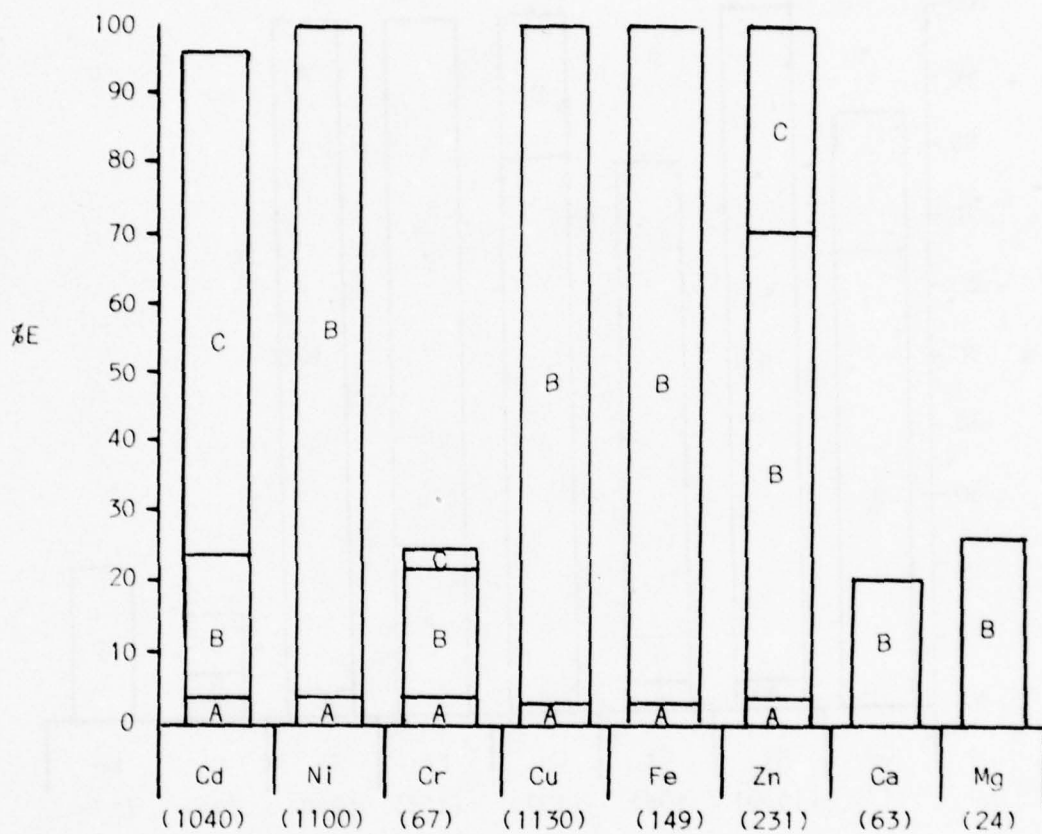


Figure (118). Sequential extraction scheme using A(8HQ, pH = 0.5), B(8HQ, pH = 4.0) and C(8HQ, pH = 5.5).

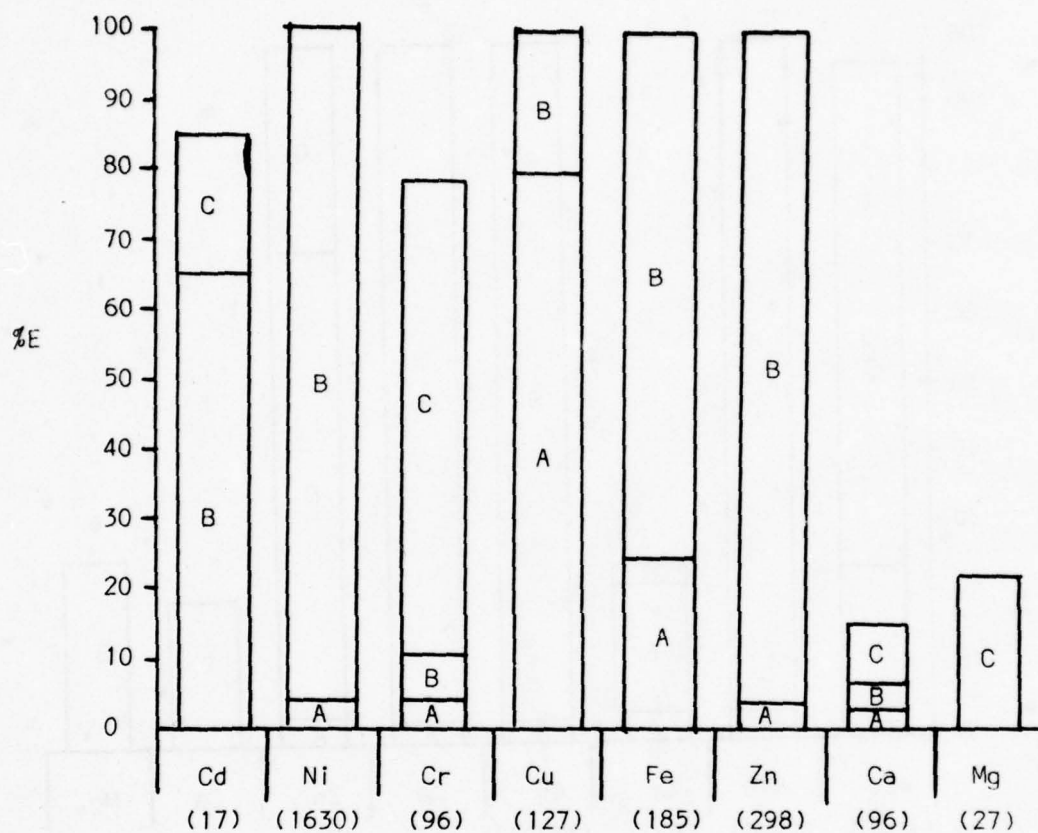


Figure (119). Sequential extraction scheme using A(TTA, pH = 3), B(8HQ, pH = 5.3) and C(8HQ, pH = 7.2).

From the earlier work it was shown that 8HQ was more selective at pH=4.0, therefore, a run was done using A(TTA, pH=2.6), B(8HQ, pH=4.0) and C(TTA, pH=7.0). Figure 120 shows the results. A again showed selective removal of copper with some Fe and Cr being extracted. B did not extract as selectively as expected. Ni, Fe, Zn and some Cd and Cu were extracted. The C solution was ineffective.

In the next run, as shown in Figure 121, A(8HQ, pH=2.5) extracted all of the Cu and Fe but also extracted some of Cd, Ni, Cr, Zn, Ca and Mg. B(8HQ, pH=4.0), however, produced a clean extraction for Ni and Zn. C(NaDDC, pH=4.0) then extracted the remaining metals Cd, Cr, Zn. The performance of B and C was encouraging since both had clean extractions containing only two elements in each.

In the next run, A(AcA, pH=5.5) was used to try to remove the Cu. As Figure 129 shows, it was relatively successful with about 80% removal, with minimum extraction of other metals. B(8HQ, pH=2.5) again extracted a little of everything and a lot of Fe. This time C(8HQ, pH=4.0) had not only Ni and Zn extraction but also about 30% Cd. This made this a little less clean than desirable. D(NaDDC, pH=4.0) again extracted the remaining metals.

TTA was used instead of AcA in a similar experiment. The results are given in Figure 123. TTA behaved similar to AcA. It extracted a little less Cu and a little more Fe. But both, in general, produced the same result. B(8HQ, pH=2.5) again shows a wide range of extraction. C(8HQ, pH=5.3) was the same as the previous run with Ni, Zn and Cd extraction. D(NaDDC, pH=5.3) again extracted the remaining metals.

It was decided to extract twice with TTA in order to obtain more complete copper recovery. 8HQ, pH=2.5 was dropped, since it lacked selectivity. The results of this run are given in Figure 124. The two TTA extraction did as expected with nearly complete Cu removal with minimal extraction of other metals except Fe. C(8HQ, pH=4.0) gave a clean extraction of Ni and Zn with minimal extraction of other metals. D(8HQ, pH=5.5) extracted most of the remaining Zn and with some Cd being extracted. E(NaDDC, pH=5.5) extracted most of the remaining elements.

If one did not have to adjust the pH for each extraction but could use one value, the time and chemical savings would be advantageous. Therefore, an experiment was run using a synthetic regenerate solution at pH=4. Figure 125 shows these results. A and B (TTA, pH=4) again extracted all of the Cu with minimal extraction of other elements. C(8HQ, pH=4.0) extracted most of the Ni and Fe. D(NaDDC, pH=4.0) extracted the remaining Cd, Cr, Fe, Zn and some Ca and Mg.

This system seemed to offer as good a separation as obtained to this point. TTA layers were producing a relatively clean solution of copper with a small amount of Fe. The 8HQ layer was extracting 75% of the nickel, 60% of the Fe and small amount of Zn. The NaDDC served as a general scavenger for removal of the remaining metals. The final water was very clean. Therefore,

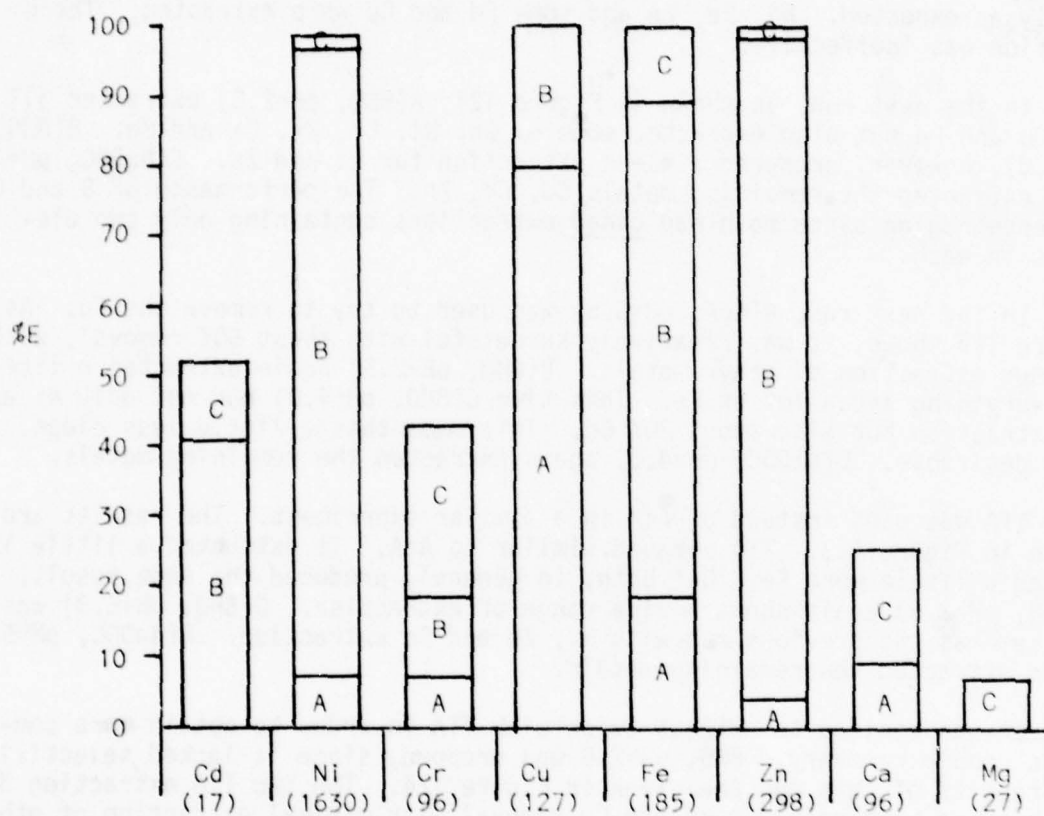


Figure (120). Sequential extraction scheme using A(TTA, pH = 2.6), B(8HQ, pH = 4.0) and C(TTA, pH = 7.0).

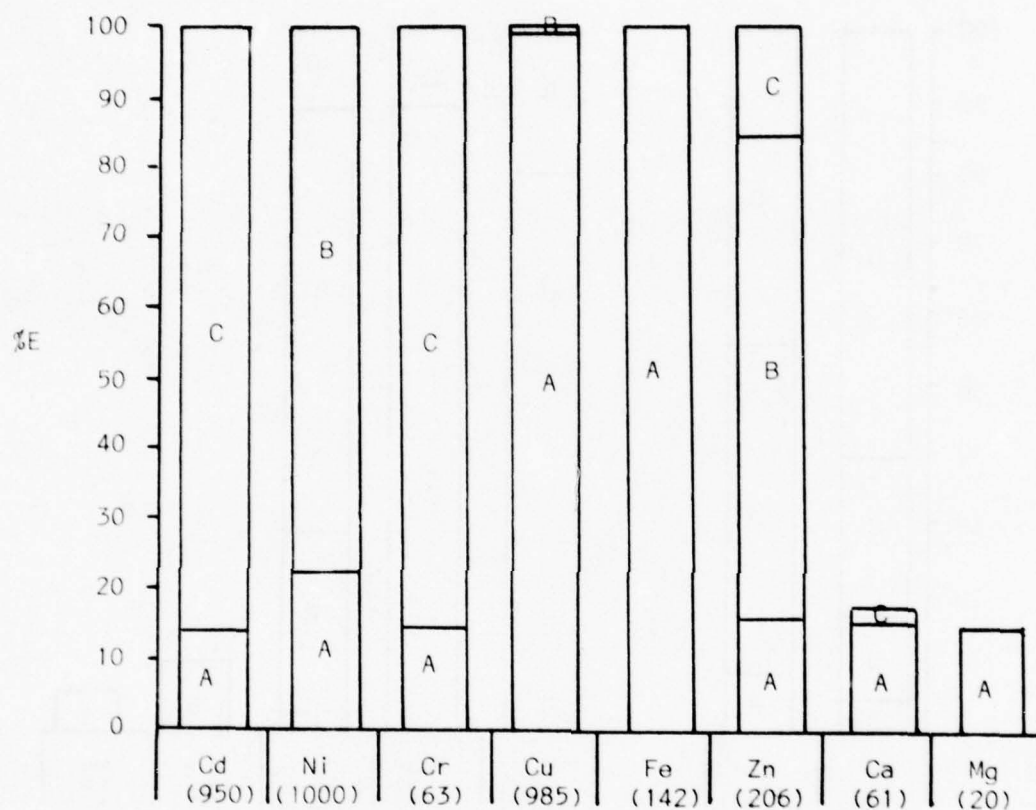


Figure (121). Sequential extraction scheme using A(8HQ, pH = 2.5), B(8HQ, pH = 4.0) and C(NaDDC, pH = 4.0).

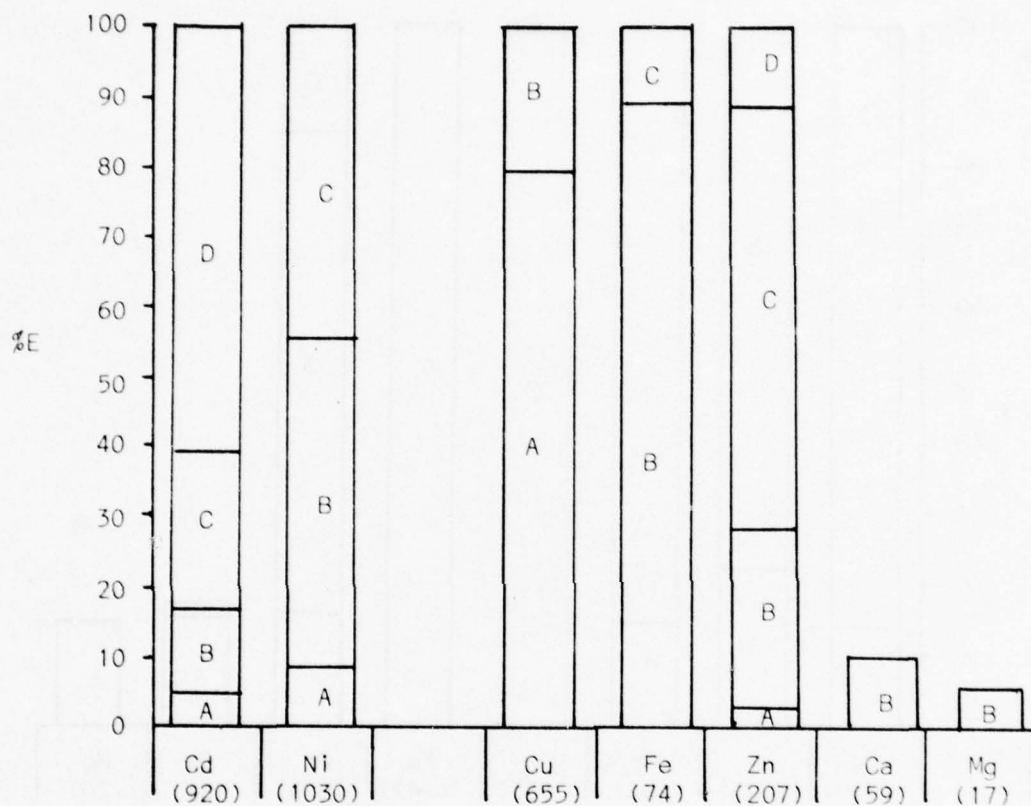


Figure (122). Sequential extraction scheme using A(AcA, pH = 5.5), B(8HQ, pH = 2.5), C(8HQ, pH = 4.0) and D(NaDDC, pH = 4.0).

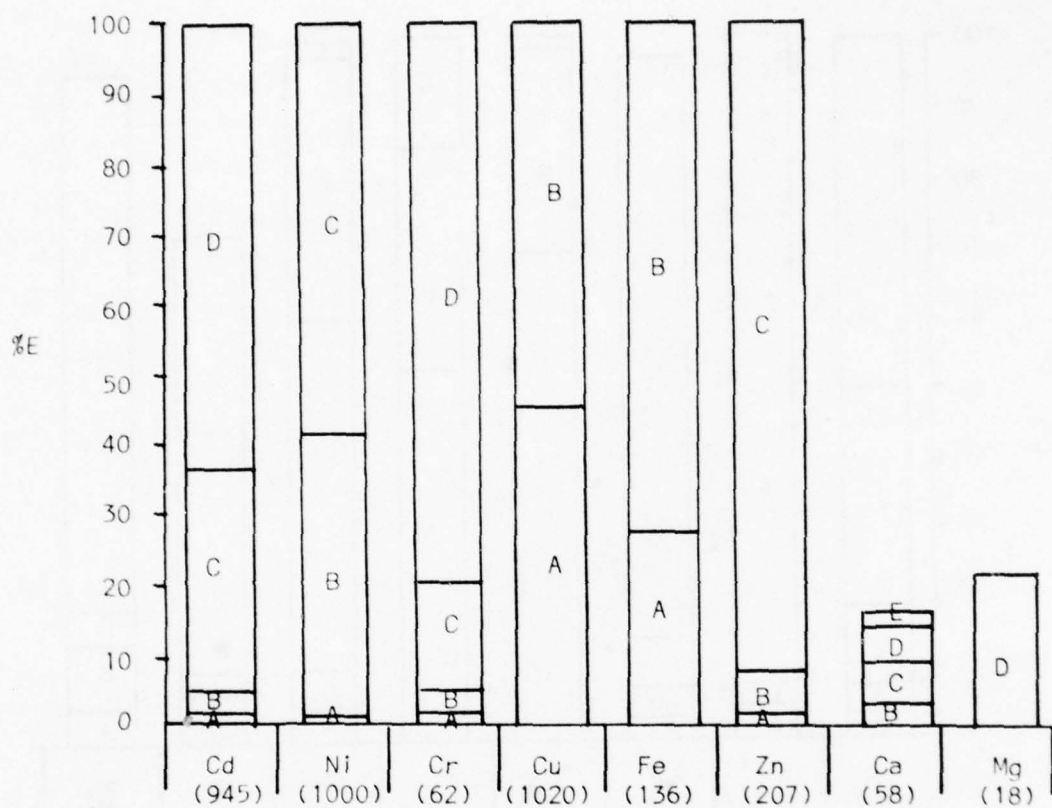


Figure (123). Sequential extraction scheme using A(TTA, pH = 3.0), B(8HQ, pH = 2.5), C(8HQ, pH = 4.0), D(8HQ, pH = 5.3) and E(NaDDC, pH = 5.3).

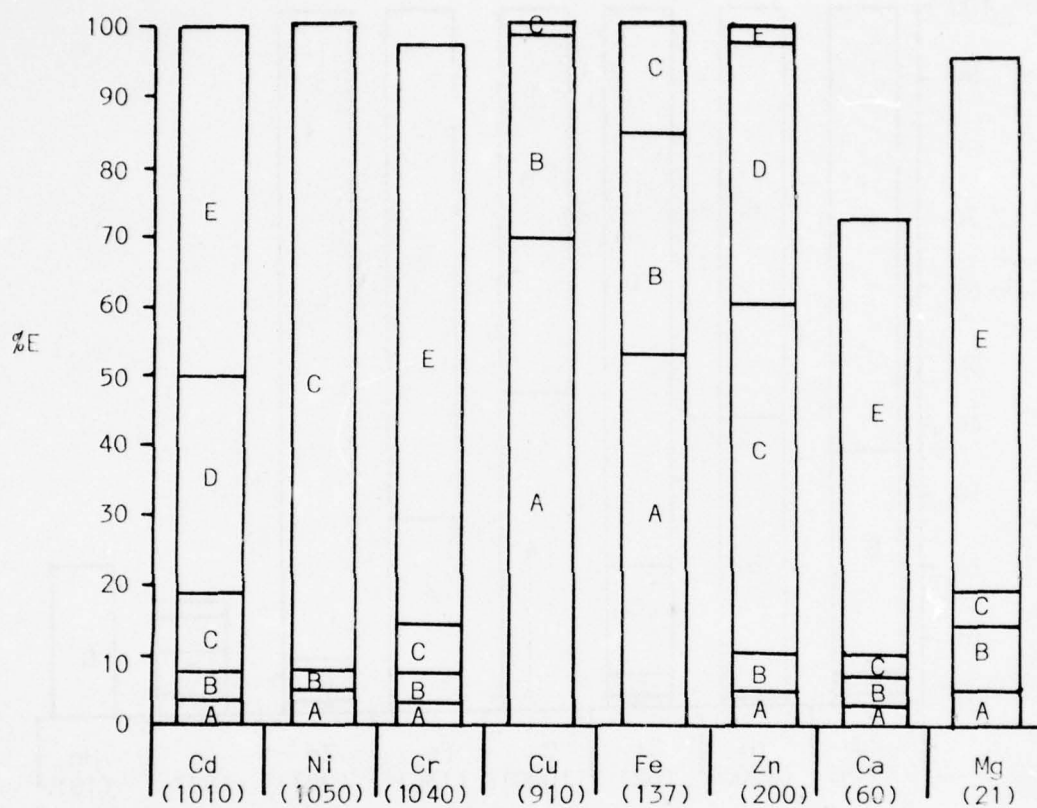


Figure (124). Sequential extraction scheme using
 A(TTA, pH = 4.0), B(TTA, pH = 4.0),
 C(8HQ, pH = 4.0), D(8HQ, pH = 5.5)
 and E(NaDDC, pH = 5.5)

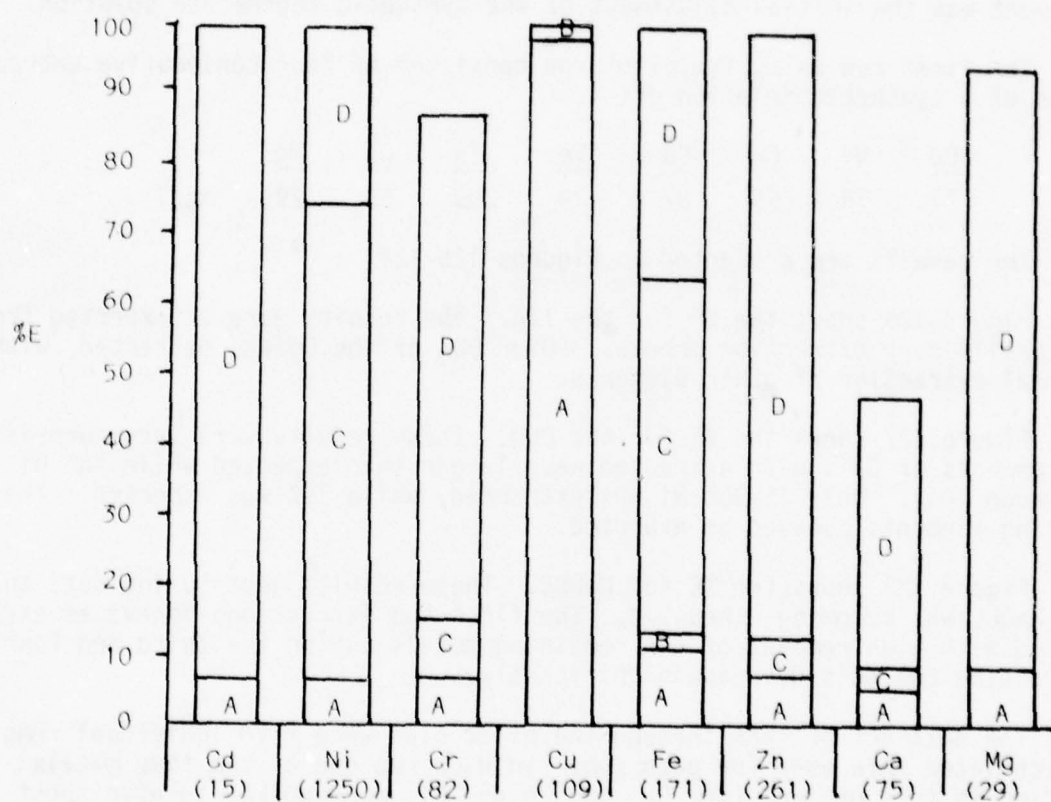


Figure (125). Sequential extraction scheme using A(TTA, pH = 4.0), B(TTA, pH = 4.0), C(8HQ, pH = 4.0), and D(NaDDC, pH = 4.0).

this scheme was selected for the pilot plant.

The pilot plant used was previously described in the methods and materials section. Since the same pH was used for all extractions, the only pH adjustment was the initial adjustment of the synthetic regenerate solution.

The first run using the pilot run consisted of four consecutive extractions of a synthetic solution of:

<u>Cd</u>	<u>Ni</u>	<u>Cr</u>	<u>Cu</u>	<u>Fe</u>	<u>Zn</u>	<u>Ca</u>	<u>Mg</u>	
11	74	65	87	124	209	65	29	mg/l

The results are presented in Figures 126-128.

Figure 126 shows the %E for the TTA. The results were as expected from the preliminary extraction schemes. Over 90% of the Cu was extracted, with minimal extraction of other elements.

Figure 127 shows the %E for the 8HQ. These results were very surprising. The amounts of Cd and Zn extracted were larger than expected while the Ni was much less. Only 15-30% Ni was extracted, while 75% was expected. The remaining elements behaved as expected.

Figure 128 shows the %E for NaDDC. These results seem to indicate that the NaDDC was becoming exhausted. The first two extractions behave as expected with high removal of the remaining metals but on the third and fourth extraction the %E's decrease significantly.

The next set of runs through the pilot plan were five individual runs. New chelates were used for each run. In each run one of the five metals studied in this project (Cr, Cu, Cd, Zn and Ni) were spiked to give about 1000 gm/l. The actual concentrations are listed below:

	<u>Cd</u>	<u>Ni</u>	<u>Cr</u>	<u>Cu</u>	<u>Fe</u>	<u>Zn</u>	<u>Ca</u>	<u>Mg</u>
Run 1	14	90	62	980	113	260	100	35
2	11	800	72	85	160	240	80	32
3	13	88	77	102	160	1140	84	33
4	890	80	71	87	150	230	78	29
5	12	76	850	87	144	225	74	28

Figure 129 shows the results of the TTA. These results are as expected. Little is extracted except Cu. The high amounts of the metals had no effect on the %E except in the case of Cu. At a high concentration, only 55% was extracted. This agrees with results observed in the preliminary sequential scheme study.

Figure 130 shows the results for 8HQ. These results are more scattered than for TTA but there appears to be no effect on %E by high levels

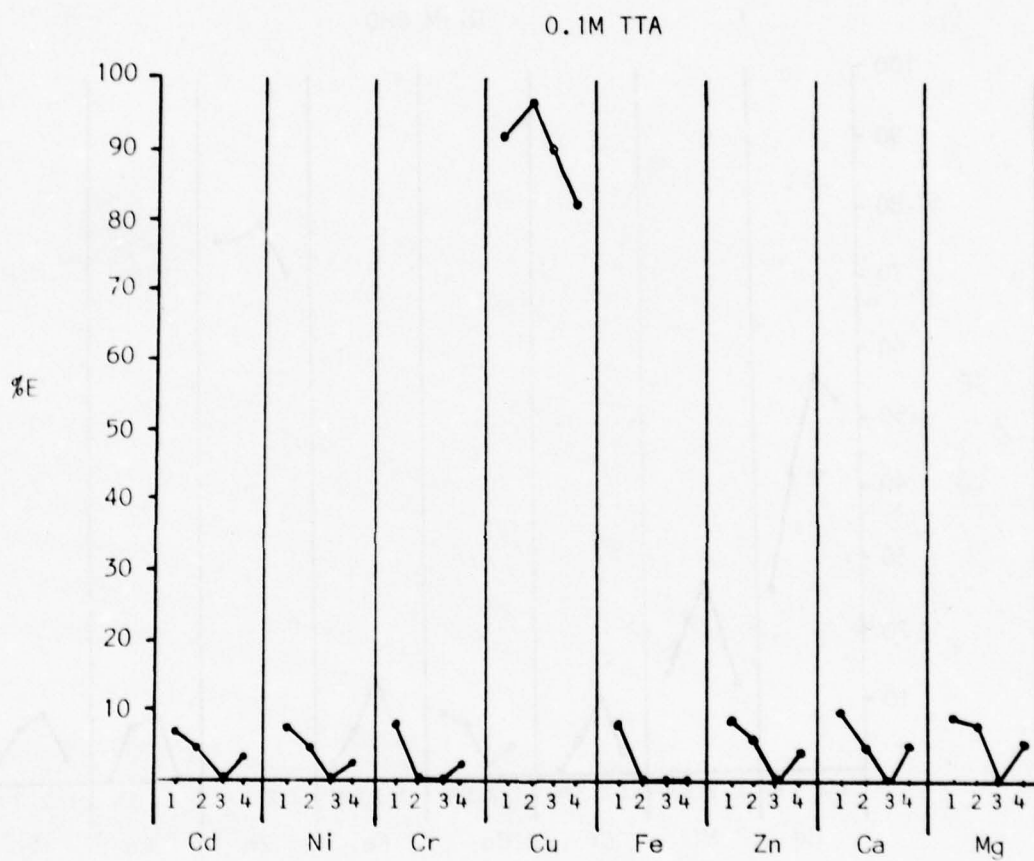


Figure (126). Percent extraction for TTA for four consecutive extractions of a synthetic regenerate solution.

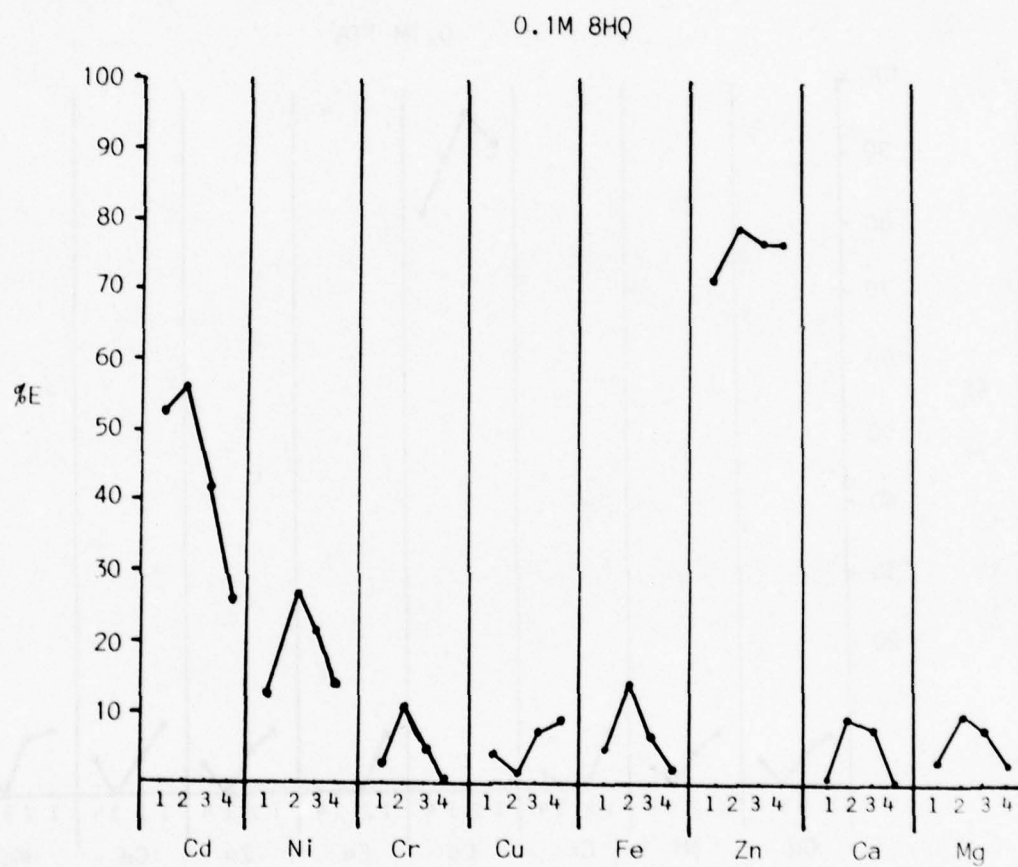


Figure (127). Percent extraction for 8HQ for four consecutive extractions of a synthetic regenerate solution.

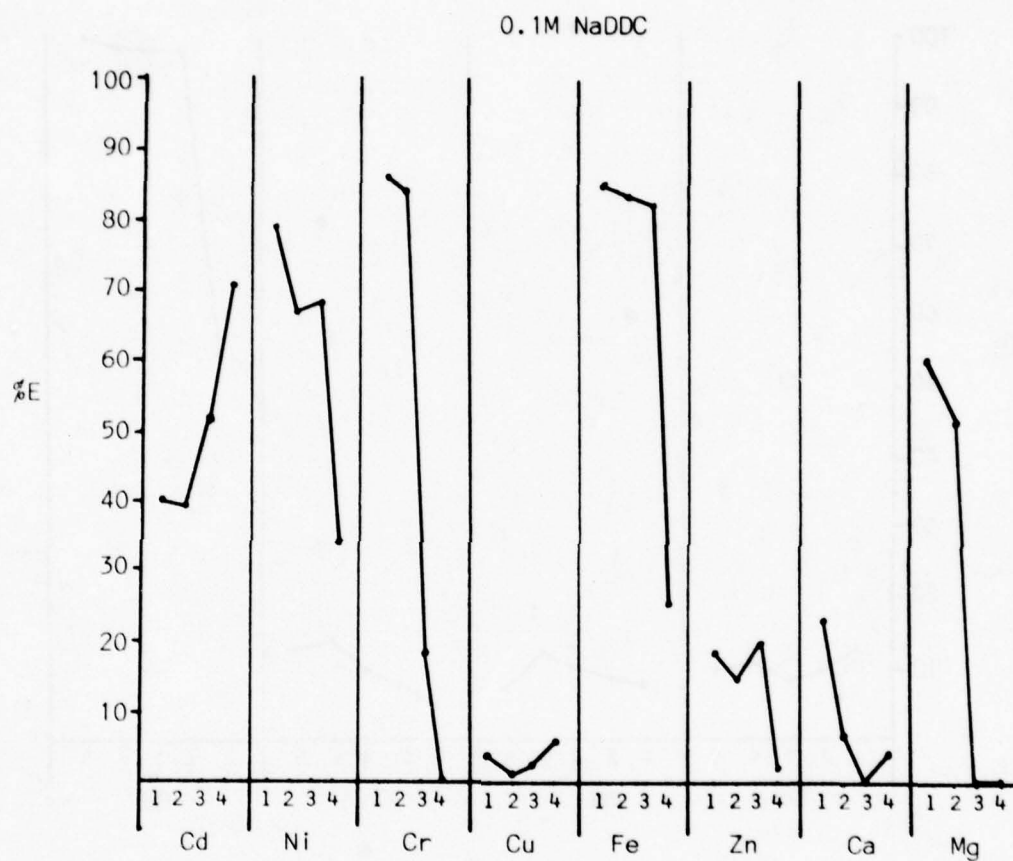


Figure (128). Percent extraction for NaDDC for four consecutive extractions of a synthetic regenerate solution.

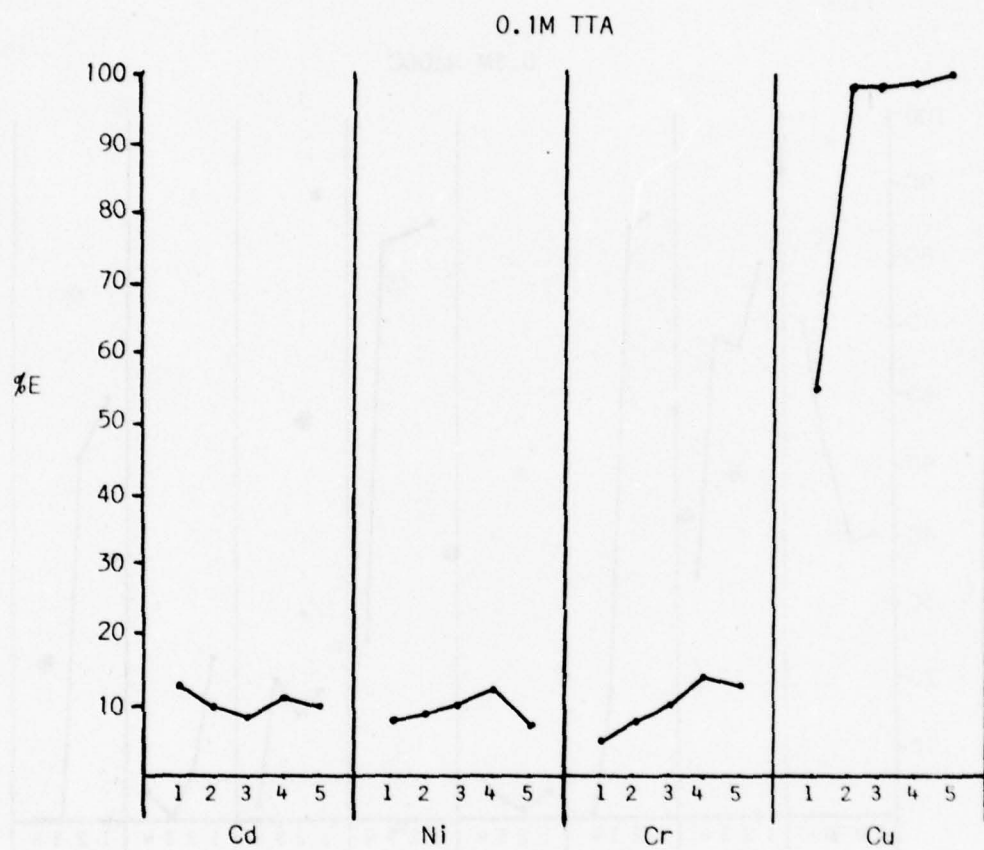


Figure (129). Percent extraction for TTA for five independent runs containing the synthetic regenerate solution spiked with various metals.

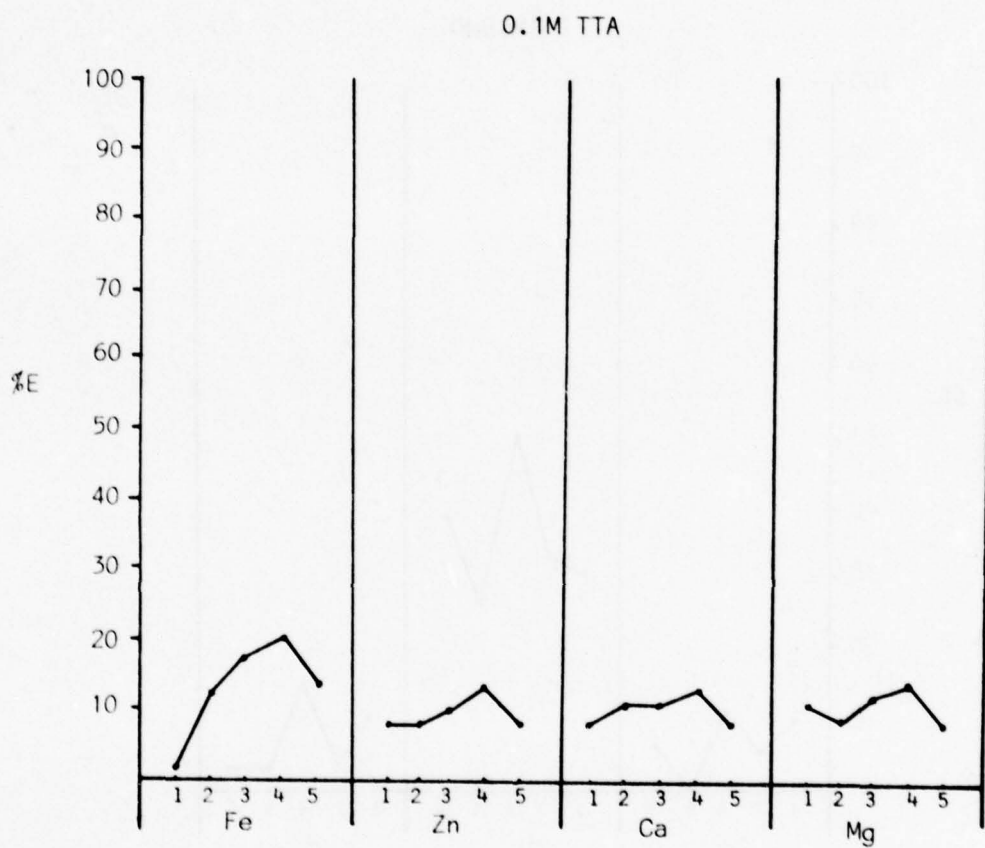


Figure (129) cont'd.

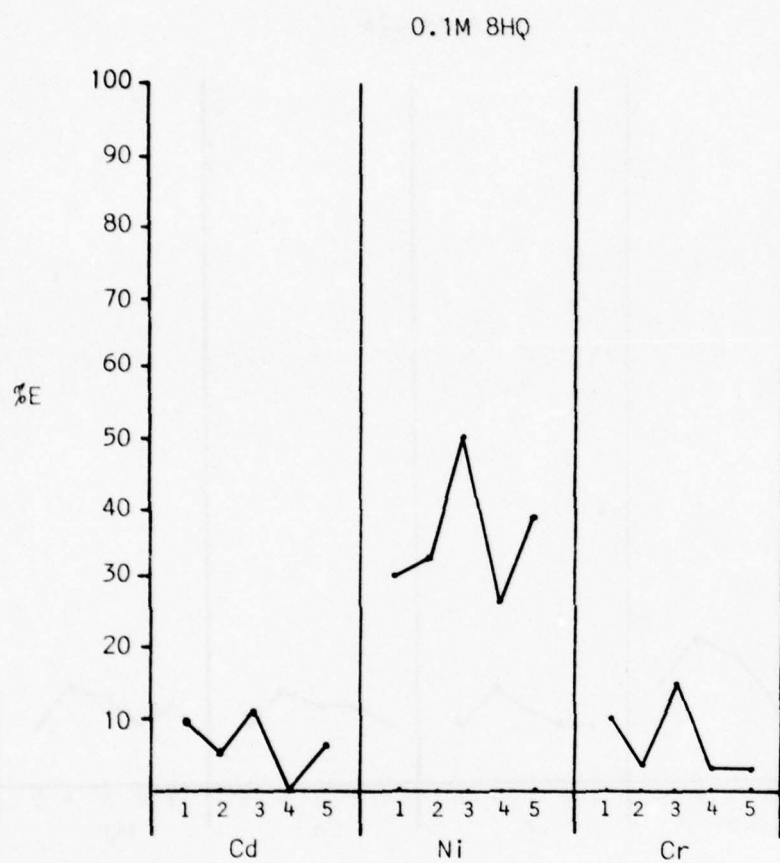


Figure (130). Percent extraction for 8HQ for five independent runs containing the synthetic regenerate solution spiked with various metals.

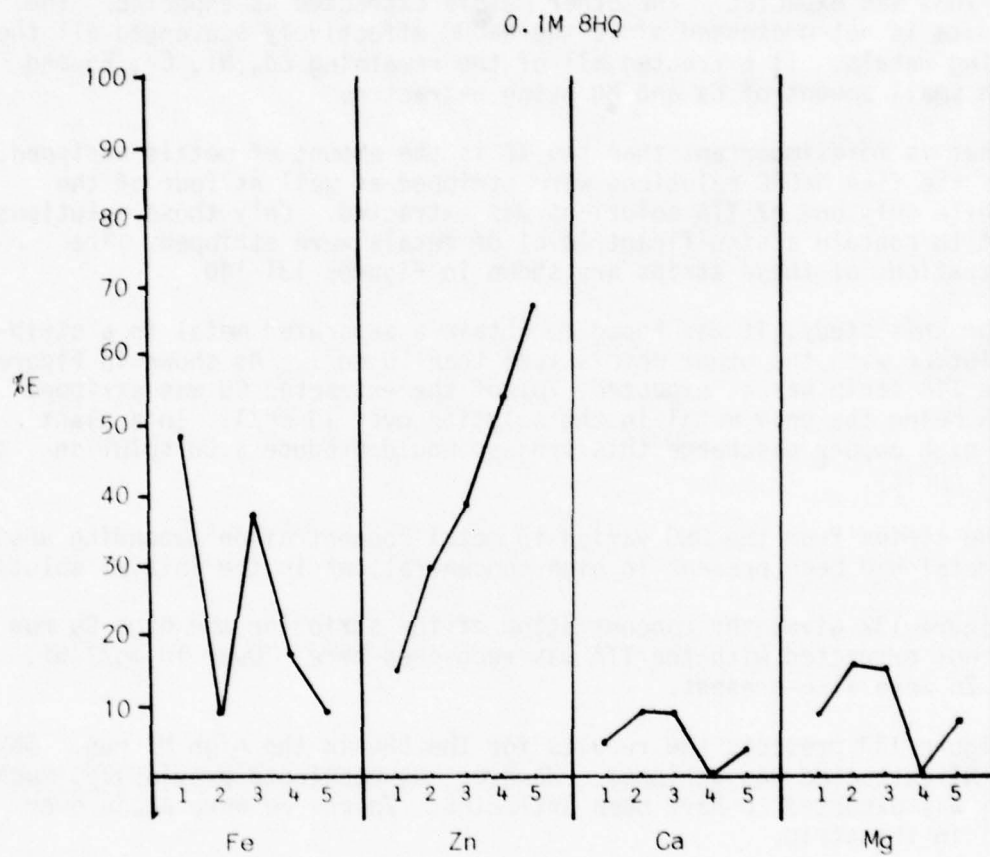


Figure (130) cont'd.

of various metals. As in the previous experiment using the pilot plant, the Ni is lower than expected. This was higher than the previous experiment however, when it had been 15-30% while now it was 30-50% but still not 75-100% was expected. The other metals extracted as expected. The NaDDC data is not presented since the NaDDC effectively scavenged all the remaining metals. It extracted all of the remaining Cd, Ni, Cr, Fe and Zn with small amount of Ca and Mg being extracted.

What is more important than the %E is the amount of metals stripped. Each of the five NaDDC solutions were stripped as well as four of the 8HQ, while only one of TTA solutions was extracted. Only those solutions thought to contain a significant level of metals were stripped. The concentrations of these strips are shown in Figures 131-140.

For this study, it was hoped to obtain a separated metal in a stripped solution with the other metals less than 10 mg/l. As shown in Figure 131 the TTA strip was as expected, 78% of the extracted Cu was stripped with Zn being the only metal in the solution over 10 mg/l. In a plant having high copper discharge this process would produce a Cu solution of high purity.

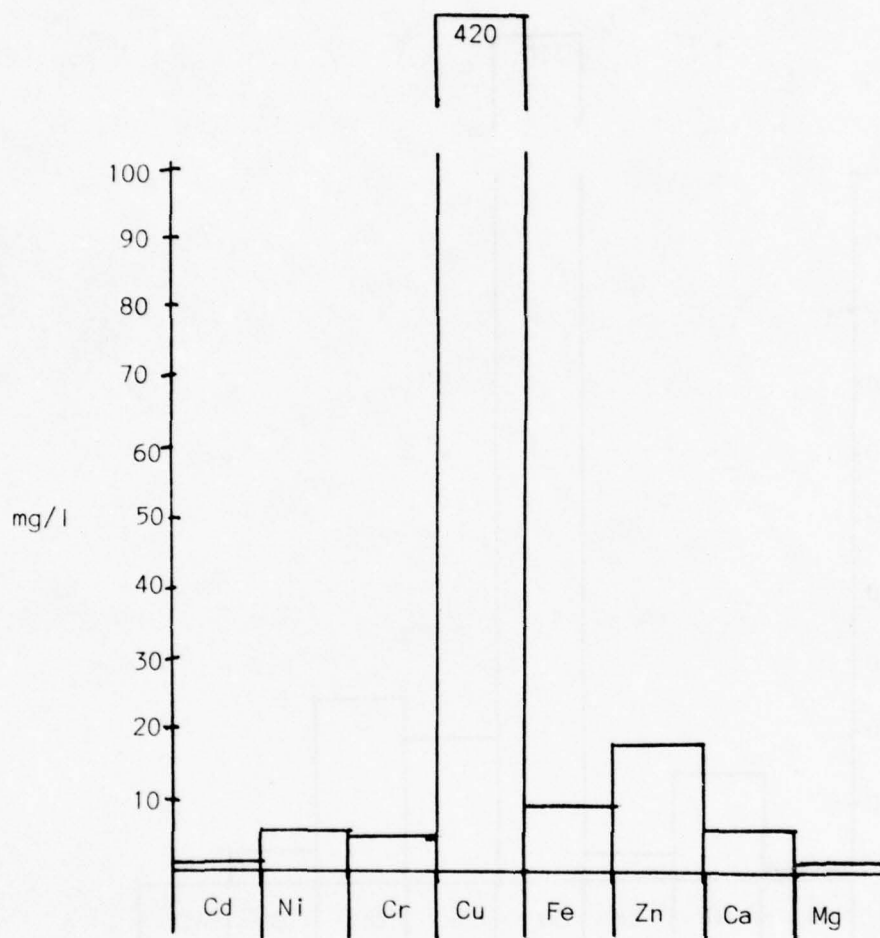
The strips from the 8HQ varied in metal concentration depending upon which metal had been present in high concentrations in the initial solution.

Figure 132 gives the concentration of the strip for the high Cu run. The Cu not extracted with the TTA was recovered here. Over 10 mg/l Ni, Fe and Zn were also present.

Figure 133 presents the results for the 8HQ in the high Ni run. 56% of the Ni extracted was stripped. However, as mentioned previously, much more Ni was expected to have been extracted. Zn and Fe were again over 10 mg/l in the strip.

Figure 134 shows the results of the high Zn run for 8HQ strip. 84% of the extracted zinc was stripped. However, Ni, Cr, Fe and Ca all exceeded 10 mg/l. Thus, the produced zinc strip was not as pure as would be desired.

Figure 135 shows the results of the high Cd run for 8HQ strip. These results indicate that an error was made in the calculation for the %E of Cd for 8HQ for this run. The calculated value was 0%, however, 145 mg/l Cd was stripped, 16% of the original starting concentration. This disagreement shows a problem in using this method. In order to calculate %E the amount of Cd in the water layer after extraction is subtracted from that amount of Cd in the starting solution. In cases of low extraction, a large number is subtracted from an equally large number, therefore, a large error can result. For these studies each value has an error of 5-10% associated with it. Therefore, the error of not seeing the 16% Cd extraction was possible simply due to errors in the measurement of the original two numbers. Again the 8HQ strip contained several metals in high levels and did not produce a clean recovered metal.



Figure(131). Metal content in stripped TTA solution from high Cu run.

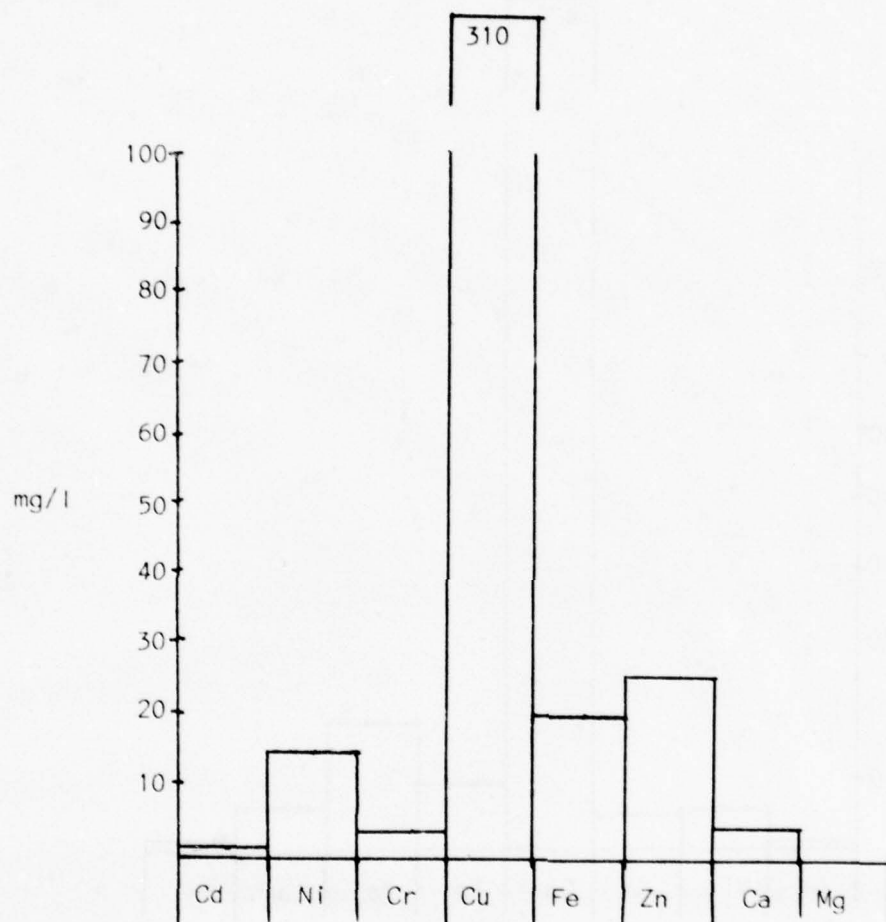


Figure (132). Metal content in stripped 8HQ solution from high Cu run.

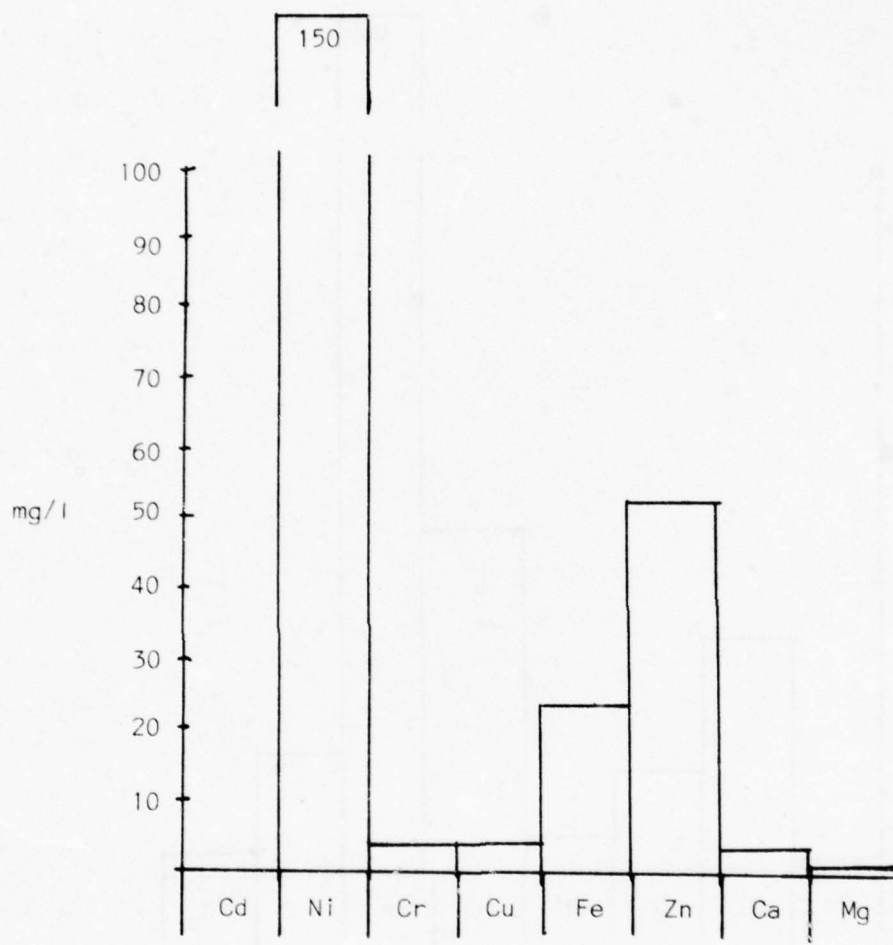


Figure (133). Metal content in stripped 8HQ solution from high Ni run.

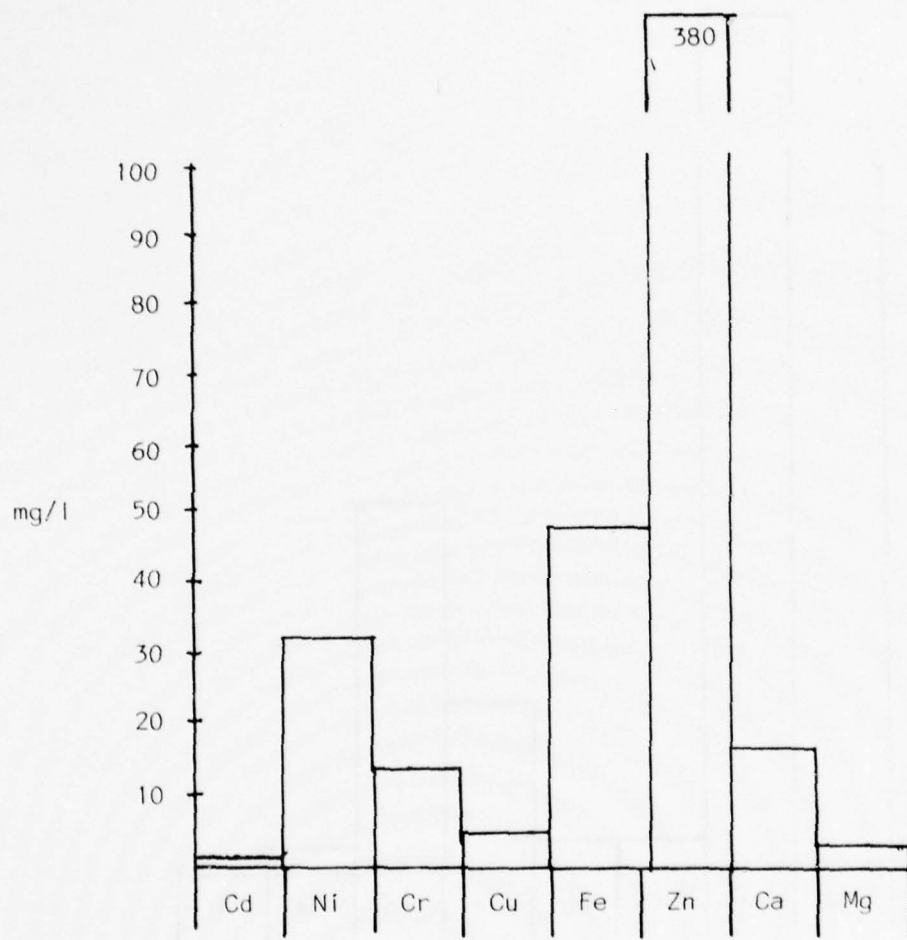


Figure (134). Metal content in stripped 8HQ solution from high Zn run.

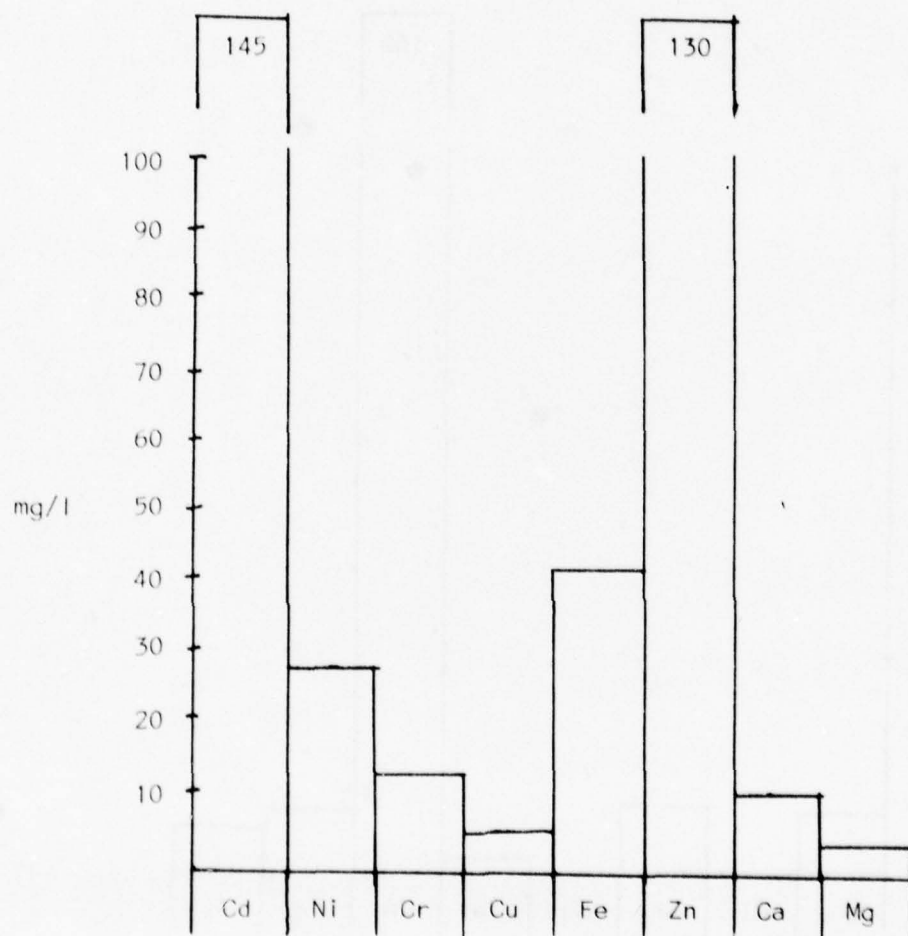


Figure (135). Metal content in stripped 8HQ solution from high Cd run.

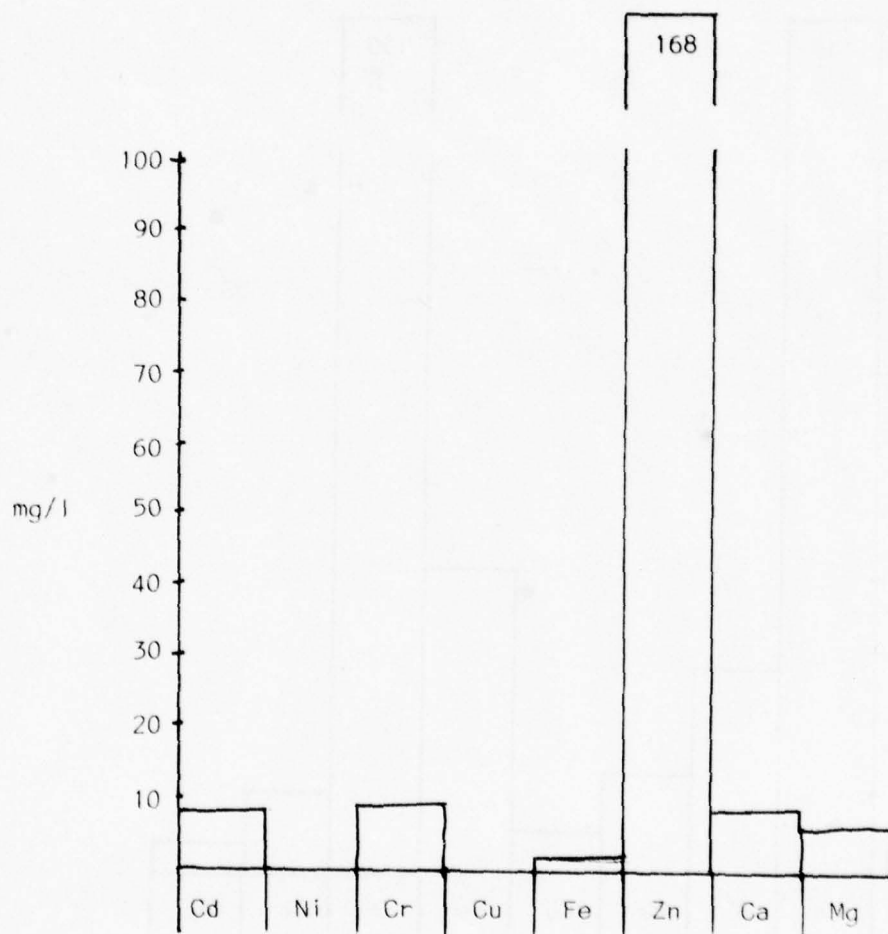


Figure (136). Metal content in stripped NaDDC solution from high Cu run.

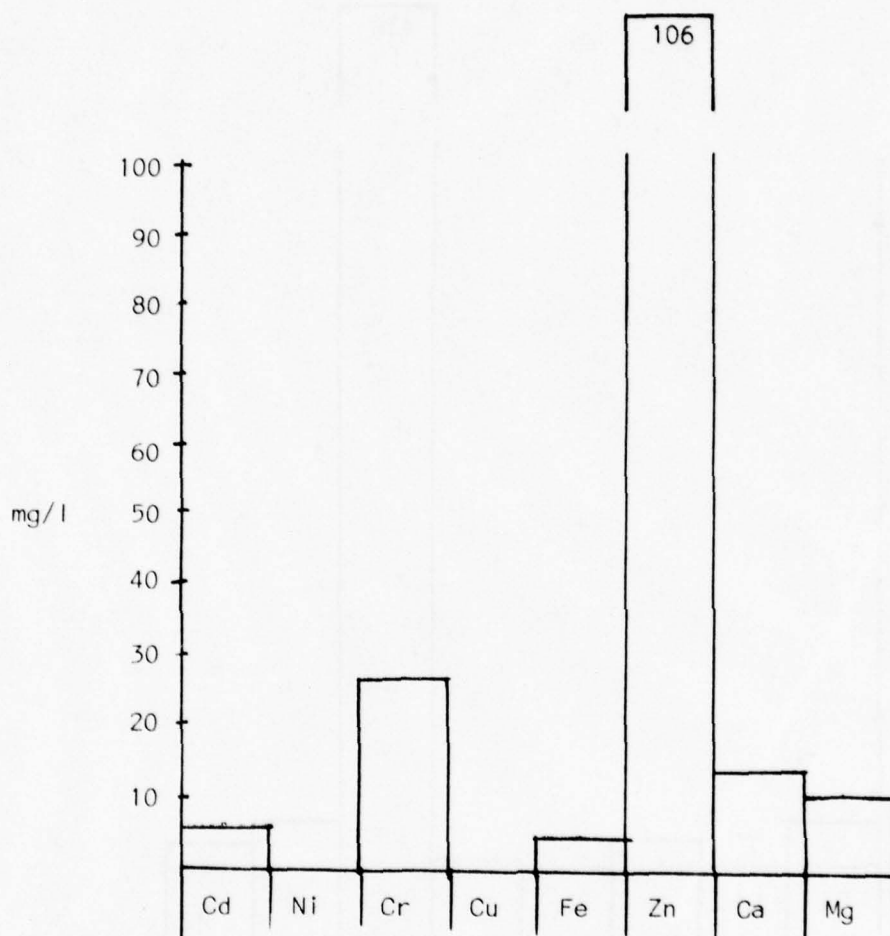


Figure (137). Metal content in stripped NaDDC solution from high Ni run.

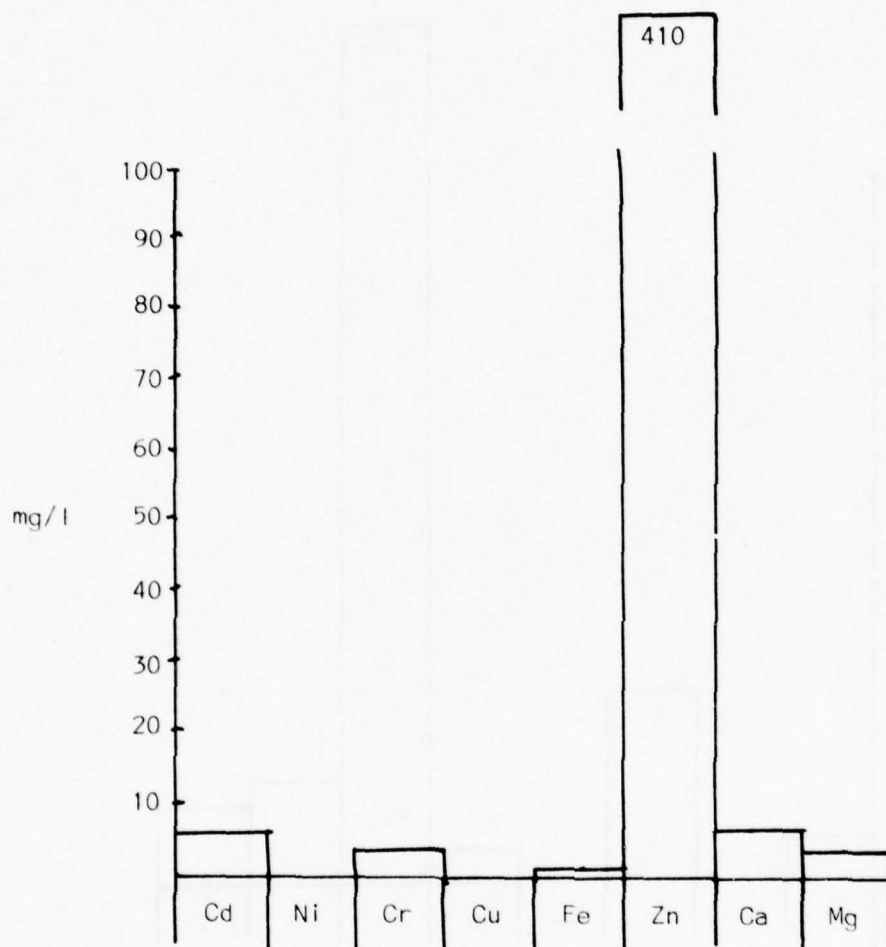


Figure (138). Metal content in stripped NaDDC solution from high Zn run.

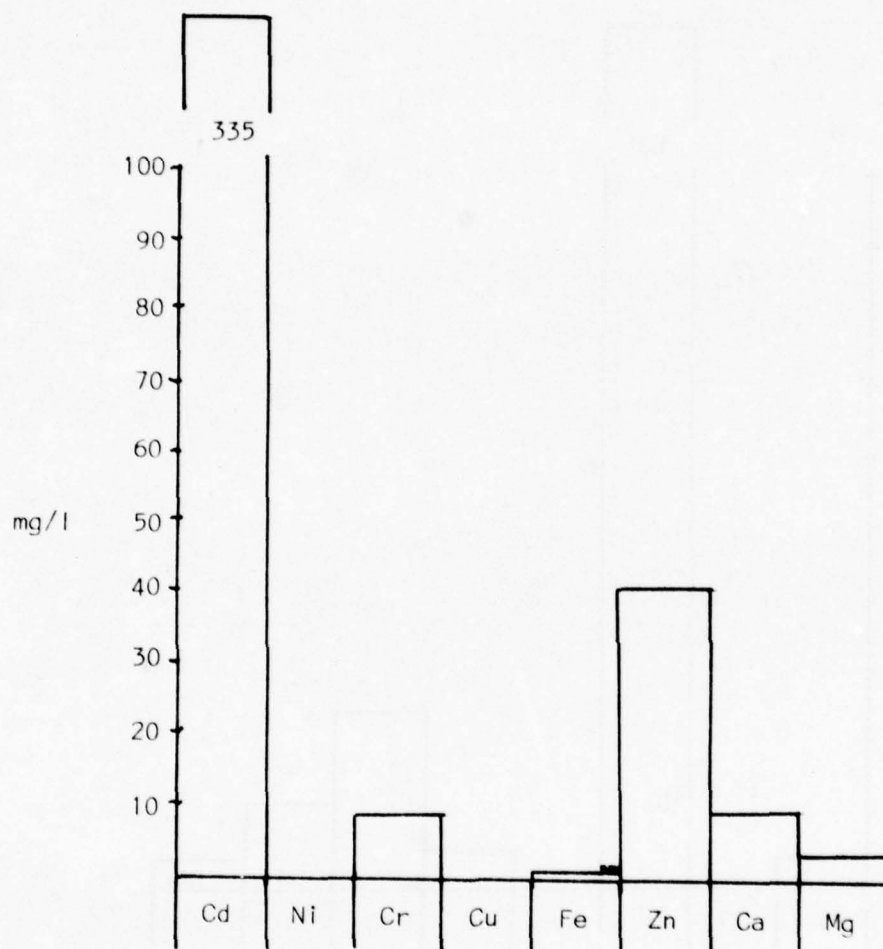


Figure (139). Metal content in stripped NaDDC solution from high Cd run.

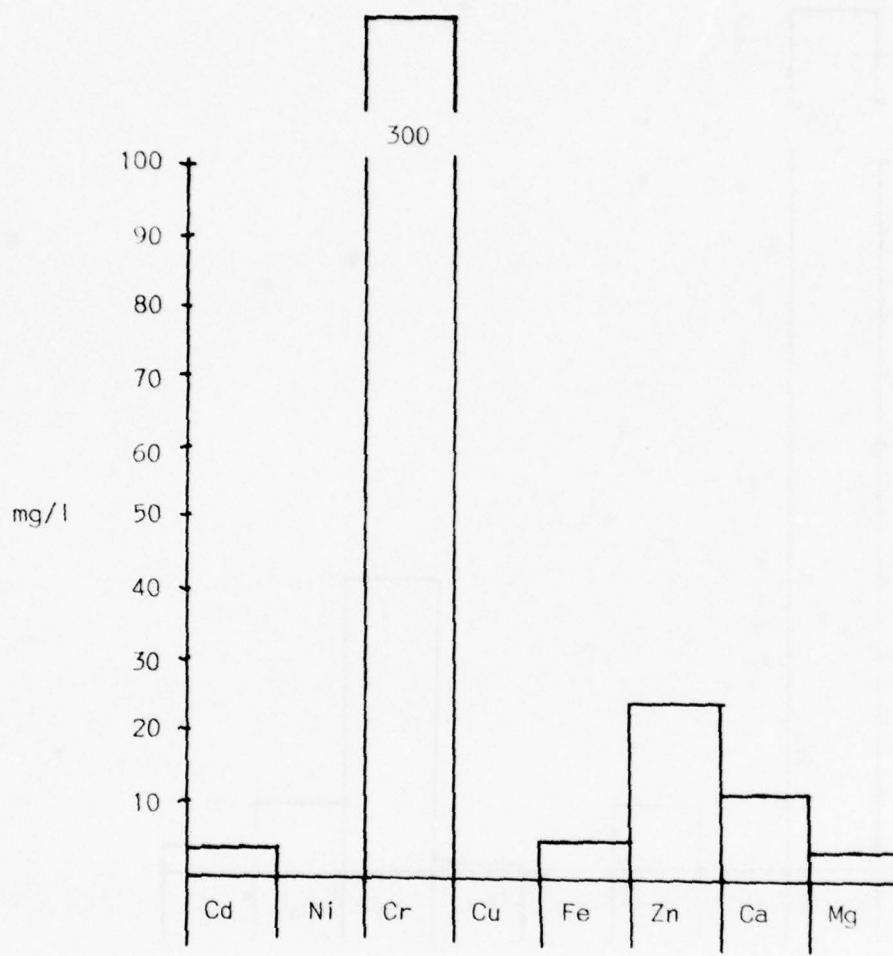


Figure (140). Metal content in stripped NaDDC solution from high Cr run.

Figure 136 shows the results of the high Cu run for the NaDDC strip. 91% of the Zn extracted was recovered with all other metals below 10 mg/l.

Figure 137 shows the results of the high Ni run for the NaDDC strip. 71% of the Zn extracted was recovered. Cr, Ca and Mg were all above 10 mg/l. Even though 460 mg/l Ni had been extracted, none was stripped.

Figure 138 shows the results of the high Zn run for the NaDDC strip. 71% of the Zn extracted was recovered. No other metals exceeded 10 mg/l. This was a clean solution of Zn and would seem to offer potential for a Zn recovery process. NaDDC, even though it extracts most metals, it does not easily release all of them, thus making it very selective and offering potential for recovery schemes.

Figure 139 shows the results of the high Cd run for the NaDDC strip. Only 43% of the Cd extracted was recovered. Zn was again present above 10 mg/l but all other metals were less.

Figure 140 shows the results of the high Cr run for the NaDDC strip. 42% of the extracted Cr was recovered. Zn and Ca were the only metals above 10 mg/l.

To summarize the results of the stripping experiments, the following conclusions can be drawn:

(1) For TTA, 78% of extracted Cu was recovered. Zn was the only metal as a significant contaminant (19 mg/l). However, most of the zinc in the original solution (260 mg/l) was not extracted. Therefore, this extraction has potential for producing a clean Cu solution even at these relatively high levels of zinc. At a lower level of zinc the solution would be even cleaner.

(2) The 8HQ performance was disappointing, especially for Ni extraction. The 8HQ gives complete release of Cd and Cu. It released 56-75% of the Ni, 62-100% Cr, 48-100% Fe, 65-100% Zn. 8HQ gives a nearly complete release of all metals extracted.

(3) The NaDDC produced the most surprising and encouraging results. This chelate does not readily release all of the metals it extracts. None of the Ni extracted was released. Less than 6% of the Fe was released, 50-80% of the Cd was released, 7-42% of the Cr was released. Zn is readily released with 55-91% recovered. Because of this retention of Ni and Fe, this chelate which previously offered potential use only as a final clean-up for left-over metals, might be useful in actually selectively recovering some of the metals.

The problem with the poor extraction of Ni using 8HQ in the pilot plant system was found to be due to insufficient shaking time and mixing. In order to obtain the extraction efficiencies which were obtained in the preliminary work, the extraction flasks had to be mixed at maximum rate and mixed for at least 15 minutes.

For the final portion of this study, it was desired to make use of the information obtained so far and apply it toward the recovery of metals in a real electroplating wastewater. Since information was available for Tinker Air Force Base, it was chosen as an example.

As described previously the Tinker Air Force Base Electroplating wastewater (from ion exchange) has only two elements, Cr^{+6} and Ni^{+2} worth recovering. The Cr is in the anion regenerant and the Ni is the cation regenerant.

Reviewing the results from our study, Cr^{+6} is not extractable. However, there are various procedures for reuse of Cr^{+6} from anion exchange columns. These include methods as simple as evaporation or a more complicated method involving reduction of Cr^{+6} to Cr^{+3} and then removal by cation exchange, stripping and oxidation back to Cr^{+6} .

The Ni would be the only metal applicable to this procedure. If 8HQ was used alone, any Ni extracted would be expected to be contaminated with Fe, Zn and Cu. TTA could be used in a pretreatment to remove the Cu and some Fe, but since there is not enough Cu to recover, this added extraction would seem to be an expensive clean-up step.

From work discussed in a previous section, it was found that certain metals could be selectively precipitated. It had been observed during this work that if the pH of the synthetic regenerate was raised to pH=5.5 a brown precipitate formed. Upon examining the water before and after the pH adjustment the following information was obtained:

	mg/l							
<u>Run 1</u>	<u>Cd</u>	<u>Ni</u>	<u>Cr</u>	<u>Cu</u>	<u>Fe</u>	<u>Zn</u>	<u>Ca</u>	<u>Mg</u>
pH=0.8	11	1720	84	110	176	257	73	32
pH=5.5	9	1410	1	10	1	191	62	27
<u>Run 2</u>								
pH=0.8	19	1840	105	120	215	274	86	35
pH=5.5	19	1640	2	14	4	240	83	29
	%E							
Run 1	18	18	100	91	100	26	15	16
Run 2	0	11	98	88	98	12	3	17

As can be seen, nearly all of the copper, chromium and iron were removed with only a small amount of nickel. This precipitation has selectively removed two of the contaminating metals. There is still, however, a large amount of zinc present in solution. Examining Figure 10, Ni should be extracted at pH=3.0 with only minimal Zn.

The following procedure was then followed:

- (1) A synthetic regenerate solution (Run 2 from above) was adjusted to pH=5.5.
- (2) The precipitate that formed was allowed to settle and the supernatant poured off.
- (3) 500 ml of this supernatant was poured into the storage reservoir of the pilot plant.
- (4) 150 ml was discharged into an extraction vessel containing 150 ml 0.25M 8HQ in chloroform.
- (5) System was stirred at maximum speed for 30 minutes.
- (6) Aqueous layer was discarded and another 150 ml was discharged into the extraction vessel.
- (7) Step 5 and 6 were repeated.
- (8) The organic layer had now extracted 3-150 ml portions of the supernatant.
- (9) The organic layer was then stripped with 2.4 M HCl for 10 minutes.

Figure 141 shows a graph with the %E for each run. Only Cu and Ni were extracted to any degree. 83% of the total Ni was extracted.

Figure 142 shows the concentration of the stripped solution. 83% of the extracted Ni was recovered. More might have been recovered with a longer stripping time. The Zn and Cu are still in the final solution but represent less than 3% of the total nickel.

This combination of precipitation and extraction is able to produce a final stripped solution containing a clean solution of Ni.

During the entire process, 8 ml of chloroform was lost. The solubility of chloroform in water (0.8%) would account for about half of this loss with the rest being carried over upon separation of layers. The chloroform and any chelate in the stripped solution might be significant if the metal is to be reused. If this is true, then the stripped solution would have to be run through an activated carbon bed for organic removal.

Summary of Liquid-Liquid Extraction Studies

The results obtained in these studies indicate that the liquid-liquid extraction technique offers potential for the recovery of metals from an ion exchange regenerate of an electroplating plant. However, at the present time it does not appear to be economical.

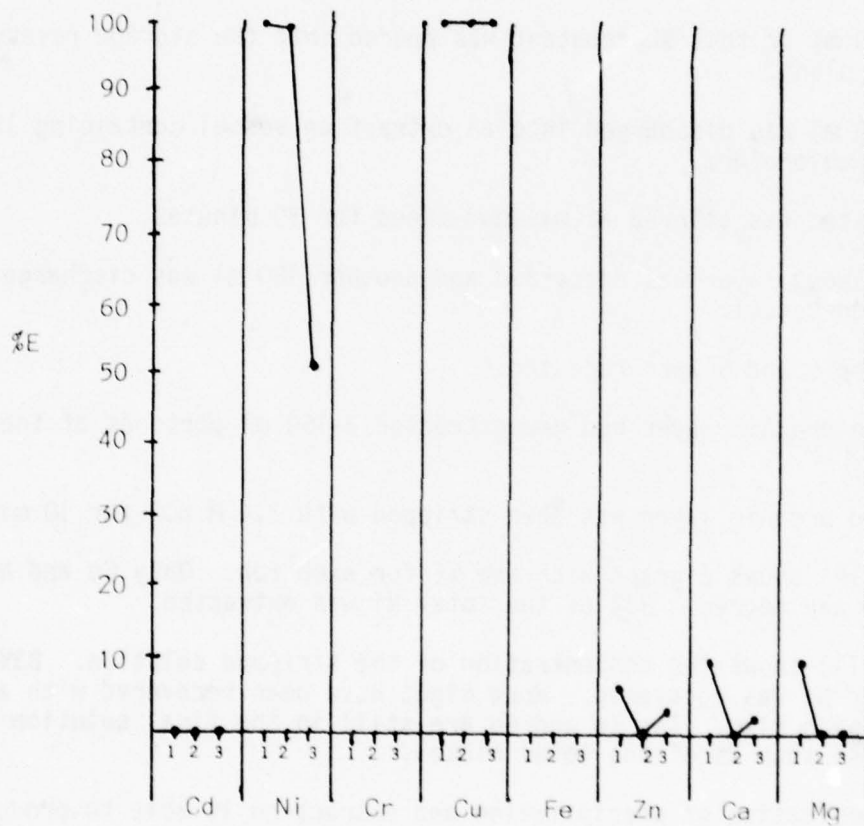


Figure (141). Percent extraction for 8HQ extraction of a precipitated synthetic regenerate solution. Three consecutive extractions.

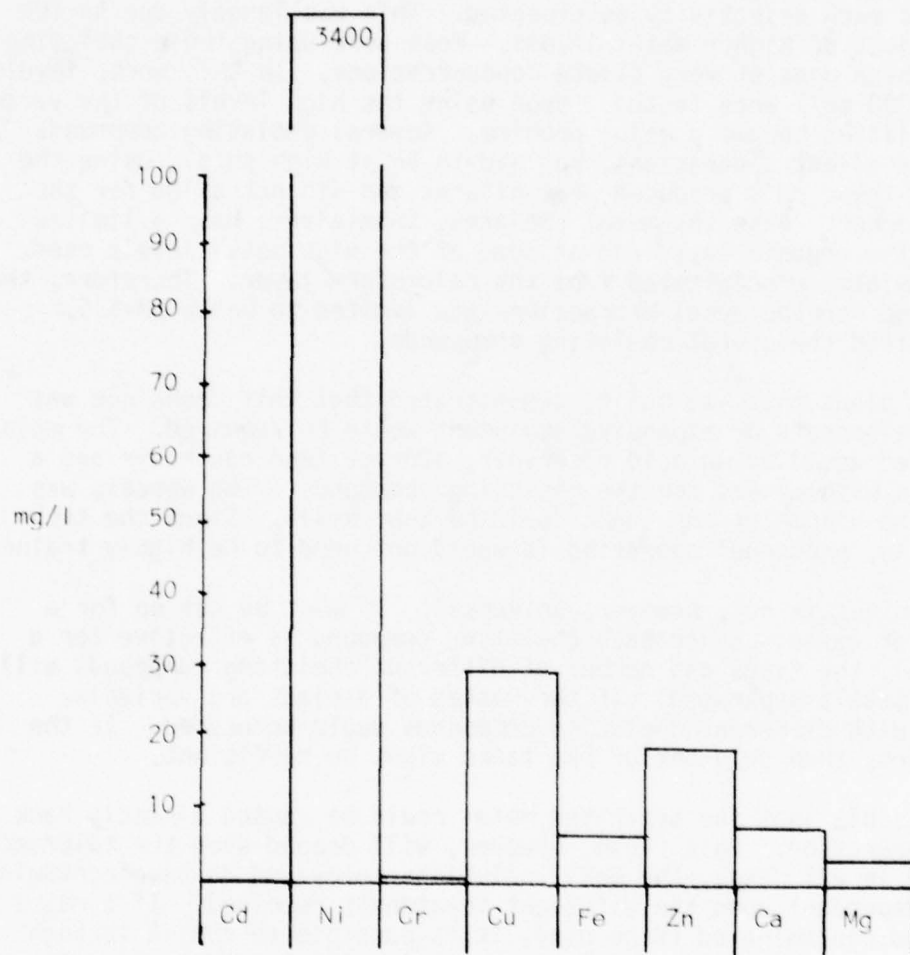


Figure (142). Metal content in stripped 8HQ solution from precipitated synthetic regenerate run.

This technique was shown to be able to separate the various metals of interest with varying degrees of success. The chelating compounds examined did not show as much selectivity as expected. This was largely due to the use in the project of higher metal levels. Most work using these chelating compounds had been done at very dilute concentrations. In this work, levels as high as 10,000 mg/l were tested. Upon using the high levels of the various metals, solubilities became a major problem. Several chelating compounds studied gave excellent separations, but had to be at high pH's. Using the high metals at these pH's produced precipitates and did not allow for the extraction to occur. Also the metal chelates, themselves, have a limited solubility in the organic layer and at some of the high metal levels used, these metal chelates precipitated from the chloroform layer. Therefore, the working pH range for the metal extractions was limited to below pH=5.5, which then limited the useful chelating compounds.

The pilot plant that was built, demonstrated that this technique was simple and no elaborate or expensive equipment would be required. The main equipment needed would be an acid reservoir, storage feed reservoir and a series of tanks with mixers for the chelating compounds. The process was very fast so the volume of the tanks could be kept small. Since the technique was simple, personnel operating it would not need to be highly trained.

This technique is not, however, universal. It must be set up for a specific type of waste. Since each chelating compound is effective for a different metal, the types and number of different chelating compounds will determine the metals separated. If the wastes of a plant are variable, several tanks with different chelating compounds would be needed. If the waste is uniform, then only one or two tanks might be sufficient.

It is possible that the separated metal could be reused directly back into the plant operation. This reuse, however, will depend upon the tolerances of the baths. In all cases, the metal solutions recovered do have contamination and are dependent upon the different treatments received. If a metal solution is too contaminated to be used, it is possible to run it through another chelate system to clean it further. This will increase the cost.

The recovered metal solutions also contain small amounts of chloroform and chelating compounds. If these organics interfere with the electroplating process, another step would have to be added; removal with activated carbon.

Because of the large number of possible variations to a plant, it is difficult to estimate a total cost. However, certain costs can be calculated. The cost of the three main chelating compounds used in this study are: 8HQ (\$35/lb.), TTFA (\$270/lb.) and NaDDC (\$44/lb.). These prices are based on small purchases and high purity. If these chemicals were purchased in quantity and of less purity, it is reasonable to assume that the cost would be 2-5 times less. Below is a comparison of the metal prices and the chelate cost assuming a factor of 3 reduction for bulk purchases:

<u>Metal</u>	<u>Metal Price (\$/lb)</u>	<u>Chelate Price (\$/lb)</u>	<u>1b Metal Recovered (theoretical) per 1b Chelate Used</u>
Ni	5.3	12 (8HQ)	2
Cr	0.8	15 (NaDDC)	3
Cd	16.	15 (NaDDC)	1
Cu	7.	90 (TTFA)	2

From these data, Cu and Cr recovery would not be economically feasible based solely upon the cost of the chelate. The value of the Ni and Cd would equal the cost of the chelate used. This does not consider the cost of the chloroform, HCl, NaOH, capital costs, as well as operating costs. All of these costs would be much more than current disposal costs.

Therefore, unless the metal prices increase dramatically, or a method of recycling the chelating compound can be found, the process is not economically feasible.

SECTION IV

CONCLUSIONS

METALS INSOLUBILIZATION STUDIES

1. The hydroxide insolubilization/precipitation of cadmium, copper, nickel and zinc yielded residual supernatant metals concentrations which were in close agreement with values predicted from theoretical equilibrium chemistry calculations.
2. The addition of sulfate ions resulted in the destabilization of $\text{Cr}(\text{OH})_3(\text{s})$ suspensions in the pH range 6.0 to 7.5 through the mechanism of adsorption for charge neutralization. The sulfate adsorption phenomenon was found to be reversible, with sulfate ions being desorbed back into solution at pH values greater than the isoelectric point of $\text{Cr}(\text{OH})_3(\text{s})$.
3. The presence of chromium in a mixed-metal solution was found to greatly affect the insolubilization/precipitation of other cations from solution through "coprecipitation".
4. The mechanism of "coprecipitation" was determined to be related to insolubilization kinetics such that, under conditions of "localized high pH", the "slow" kinetics of chromium hydroxide insolubilization allowed for the insolubilization of other metals. No evidence of metal ion adsorption or ion inclusion, mechanisms reported by other investigators, was seen to occur.
5. Mixed-metal systems containing little or no chromium were found to function according to equilibrium chemistry predictions. Efficient separation of two or more metals as $\text{Me}(\text{OH})_x$ species was often achieved, offering the possibility for metals recovery through "selective hydroxide precipitation".
6. "Coprecipitation" is not characteristic of all trivalent cations.

SLUDGE CHARACTERIZATION STUDIES

7. Nickel hydroxide sludges were characterized by high specific resistance values, low cake solids concentrations, and minimal solids penetration during dewatering.
8. Chromium hydroxide sludges were characterized by low specific resistance values, high cake solids concentrations, and major problems related to solids penetration.
9. The use of lime instead of sodium hydroxide resulted in the

formation of a chromium hydroxide floc which was more resistant to "break-up" during dewatering, as evidenced by significant decrease in solids penetration.

10. The addition of small doses of polyelectrolyte to chromium hydroxide sludges will often significantly reduce the amount of solids passing into the vacuum filtrate.
11. Cupric hydroxide sludges were characterized by low specific resistance values, widely varying cake solids concentrations, and problems related to solids penetration. However, the "aging" of cupric hydroxide to cupric oxide helped to alleviate most problems of solids penetration.

FACTORS AFFECTING DEWATERING

12. Of the sludge parameters investigated, particle size was found to have the most important role in characterizing the resistance of metal hydroxide sludges to dewatering.
13. As the mean sludge floc size increased, the specific resistance of metal hydroxide sludges decreased significantly.
14. Parameters such as insolubilization pH and variations in metal content were found to relate to sludge specific resistance by affecting the size of flocs formed during insolubilization/precipitation.
15. No one size fraction could be identified as being most characteristic of metal hydroxide sludge dewatering. Rather, the sludge mean floc size and size distribution most adequately accounted for variations in specific resistance observed.
16. Accurate, predictive sludge dewatering models can be developed to relate specific resistance to measureable sludge parameters. In the case of metal hydroxide sludges, particle size and the fraction of "fines" were found to be the most crucial physical parameters necessary to characterize the resultant specific resistance.
17. Solids penetration is a major problem when considering the dewatering of certain metal hydroxide sludges. Furthermore, solids penetration could not be correlated to the relative fraction of "fine" particles present in a sludge. Instead, floc strength appears to be a major determining factor in the amount of solids penetration which occurs during dewatering.
18. None of the physical sludge parameters evaluated were found to be a good indicator of sludge compressibility. Particle size offered a minimal correlation to "s". Most sludges evaluated had coefficient of compressibility, "s", values near 1.0. Finally, the

variation in "s" during polymer conditioning studies was at best considered random and unreliable.

19. Synthetic organic polymers of high molecular weight (greater than 10^6) were found to be efficient conditioning agents for metal hydroxide sludges.
20. Polymers condition metal hydroxide sludges through increases in particle size, the mechanism of action being interparticle "bridging".

GRAVITY THICKENING

21. The rate of metal hydroxide suspension thickening was seen to be affected by solids concentration as well as by changes in the characteristic floc size of the suspension.
22. Polyelectrolytes enhanced the rate of thickening through increases in particle size.
23. It is possible to correlate the thickening rates and dewatering rates of metal hydroxide suspensions.

DUAL MEDIA FILTRATION

24. Dual media filtration with cationic polymer addition can effectively clarify a metal hydroxide suspension.
25. A cationic polymer dose of 0.5 mg/l was found to be as effective as higher doses.
26. Filtration efficiency is very sensitive to the liquid application rate. Performance was always better at 2 gpm/ft² than at 4 gpm/ft².
27. Precoat filtration was found to perform at a level comparable to direct polymer addition to the slurry.
28. Anionic polymers were not useful because they caused high head losses at the filter surface.

DIATOMACEOUS EARTH FILTRATION

29. Diatomaceous earth filtration provided effluent turbidities that were superior to those obtained by dual media filtration.
30. Most grades of diatomaceous earth performed well. The choice of media was not critical.

31. A flow rate of 0.5 gpm/ft^2 and a precoat addition rate of 0.15 lb/ft^2 were found to be optimum.

LIQUID-LIQUID EXTRACTION

32. Liquid-liquid extraction can be used to separate metals from a mixed metal solution. The separated metals can be obtained in a reasonably pure form.
33. Although the liquid-liquid extraction process was found to effectively separate metals, the value of the recovered metals could not offset the extraction cost.
34. Inability to recover and reuse the metal chelates is the major cost factor which renders this process uneconomically feasible.
35. Chelating compounds which can be recovered are not selective enough to separate metals so they can be reused.

SECTION V

RECOMMENDATIONS

METAL INSOLUBILIZATION

The concentration of metals from an ion exchange regenerant solution could be effectively reduced by chemical precipitation as metal hydroxides. Individual metals were found to precipitate in a manner predicted by equilibrium chemistry. Mixed metal systems were more complex. Solutions containing a significant quantity of chromium were found to produce conditions of "coprecipitation" wherein other divalent cations were insolubilized at pH values far below that predicted necessary for their removal from solution.

Sedimentation of metal hydroxide flocs was directly related to the size of particulates formed during the insolubilization phase of treatment. Certain species such as $\text{Cr}(\text{OH})_3$ (5) were characterized by the presence of extremely fine particles for insolubilization pH values outside the range 7.5 to 10.5, resulting in the formation of relatively stable suspensions. Insolubilization at pH values near the isoelectric point resulted in good settling characteristics.

SLUDGE DEWATERING

Particle size was also found to be a major factor in determining the rate of hydroxide sludge thickening and dewatering. Particles of larger characteristic size produced increased interfacial settling velocities and low specific resistance values. Vacuum filtration was examined extensively and found to be an applicable procedure for the dewatering of metal hydroxide sludges. Most sludges were found to dewater well and produce cake solids concentrations in the range of 11 to 17%, with slightly higher levels of 21 to 25% solids obtained for chromium hydroxide sludges. In cases where higher resistance to filtration was noted, the addition of organic polyelectrolytes resulted in improvement in the dewatering rate.

FILTRATION

Either filtration process could be used to upgrade effluents from the precipitation process for recycle of the effluent back through the ion exchange units. The diatomaceous earth pressure precoated filter should be considered in polishing operations involving metal hydroxides as this filter produced a high quality filtrate and was generally superior to the dual media filter. Neither filtration process provided metals removal sufficient for direct effluent discharge. Organic polyelectrolytes were required for dual media filtration but the dose requirements were not critical.

LIQUID-LIQUID EXTRACTION

The liquid-liquid extraction process was evaluated to determine if the metals from a mixed metal system could be separated and recovered economically. Liquid-liquid extraction was found to be a technically feasible

procedure but is not an economically viable procedure. The major economic difficulty with this procedure is that the chelates cannot be recovered and reused and therefore costs of the separation are unreasonably large.

The specific recommendations made for the treatment of metal-bearing regeneration backwash water similar to that found at the U.S. Air Force Logistic Center located in Oklahoma City, OK (OC-ALC) are:

1. The concentration of various metals in the regeneration backwash should be monitored frequently for the control of the neutralization process. Since coprecipitation of metals may suppress the equilibrium pH of precipitation of individual species, alkalimetric titration of mixed metal wastes should be performed to determine both the dosage of alkali and precipitation pH of the various metals. Insolubilization of mixed metals is optimum in the pH range of 7.5 to 10.5.
2. Use of lime is recommended instead of caustic soda despite the expected increased volume of sludge. Besides being less expensive, lime can enhance the dewaterability of mixed metal hydroxides by increasing their shear strength.
3. It is recommended that chromate waste stream be separated since the presence of chromium may make dewatering of the hydroxide sludges difficult.
4. Sufficient time must be allowed in the precipitation and settling process to complete insolubilization and allow for some "aging" of metal hydroxides prior to dewatering. Problems of "bleeding" of particulates through vacuum filter media during dewatering may be partly overcome if certain metal hydroxides, such as those of copper and chromium, are aged.
5. Addition of small amounts of high molecular weight polyelectrolytes as a filter aid in dewatering should be used to increase the strength of hydroxide flocs by using polyelectrolytes, since this appears to be the crucial parameter controlling solids penetration.
6. The proposed model for specific resistance may be used conveniently to predict specific resistance of a metal hydroxide sludge from a knowledge of its particle size and size distribution.
7. Either dual-media granular filter or diatomaceous earth precoat filter may be used to rid the clarifier overflow and vacuum filtrate of trace carryover particulates. Diatomaceous earth filters yield a superior quality of effluent and hence recommended for the polishing of effluents from the hydroxide treatment operations.
8. The metal waste streams should be segregated in the electroplating shops and, wherever economics warrant it, recovery should be accomplished by evaporation.

9. Separation and recovery of mixed wastes by liquid-liquid extraction is not economically feasible.
10. Further research is recommended to investigate methods of reducing sludge volumes and to determine environmentally safe methods for the ultimate disposal of dewatered metallic residues.

REFERENCES

1. McDonald, C. W., "Removal of Toxic Metals from Metal Finishing Wastewater by Solvent Extraction", EPA 600/2-78-011, Feb., 1978.
2. Cherry, R. H., Jr., "Removing Chromium and Cyanide and Treating Electroplating Sludges", Finishers Management, p. 35, July 1971.
3. Iannmartino, N. R., "Mercury Clean Up Rates-II", Chemical Engineering, February 3, 1975.
4. Patterson, J. W., Technology and Economics of Industrial Pollution Abatement, Illinois Institute for Water Quality, Document No. 76/22, 1976.
5. Trippler, A. B., Jr., R. H. Cherry, Jr. and G. R. Smithson, Jr., The Reclamation of Metal Values from Metal-Finishing Waste Treatment Sludges, EPA Report No. 670/2-75-018.
6. Novak, J. T., et al. Optimum Dewatering and Metal Recovery of Metal Plating Sludges, U. S. Air Force, Report No. CEEDO-TR-78-15, Tyndall AFB, March 1978.
7. Pribil, R. and V. Vesely, "The Extraction of Cadmium and Zinc and Their Complexometric Determination in the Presence of Other Elements", Collect. Czech. Chem. Commun., 37, 13-21, 1972.
8. Florence, T. and J. Farrar, "Liquid-Liquid Extraction of Nickel with Long-Chain Amines from Aqueous and Nonaqueous Halide Media", Anal. Chem., 40, 1200-1206, 1968.
9. McDonald, C.W. and T. Rhodes, "Liquid-Liquid Extraction of Zinc with Aliquat 336-S-I from Aqueous Iodide Solutions", Anal. Chem., 46, 300-301, 1974.
10. Stary, J., The Solvent Extraction of Metal Chelates, The McMillan Co., N.Y., 1964.
11. Brooks, P. T., et al., "Processing of Superalloy Scrap", J. Metals, 22, 25, 1970.
12. Reinhardt, H., "Solvent Extraction for Recovery of Metal Waste," Chem. and Ind., 210-213, March, 1975.
13. Jenkins, S.H., Knight, D. G., and Humphreys, R. E., "The Solubility of Heavy Metal Hydroxides in Water, Seqage and Sewage Sludge I. The Solubility of Some Metal Hydroxides", International Journal of Air and Water Pollution, 8, 537, (1964).

14. Patterson, J. W., Scala, J. J., and Allen, H. E., "Heavy Metal Treatment by Carbonate Precipitation", Proceedings of the 30th Purdue Industrial Waste Conference (1975).
15. Robinson, A. K., "Sulfide vs Hydroxide Precipitation of Heavy Metals from Industrial Wastewater", presented at EPA/AES First Annual Conference on Advanced Pollution Control for the Metal Finishing Industry (1978).
16. Stumm, W., and Morgan, J. J., Aquatic Chemistry; An Introduction Emphasizing Chemical Equilibria in Natural Waters, Wiley-Interscience, (1970).
17. Eckenfelder, W. W., and O'Connor, D. J., Biological Waste Treatment, Permagon Press, NY, (1961).
18. Standard Methods for the Examination of Water and Wastewater, 14th Edition, American Public Health Association, American Water Works Association, and Water Pollution Control Federation, (1975).
19. Novak, J. T., and O'Brien, J. H., "Polymer Conditioning of Chemical Sludges", Journal of the Water Pollution Control Federation, 47(10), 2397, (1975).
20. Thomas, M. J., and Theis, T. L., "Effects of Selected Ions on the Removal of Chrome (III) Hydroxide", Journal of the Water Pollution Control Federation, 48(8): 2032, (1976).
21. Canale, R. P., and Borchardt, J. A., "Sedimentation", in Physico-chemical Processes for Water Quality Control, (W. J. Weber, Jr., Editor), Wiley-Interscience, (1972).
22. Riddick, T., Control of Colloid Stability Through Zeta Potential.
23. Zievers, J. F., Crain, R. W. and Barclay, F. G., "Waste Treatment in Metal Finishings, U.S. and European Practices", Plating, 55, 1171 (1968).
24. Patterson, J. W., Wastewater Treatment Technology, Ann Arbor Science Publishers, (1975).
25. Tewari, S. N., et al., "The Nature of Hydrated Chromium Oxide: IV. The Solubility of Different Samples in Sulfuric Acid", Kolloid-Z, (130), 169 (1953); Chem Abs. 47:7291.
26. Knyazev, E. A., "The Solubility of Hydroxides", translated from Zhurnal Fizicheskoi Khimii, 49, 1534, (1975).
27. Plotnikov, V. I., "Coprecipitation of Small Amount of Cadmium With Some Metal Hydroxides", Zhur. Neorg. Khim., 4, 2775 (1959); Chem Abs. 54:19101C.

28. Simon, J., et al., "Sorption Effects on Metal (III) Hydroxide Precipitants III. Sorption and Coprecipitation of Cd Ions by Freshly Precipitated $\text{Cr}(\text{OH})_3$ ", Fresenius' Z. Anal. Chem., 264(1), 4, (1963); Chem. Abs. 78:15191Z.
29. Ermolenko, et al., "Phenomenon of Mutual Protection, Structure and Phase Transition of a Mixed $\text{NiO-Cr}_2\text{O}_3$ Catalyst", Vest. Akad. Navuk Belarus, SSR Scr. Khim. Minsk, USSR; Chem. Abs. 70:23251S.
30. Wilkens, R., and Eigen, W., "Formation of Metal Complexes", in Mechanisms of Inorganic Reactions, (1966).
31. Chalyi, V. P., "Kinetics and Mechanisms of Aging of Metallic Hydroxides VIII: Speed of Solution of Hydroxides". Ukr. Khim. Zh., 28(9), 1005 (1962); Chem. Abs. 59:9398A.
32. Krusenstjern, A., "Neutralization of Plating Wastes With Calcium and Sodium Hydroxide", Metalloberflaeche, 18(3), 65 (1964).
33. Pattengill, L., Masters Thesis, University of Missouri - Columbia, (Dec. 1976).
34. Bargman, R. D., Garber, W. F., and J. Nagano, "Sludge Filtration and Use of Synthetic Organic Coagulants at Hyperion", Sewage and Industrial Wastes, 30 (9), 1079, (1958).
35. Coackley, P., and Allos, R., "The Drying Characteristics of Some Sewage Sludges", Inst. of Sew. Purif., Pt. 6, 557, (1962).
36. Dixon, J. K., La Mer, V. K., and Linford, H. B., "Factors Affecting Filtration Rates of Flocculated Silica", Journal of the Water Pollution Control Federation, 39(4), 647, (1967).
37. Karr, P. R. and Keinath, T. M., "Influence of Particle Size on Sludge Dewaterability", Journal of the Water Pollution Control Federation, 50(8), 1911 (1978).
38. Gale, R. S., "Filtration Theory with Special Reference to Sewage Sludges", Water Pollution Control, 622 (1967).
39. Simmons, C. S., and Dahlstrom, D. A., "Steam Dewatering of Filter Cakes", Chem. Engr. Prog., 62(1), 75, (1966).
40. McVaugh, J., and Wall, W. T., Jr., "Optimization of Heavy Metals Wastewater Treatment. Effluent Quality Versus Sludge Treatment", 31st Purdue Industrial Waste Conference, (1976).
41. Grace, H. P., "Resistance and Compressibility of Filter Cakes. Pt. II: Under Conditions of Pressure Filtration" Chem. Engr. Prog., 49(7), 367, (1953).

42. Hannah, S. A., Cohen, J. M., and Robeck, G. G., "Measurement of Floc Strength by Particle Counting", Journal of the American Water Works Association, 59(9), 1149, (1967).
43. King, P. H. et al, Treatment of Waste Sludges from Water Purification Plants, Virginia Water Resources Research Center Bulletin #52, (1972).
44. Stumm, W., and O'Melia, C. R., "Stoichiometry of Coagulation", Journal of the American Water Works Association, 60(5), 514, (1968).
45. La Mer, V. K., and Healy, T. W., "Adsorption-Flocculation Reactions of Macromolecules at the Solid-Liquid Interface", Reviews of Pure and Applied Chemistry, 13, 112, (1963).
46. Schaefer, R., Master's Thesis, University of Missouri - Columbia, (1976).
47. Vesilind, P. A., Treatment and Disposal of Wastewater Sludges, Ann Arbor Science Publishing Inc., 1974.
48. Yao, K. M., Habibian, M. T., and O'Melia, C.R., "Water and Wastewater Filtration - Concepts and Applications", Envr. Science and Technology, 5(11), 1105 (1971).
49. Ghosh, M. M., Jordan, T. A., and Porter, R. L., "Physicochemical Approach to Water and Wastewater Filtration", Jour. Envr. Engineering Division, ASCE, 101, EE1, 71 (1975).
50. Stump, V. L. and Novak, J. T., "Mixing of Polyelectrolytes for Direct Filtration", Proceedings 97th Annual Conf. AWWA, 1977.
51. Cleasby, J. L., "Filtration" in Physicochemical Processes for Water Quality Control, ed. W. W. Weber, Wiley-Interscience, New York (1972).

APPENDIX A

ESTIMATION OF CURRENT BED UTILIZATION

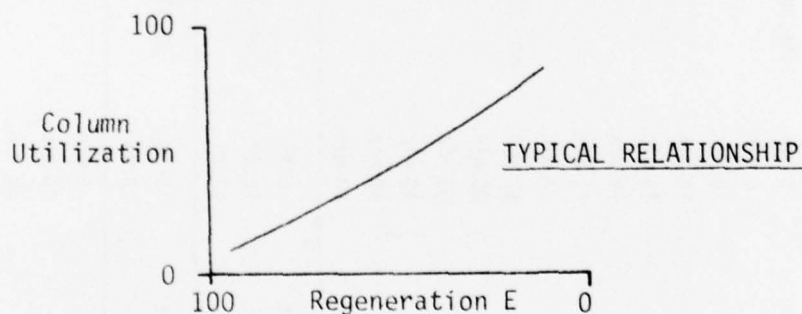
Column Utilization

In practice, the ratio of operating to theoretical exchanger capacity is at a level considerably below its theoretical capacity. The exchange reactions are equilibrium reactions and a large quantity of regenerant would be required to drive the reaction to completion. Although increasing the quantity of regenerant per unit volume of resin in regeneration increases the operational capacity of the exchanger, the resulting bed capacity is not directly proportional to the increase in regenerant required.

Efficiency

The term "Efficiency" is used to designate the degree of utilization of regenerant. E is the ratio of the operating exchange capacity of a unit to the exchange capacity that theoretically could be derived from a specific weight of applied regenerant. Efficiency refers only the output of an exchanger relative to the input of regenerant, on an equivalent basis.

This suggests that higher efficiencies are achieved with lower levels of regeneration. However, low bed capacities also result at low regeneration levels. In practice, some efficiency is generally sacrificed to obtain a reasonable column utilization.



Typical E 's = 45-70%

Typical Column Utilization = 30-65%

OC-ALC Cation Column

Dowex HCRS

135 ft³ Wet Volume

Total Capacity: 4.8 meq/gm

1.8 meq/wet ml

} from product literature

TABLE A-1
COMPOSITION OF METALS IN SAMPLES FROM REGENERANT STREAMS AT TINKER AFB

Sample I.D.		Na	Zn	Ni	Mg	Cu	Cd	Cr	Fe	Ca
Cation Regenerant	0	1202.00	2.06	2630.	142.	8.0	.24	9.5	19.8	394.00
	3 min.	1496.00	3.50	3020.	169.	9.4	.26	9.4	18.9	476.00
	6 min.		2.95	2340.	163.	9.7	.19	9.2	18.2	464.00
	9 min.		3.20	2680.	155.	9.7	.24	9.4	16.8	444.50
	12 min.		3.00	2910	137.	8.5	.22	8.1	14.5	393.00
	15 min.		2.05	2390.	115.	7.5	.16	6.6	11.3	332.00
	18 min.		1.60	1920.	95.1	6.0	.14	4.5	8.4	271.00
	21 min.		1.25	970.	72.7	4.4	6.6	2.7	5.9	207.00
	24 min.		1.12	770.	58.9	3.5	5.5	1.9	4.3	168.00
	27 min.	400.30	.83	490.	39.1	2.4	3.9	.75	3.1	112.00
	30 min.		.65	385.	30.1	1.8	2.8	.3	2.4	86.10
Rinse Water Influent	35 min.		.43	220.	18.9	1.1	1.7	<.2	1.6	53.40
	40 min.		.22	200.	10.9	.64	.64	<.2	1.1	31.10
	45 min.		.16	102.	7.2	.44	.42	<.2	.81	19.90
	50 min.		.11	67.	4.9	.29	.28	<.2	.63	14.00
	8:30		.04	1.4	1.9	.11	.08	4.4	.05	3.6
	10:30	24.17	<.03	3.8	2.7	.13	.13	4.4	.04	5.5
Rinse Water Effluent	12:30		<.03	3.1	2.1	.09	.22	<.2	.07	4.5
	10:30	25.11	<.03	2.3	2.8	<.06	.50	1.2	.05	5.9
	12:30		<.03	2.4	2.4	.06	.16	.5	<.03	5.2
Cation Backwash	5 min.		.33	12.9	30.6	.28	.30	<.2	.96	73.40
	20 min.		<.03	3.0	1.7	<.06	.12	<.2	.06	3.40
	30 min.		<.03	.9	1.0	<.06	<.07	<.2	.04	1.90

$$\rho \text{ as Dry wt/wet vol.} = \frac{1.8 \text{ meq}}{\text{ml}} \cdot \frac{\text{gm}}{4.8 \text{ meq}} \cdot \frac{10^3 \text{ ml}}{1}$$

$$= 375 \text{ gm/l}$$

$$\text{Column Utilization} = \frac{\text{operating capacity}}{\text{total capacity}}$$

$$\text{Total capacity} = 1.8 \frac{\text{meq}}{\text{ml}} \cdot \frac{10^3 \text{ ml}}{1} \cdot \frac{28.32 \text{ l}}{\text{ft}^3} (135 \text{ ft}^3)$$

$$= 6.9 \times 10^6 \text{ meq}$$

$$= 1800 \text{ meq/l resin}$$

$$\text{Operating capacity} = \text{meq's removed/l resin}$$

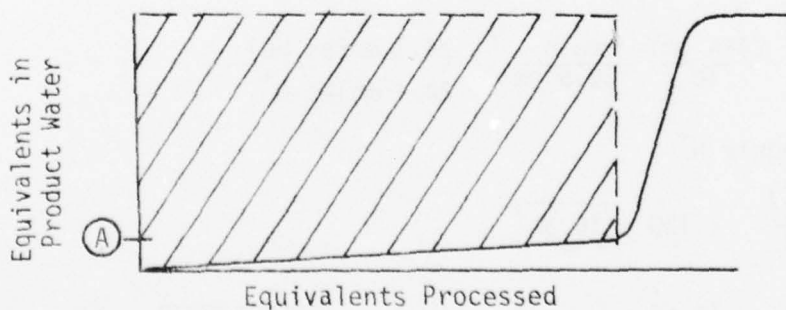
Estimate from regenerant Data collected January 1978 and shown in Table A-1 is 140 meq/l including Na^+

$$\frac{140 \frac{\text{meq}}{\text{l}} (10^3 \text{ Gal Regen.}) 3.785 \frac{\text{l}}{\text{Gal}}}{135 \text{ ft}^3 \text{ Resins}} \cdot \frac{\text{ft}^3}{28.32 \text{ l}} = 139 \text{ meq/l resin}$$

$$= 3.925 \text{ eq/ft}^3 \text{ resin}$$

NOTE: This is not the best way to determine operating capacity but the only way given the data we have from Tinker. Using the regenerant data we inherently assume each cation introduced into the column is removed by the HCl

Usual Method:



(Vol. of water processed for constant waste)

When TDS or conductivity in product water reaches level A, then regeneration is required.

operating capacity = cross hatched area

would need to monitor: a) Flows
b) Influent concentrations
c) Effluent concentrations

ie: A comprehensive Mass Balance

using our best estimate of operating capacity,

$$\text{Column Utilization} = \frac{139 \text{ meq/l resin}}{1800 \text{ meq/l resin}} \times 100 = 7.7\%$$

Tinker Regeneration E

100 Gal of Tech. Grade HCl in 100 gal. H₂O

Tech. Grade = 31.45% HCL by wt.

5 gallons @ \$9.55

FSN 6810-00-236-5665

$$E = \frac{\text{operating capacity}}{\text{Theoretical exchange capacity based on regen. applied}}$$
$$(5 \text{ gal})(62.4 \frac{\text{lb}}{\text{ft}^3}) \frac{1 \text{ ft}^3}{7.48 \text{ gal}} (.3145) = 13.12 \text{ lb HCl/5 gal}$$
$$= \boxed{2.62 \text{ lb HCl/gal}}$$

$$100 \text{ gal} (2.62 \text{ lb} \frac{\text{HCl}}{\text{gal}}) = 262 \text{ lb HCl}$$
$$= 1.94 \text{ lb HCl/ft}^3 \text{ resin}$$

$$1.94 \text{ lb HCl/ft}^3 \left(\frac{454 \text{ gm}}{\text{lb}} \right) \frac{\text{mole}}{36.5 \text{ gm}} = 24.1 \text{ moles HCl}$$
$$= 24.1 \text{ moles H}^+$$

$$1 \text{ mole H}^+ = 1 \text{ equiv H}^+$$

$$E = \frac{3.925 \text{ eq/ft}^3}{24.1 \text{ eq/ft}^3} \times 100 = \boxed{16.3\%}$$

$$\left(\frac{20 \text{ containers}}{\text{regen}} \right) \frac{\$9.55}{\text{container}} 180 \text{ regens/yr.} = \boxed{\$34,000/\text{yr}}$$

Softening

It is noteworthy that on an equivalent basis approximately 90% of the total operating capacity is being utilized to remove Ca and Mg ions. The majority of this hardness comes from the 25,00 GPD well make up water which contains 42 mg/l and 20 mg/l compared to only 2.3 mg/l and 2.0 mg/l in the OC-ACL rinsewater.

A softening process which employs and H^+ strong acid cation resin should be installed upstream of the rinse sump on the make up water line. Column utilization may not increase but cycle time should go from 2 days to approximately 2 weeks and metal concentrations in the regenerant will be much higher an advantage with respect to recovery.

The problems associated with utilization and regeneration E are physical in nature.

1. Loss of resin
2. Air locks (consider degasing the influent)
3. Improper distribution system
4. Hydroxide fouling in the anion column
5. Channeling/short circuiting

APPENDIX B

CALCULATION OF SIMULATED SAMPLE CONTENT FOR CATION REGENERANT

I. Method A

1. Assume 50% column utilization is desirable and regeneration is conducted to achieve this value.

$$\begin{aligned}\text{Total capacity} &= (135 \text{ ft}^3) (1.8 \text{ meq/l}) \\ &= 6.9 \times 10^6 \text{ meq}\end{aligned}$$

$$50\% = \frac{\text{operating capacity}}{6.9 \times 10^6 \text{ meq}} \times 100$$

$$\text{Operating Capacity} = 3.45 \times 10^6 \text{ meq}$$

Based on a regenerant volume of 1000 gal, the equivalent concentration in the regenerant is 912 meq/l.

2. An alternate calculation is as follows:

Typical operating capacity for Dowex strong acid resin regenerant with 6 lb. 100% HCl/ft³ resin.

25 kg/ft³ resin (as CaCO₃)

$$\begin{aligned}\frac{(25 \text{ kg CaCO}_3/\text{ft}^3)(135 \text{ ft}^3)}{1000 \text{ gal} \times 3.785 \text{ l/gal}} &\times \frac{10^3 \text{ gm}}{\text{kg}} \times \frac{.0648 \text{ gm}}{\text{grain}} \times \frac{\text{eq}}{50 \text{ gm}} \times \frac{10^3 \text{ meq}}{\text{eq}} \\ &= \underline{1150 \text{ meq/l}}\end{aligned}$$

Use 1000 meq/l for simulated samples

Assume make-up water softened with strong acid H⁺ resin, removing all cations from rinse water

The simulated sample content is shown in Table B-1.

II. Method B

1. Assume 2000 gal regeneration and backwash flow
2. Two samples were taken at Tinker AFB and the metal content measured. One sample, designated as sample #1, was a grab sample taken during the regeneration cycle. Sample #2 was a composite sample and represents the composite metal concentration in one regeneration cycle.

TABLE B-1

Simulated Sample Content Calculated Using Method A

Ions of Interests	Equivalent Weight	Measured Ions in a Sample*		Simulated Sample Based on a Total Ion content of 1000 meq/l	mg/l
		mg/l	meq/l	meq/l	
Ni(II)	29.4	8.7	.296	5.4	1588
Cu(II)	31.8	.02	.0006	.01	3.2
Zn(II)	32.7	.01	.0003	.01	3.3
Na(I)	23	112	4.87	88.08	20,260
Fe(II)	27.9	.05	.002	.04	11.2
Cr(III)	17.3	.95	.005	1.00	173
Cd(II)	56.2	.22	.004	.07	39.3
Ca(II)	20	2.3	.115	2.10	420
Mg(II)	12.2	2.0	.164	2.97	362
Al(III)	9	.2	.022	.4	36
Total			5.529	100	

*Data taken from a cation regenerant sample from Kirtland A.F.B.

These values, presented in Table B-2, show that both the grab sample and composite sample contain similar ion contents. Therefore, these values were averaged and used to calculate the synthetic waste metal content.

The criteria utilized in developing the proposed synthetic regeneration waste solution are as follows:

(1) Both Samples #1 and #2 contained approximately 95 meq/l of cations (excluding H^+ , Na^+ , K^+ , etc.) This was assumed to be the representative cation exchange capacity (CEC) of the resin that could be realized under the operating conditions. This is at best a judgment decision. Since the present ion exchange system at Tinker AFB is assumed to be exhausted on the basis of conductance measurements after both anion and cation exchanges, it is impossible to determine exactly what percentages of the CEC and also total exchange capacity are utilized when the system is regenerated.

(2) All calculations were made assuming that proper equipment for the removal of hardness from make up water will be installed. Thus, it was assumed that 90% of the present levels of calcium and magnesium would be removed through pretreatment.

(3) Other elements under consideration (Ni, Cr, Cu, Cd, Zn and Fe) were considered to remain in the same proportions as were obtained by averaging their respective concentrations present in Sample #1 and #2. These calculations are shown in Table B-2.

TABLE B-2.

Sample Calculations for Synthetic Cations Regeneration Waste

Metal	Sample #1	Sample #2	Ave. Conc.		% of Equivalence (excluding Ca & Mg)
			mg/l	meq/l	
Cd	2.6	1.2	1.9	0.03	0.40
Ni	210.1	74.2	142.1	4.84	65.0
Cr	11.5	5.2	8.35	0.48	6.44
Cu	4.5	18.7	11.6	0.37	4.97
Fe	20.0	14.7	17.4	0.95	12.75
Zn	39.0	12.0	25.5	0.78	10.47
Ca	990.0	960.0	975.0	48.7	--
Mg	420.0	390.0	405.0	33.7	--
Pb	6.0		6.0	.058	

Because insufficient data existed for the chemical composition (metals,

in particular) of the rinse water, its use in developing the metallic composition of the simulated cation exchange regeneration wastewater was precluded.

From the average ratio of various metals present in the two waste samples, it is possible to predict the concentration of each metal, assuming 95 meq/l to be the total concentration of all metals the results of these calculations are shown below:

TABLE B-3

Composition of Synthetic Waste Calculated Using Method B.

<u>Element</u>	<u>meq/l</u>	<u>mg/l</u>
Cd	0.3	18.5
Ni	59.9	1550.0
Cr	5.3	91.0
Cr	4.1	129.0
Fe	10.4	191.0
Zn	8.6	279.0
Ca	4.9	97.0
Mg	3.3	40.0
<hr/>		
95.8 meq/l		

The synthetic waste were prepared by utilizing nitrate or chloride salts of each metal and dissolving them in distilled water. Hydrochloric acid was used to lower the pH to 1.4-1.5, the normal pH range of the backwash waste samples from Tinker AFB. Also, NaCl was added iff additional ionic strength was needed.

Because the synthetic sample in Table B-3 was calculated based upon actual Tinker AFB samples, this synthetic waste sample was selected over that shown in Table B-1.

INITIAL DISTRIBUTION

DDC/DAA	2	HQ AFESC/DEV	1
HQ AFSC/DL	1	USAFSAM/EDE	2
HQ AFSC/SD	1	HQ AFISC	2
HQ USAF/LEEV	1	HQ AUL/LSE 71-249	1
OSAF/MIQ	1	HQ USAFA/Library	1
OSAF/OI	1	HQ AFESC/TST	2
AFIT/Library	1	OL-AD; USAF OEHL	1
AFIT/DE	1	OUSDR&E	1
EPA/ORD	1	USAF Hospital, Weisbaden	1
AFIT/LSGM	1	VPI and SU	1
USA Chief, R&D/EQ	1	University of S. Carolina	1
USN Chief, R&D/EQ	1	AFLC/MA	1
WR-ALC/DEE	1	Industrial Env Research Lab	1
WR-ALC/MAA	1	AFRCE/ER	1
OC-ALC/DEE	1	USAMBRDL	1
OC-ALC/MAA	1	AFLC/DE	1
SM-ALC/DEE	1	US Army/CERL	1
SM-ALC/MAA	1	USA Environ Hygn Agency	1
SA-ALC/DEE	1	University of MO-Columbia	10
SA-ALC/MAA	1	HQ AFESC/RDVM	10
O-ALC/DEE	1	AFRCE/CR	1
O-ALC/MAA	1	AFRCE/WR	1
AFOSR/CC	1	NEPSS	1
OEHL/CC	1	NCEL, Code 25111	1